

AVAILABLE DATA

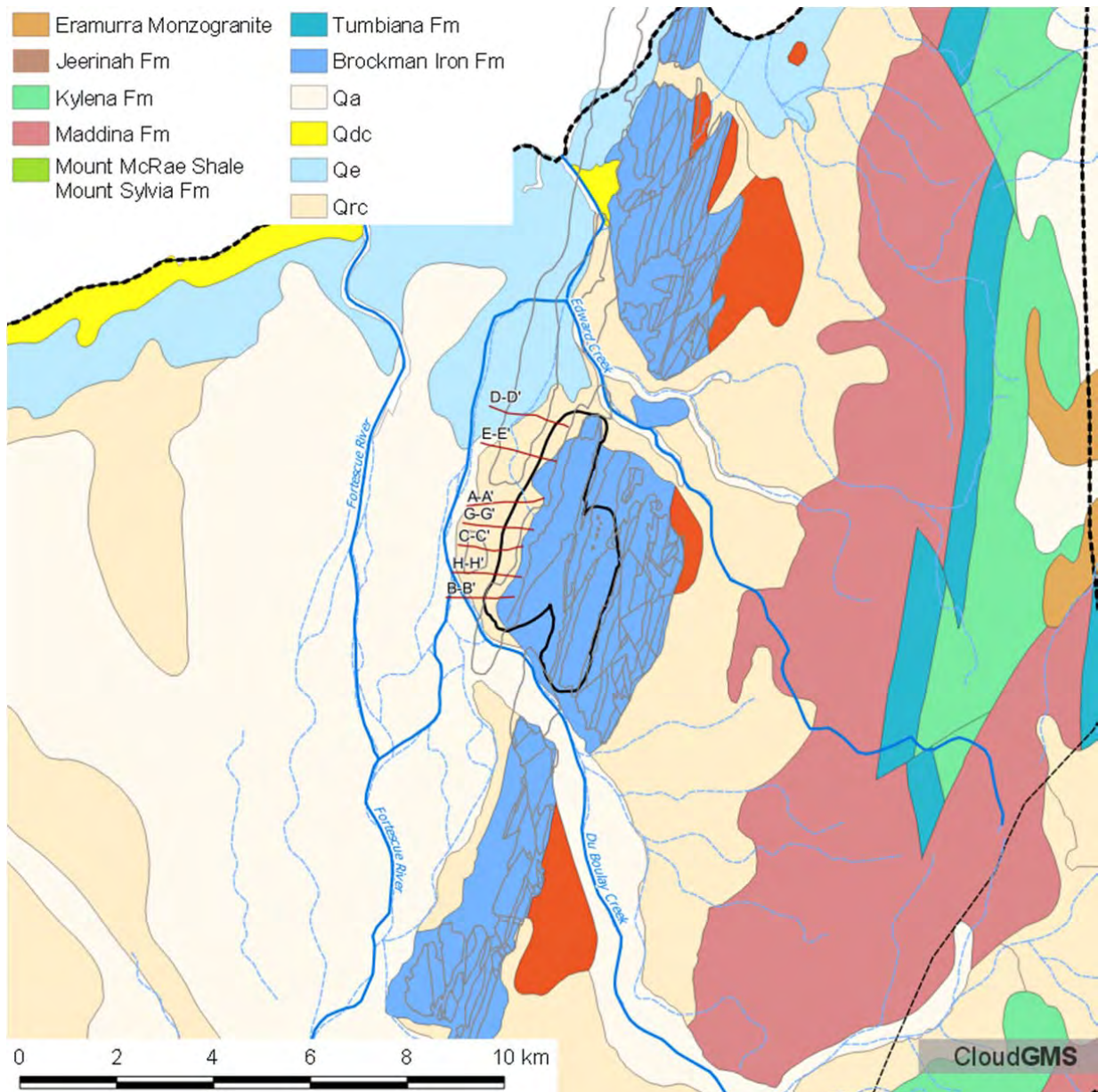


Figure 2-17 Location of sections delineating the depth and extent of the alluvial sediments to the west of the pit (Global Groundwater 2010) and mapped extent of alluvial sediments (Qrc).

2.9.2 Depth of basement weathering and water filled fractures

Typically, the Hamersley Group is weathered to approximately 40 – 45 metres below ground level and contains some minor groundwater. Underlying the weathered layer is fresh bedrock which does not contain any significant groundwater, except where fractures occur.

Recent mapping of the depth of weathering extends to below -120 mAHD adjacent to the location of Sump 03 (Figure 2-18) and fracture mapping shows enhanced permeability may extend to depths of greater than -170 mAHD (Figure 2-19) primarily within faulted parts of the Yandicoogina Shale (CPMM, 2014) forming a 'bathtub' shape in the west of the current East Pit. Clearly, this large volume of rock with likely enhanced storage and permeability indicates there is likely to be a volume of water stored beneath Lake Sino in the vicinity of Sump 03 depicted as cyan squares (refer to Figure 2-18).

AVAILABLE DATA

The following comments / discussion of the weathering and fracture mapping (CPMM, 2014) have been reproduced herein.

This weathered zone 'bathtub' is bounded by fresh rock and packer test results indicate the hydraulic conductivity of fresh rock is typically very low, so the walls of the 'bathtub' form a barrier to water flow (SWS, 2011). However, the water-bearing fracture depth shows that the 'bathtub' lies above a region of deep water-bearing fractures, likely associated with the intersection of two faults. So water is able to migrate in a roughly north-south direction indicating possible connection between sumps 03 and 05 / 08. As a first pass, using a basic 'text-book' estimate, a storage coefficient of 0.02 (2% total volume of available water) for a clay, unconfined aquifer implies a water volume of 3 GL in the weathered material. However, this number is sensitive to the storage coefficient, so could range anywhere from 500 ML to 5 GL. Similarly a further 1.5 GL may be stored in the fractured rock beneath.

These maps (Figure 2-18 and Figure 2-19 below) provide good targeting information, indicating more prospective areas for dewatering. The map agrees with known airlift yields from early drill holes. A small network of 5 or 6 bores on the western margin targeting deep fractures may be useful to dewater the area prior to mining and may allow mining to progress unimpeded by excess water.

Although the method to determine the depth of weathering is subjective, it compares well with local geological understanding and offers some hydrogeological interpretation. The associated changes in hydraulic conductivity with weathering and faulting around the pit are useful to explain the variations in water level and salinity, and why perched water in sumps has not drained towards the lower parts of the pit.

This data also indicates that water ingress is likely from the deep zone of weathered material to the west of the current extent of the East Pit, independent of the Fortescue Alluvial aquifer system. Advanced dewatering in this area will be required to enable rapid vertical mining. Although the comments are in reference to the east pit shell, similar lithologies and depth of weathering are observed in the limited drill hole data to the west of the west pit shell and the discussion may also be pertinent to this area.

The geological block model and depth of weathering mapping suggests that similar conditions may occur to the west of the extension of the west pit. The hydraulic parameters of the weathered material are largely unknown, and as such still constitute a major uncertainty with the modelling. To address this uncertainty a range of parameter combinations are investigated to determine the importance of the hydraulic characteristics of the weathered material on key model outcomes.

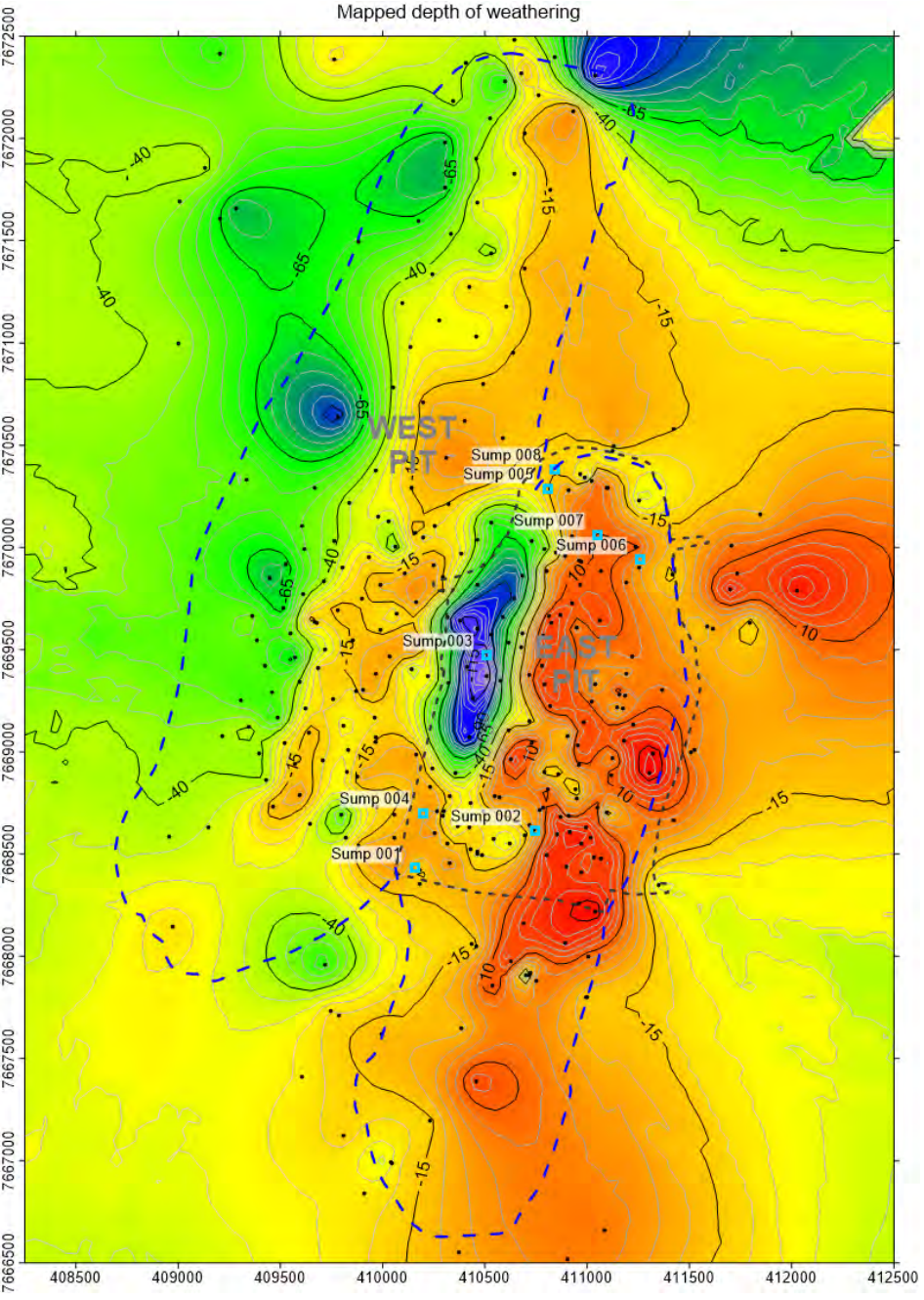


Figure 2-18 Mapped depth of weathering in mAH (after CPMM, 2014) identifying sump locations (cyan squares) and borehole data points (black dots).

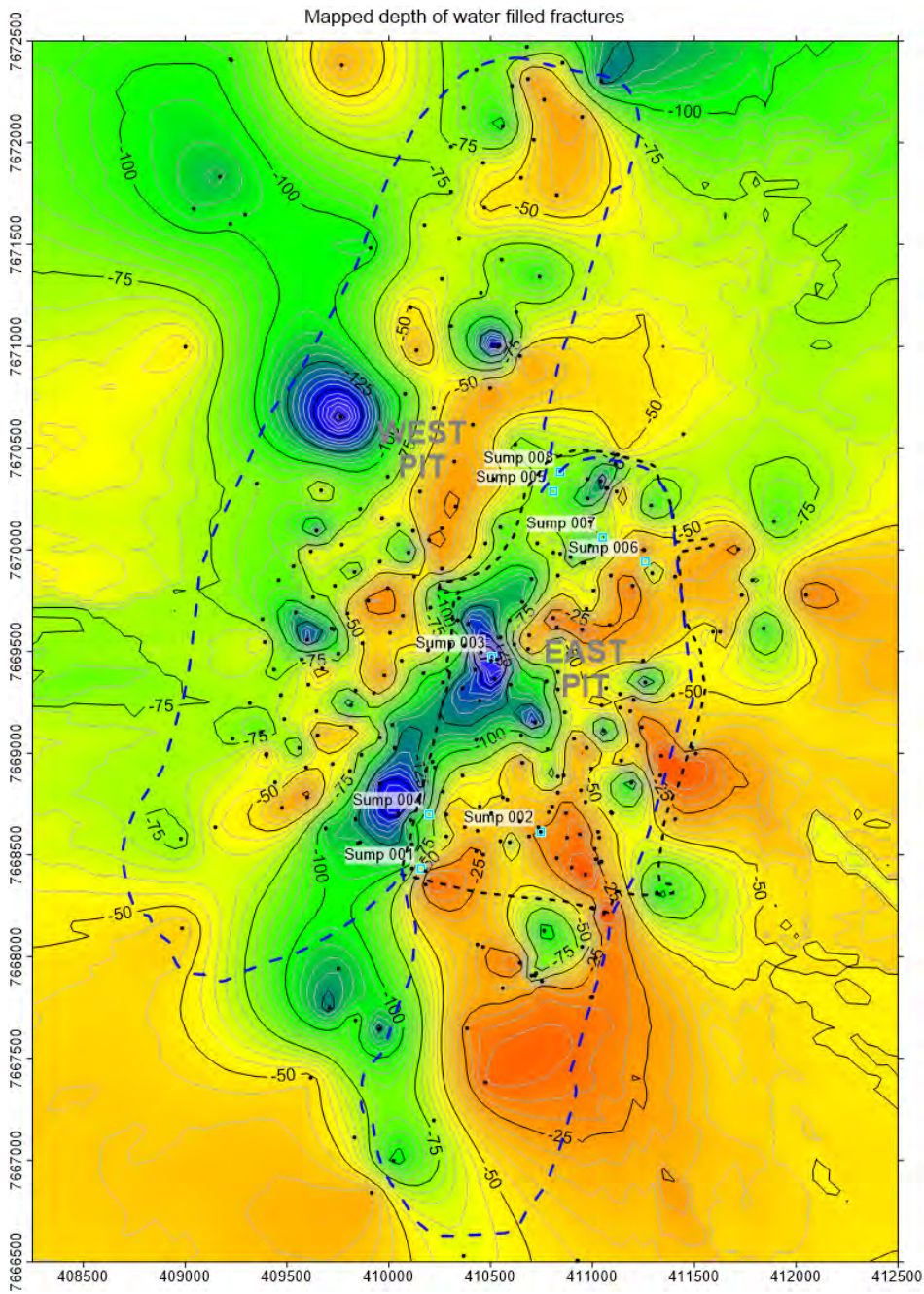


Figure 2-19 Mapped fracture depth in mAGD (after CPMM, 2014) identifying sump locations (cyan squares) and borehole data points (black dots).

2.9.3 Geological block model

The geological block model in the vicinity of the mine was provided by CPM in 3D DXF format. The block model was imported into Leapfrog Hydro (ARANZ Geo Ltd, 2017) and has been used primarily for visualization and conceptual interpretations. The geological units represented in the block model include the Dales Gorge member (D1-D4), Joffre member (J1-J6) Weeli Wollli formation (WW1-WW4) Whaleback Shale (WS1-WS2) and Yandicoogina Shale (YS).

AVAILABLE DATA

The Fortescue Alluvial aquifer system has been incorporated as an erosional unit based on the geological logs from the GSWA 1983 investigation (Commander, 1989) and the Global Groundwater 2009 investigations.

Cross sections can be generated from the Leapfrog Hydro block model to provide context for the local geological setting for the pit. The geological model indicates that the superficial sediments, denoted Cz below, are underlain by deeply weathered Weeli Wolli Formation (WW1-WW4) and dolerite sills (SILL1-SILL3).

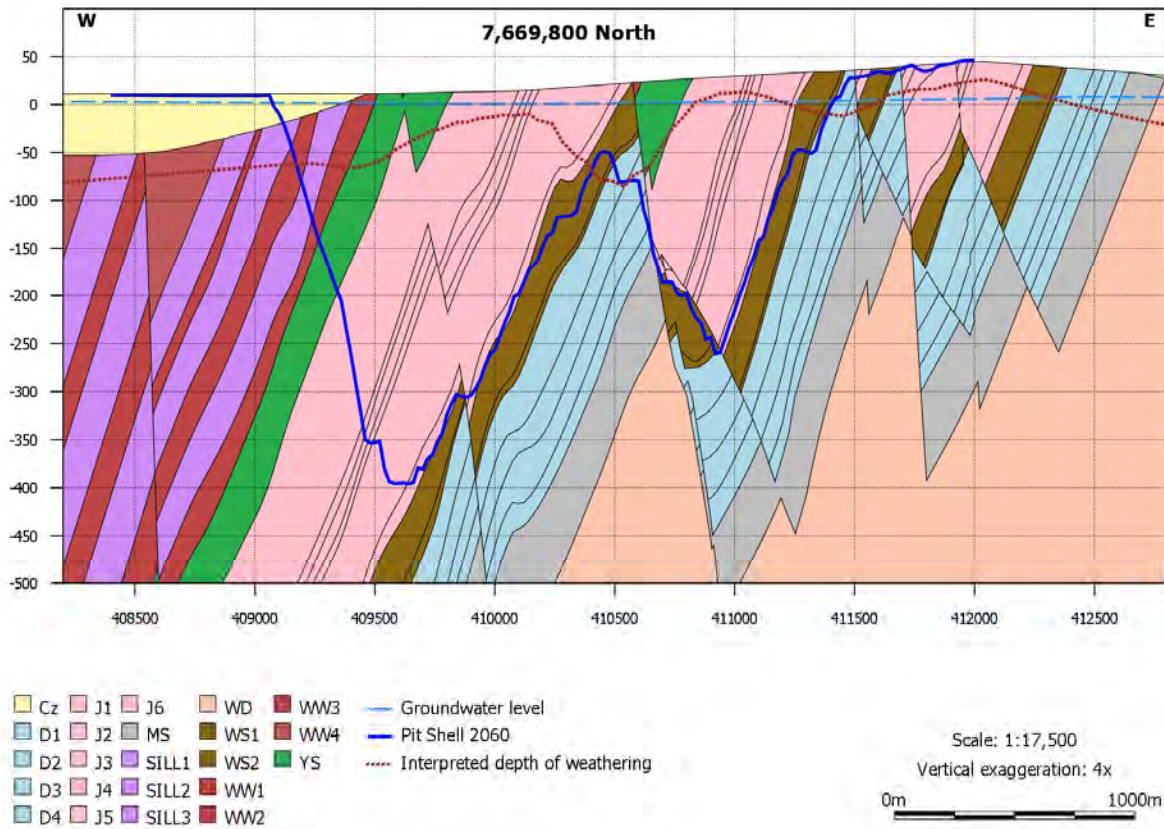


Figure 2-20 Leapfrog Hydro geological section along 7669800 mN of the modified CPM geological block model showing the relationship between the alluvial sediments, weathering surface and formations of the Hamersley Group, the final pit shell and regional groundwater level.

2.10 Regional geophysics

Airborne magnetics is available from the Geological Survey of Western Australia as a 40 metre grid and processed to 1st vertical derivative to accentuate short wavelength features such as geological structures and contacts. (<http://www.dmp.wa.gov.au/Geological-Survey/Regional-geophysical-survey-data-1392.aspx>). The magnetics data is presented below in Figure 2-21.

The Brockman Iron Formation (Dales Gorge Member, Joffre Member, Whaleback Shale Member and Yandicoogina Shale Member) of the Hamersley Group is the most obvious features in the magnetics data. The Brockman Iron Formation shows a much higher magnetics signature with a 'highly textured' appearance. The 'highly texture' appearance is a result of the juxtaposition of the magnetic formations against the less magnetic formations and the occurrence of structural features. Structural features can

AVAILABLE DATA

increase the rate of alteration the magnetic minerals to less magnetic minerals due to enhanced weathering.

Regionally, the texture of the 1VD magnetics data highlights the contacts between the Hamersley Group and the Fortescue Group (Jerrinah, Maddina and Kylenea Formations) to the east and the Cretaceous aged Winning Group to the west.

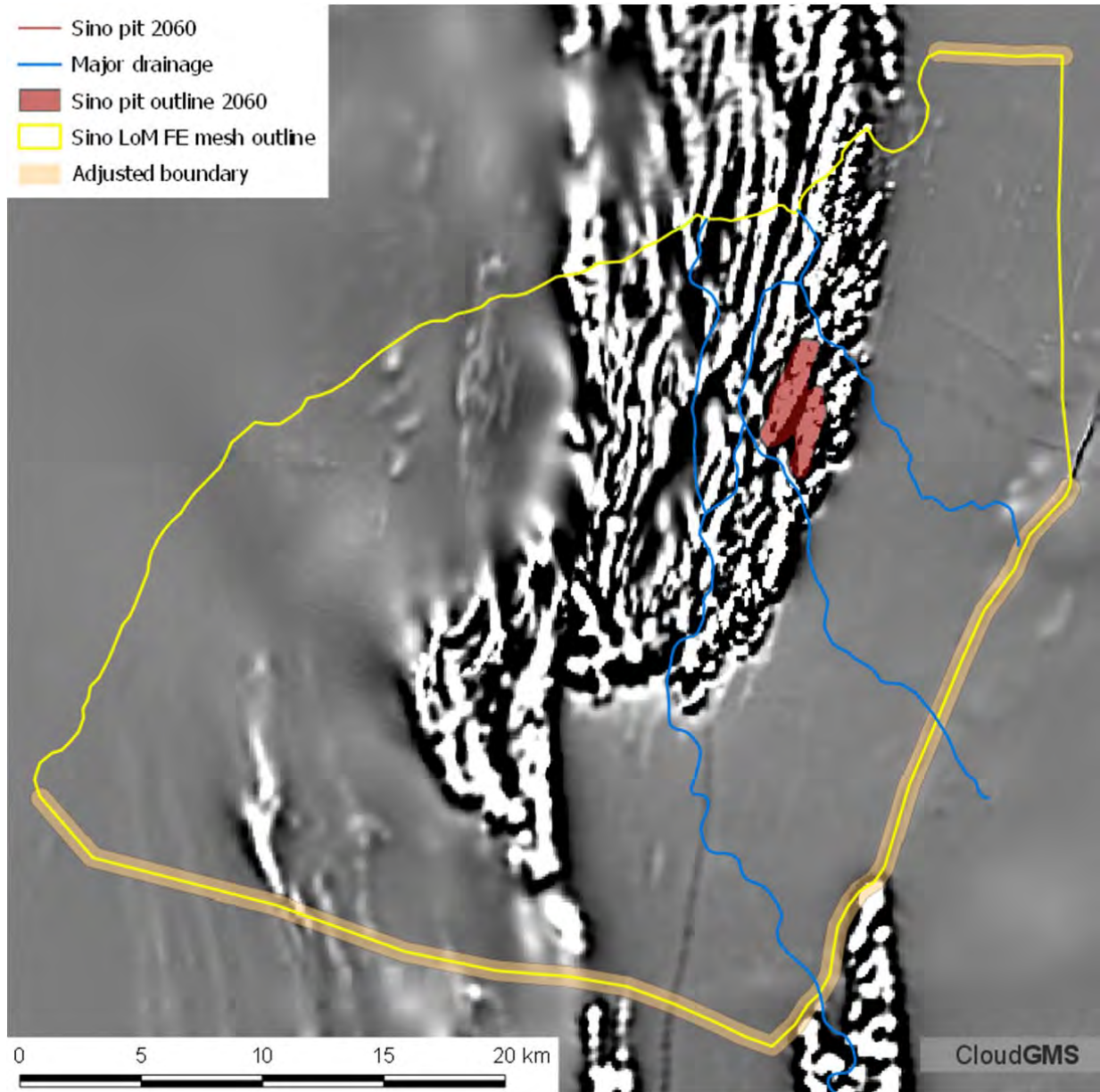


Figure 2-21 Regional aeromagnetics data processed to 1VD to accentuate short wavelength features such as geological contacts and structures.

The magnetics data (along with geological mapping) indicates a series of parallel, westerly dipping faults has disrupted the Hamersley Group succession, which have resulted in the partial loss, repetition or absence of several major geological units and in some areas have juxtaposed the BIF units against themselves to give unusually wide areas of outcrop. The aeromagnetic data indicate that the faults gradually change strike, trending increasingly northwestward to the north (offshore), and south-southwestward to the south.

Large scale anisotropy is likely aligned with the strike of the units.

Along with geological mapping the regional geophysics provides evidence to support changes to the south eastern and southern boundaries of the groundwater model, which have been highlighted above in Figure 2-21.

2.11 Groundwater dependent ecosystems

Descriptions of local and regional flora and fauna for the lower Fortescue River are discussed by Loomes (2010). The document provides an assessment of the ecological values, the ecosystems dependent on the shallow alluvial aquifer, the conceptual links between the pools and groundwater and possible impacts due to development.

Three types of ecosystems were identified as possibly being dependent on the shallow alluvial aquifer of the lower Fortescue River (Loomes, 2010);

- river pools – aquatic and emergent macrophytes, phytoplankton, fish, macroinvertebrates and terrestrial vertebrate fauna
- riparian vegetation – phreatophytic vegetation and dependent terrestrial fauna
- aquifer ecosystems – stygofauna.

2.11.1 River pools

Permanent or near permanent (freshwater) pools occur within the lower Fortescue River project area where the river channel intersects the water table.

Pool permanency was characterised by analyses of satellite imagery (Department of Water, 2009). Permanency was assessed based on pool occurrence across seven sets of Landsat imagery spanning 1999 to 2007. Pools were defined as permanent if they were present across all image sets; semi-permanent if present in 60 – 99% of image sets and intermittent if present in <60% of image sets.

The Department of Water has identified two permanent pools (Mungajee and Tom Bull), five semi-permanent pools (Bilano, Stewart, Churdo, Jilan Jilan and one unnamed) and two unnamed intermittent pools in the project area (Figure 2-5). Although Tom Bull Pool has been identified as being permanent its permanence may be due to its proximity to the river mouth and possible inundation by spring tides and therefore, Tom Bull Pool is likely to be brackish. The permanency rating of Mungajee Pool is also questionable (Morgan et al 2009).

Loomes (2010) provided conceptual models for the connections between groundwater and the various pools in the area, however, limited information exists to verify their dependence on groundwater. Broadly speaking the pool / groundwater interaction processes are summarised as:

- The Fortescue River and its pools are connected to and interact with the underlying alluvial aquifer.
- The direction of interaction changes seasonally in response to flooding, evaporation from pools or transpiration by riparian vegetation. The permanence of the interaction is determined by the level of the groundwater in relation to the base height of the pool.
- When the river is in flood there is connectivity between pools, the floodplains and the riparian zone. During river flow events groundwater is recharged from the surface water and the watertable rises.

AVAILABLE DATA

- During periods of no flow the hydraulic gradient between the groundwater and the pools reverses and groundwater discharges into the pools. Intermittent pools begin to dry out as the watertable drops below the base height of the pool and the groundwater becomes disconnected.
- Drought conditions and declining groundwater levels result in shallower pool depths and semi-permanent pools disconnecting from the groundwater. This greatly reduces the area of available aquatic habitat. Permanent pools have demonstrated long-term connectivity to the groundwater and are expected to be maintained by groundwater discharge during these drought periods. Because of this, these pools provide critical habitat and are an important refuge for native flora and fauna.
- Bilanoo and Mungajee pools provide habitat for all fish taxa known from the Fortescue River catchment, including previously unidentified species and taxa with restricted distribution (Morgan et al. 2009). As the Fortescue River has the highest diversity of freshwater fish taxa of all Pilbara rivers including those requiring deep, permanent pools (Morgan et al. 2009), it is likely that these two pools have high habitat value and are highly sensitive to groundwater decline (Loomes, 2010).

Given that the identified permanent and semi-permanent pools are primarily reliant on groundwater for their persistence, the changes to groundwater levels are used as a metric to determine the impacts (if any) during the life of the mine and post closure.

The closest permanent pool in the Fortescue River is Tom Bull Pool located approximately 2000 m west of the mine leases and this is tidal. Tidal influence extends up the River to at least the western boundary of the central mine lease (M 08/124). The next closest ephemeral to semi-permanent river pool is Mungajee Pool (Morgan et al, 2009), approximately 3.2 km southwest of the mine lease area, which does not appear to be tidal.

There are no non-tidal permanent surface water pools in Du Boulay Creek or the Fortescue River in the vicinity of the mining leases, and pools in the river upstream of the tidal influence are ephemeral to semi-permanent. This is supported by interpretation of geological section and hydrograph data given in Commander (1994), which shows watertable elevations below the base of the current bed of the Fortescue River over the bulk of the Fortescue River floodplain except for short periods after major recharge events.

2.11.2 Groundwater dependent vegetation

Groundwater dependent vegetation within the project area can be broadly divided into two groups (Phreatophytic and Vadophytic) depending on the degree of dependence on groundwater availability.

Phreatophytic vegetation is that which relies directly on the groundwater table for water uptake. Phreatophytes can respond to significant and/or rapid groundwater drawdown by a decline in health and eventual death.

Vadophytic vegetation primarily sources water from the vadose or unsaturated zone above the water table. While the vadose zone has a close association with groundwater through capillary action, it can also be supported by the downward infiltration of rainfall and river recharge.

Vegetation mapping has been undertaken by Maunsell (2007) as part of the Environmental Impact Assessment for the Balmoral South Iron Ore Project and is limited to existing tenements. Three species commonly associated with groundwater have been identified in the Project Area; *M. argentea* (Cadjeput), *E. camaldulensis* (River Red Gum), and *E. victrix* (Coolibah) (Maunsell, 2007). Of these three, Cadjeput is the only true, or obligate, phreatophyte. River Red Gum and Coolibah are classified as vadophytes, while River Red Gum is often a facultative (opportunistic) phreatophyte. However, in semi-arid environments it is often river flooding which enables the River Red Gum to survive (CSIRO Website).

AVAILABLE DATA

These three tree species are considered key indicator species for ecosystems dependent on groundwater within the Project Area. These species are also the dominant over-storey species of the riparian zone within the Project Area and are therefore of ecological significance on a local scale. Based on Maunsell's (2007) report, groundwater associated vegetation has been categorised into three groups (high, moderate and low) depending on vegetation type and dependence on groundwater.

High Groundwater Dependence

The only true or obligate phreatophyte mapped within the project area is *Melaleuca argentea* (Cadjeput). This species is restricted to creek lines and is referred to as an obligate phreatophyte. Only one isolated stand of Cadjeput is reported and occurs on Du Boulay Creek. Maunsell suggest that drawdowns in excess of 1m are likely to result in degradation to Cadjeput.

Moderate Groundwater Dependence

This group is typified by scattered riverine trees and Woodlands to Open Woodlands of *E. camaldulensis* (River Red Gum) and *E. victrix* (Coolibah). River Red Gums are typically described as a tree that is periodically dependent on groundwater during phases of their life (i.e. facultative phreatophyte). Coolibah is classified as a vadophyte. This vegetation community is predominantly associated with the main drainage channels. Maunsell suggest that drawdowns in excess of 5m may result in degradation, however, evidence also suggests that, if the rate of water level decline is slow enough, the tolerance to water level decline can be greater. Seasonal water level fluctuations in excess of 6m have been reported in the vicinity of the Fortescue River (Commander, 1993) where stands of River Red Gum and Coolibah are prevalent. GDV is likely to be sustained by soil moisture and groundwater within alluvial aquifers.

Recent work in similar climatic and physical conditions (Pfausch, et al., 2014) have shown how anthropogenic modification of water tables can affect water use of eucalypts (*E. victrix*) that dominate these zones, and that the effects of falling groundwater on facultative phreatophytes requires both consideration of rates of drawdown and antecedent groundwater levels. For example, trees accessing shallow groundwater may be more sensitive to drawdown compared with trees growing above groundwater at greater depth. The net result is a range in dependence on groundwater by trees across a landscape and variable responses to water availability. Water use of phreatophytes is intimately linked to soil water availability. Under conditions where tree water use (transpiration) generates increasingly negative water potentials inside the plant, signals from roots and/or the atmosphere serve to reduce stomatal conductance (gs), effectively reducing water loss. Trees can limit water losses by abscission of foliage, and for eucalypts, abscission of foliage has long been linked to acute water shortages at the end of summer.

The researchers demonstrate a remarkable capacity of *E. victrix* to sustain a significant short-term decline in depth to groundwater and suggest repeated (even if intermittent) monitoring of selected parameters like tree water use will be required.

Low Groundwater Dependence

This group comprises open woodland to scattered trees of *E. victrix* (Coolibah) and is associated with smaller drainage channels and the inter channel floodplains of larger drainage channels.

Trees in this area are often shorter in stature to those in the moderate areas suggesting decreased reliance on groundwater. Little information is available as to the tolerances of Coolibahs to changes in groundwater levels. While a gradual decline of the watertable would probably not affect Coolibahs, the effects of a long-term decline in the groundwater level would depend on the adaptive ability of individuals and their dependence on the vadose zone moisture (Maunsell, 2007). Areas in the central portion of Figure 2-22 designated as having no dependence are identified as being dominated by Mesquite, so although there may be some dependence there is little conservation value.

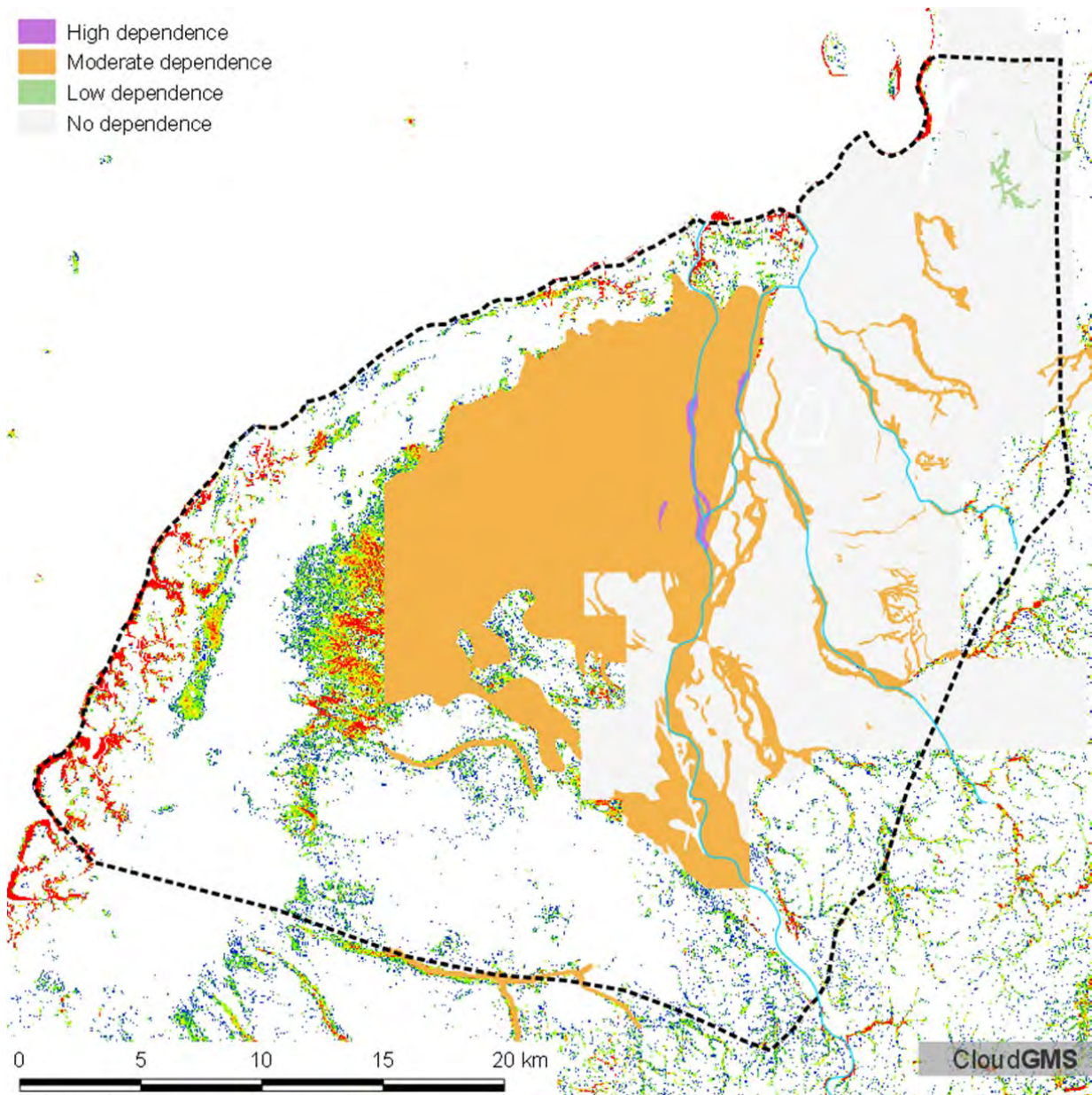
AVAILABLE DATA

Figure 2-22 Mapped groundwater dependence of vegetation within the project area. Areas in the central portion designated as having no dependence are identified as being dominated by Mesquite.

2.11.3 Mesquite mapping

Mesquite is an invasive weed and has colonised large areas of the lower Fortescue River floodplain. Anderson et al, (2004) presented mapping of the mesquite across the floodplain.

2.11.4 Leaf Area Index (LAI)

Where fresh groundwater discharges to the surface, the constant availability of water sustains plant photosynthetic activity longer in summer in that area (Tweed, et al., 2007). Areas where shallow saline groundwater is close to, or discharges to the surface, are also evident from the limited vegetation activity. Soil subject to saline groundwater accumulates salts, thus limiting photosynthetic activity of salt sensitive

AVAILABLE DATA

vegetation throughout the entire year whilst supporting photosynthetic activity of salt-tolerant vegetation (Tweed, et al., 2007).

Areas of vegetation that use groundwater typically exhibit low seasonal variability of photosynthetic activity. The inter-annual variability of the vegetation activity can also contain useful information to assist mapping of groundwater discharge areas (Tweed, et al., 2007).

Vegetation that is relatively lush in comparison to surrounding areas is often associated with discharge areas. Leaf area index (LAI) is often used as an indicator to identify this type of vegetation. LAI is defined as the one sided green leaf area per unit ground area in broadleaf canopies. LAI is, therefore considered a strong indicator of water availability in semi-arid to arid environments (Hatton & Evans, 1998) and can be used as a proxy for vegetation water use.

Total LAI was estimated using the product MOD15A2 centred on the project area (201 km wide × 201 km length) from the MODIS 163 Land Product Subsets project (<http://daac.ornl.gov/MODIS/>).

ORNL DAAC. 2008. MODIS Collection 5 Land Products Global Subsetting and Visualization Tool. ORNL DAAC, Oak Ridge, Tennessee, USA. Accessed September 05, 2016. Subset obtained for MOD15A2 product at 21.15S,134.3E, time period: 2000-02-18 to 2016-09-05, and subset size: 201 x 201 km. <http://dx.doi.org/10.3334/ORNLDAAC/1241>

Leaf area index (LAI) from the MOD15A2 images for April 2006 and November 2007 and are presented below in Figure 2-23 a) and b) respectively. The areas where LAI is greater than 0.4 in the 2007 image, are consistent with areas identified in the vegetation mapping as being highly groundwater dependent.

The high LAI (>0.8) evident in Figure 2-23a is related to the growth of annual grasses in the understorey as a result of rainfall. The areas where LAI is 0 (red cells) reflect the presence of highly saline conditions along the coast where very limited vegetation communities can exist.

LAI of greater than 0.4 covers an area of approximately 17 km². The areas where LAI are between 0.2-0.4 are consistent with areas mapped as sparse mesquite by Anderson et al, (2004).

The LAI for the dry period (Nov 2007) is used to determine the zonation of ET fluxes in the areal recharge / discharge parameter expression (refer to section 4.9.1).

AVAILABLE DATA

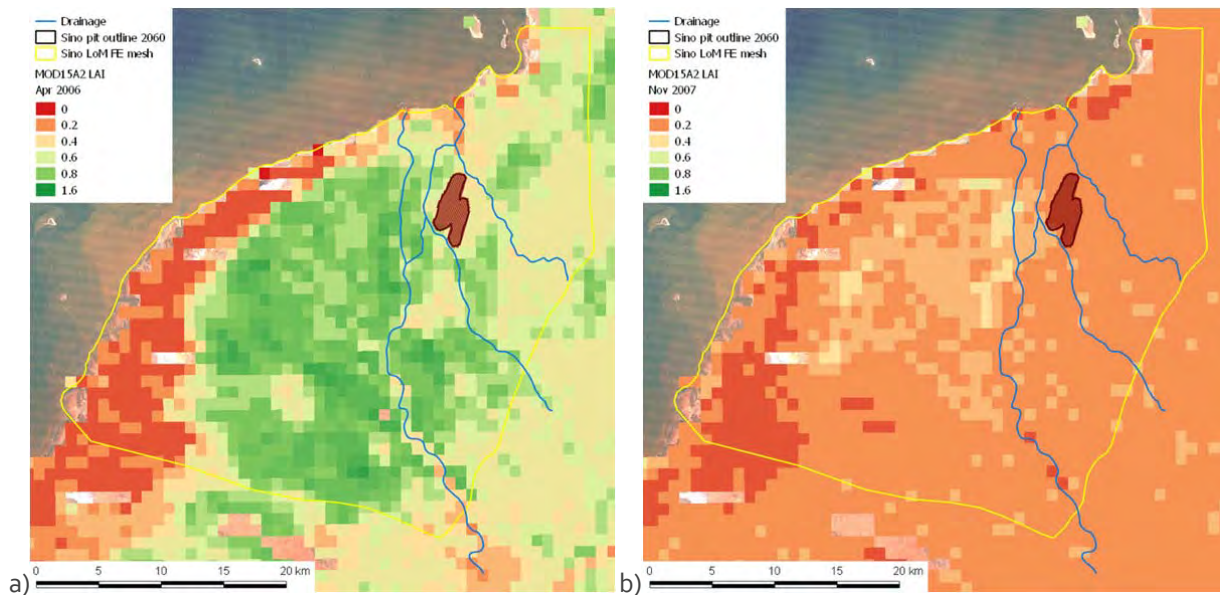


Figure 2-23 Comparison of MODIS images demonstrating the variation in LAI between wet and dry periods a) LAI April 2006 and b) LAI for Nov 2007. The persistence of LAI > 0.4 suggests areas where vegetation is persisting and accessing groundwater.

2.11.5 Subterranean fauna

With any drawdown in water levels there is the potential for localised impact on stygofauna through the potential loss of habitat due to groundwater level decline in both the basement rock aquifers and in the local creek alluvium.

Stygofauna surveys undertaken to date (Maunsel, 2007) indicate that all taxa identified have wider distributions (Halse et al. in prep.) and it is unlikely that the cumulative impact of developing the Sino Expansion will have a significant adverse effect on stygofauna conservation (Aquaterra, 2009).

2.11.6 Groundwater dependent vegetation (GDV) monitoring sites

Site specific groundwater dependent monitoring sites are presented as part of the Groundwater Dependent Vegetation Monitoring Plan (Astron, 2015). These sites are presented below in Table 2 and in Figure 2-24.

The sites listed in Table 2 will be used to assess the impacts of the mine on the GDV and the modelling results compared to the trigger values currently employed.

In term of groundwater dependent vegetation, currently site 13 is the only monitoring site that supports *M. argentea*, which as identified above in section 2.11.2 is an obligate phreatophyte (ie it is totally groundwater dependant). This site is also heavily utilised as a watering point by cattle.

AVAILABLE DATA

Table 2 Groundwater dependent vegetation (GDV) monitoring sites identified by Astron (2015).

Zone	Active	Astron site	Monitoring bores	Catchment
Reference	Current	8	FCP23A	Fortescue River
	Current	-	FCP10A	Fortescue River
1	Current	13	09AC489, 09AC490, 09AC534, 09AC537, 09AC539	Du Boulay Creek
	From 2018	5	07RC156, 09AC546, 09AC547	Du Boulay Creek
2	Current	2	07RC149, 07RC150	Du Boulay Creek
	Current	6	07RC151, 13DD732	Du Boulay Creek

FCP23A trigger = 4.20 mAHD

Zone 1 trigger = 2 standard deviations below baseline mean

Zone 2 trigger = 3 standard deviations below baseline mean

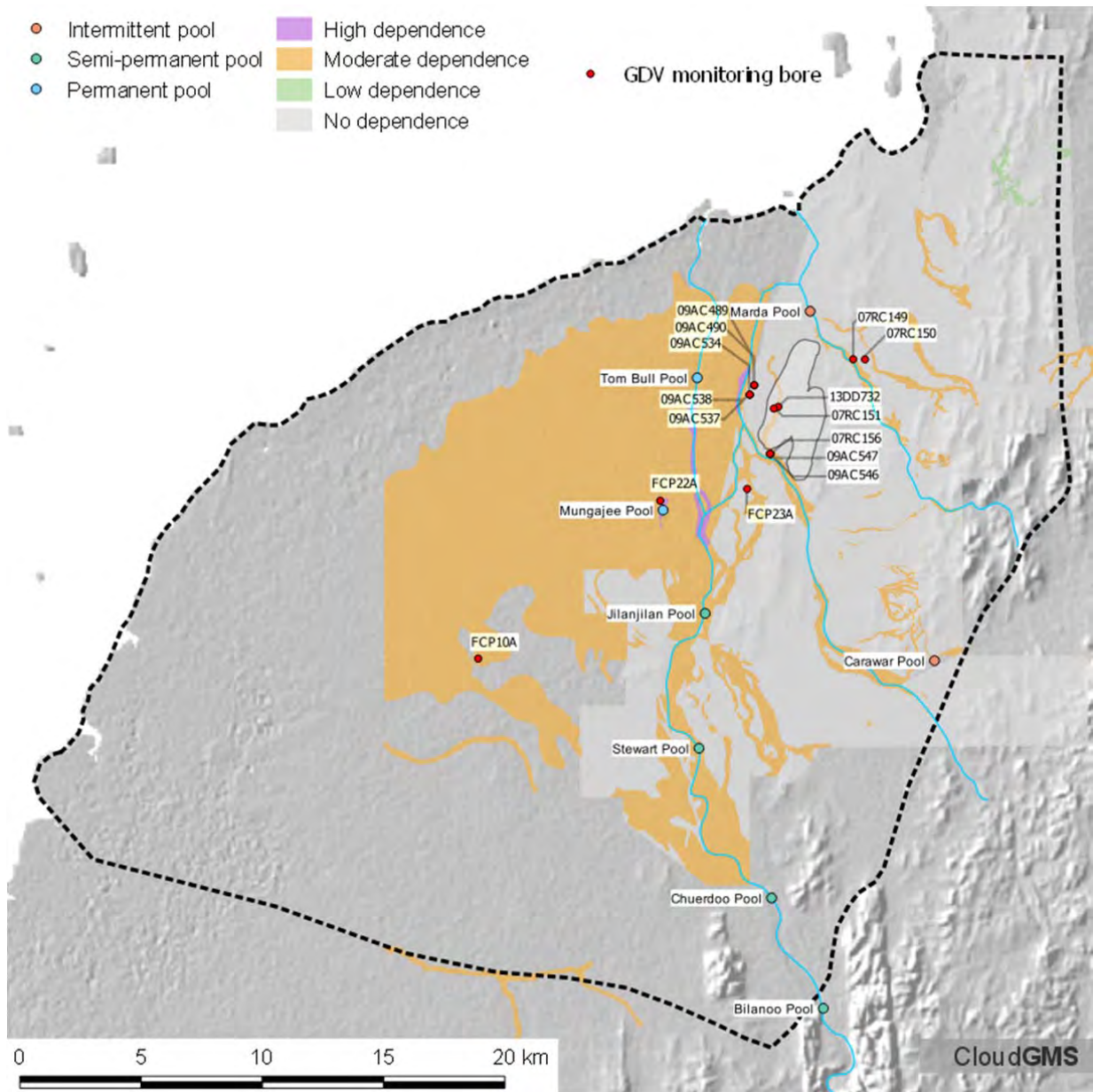


Figure 2-24 Locations of groundwater dependent vegetation monitoring bore sites identified by Astron (2015).

3 Hydrogeological conceptualisation

3.1 Regional Geology

The project area is located along the western edge of the Hamersley Province. The Hamersley Province of the Pilbara region in the north-west of Western Australia is one of the major iron ore provinces in the world. The 2.4 billion year old Hamersley Group outcrops over an area approximately 400km long East-West and 200km long North-South and contains a number of world class iron ore deposits.

The eastern part of the project area is characterised by two series of north-north-easterly trending ridges (refer to Figure 2-2) of outcropping Lower Proterozoic aged rocks of the Mount Bruce Supergroup, which are part of the Hamersley Basin. These rocks dip steeply to the west northwest and become younger from east to west. The sequence is however impacted by faulting resulting in some repetition or absence of the units within the stratigraphic sequence.

The average strike direction of the units is around 15° north-northeast. The eastern most and highest set of ridges consist of steeply west north-westerly dipping basalts and volcanic tuffs of the Kylenea and Maddina Volcanic units.

The western series of ridges identified in the Balmoral area are made up of banded iron formation (BIF), chert and shale of the Brockman Iron Formation and to a lesser extent the Mt McRae Shale/Mount Sylvia Formations. The sequence dips at approximately 45° to the west northwest and strikes north north-easterly.

The Balmoral area is divided into three deposits of high-grade magnetite, the North (MLs 08/118-122), Central (George Palmer, MLs 08/123-125) and South (Susan Palmer, MLs 08/126-130) blocks, based on areas of outcrop separated by substantial creek drainages. The central deposit is the George Palmer deposit, and is the focus of the Sino Iron Project being developed by CITIC Pacific.

To the west of the Fortescue River floodplain are the Late Devonian to Cretaceous aged Winning Group of the Carnarvon Basin.

The Winning Group onlaps the western edge of the Hamersley Basin. The sediments overlie Proterozoic basement rocks of the Peedamullah Shelf, which runs along the Onslow coast and extends inland for up to 60 km. The sedimentary sequence is mostly less than 500 m thick and less than 90m thickness in the project area, but increases to 700 m to the south-west.

The Winning Group comprises a basal coarse-grained section of the Yarraloola Conglomerate, overlain by finer-grained sediments dominated by shale. The Yarraloola Conglomerate is often referred to as the basal Cretaceous sand and conglomerate and consists of rounded gravels, varying from very well cemented to loose, with minor sands and clays. It is interpreted to occupy buried channels where the major drainages enter the coastal plain. The units directly over lie on the Proterozoic basement rock.

Unconformably overlying the Carnarvon Basin sediments is a relatively thin (<40m thick) veneer of Cainozoic superficial sediments, consisting of the Tertiary-aged Trealla Limestone that consists of clays, marl and crystalline limestone and the Quaternary aged Fortescue River alluvial and associated detrital scree deposits that have formed scree fans extending from the outcropping Proterozoic bedrock.

The Fortescue River is considered to have eroded and carved paleochannel(s), possibly along the edge of the contact between the Hamersley Basin sequence and the younger Carnarvon Basin sedimentary sequence that overlies granitic Achaean basement. The paleochannel(s) has been progressively backfilled.

SINO EXPANSION LIFE OF MINE GROUNDWATER MODEL
HYDROGEOLOGICAL CONCEPTUALISATION

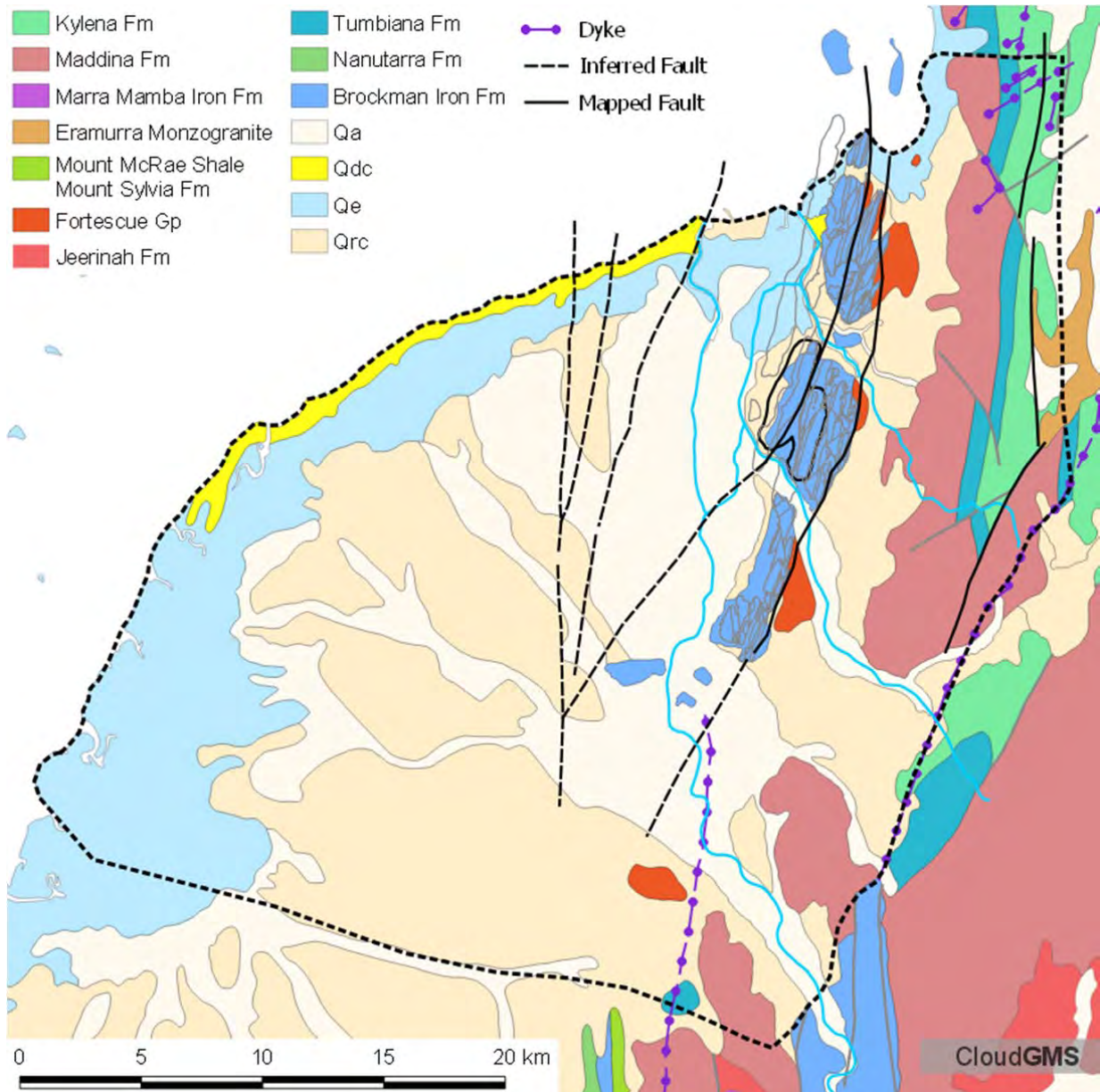


Figure 3-1 Regional surface geology of the project area (modified from Geoscience Australia). Structural features modified from (Hickman & Strong, 2003)

Descriptions of the units in the project area are detailed in the following sections.

3.1.1 Lower Proterozoic

The geological section presented above in Figure 2-20 indicates the stratigraphic relationships of the Lower Proterozoic rocks in the vicinity of the mine. The majority of the resource is located within the Joffre Member, with the footwall unit of the mining operations to be developed along the contact with the underlying Whaleback Shale Member. Underlying the Whaleback Shale is the Dales Gorge Member that in turns overlies the Mount McRae Shale and Mount Sylvia Formations to the east. To the west of the Joffre Member is a sequence of the Yandicoogina Shale Member, overlain by banded iron formations of the Weeli Wolli Formation.

The magnetite BIF is oxidised at surface, with the replacement of magnetite by hematite and/or goethite accompanied by a loss of magnetism. Oxidation typically penetrates to a depth of 40-50m and has enhanced the hydraulic conductivity of this area of the formation compared to the fresh rock below.

The McRae Shale consists of mudstone, siltstone, chert, iron-formation, and dolomite. Thin bands of shard-bearing volcanic ash in upper parts.

The Brockman Iron Formation consists of 4 members:

- Joffre member (J1-J6 ~300m true thickness) comprise well-banded BIF made up of chert and iron oxides.
- Whaleback Shale member (WS1-WS2 ~60m thick) comprises thin bands of iron formation rocks with significant sheet-silicate content causing a shaly appearance.
- Dales Gorge member (D1-D4 ~150m thick) is predominantly well-banded iron formation made up almost entirely of chert and iron oxides. Includes ferruginous volcanic tuffs, 2-3m thick with 10-20cm of potassium feldspar/stilpnomelane spherules.
- Yandicoogina Shale member (YS ~60m thick) (including breccia) comprises alternating chert and thin shale, and regionally it is intruded by dolerite sills.

The Weeli Wolli Formation (WW1-WW4 ~600m thick) overlies the Brockman Iron Formation and are comprised of banded iron-formation (commonly jaspilitic), mudstone, siltstone; common interlayered metadoleritic sills.

3.1.2 Cretaceous aged sediments

The Early Cretaceous Yarraloola Conglomerate unconformably overlies and infills incised valleys in the Precambrian basement. It crops out in places adjacent to the Precambrian bedrock along outliers located north of the Balmoral Homestead. It was intersected in three wells during the GSWA exploration program (Commander, 1993) and consists of angular to rounded pebble gravel (mainly derived from Mount Bruce Supergroup) with minor beds of sand and clay formed as stream deposits in a fluvial environment.

Further to the west the Early Cretaceous Muderong Shale unconformably overlies the Precambrian basement and comprises grey-green siltstone with a basal greensand (Mardie Greensand Member). As the groundwater exploration bores were generally stopped in the Trealla Limestone, the Muderong Shale was only intersected in the petroleum exploration bores at depths of 74 m (Coonga 1) and 93 m (Mardie West 1).

3.1.3 Tertiary aged sediments

The Middle Miocene Trealla Limestone unconformably overlies the Yarraloola Conglomerate or Muderong Shale. It consists of interbedded clay, marl and fine grained limestone, and typically forms the lower confining beds of the lower Fortescue River alluvial sequence.

The Middle Eocene Robe Pisolite (also known as Channel Iron Deposits) consists of pisolitic, oolitic and massive limonite, minor terrigenous siliciclastic material, goethite and hematite deposits; developed along palaeodrainage lines; dissected by present day drainage. The Robe Pisolite has been identified in the drilling by Global Groundwater (2010) and is overlain by the Trealla Limestone where it is present. Where the Trealla Limestone is absent the Robe Pisolite separates the alluvial sediments from the Yarraloola Conglomerate.

3.1.4 Quaternary aged sediments

Quaternary alluvial deposits are up to 30 m thick and form part of an alluvial fan associated with the discharge of the Fortescue River onto the Ashburton plain. The alluvium is deposited on the pre-existing erosional surface and unconformably overlies Precambrian, Cretaceous and Tertiary rocks. The present surface is dominated by clayey over-bank deposits with gravel beds in drainage channels and in subsurface paleochannels. The gravel consists of rounded pebbles up to 100 mm in diameter of basalt, chert, tuff, jaspilite and minor quartz, derived from the surrounding Precambrian basement. These are partially cemented adjacent to semi-permanent river pools. Over-bank deposits comprise dense red to yellow ferruginous clays and pink to white silty and sandy clays. The gravel deposits thin outwards from the main drainage channels into predominantly clayey sequences that are locally ferruginous and silicified. Calcrete is locally formed in a close zone of watertable fluctuation, typically at depths between 4 and 12 m below the surface (Haig, 2009).

3.2 Regional structure

Hickman & Strong, (1998) present evidence of thrusting of the Brockman Iron Formation over the Jeerinah Formation to the east and suggest that they are separated by an exposure gap of 10 to 20 m. Across this gap the Mount McRae Shale, and Mount Sylvia, Wittenoom, and Marra Mamba Iron Formations, with a continual stratigraphic thickness of 480 m, have been tectonically removed. The strike and inclination of bedding in the Brockman Iron Formation are structurally discordant to the strike and inclination in beds of the adjacent Jeerinah Formation, indicating faulted contacts.

Faulting plays an essential role for the interpretation of the geology of the area. Major faulting exists between the western and eastern ridges that trends parallel to the regional strike. These major faults coupled with smaller en echelon faults, have resulted in the partial loss, repetition or absence of several major geological units. Faulting is quite extensive on the western side of the deposit with multiple repetitions of the Joffre member. Extension of the BIF to the South is limited by a thrust fault that terminates the sequence. Dolerite dykes have intruded along many of these sheared zones.

The Balmoral deposits are dissected by a series of faults, with two dominant sets trending NNW-SSE or NE-SW, which in some areas juxtapose the BIF units against themselves to give unusually wide areas of outcrop. Thin dolerite dykes, generally less than 5m but occasionally up to 30m thick, intrude along or parallel to the faults. Initially the faults and dykes were considered to dip steeply to the west, though more recent work suggests that they dip moderately to the east or south-east as indicated previously in the block model (refer to Figure 2-20).

Large scale folds have not been observed in the Balmoral area. Dolerite intrusions are common throughout the Hamersley Basin. They are generally post-tectonic in emplacement history and form linear dykes or sills. In the Hamersley ranges as a whole the dolerite dykes are common in competent rocks, such as the chert and banded iron lithologies. The Balmoral area is no exception to this rule with numerous thin dolerite dykes, although dolerite sills have not been identified in any of the drill holes.

The major dyke directions in the Balmoral Area are NNE and NE.

Dolerite dykes do not represent a significant volume at Balmoral, however, they do lead to a reduction in the quality of and quantity of proximal magnetite ore due to:

- Regionally, dolerite dykes have been found to host aquifers, although within the vicinity of the Sino pit they do not appear to represent significant aquifers. They alter quickly and are a source of wall rock alteration and thus result in deeper oxidation of the host rock.

- Large dykes have caused contact metamorphic reactions, resulting in an increase in the magnetic weight recovery and silica in concentrate in areas proximal to the dykes.

3.3 Hydrogeology

The project area comprises two groundwater systems:

- A shallow groundwater system with relatively high permeability and storage characteristics; and
- A deeper groundwater with low permeability and storage characteristics.

The major aquifer of the area is the Lower Fortescue River alluvial sediments, the underlying Yarraloola Conglomerate is a less significant aquifer and appears to have limited storage and recharge (Haig, 2009).

3.3.1 Superficial groundwater system

The superficial groundwater system comprises the following units:

- Alluvial gravels;
- Trealla Limestone and Robe Pisolite; and
- Yarraloola Conglomerate

The lower Fortescue River alluvial aquifer extends over the alluvial fan deposit to the west of the present-day Fortescue River. It is defined by highly transmissive gravel beds deposited through the central area of the alluvial fan with a saturated thickness up to 15 m and an aerial extent of approximately 200 km². The extent and thickness of the saturated gravel aquifer is presented below in Figure 3-2. The aquifer grades laterally into much lower transmissivity clay and silt deposits of the floodplain to the south.

It is believed that the alluvial layer is an extensive and unified aquifer with measured hydraulic conductivity in the range of 63-190 m/day (Commander, 1993). This aquifer receives rainfall recharge and river recharge from the Fortescue River, and ultimately discharges into the sea.

The lower clay layer and underlying Trealla Limestone provide an aquitard between the alluvial aquifer and the Yarraloola Conglomerate aquifer.

In general, the Yarraloola Conglomerate fills erosional features in the Precambrian basement rock. The distribution is incompletely known and appears to be confined to narrow channels in the erosional surface of the underlying Proterozoic rocks. At the lower Fortescue River, the Yarraloola Conglomerate aquifer is confined by up to 30 m of Trealla Limestone, although this is much thinner along the margins of the basin.

The average thickness of the Yarraloola Conglomerate aquifer is estimated to be 40 metres, thinning towards the flank of the basin. The rate of water exchange between this aquifer and the alluvial aquifer is largely determined by the thickness of the aquitard between them, which has an average thickness of 17 m.

SINO EXPANSION LIFE OF MINE GROUNDWATER MODEL
HYDROGEOLOGICAL CONCEPTUALISATION

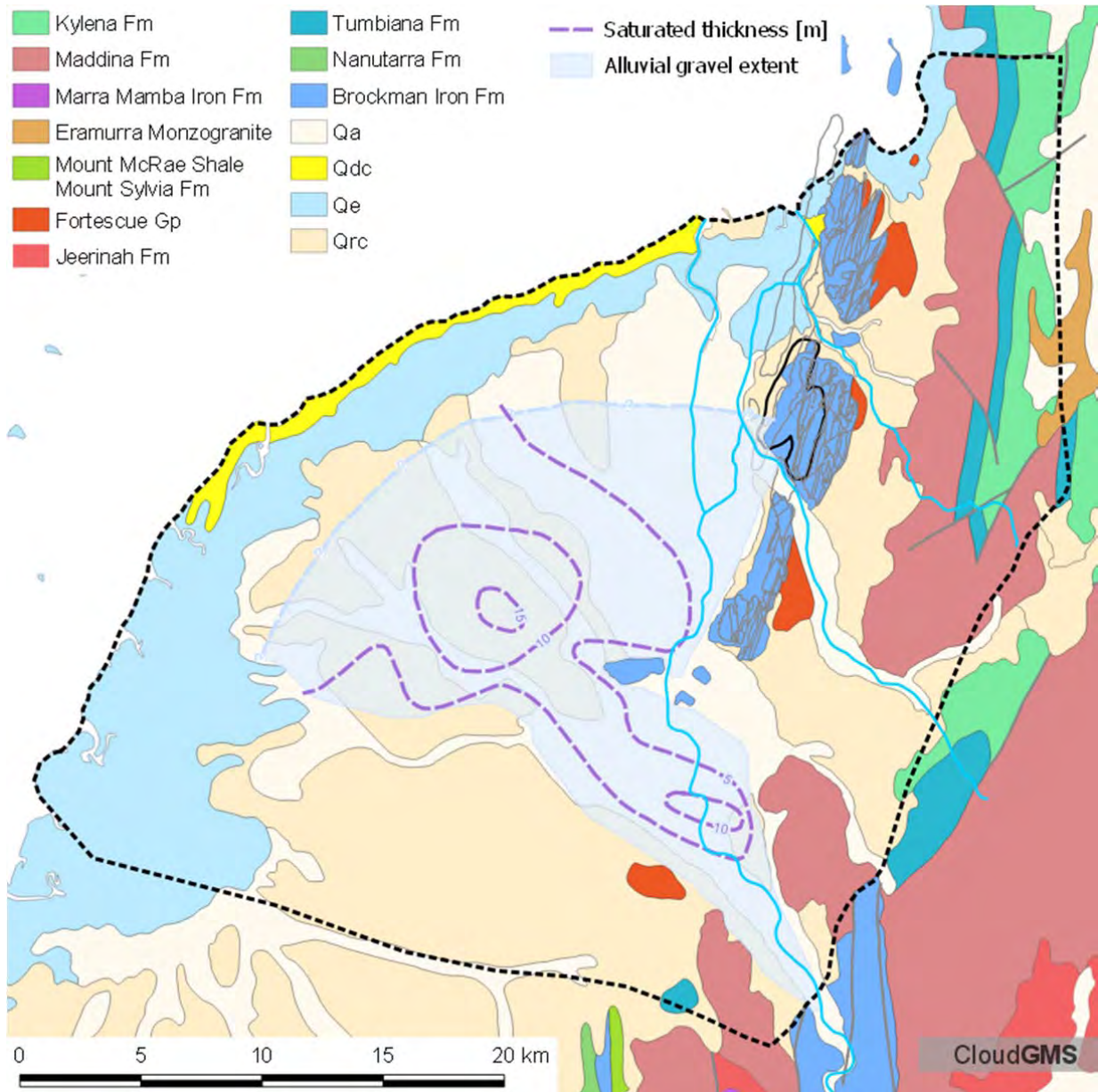


Figure 3-2 Extent of alluvial gravels and saturated thickness (after Commander (1993))

3.3.2 Basement groundwater system

The weathered layer of the Hamersley Group stores groundwater, but have only limited recharge through fractures exposed at the land surface.

The eastern most and highest ridge consist of steeply west north-westerly dipping basalts and volcanic tuffs of the Kylena and Maddina Volcanic units of the Fortescue Group. These units have been interpreted to play no active role in the hydrogeology of the proposed mining area (MWH, 2010b).

3.3.3 Structural features

Several faults have been mapped in the vicinity of the pit. The locations of these features are presented below in Figure 3-3.

Although there are several mapped faults, to date only one feature NE Fault-1 appears to be hydrogeologically significant. The NE Fault-1 extends through the north western portion of the current East Pit. The recent discharge from the dewatering sumps within the pit has been considerably more (particularly at Sump07) than would be expected based on the expected hydraulic properties of either the weathered or fresh basement rocks. Examination of the geological block model indicates that the area is different to other areas intersected by the pit:

- There is a fault showing large vertical displacement;
- The footwall consists of Dales Gorge Member; and
- The hanging wall consists of the Yandicoogina Shale.

It is expected that secondary permeability has been developed in the Dales Gorge Member associated with the NE Fault-1. The presence of such a feature may explain the extended period of excess inflows and the highest flows from Sump05 and Sump07, both are located along the fault on the foot wall side.

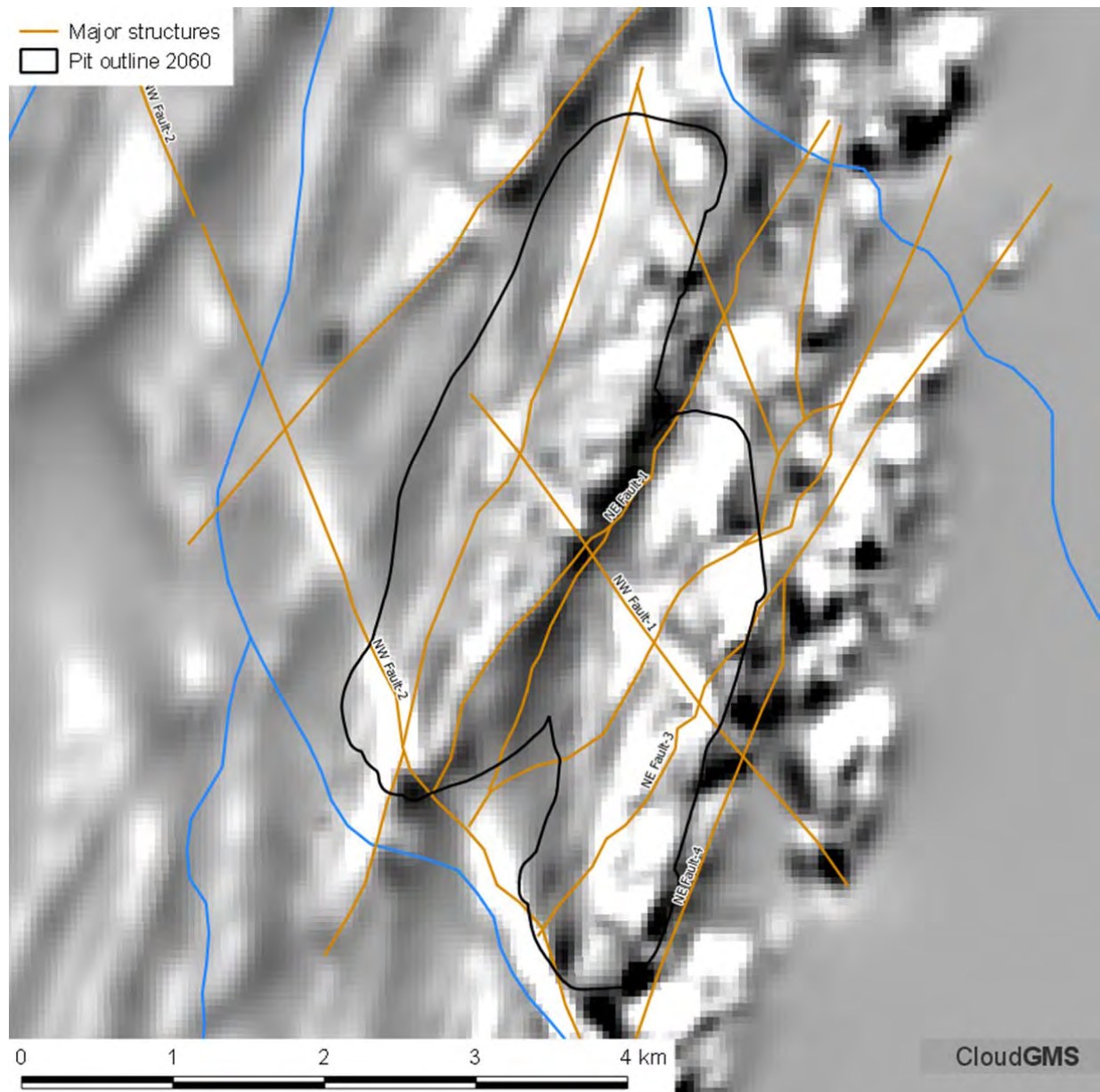


Figure 3-3 Location of major faults in the vicinity of the pit based on geological block model overlying 1VD aeromagnetics data.

3.4 Aquifer testing and hydraulic parameters

3.4.1 Superficial aquifers

The GSWA investigation of the lower Fortescue River alluvial aquifer step-rate tests, constant-rate pumping tests of eight hours duration were conducted on five bores (Commander, 1989). Limitations of pump and casing size resulted in relatively low discharge rates of 18 to 1063 kL/day (2.66 to 6.83 L/s), with drawdown in observation bores (20 m from pumping bore) less than 0.5 m.

Drawdown data from the GSWA testing was interpreted using delayed yield non-equilibrium type curves. Estimations of transmissivity ranged between 380 and 1760 m²/day in the alluvial aquifer.

Alluvium hydraulic parameters based on pumping tests at three bores in the alluvial aquifer as reported by Commander (1993) can be summarised as:

- Hydraulic conductivity of the alluvium ranged from 63 to 190 m/d.
- a specific yield of 0.3 from samples of river gravel, however a specific yield of 0.1 was assumed to be more representative of the alluvial sediments as the gravel has a proportion of clay in the matrix.

Aquaterra (2008) conducted pumping tests at three bores and calculated:

- Hydraulic conductivity in the range 8.5 to 194.3 m/day.

Alluvium hydraulic parameters close to the western margin of the proposed pit as reported by Global Groundwater, (2010) can be summarised as:

- Hydraulic conductivity of the alluvium ranged from 54 to 136 m/day and averaged 80 m/day, which compares favourably with values obtained from earlier test pumping reported by Commander (1989) and Aquaterra (2009).
- Hydraulic conductivity of the Yarraloola Conglomerate in the deeper production bores ranged from 2 to 39 m/day and averaged 12 m/day.
- The coefficient of storage it is expected that values in the order of 1×10^{-4} are probably representative of the Yarraloola Conglomerate aquifer. However, in terms of drainable porosity, the specific yield of these strata is likely to be similar to that of the alluvium.

Global Groundwater (2010) identified that the values are generally higher than those derived from earlier test pumping in the Yarraloola Conglomerate. They also identified that three of the four earlier tested bores were low to very low yielding with much greater drawdown than encountered in the bores constructed on Sino Iron's mining lease areas and therefore suggested that the difference is not anomalous.

It should also be noted that the hydraulic parameters determined by Global Groundwater (2009) for the Yarraloola Conglomerate are considerably greater than the values assumed in the vicinity of the pit in the MWH (2010) study.

3.4.2 Weathered basement

No estimates of the hydraulic parameters for the weathered basement rocks are available, however, previous modelling studies (MWH, 2010 and SWS, 2013) indicated hydraulic conductivity values ranging from 0.08 – 5.0 m/d in the vicinity of the pit and regionally of the order of 1 m/day and specific yield of between 0.01 and 0.1.

3.4.3 Unweathered basement

Estimates of the hydraulic parameters are presented below in Table 3. Each of the basement rock units are typically several orders of magnitude lower than the overlying weathered material and superficial sediments. The values come from the following two sources:

- The drainage test and subsequent analysis performed by SWS in 2013. This test targeted the confined fresh (unweathered) Brockman Iron Formation units, with a primary focus on the Whaleback Shale.
- Packer tests, falling head tests and geophysical analysis performed on several holes drilled in the eastern (or footwall) slope undertaken by SWS in 2011.

Table 3 Initial hydraulic conductivity ranges used in the current study based on previous studies.

Units	Kh / Kv [m/d]	Sy [%]	S [m ⁻¹]
Calibrated in previous studies			
Weathered zone – regional	1.0 / 0.1	10	1.00E-04
Weathered zone – northwest	2.0 / 0.2	10	1.00E-04
Weathered zone – northeast layer 1	5.0 / 0.5	10	1.00E-04
Weathered zone – northeast	0.75 / 0.075	10	1.00E-04
Weathered zone – central	0.08 / 0.008	10	1.00E-04
Weathered zone – NE Fault-1 zone	100.0 / 100.0	10	1.00E-04
Weathered zone – south and southeast	0.01 / 0.001	10	1.00E-04
<hr/>			
Alluvium – mine area	10.0 / 1.0	10	1.00E-04
Alluvium – central region	80.0 / 8.0	10	1.00E-04
Alluvium – south region	1.0 / 0.1	10	1.00E-04
Trealla limestone	0.01 / 0.001	1	1.00E-06
Yarraloola conglomerate	10.0 / 1.0	5	1.00E-04
Yandicoogina shale	0.0001 / 0.0001	1	1.00E-06
Mt Sylvia shale	0.0001 / 0.0001	1	1.00E-06
<hr/>			
Calibrated based on SWS (2013a) - injection test modelling			
Weeli Wolli formation / Yandicoogina shale	0.0003	1	1.00E-06
Joffre member	0.01	1	1.00E-06
Whaleback shale / Dales Gorge member	0.001	1	1.00E-07
Mt McRae shale	0.0001	1	1.00E-06

3.4.4 Anisotropy

The superficial sediments are expected to show some anisotropy, typically a ratio of Kh:Kv of 10:1 is assumed, and this has been adopted in this study.

The unweathered basement rocks are expected to be relatively isotropic due to the nature of the sediments and their diagenic history, an Kh:Kv anisotropy ratio of 1:1 is assumed, and has been adopted in this study.

3.5 Hydrostratigraphic units (HSUs)

In order simulate groundwater dynamics in the aquifer system and to predict the environmental impacts of future groundwater abstraction, it is necessary that the model includes the following geological formations:

1. Alluvial aquifer - the major source of potential water supply for the area;
2. Trealla Limestone - an aquitard between the alluvial aquifer and the Yarraloola Conglomerate aquifer;
3. Yarraloola Conglomerate;
4. Weathered Hamersley and Fortescue Groups - a minor aquifer in weathered bedrock where groundwater exists in fractures.
5. Fresh Hamersley Group and Fortescue Group rocks - tight and relatively impermeable.

HYDROGEOLOGICAL CONCEPTUALISATION

The alluvial sediments to the west of the mine site constitute the main aquifer in the region. They are **laterally significant and probably present the highest hydraulic conductivity of any sediment in the area.**

The Yarraloola Conglomerate may represent a significant aquifer, although it is thought to be poorly connected from the other aquifer system by the Trealla Limestone above and the Weeli Wollli Formation to the east, both of which are not expected to present high hydraulic conductivities.

The depth of weathering in the vicinity of the mine site was presented in section 2.9.2. and indicates significant weathering of the basement rocks occurs down to approximately 40 to 50 m below ground surface. The weathering enhances the hydraulic conductivity of this area of the formation compared to the fresh rock below, although the nature of weathering is expected to be spatially variable.

The geological units described in the previous section have been grouped into hydrostratigraphic units for incorporation in the groundwater model. The grouping is based primarily on similar hydraulic parameters.

Table 4 Hydrostratigraphic units

HSU	Geological units	Description
1	Cenozoic alluvial sediments	Alluvial aquifer – the major source of potential water supply for the area.
2	Alluvial sediments to the east of the outcropping Hamersley Group	Minor alluvial / colluvium aquifers where they exist below the groundwater table.
3	Cenozoic clay sediments to the south – southeast of the lower Fortescue alluvial sediments	Clay aquitard bounding the southeastern edge of the alluvial sediments.
4	Weathered Fortescue Group	Weathered Bedrock (Fortescue Group): - a minor aquifer in weathered bedrock where groundwater exists in fractures.
5	Weathered Hamersley Group	Weathered Bedrock (Hamersley Group): - a minor aquifer in weathered bedrock where groundwater exists in fractures.
6	Tertiary aged sediments	Trealla Limestone – an aquitard between the alluvial aquifer and the Yarraloola Conglomerate aquifer.
7	Cretaceous aged sediments lower.	Cretaceous aged Yarraloola Conglomerate: - aquifer of limited aerial extent.
8	Fresh Fortescue Group	Fresh Bedrock (Fortescue Group); - tight and relatively impermeable.
9	Joffre Member	Fresh Joffre member (Hamersley Group); - tight and relatively impermeable.
10	Whaleback Shale and Dales Gorge Member	Combined fresh Whaleback Shale and Dales Gorge members (Hamersley Group); - tight and relatively impermeable.
11	Weeli Wollli Formation and Yandicoogina Shale	Combined fresh Weeli Wollli Formation and Yandicoogina Shale (Hamersley Group); - tight and relatively impermeable.
12	McRae Shale	Fresh McRae Shale Formation (Hamersley Group); - tight and relatively impermeable.

3.6 Groundwater processes

3.6.1 Recharge processes

Fortescue River Alluvium

The Fortescue River is a major source of groundwater recharge for the alluvial aquifer and is considered very much greater than that due to direct recharge from the surface (Commander, 1993). Observed groundwater levels at monitoring bores show that the closer a monitoring bore is to the river, the larger the fluctuations in groundwater levels (Commander, 1993). Groundwater levels in bores close to the river rise rapidly when

river flows and decline soon after the river ceases to flow, and fluctuate as much as 6 m. The volume of recharge is controlled by the duration of flow, frequency of flow, depth of flow and the available storage of the aquifer (Haig, 2009).

Previous modelling used the entire discharge record as a constraint on the transfer boundary conditions used to represent recharge from the Fortescue River. Although this would result in recharge as per the above mentioned mechanism, this produced many events that were not evident in the groundwater level hydrographs.

Previous experience studying recharge from ephemeral drainage in arid environments indicates that flows within the main channel of a river may only provide limited recharge and that recharge is more likely during overbank flow periods. A threshold in discharge is therefore required before overbank flows are generated and recharge occurs. In the case of the Fortescue River this mechanism appears to be taking place as the groundwater level hydrographs do not respond to all flow events, even where the observation bore is in close proximity to the river (ie FCP18A).

Proterozoic Basement Rocks

Some direct rainfall recharge may also occur in the area of outcropping weathered Hamersley Group through fractures exposed to the land surface.

These basement aquifers are recharged by the infiltration of rainfall and local runoff in areas of outcrop and via leakage from overlying residual soils and sediments in areas of subcrop. The aquifers discharge by baseflow to local drainages and by throughflow to the Fortescue River alluvium and coastal sediments.

3.6.2 Discharge processes

Fortescue River Alluvium

Discharge from the alluvial gravel aquifer is by a combination of evapotranspiration from phreatophytic vegetation in the north-west of the area, also as direct evaporation from the near shore tidal flats where the fresh groundwater is close to the surface above a saline water interface and throughflow to the ocean. The MWH (2010) modelling study estimated the discharge due to these mechanisms is to be on average 10.1 and 3.3 GL/year respectively.

There may also be some instances or reaches of the river where there are some minor flows or discharge from the alluvial aquifer to the Fortescue River, however, these are not expected to be a significant proportion of the overall catchment water balance.

Evapotranspiration by the mesquite, which has relatively deep roots and is a weed in the region may be considerable. Mesquite may take up water from as deep as 10mbgl. Before the advent of mesquite, it is likely that most of the groundwater discharge was to the bare tidal flats, with the groundwater flow taking place over a saltwater interface (MWH, 2010a).

Commander (1993) calculated the discharge as depletion in storage volume in the alluvium during a period of low river flow when the groundwater levels declined. A specific yield of 0.1 was used and the change in groundwater levels between 12 November 1985 and 26 November 1986 were measured. The total depletion in storage volume was calculated to be 11 GL and was equated to the average annual discharge from the aquifer. The value of specific yield of 0.1 was considered to be conservative and thus the above value is a minimum estimate of discharge (Commander, 1993).

In addition to discharge into the Indian Ocean, evapotranspiration is another important discharge from the aquifer. High evaporation exists in the coastal zone where groundwater level is shallow.

Proterozoic Basement Rocks

The basement aquifers discharge by baseflow to local drainages and by throughflow to the Fortescue River alluvium and coastal sediments. As such groundwater flow in the basement rock aquifers is generally from topographic highs towards the Fortescue River and the coast, with some local convergence about creeks during non-flood periods.

3.6.3 Regional groundwater flow

Groundwater flow in the region is generally to the northwest towards the ocean, with local groundwater flows being influenced by topography, recharge and discharge zones. The regional groundwater level contours as measured at the start of 2013 are shown in Figure 3-4.

Regionally groundwater flow within the superficial aquifer systems is from southeast to the northwest. Locally groundwater generally flows away from the river toward the northwest and discharges into the sea with groundwater level decreasing from 25 m AHD in the south, to less than 1 m AHD within 2 km of the tidal flats. Hydraulic gradient is highest when the Fortescue River reaches the peak water level and then gradually decreases with the fall of the river water level and during no flow period.

As such, groundwater level contours tend to be parallel to the coast with flow in a north-westerly direction, however there is divergence of groundwater flow away from the main river channels at times of river flow and local convergence of groundwater flow about the river channels in periods of little to no flow.

Limited groundwater level data exists for the basement groundwater system (refer to Figure 3-4 below), however, on a regional scale groundwater flow in the basement rock aquifers is expected to be generally from the topographic highs to the east towards the Fortescue River and the coast, with some local convergence about creeks during non-flood periods.

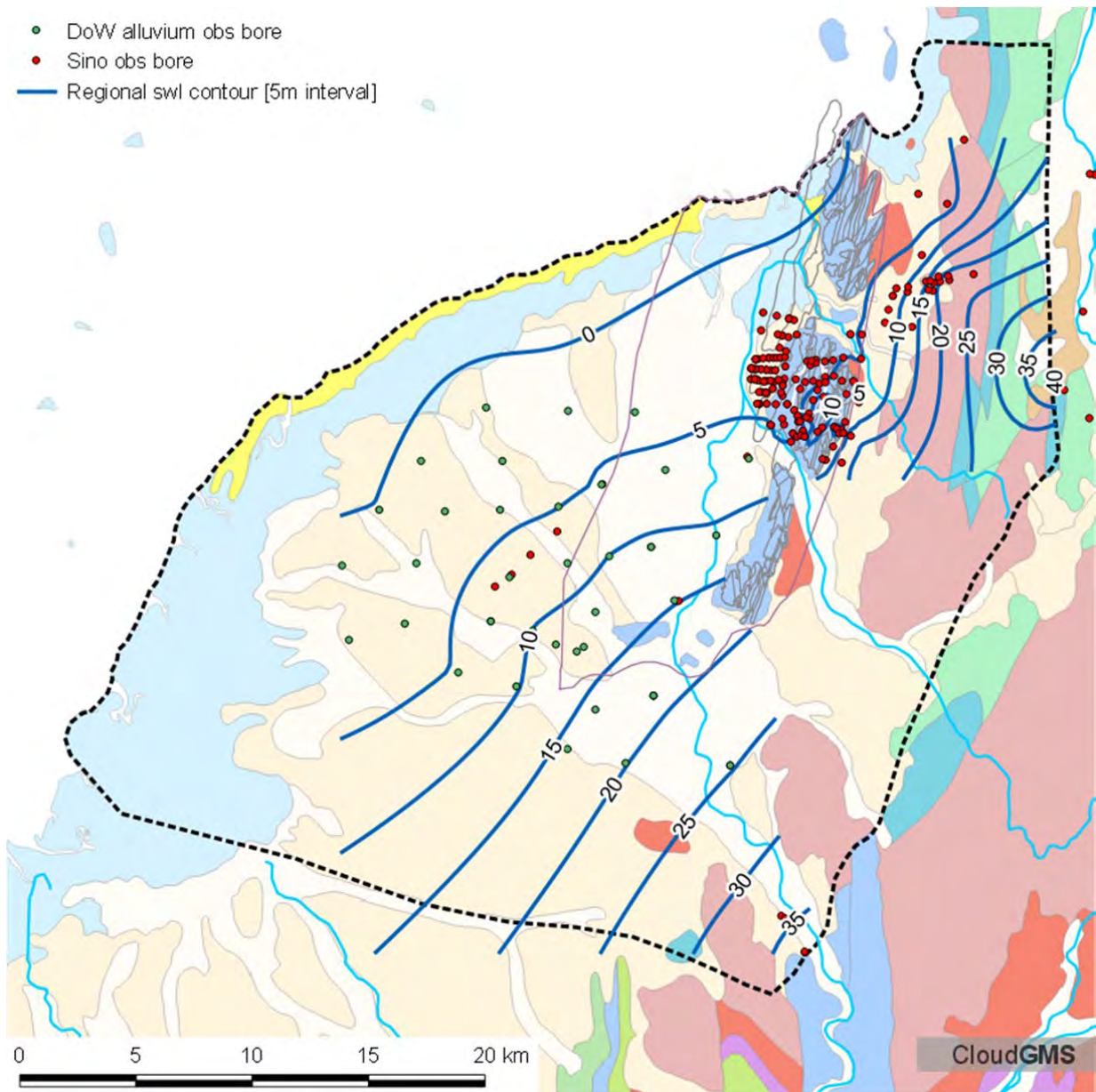


Figure 3-4 Pre mining regional groundwater contours derived from average swl values for DoW and CPM standpipe observation bores.

3.6.4 Local groundwater flow

The groundwater levels before mining commenced are likely to have been between 2 and 10 m AHD across the site, highest in the southeast and east and lowest towards the coast in the northwest. Mining activity began to perturb the groundwater system in the weathered zone from 2008 with the drilling and commissioning of production bores and then with the development of the open pit beneath the water table in 2009.

**SINO EXPANSION LIFE OF MINE GROUNDWATER MODEL
HYDROGEOLOGICAL CONCEPTUALISATION**

Although the regional groundwater flow is from the east and southeast and locally contours show steep gradients in the southern and southeastern areas of the pit, the majority of groundwater pumped from the in-pit sumps has been from the northern pit domain (sumps 05, 06, 07, 08 & 09). This has been due to the presence of high permeability feature interpreted to be associated with a NE trending faults, particularly NE Fault-1 (refer to section 3.3.3).

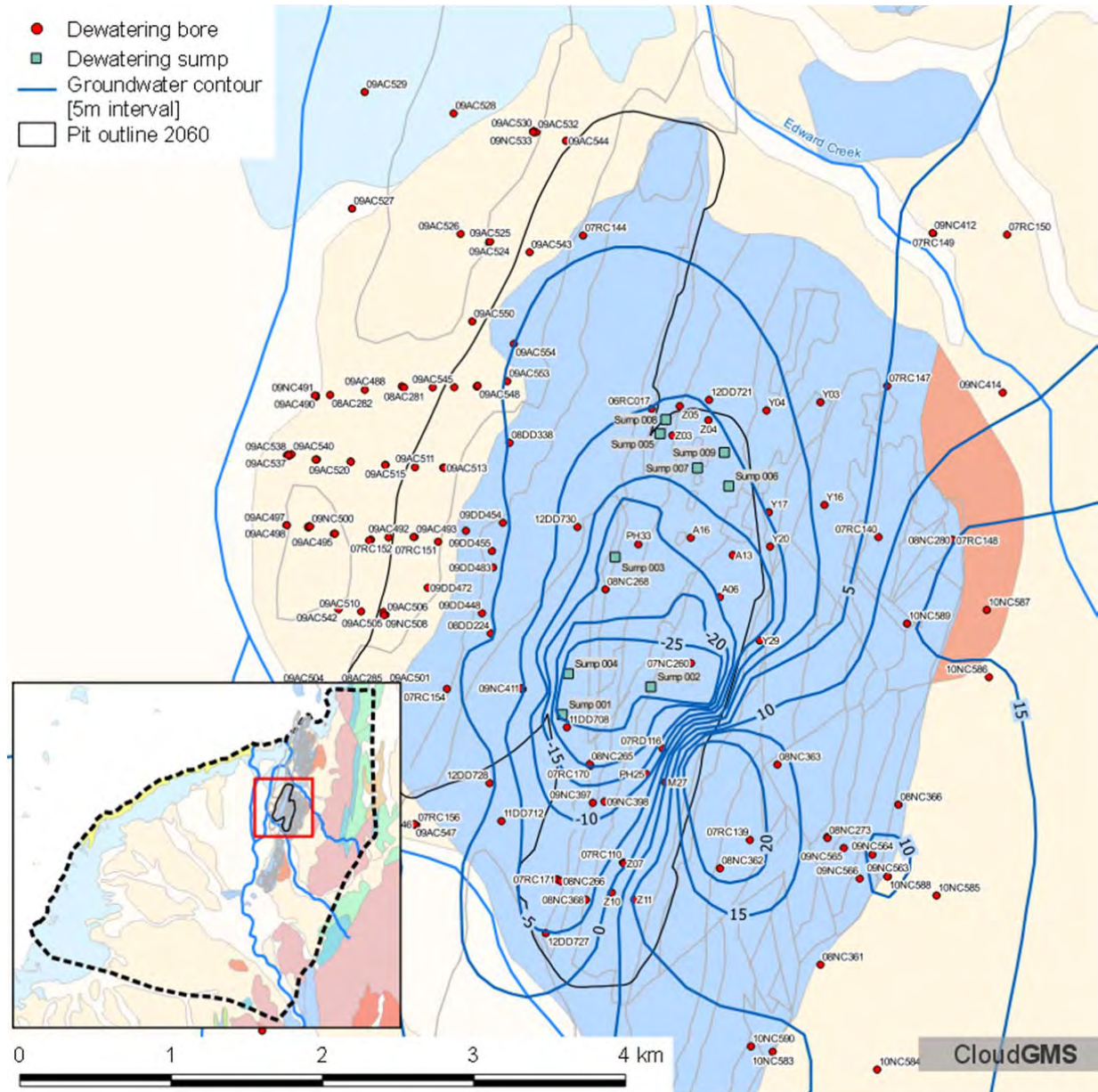


Figure 3-5 Groundwater contours in the vicinity of the current pit.

3.7 Water balance

The alluvial aquifer receives direct recharge from rainfall and indirect recharge via infiltration through the bed of the Fortescue River system. The weathered rock aquifer will receive direct recharge only from rainfall. Although recharge is likely to vary significantly depending on the intensity and occurrence of rainfall events, the previous modelling (MWH, 2010a) estimated these inflows to be on average:

Diffuse rainfall recharge to the alluvial and weathered rock aquifers is estimated at 4.5 GL/year (1 – 2% of rainfall). Model domain area 1015 km² and average annual rainfall of 267mm.

Recharge to the alluvial aquifer from river losses are estimated at 8.8 GL/year (MWH, 2010a). This was based on a percentage of river flow and did not consider the mechanism proposed by Haig (2009).

Discharge of groundwater from the system is expected to occur via either evapotranspiration (due to the shallow groundwater level and deep rooted trees) or flow into the sea. The modelling study estimated these components to be on average 10.1 and 3.3 GL/year respectively (MWH, 2010a).

3.7.1 Recharge

Fortescue River Alluvium

Following the flow event resulting from Cyclone Chloe in February 1984, recharge was estimated by calculating the volumetric change in the saturated aquifer between March and July of 1984. A specific yield of 0.1 was assumed for the alluvial gravels and the change of water levels was determined from hydrographs. The recharge during the flood event caused by Cyclone Chloe was estimated to be 22.7 GL (Commander, 1993).

Rainfall recharge occurs in areas covered with alluvial sands and gravels, as illustrated in water levels at some bores that rose following local rains but did not give rise to significant stream flow events (Commander, 1993 as cited in MWH, 2010).

Recharge to the Yaraloola Conglomerate is from downward leakage from the overlying alluvium where sections of the Trealla Limestone have eroded away.

Proterozoic Basement Rocks

Some direct rainfall recharge may also occur in the area of outcropping weathered Hamersley Group through fractures exposed to the land surface.

These basement aquifers are recharged by the infiltration of rainfall and local runoff in areas of outcrop and via leakage from overlying residual soils and sediments in areas of subcrop.

3.7.2 Discharge

Fortescue River Alluvium

The MWH (2010a) modelling study estimated the discharge due to evapotranspiration and flow to the sea is to be on average 10.1 and 3.3 GL/year respectively.

Commander (1993) calculated the discharge as depletion in storage volume in the alluvium during a period of low river flow when the groundwater levels declined. A specific yield of 0.1 was used and the change in groundwater levels between 12 November 1985 and 26 November 1986 were measured. The total depletion in storage volume was calculated to be 11 GL and was equated to the average annual discharge from the aquifer. The value of specific yield of 0.1 was considered to be conservative and thus the above value is a minimum estimate of discharge (Commander, 1993).

Proterozoic Basement Rocks

The basement aquifers discharge by baseflow to local drainages and by throughflow to the Fortescue River alluvium and coastal sediments. As such groundwater flow in the basement rock aquifers is generally from topographic highs towards the Fortescue River and the coast, with some local convergence about creeks during non-flood periods.

3.7.3 Groundwater abstraction

In terms of mining activities, the weathered Brockman Iron Formation is the first major aquifer that the open pit will directly intersect. Later in the mine life the open pit may also intersect the alluvial deposits to the west.

The main stress to the groundwater system from mining related activities (pit inflow and abstraction) has been to the weathered Brockman Iron Formation. This is because the abstraction bores are most likely to take the majority of their water from the portion of the screened interval that intersects the weathered zone and the majority of the pit does not exceed -30 or -40 mAHD at this moment, which, according to the block model, is roughly the location of the transition between weathered and fresh material.

As of January 2016 a total of 22 production bores have been drilled at the site (abstracting a total of just over 5 GL since 2009). The production bores are relatively shallow, ranging in depth from approximately 44 mBGL to 170 mBGL and the main abstraction targets are the and weathered rock aquifer located around the mine area with some abstraction from the Fortescue River alluvium. Average annual abstraction rates for the production bores are 16 L/s in 2008 (509 ML/year), 37 L/s in 2009 (1,157ML/year), 49L/s in 2010 (1,541ML/year), 36L/s in 2011 (1,125ML/year) and 25L/s in 2012 (793 ML/year). The abstraction profiles are presented above in Figure 2-11 and Figure 2-12.

In-pit dewatering occurs via pumping from several in-pit sumps. Up to January 2013 a total of 2 GL had been abstracted from the sumps Figure 2-13 and Figure 2-14. Initial abstraction (May 2009 to June 2011) was relatively minor with an average monthly abstraction rate of less than 10 L/s. After this period additional sumps within the pit area were constructed, with a recorded abstraction rate of approximately 36 L/s from Sump 001 (South wall) for July and August 2011. Average monthly abstraction approximately doubled after August 2012 to 77 L/s (~200 ML/month). Between September 2012 and January 2013 about 30% of pumping was from sumps located along the South wall (Sumps 1 and 2) and about 70% from sumps located in the northwest section of the mine (Sumps 3 and 5), with minor flows recorded for Sump 6 in the northeast sector.

Of further interest is the fact that the deepest part of the pit (Sump 1) attracts a much more limited inflow than the north of the pit, which is 20 m or so shallower (Sumps 5 and 6).

3.7.4 Throughflow Rate

Commander, (1993) used an average hydraulic conductivity about 130 m/d for the alluvial sediments (refer to section 3.4.1) to obtain an estimate of groundwater throughflow of between 2.3 GL/annum and 9.2 GL/annum.

MWH, (2010a) used the average of the available hydraulic conductivity of 134 m/d and calculated average throughflow rate of 11.0 GL/year.

The difference between estimated total groundwater recharge and the throughflow is in the range of 0.4 - 3.4 GL/year, which is the estimated amount of groundwater lost due to evapotranspiration in the area upstream of the cross-section (MWH, 2010a).

Table 5 Estimated water budget of the Fortescue floodplain area.

Component	Flux [GL/yr] MWH 2010a
Inflows	
Diffuse / direct recharge	4.5
Localised / indirect recharge	6.9 – 8.9
Outflows	
Evapotranspiration	0.4 – 3.4
Throughflow to the coast	11.0

3.8 Water quality

The gravel deposits coincide with a fresh water lobe, typically less than 1000 mg/L TDS, which grades outwards into saline groundwater near the coastal interface and margins of the alluvial fan. The low salinity is a result of recharge from periodic river flow.

A salt water interface is known to exist in both the alluvial and bedrock groundwater systems. The presence of a tidal fluctuation that oscillates considerable distances inland from the ocean via tidal flats and estuaries has resulted in the salt water interface occurring close to the ground surface several kilometres inland from the ocean.

Existing monitoring bores within the alluvium and bedrock groundwater systems have been profiled for salinity and have confirmed the existence of the salt water interface at depth.

Fugro geophysical data shows that the distance between the sea shoreline and seawater interface increases from northeast to southwest. Most likely this is resulted from the decrease in groundwater flow velocity from the northeast to the southwest. Groundwater flows faster in the northwest part of the alluvial aquifer, since it receives direct recharge from the Fortescue River. With the increase in the distance away from the river, the influence of river recharge declines and thus groundwater flow velocity decreases, as a result, the seawater interface moves further inland.

As salt transport and density effect on groundwater flow are not simulated in the groundwater flow model, a reasonably simple treatment of the coastal boundary is adequate for the model. Based on existing studies, fresh water discharges into the ocean usually only through the top layer of the aquifer due to density effect and the (Ghyben-Herzberg) seepage face effect. Therefore, we propose to simulate deep layers along the coast as no flow boundary and the top part of the alluvial layer as constant head boundary, with a value of 0.5 mAHD, through which fresh water may discharge into the ocean. The influence of groundwater utilisation on the movement of the seawater interface can be qualitatively investigated through the particle tracking method.

The groundwater quality of the region has been discussed in detail in previous reports (Aquaterra 2001, Aquaterra, 2007 and Commander, 1993). A brief summary of groundwater quality is presented in this section of the report and water quality distribution in the superficial sediments of the Fortescue River floodplain is presented below in Figure 3-6.

There are basically three groundwater quality types in the region:

Fresh groundwater (<1,000mg/L Total Dissolved Solids, TDS) in the central part of the Fortescue River alluvium. This fresh water forms a “lobe” elongated along the main channels of the River as a result of recharge.

Marginal to brackish groundwater (1,000mg/L to around 2,000mg/L TDS) in the basement rock aquifers and on the flanks of the Fortescue River alluvium where throughflow from the basement rocks mixes with the fresh water in the alluvium.

Brackish to saline groundwater (greater than 5,000mg/L TDS) adjacent to the coast, where there is a saline water interface between the fresh groundwater flowing northwards and seawater. This interface dips to the south (i.e. inland) forming a "salt water wedge" and groundwater salinity would increase with depth in the near coastal and tidal flats areas. The groundwater is predominantly sodium chloride type water typical of mature groundwater with long residence times and little influence from recharging groundwater.

Groundwater within the superficial sediments underlying the Fortescue River floodplain, with the exception of the flanks and in the near coastal zone, generally conforms to the drinking water guidelines (refer to Figure 3-6). Regional groundwater quality data to the east and south of the mine site have been added to the contours presented by Haig (2009).

Groundwater within the Basement Rocks generally does not meet drinking water guidelines, mostly in relation to salinity (TDS) and chloride, but in some cases also with regards to sulphate, manganese, barium, nickel, boron and cadmium. However, groundwater with the Basement Rock is generally within the guidelines for stock water usage, except in coastal areas or adjacent to the tidal flats.

Groundwater quality across the mining leases is highly variable from marginal to hypersaline. Bores with marginal quality drilled within the Brockman Iron Formation, Mt McRae Shale, Maddina Formation and Jeerinah Formation (10NC587 and 10NC590) are found to the south and east of the pit. The marginal bores are surrounded by brackish quality water from bores (08NC265, 08NC362, and 08NC363) within similar geology and including the Weeli Wolli Formation. Saline water is found moving north through tenement M 08/124 within the Brockman and Jeerinah Formations (ex-production bores 08NC268, 08NC280 and 09NC414) and becomes hypersaline in the very north of tenement M08/123 (Bore 09NC412).

Low TDS bores typically feature TDS < 6000 mg/L. Direct comparisons between profiled bores from previous years shows most are unchanged.

High TDS bores are well-stratified, with some bores showing more than two stratification layers. The salinity in the bores is typically unchanged, with the saline wedge evident at similar depths to previous years. In the pit itself hypersaline water is present at -8m AHD in the northern sumps.

Comparison of the salt water wedge and the water quality contours suggests that the wedge occurs within the >3000 mg/L contour.

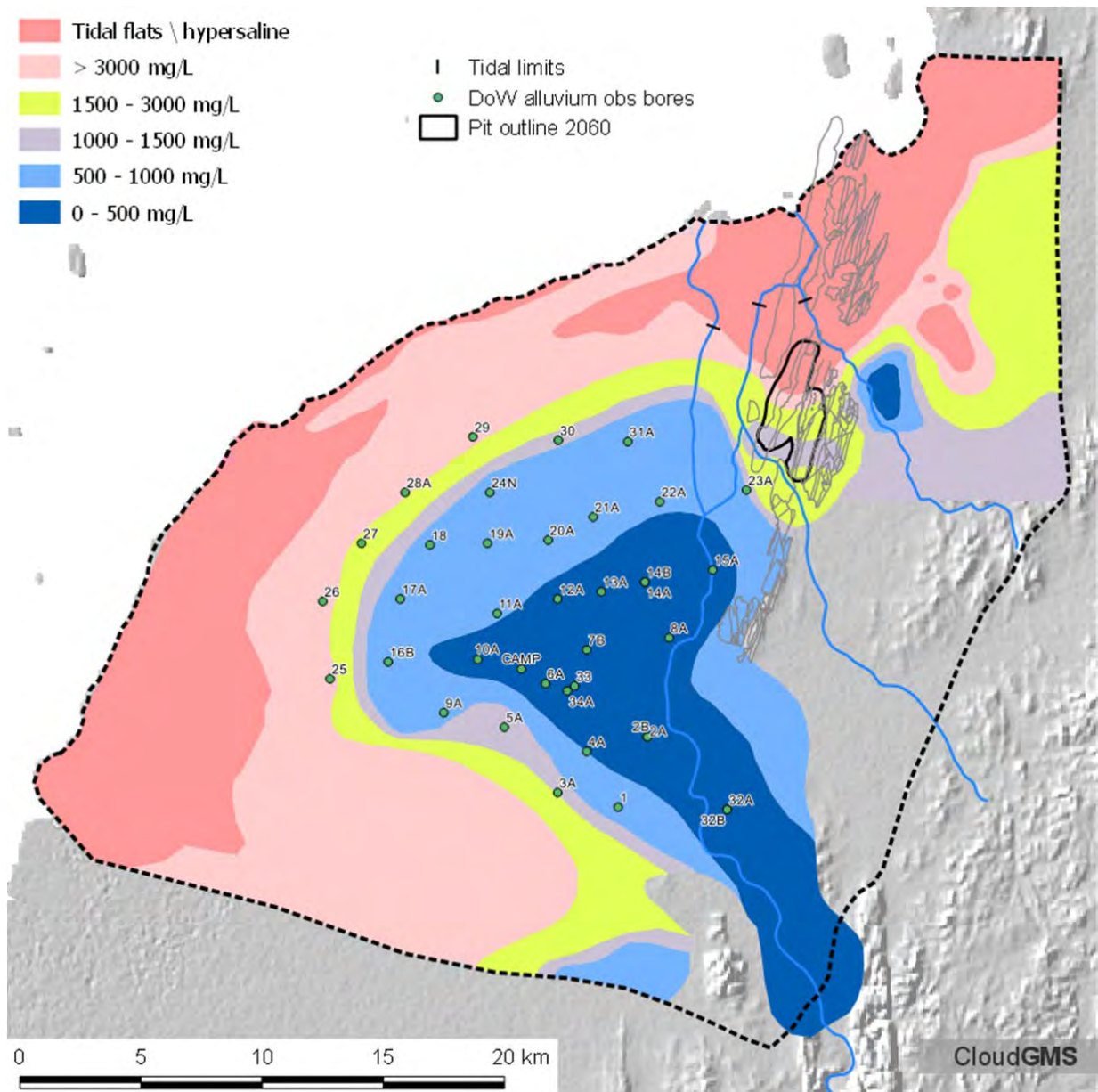


Figure 3-6 Water quality distribution in Fortescue River floodplain superficial sediments (modified from Haig, 2009).

3.9 Summary of Conceptual Model

The hydrogeology of the project area is essentially comprised of two groundwater systems:

- c) younger, superficial aquifer system comprising sands, silts/clays and gravels; and
- d) older, deep, low permeability, low storage aquifer system comprising cherty banded iron formation and mafic volcanics.

The Fortescue River is the major surface water feature within the project area, with the riverbed being located within the alluvial sediments. The Fortescue River is the major source of recharge to the superficial aquifer system.

Direct infiltration from precipitation recharges the groundwater system. A significant part of this water discharges back into creeks and as evapotranspiration. The deep groundwater system also receives recharge from the shallow groundwater system due to the differences in hydraulic head and the existence of a vertical downward gradient.

During mining conditions the major sources of inflow to the proposed pits would be: groundwater storage of the weathered rocks of the deep groundwater system (during initial stages of pit excavation); (b) groundwater storage of the deep groundwater system (during late stages of pit excavation); (c) direct inflow from precipitation; and (d) through the alluvial sediments where the pit intersects appreciable thicknesses and as leakage to the weathered basement groundwater system through overlying sediments.

Both pits will be excavated from the ground surface through the Brockman Iron Formation unit to a depth of ~ 410 m.

Based on the climatic, hydrological, geological and hydrogeological conditions described above, a conceptual model for the development of a groundwater numerical model that can be used to quantify dewatering requirement and environmental impacts of dewatering at the Sino Iron Project mine site is summarised below:

- The model covers the lower Fortescue River catchment, with the Indian Ocean as the northwest boundary and low permeability formations (Fortescue Group) as south and east boundaries.
- The model extends from the natural ground surface (essentially the groundwater table) to beyond the maximum mining depth of ~400 mBGL.
- Geologic formations considered in the model are:
 - The superficial aquifer system comprising separate layers for the Quaternary alluvial aquifer, Trealla Limestone aquitard and Yarraloola Conglomerate aquifer;
 - Weathered basement rocks (Hamersley Group, Fortescue Group),
 - Fresh basement rocks (Hamersley Group, Fortescue Group).
- Individual structural features within the separate geological groups (Hamersley Group and Fortescue Group) are considered where they have been identified as being hydrogeologically significant. Narrow zones of higher hydraulic conductivity and storage will be used to represent these features.
- Although tidal effects have been observed in monitoring bores they will not be considered in detail, thus for the purposes of this study the coast is considered as a constant head (inflow or outflow) boundary, at an elevation set at 0.5 mAHD.
- Surface water flow duration in the Fortescue River is an important process for recharge to the alluvial aquifer in the model area. The historic discharge record is used to determine the timing and duration of recharge events.
- Rainfall recharge is less significant than river recharge.
- Discharge from the alluvial aquifer occurs as evapotranspiration from phreatophytic (groundwater-dependent) vegetation fringing the Fortescue River and evaporation from river pools and the tidal flats. Evapotranspiration from dense stands of the exotic tree species, Mesquite (*Prosopis pallida*), is thought to be considerable and to influence local groundwater levels.

- Density effects on groundwater flow are not simulated in the groundwater flow model, as such a reasonably simple treatment of the coastal boundary is adequate for the model. Based on existing studies, fresh water discharges into ocean usually only through the top layer of the aquifer due to density effect and the (Ghyben-Herzberg) seepage face effect. Therefore, we propose to simulate deep layers along the coast as no flow boundary and the top part of the alluvial layer as constant head boundary, through which fresh water may discharge into the ocean.
- Some pools appear to have the potential for close hydraulic connections with groundwater in the alluvial aquifer. They are included in the model as monitoring sites to examine the impacts associated with the mine development.
- The average annual groundwater discharge/recharge is likely in the range of 11.4-14.4 GL/year.
- Pit development is considered at yearly intervals from 2016 to 2021 and 5 yearly intervals from 2025 to 2060.

4 Groundwater model design

4.1 Model design strategy

The model has been designed to meet the following criteria:

- Designed to run as quickly as possible to undertake uncertainty analysis.
- Refined in the areas of interest: the pit and river features.
- Designed to incorporate features that may be impacted by the mine pit.

4.2 Code used to construct model

The FEFLOW (Finite Element subsurface FLOW and transport system v 7.009) modelling code developed by DHI-WASY GmbH (Diersch, 2015). This code is an industry standard groundwater modelling tool used by many jurisdictions to study groundwater level behaviour within groundwater systems.

FEFLOW handles a broad variety of physical processes for subsurface flow and transport modelling and simulates groundwater level behaviour indirectly by means of a governing equation that represents the Darcy groundwater flow processes that occur in a groundwater system.

4.3 Model settings

The model settings used in this study are detailed below in Table 6.

Table 6 Feflow model settings

Model code	FEFLOW
Software version	7.0.9 (x64)
Mesh	
Element geometry	Triangle prism
Free surface	3D free surface (free and movable mesh)
Head limits for unconfined conditions	
Top of model domain	Unconstrained head
Storage change in phreatic top layer	Extend storage of unconfined layer to water table
Bottom of model domain	Unconstrained head
Numerical parameters	
Time stepping	Adams-Bashforth/Trapezoid rule (AB/TR) predictor-corrector
Error tolerance	
Euclidian L2 integral (RMS) norm	10e-03
Maximum number of iterations per timestep	12
Equation System Solver	Preconditioned conjugate-gradient method

4.4 Model Extent

The proposed model extent was based on the previous groundwater modelling studies (MWH, 2010a; SWS, 2013a) covering the whole of the Lower Fortescue River catchment downstream of Bilanoo gauging station.

The geological mapping of the regional geophysics provides evidence to support changes to the boundary of the previous groundwater models and the updated model boundary is illustrated below in Figure 4-1.

The following adjustments to the original model boundaries were made:

- the south-eastern portion of the boundary to remove the region of outcropping Brockman Iron Fm.
- realign the southern boundary around some of the more prominent outcrop and to match the observed drainage within the floodout of the Fortescue.
- realign the southern half of the eastern boundary to coincide with a regional linear feature that is interpreted to be a fault possibly associated with the Sholl Shear Zone (Hickman & Strong, 2003) that has been intruded by dolerite.

The boundary conditions are:

- Northwest boundary along the Indian Ocean: is a constant head boundary at the surface and the head along this boundary is set at an elevation of 0.5 metres AHD.
- Eastern boundary approximately aligns with a mapped thrust fault between the Fortescue Group to the east and the Dampier granitoid complex to the east (Hickman & Strong, 1998; Hickman & Strong, 2003). This boundary is considered a reasonable distance from the pit and the alluvial aquifer and it can be assumed as a no-flow boundary given the low conductivity and limited recharge for the weathered Hamersley Group.
- Southern boundary located along the upstream limit of the alluvial and Yarraloola aquifers. It can be approximately treated as a no-flow boundary as it is perpendicular to groundwater flow and given the low conductivity of the weathered Hamersley Group and only a very small part of the cross-section being alluvial sediments.
- The upper boundary of the model is the land surface, the upper slice is coincident with the groundwater table during simulation as such, rainfall recharge and evapotranspiration are applied at this surface as specified areal fluxes .
- The Fortescue River is represented as a third type boundary with fluxes being determined by the head difference between the river and the aquifer, and the conductance of the river bed (transfer rate). The maximum flow constraint is used to represent flow / cease to flow conditions and provide an upper limit to the infiltration from the river to the aquifer.

4.5 Supermesh development

FEFLOW contains the functionality to generate a finite element mesh from a super element mesh, which consists of the model boundary polygon and line and point features relevant to groundwater flow processes (eg. lithological boundaries, creeks, groundwater bores etc.).

The super element mesh and boundaries for the project area model were constructed taking into account the following key hydrological features:

- sub-cropping geological contact between Proterozoic rocks;
- the extent of the alluvial sediments;
- the Fortescue River;
- the 100m spaced lines defining the final pit footprint; and

- the locations of dewatering bores.

The supermesh elements (points, polylines and polygons) used to generate the finite element mesh are presented below in Figure 4-1.

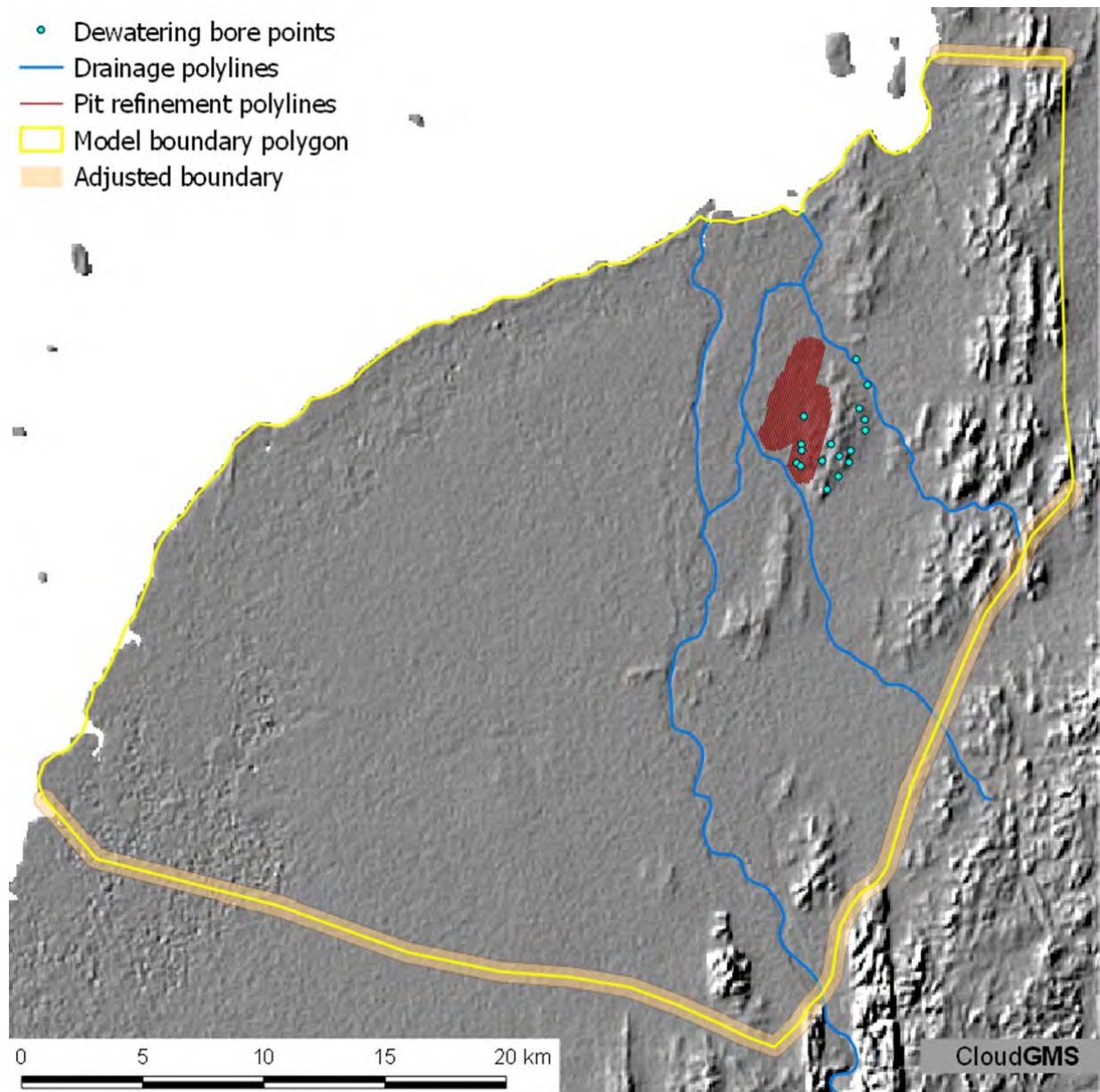


Figure 4-1 Elements used in the construction of the finite element mesh.

4.6 Model mesh

The mesh generation is based on an initial (proposed) number of elements to be generated, either for the entire mesh or for each of the super element polygons. For the Triangle mesh generation algorithm, an automatic mesh refinement at all or at selected polygon borders, at all or at selected lines, and around all points is possible.

Mesh generation typically is an iterative process, changing the generator settings and element numbers until a satisfactory finite-element mesh is obtained. Quality criteria for the mesh are somewhat subjective, but include the following:

- Obtuse angles in finite elements shall be avoided. The more obtuse the angle, the poorer the solution quality at the corresponding node. Therefore, the number of obtuse-angled elements shall be especially low in areas of focus.
- The transition from coarse to fine parts of the mesh shall be smooth.
- Structures such as well locations, natural elements (rivers, etc.) and technical installations have to be considered in the mesh.
- In specific areas, a fine mesh may be required to cover the physical processes in sufficient detail (e.g., around wells, in zones of contaminant movement).

The mesh was generated using the automatic Triangle option (Shewchuk, 2005). This feature offers the ability to define the local variation of mesh density by allowing for the refinement of the mesh around specified point and line features. The model mesh was also refined along the major structures and drainage features previously identified.

A 'proposed' mesh density of 5000 elements was used in the Generate Automatically option to create the mesh. The regional mesh was then smoothed by selecting all nodes not defined by a supermesh input feature identified previously (section 4.5) and applying the smoothing option. The mesh smoothing option uses a Laplacian operator to improve the mesh quality, leading to more regularly shaped triangular elements (Diersch, 2015).

The 'proposed' or initial seed number of elements was set to 5000, the final mesh comprises:

- 400335 finite elements (26689 finite elements per layer); and
- 216144 nodes (13509 nodes per slice).

The finite element mesh was generated using the following settings for the Triangle generator in the Mesh Generator Options:

Triangle mesh generation settings.

Property	Value	Unit
Quality mesh	True	
Minimum angle	>= 30 degrees	Degrees
Force all triangles to be Delaunay	True	
Fill all possible holes in mesh	False	
Delaunay meshing algorithm	Divide-and-conquer	
Steiner point insertion	Allow at all borders	
Mesh anisotropy	1.0	
Refine polygons	False	
Edge refine mode	Selected	
Polygon gradation	2	
Polygon target size	0.2	
Refine lines	True	
Line gradation	4	
Line target size	250	metre
Refine points	True	
Point gradation	5	
Point target size	250	metre

Currently each numerical layer was divided into 26689 numerical elements (Figure 4-2). The grid density is highest around ore bodies with the average area of a triangle element being about 5000 m² (or triangle side length of about 100 m).

A coarser grid with an average elemental area of 20000 m² (or triangle side length of about 200-250 m) was used in the vicinity of the river and alluvial gravels in order to describe river recharge. For areas covered by alluvial clay and weathered bedrocks, the grid density is even larger with an average elemental area of about 130000 m² (or triangle side length of about 550 m), since these areas are less significant in terms of available groundwater resources.

The final mesh generated for the FEFLOW model is presented below in Figure 4-2.

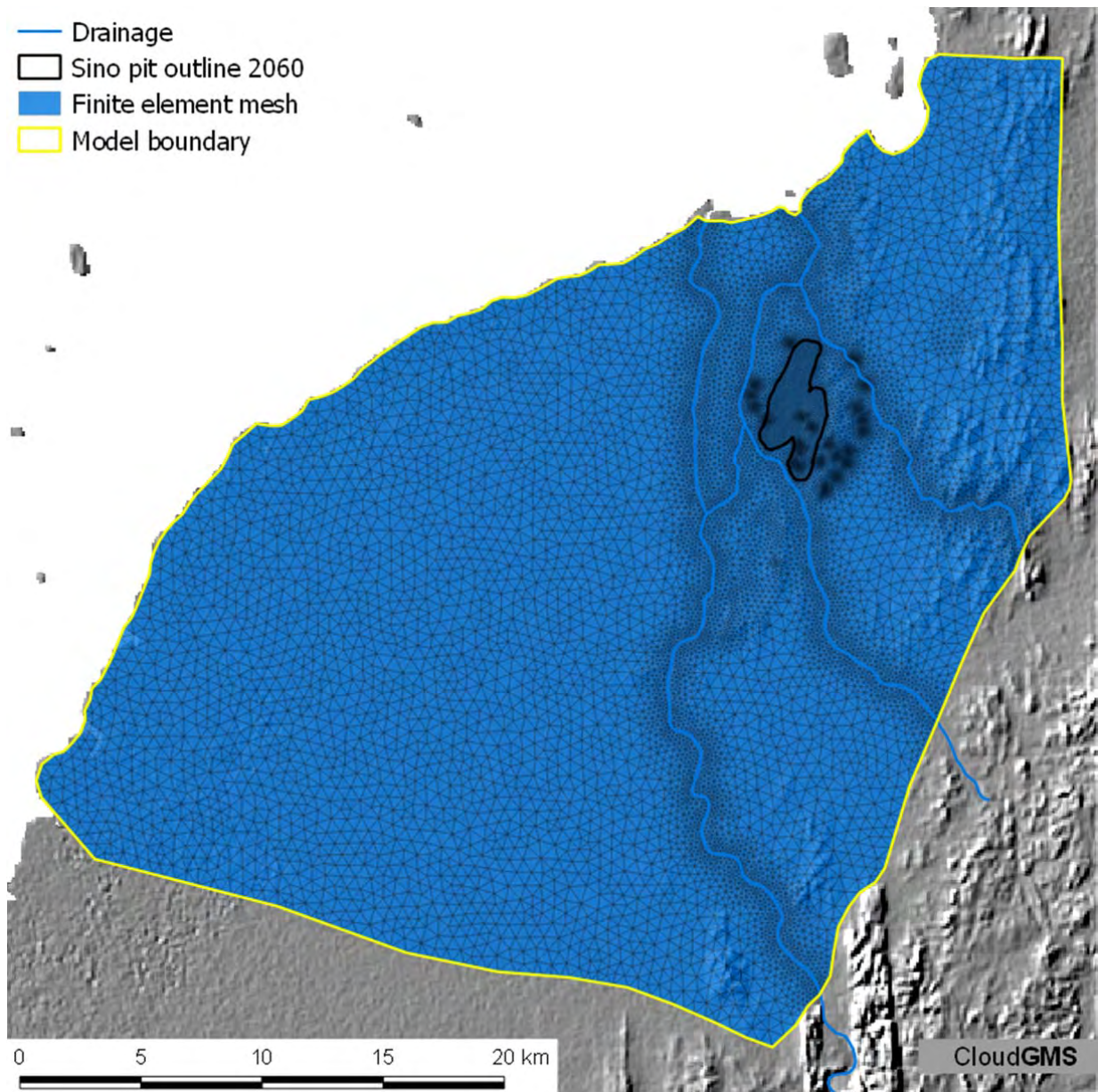


Figure 4-2 Finite element mesh showing refinement around important features within the project area.

4.7 Layer geometry

Based on the conceptual model the model domain is discretized vertically into 15 layers. Section 3.5 identified 13 hydrostratigraphic units, one numerical layer was used to represent each of the upper three superficial formations. The weathered basement rocks (HSU 4 and HSU 5) are separated into 2 layers, and the unweathered formations (HSU 6-9) were divided into 10 numerical layers, resulting in a total of 15 numerical layers. Not all geological formations exist everywhere in the model domain, therefore a numerical layer may contain more than one geological formation. The distributions of geological formations represented in each layer are described below in Table 7 and the spatial distributions of the HSUs in each layer are presented below in section 4.8.

SINO EXPANSION LIFE OF MINE GROUNDWATER MODEL
GROUNDWATER MODEL DESIGN

The layer geometry of the numerical model was generated using the Leapfrog geological modelling platform. The stratigraphy of the superficial sediments (alluvial gravels, Trealla Limestone and Yarraloola Conglomerate) using the available geological logs (Commander, 1989; Global Groundwater Pty Ltd, 2010). In the areas where geological information was not available the surfaces presented by MWH (2010) were used.

In areas where the superficial sediments are not present the layer represents either the weathered rocks of the Fortescue Group or Hamersley Group the minimum layer thickness in these area is 10 metres, this has resulted in 5 layers representing the weathered material (HSU 4 & 5) where the superficial sediments are absent.

Slices 6 to 15 are set at equal distances between the lower surface of the weathered zone, which defines the elevation for the bottom of layer 5 (ie slice 5), and the bottom of the model at -600 mAHD. This has resulted in the layers used to represent the unweathered Hamersley and Fortescue Group rocks varying in thickness from 65 m in the east to 50 metres along the coast.

Table 7 FEFLOW layer and corresponding HSUs

Layer	HSU		Comment
1	1 & 3 4 & 5	Alluvial sediments and clays, weathered basement rocks	HSU 4 & 5 represent weathered basement rocks to the east of the superficial sediments
2	2, 3 & 6 4 & 5	Tertiary sediments, weathered basement	HSU 4 & 5 represent weathered basement rocks to the east of the superficial sediments
3	3 & 7 4 & 5	Cretaceous sediments (HSU 7), weathered basement rocks	HSU 4 & 5 represent weathered basement rocks to the east of the superficial sediments
4 -5	4 & 5	Weathered Fortescue and Hamersley Group basement rocks	
6-15	8, 9, 10, 11, 12 & 13	Unweathered Fortescue and Hamersley Group basement rocks	Vertical discretisation to enable representation of 45° dip of the Hamersley Gp.

A west to east cut away section of the model domain at 7670000 mN is presented below in Figure 4-3. The section shows the model layer structure and the model zones used to parameterise the model.

The accuracy of the layer geometry is constrained by the available geological information. The geometry of the contact between the superficial sediments and the weathered Hamersley Group.

SINO EXPANSION LIFE OF MINE GROUNDWATER MODEL
GROUNDWATER MODEL DESIGN

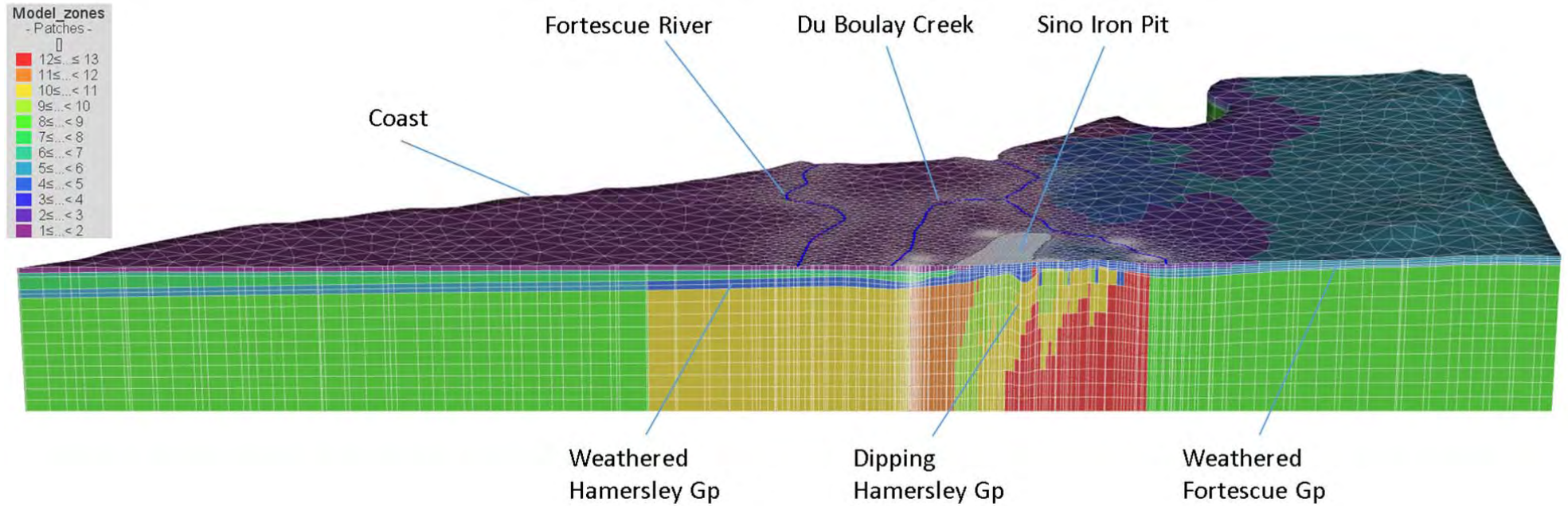


Figure 4-3 West-East cutaway section of the FEFLOW model showing the layering and the model zones representing the HSUs.

4.8 Material properties

Material parameter distributions in the model are assigned to parameter zones based on hydrostratigraphic units (HSUs) discussed in section 3.5. Material parameters are assigned to the zones using the utility PLPROC (Doherty, 2015).

- The weathered Hamersley Group was assigned using a zone corresponding to HSU 4.
- The weathered Fortescue Group was assigned using a zone corresponding to HSU 5.
- Each of the hydrostratigraphic units representing the unweathered basement (HSU 8, 9, 10, 11 & 12) were assigned using a zone for each unit.

The zonal distribution of for the upper 8 layers are presented below in Figure 4-4, Figure 4-5, Figure 4-6 and Figure 4-7. Layers 9 to 15 have not been presented as they only differ from layer 8 in the spatial distribution of HSUs 8, 9, 10, 11 and 12 which are offset to the west to represent the dipping units of the Hamersley Group. The distribution of pilot points used to describe the hydraulic conductivity of the weathered zone (HSU 4) is also presented.

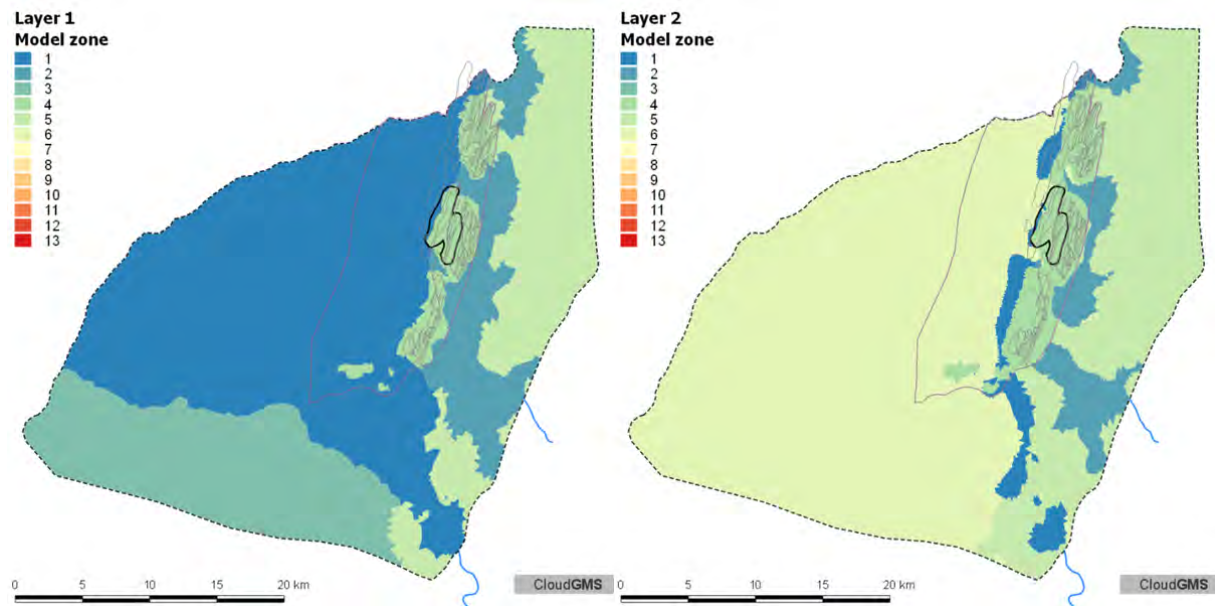


Figure 4-4 Distribution of layer 1 and layer 2 parameter model zones.

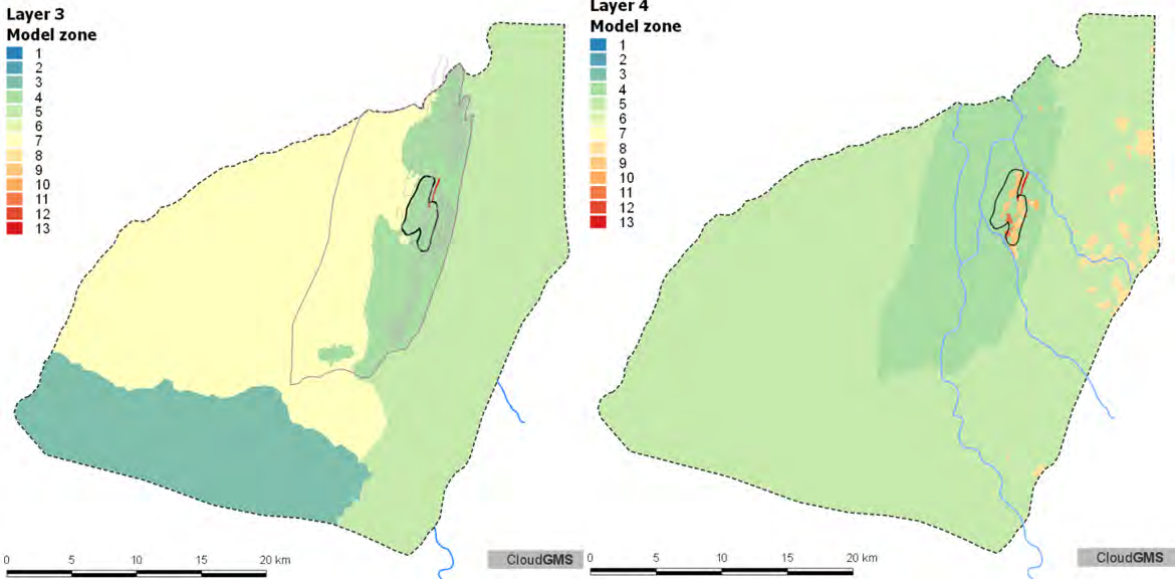


Figure 4-5 Distribution of layer 3 and layer 4 parameter model zones.

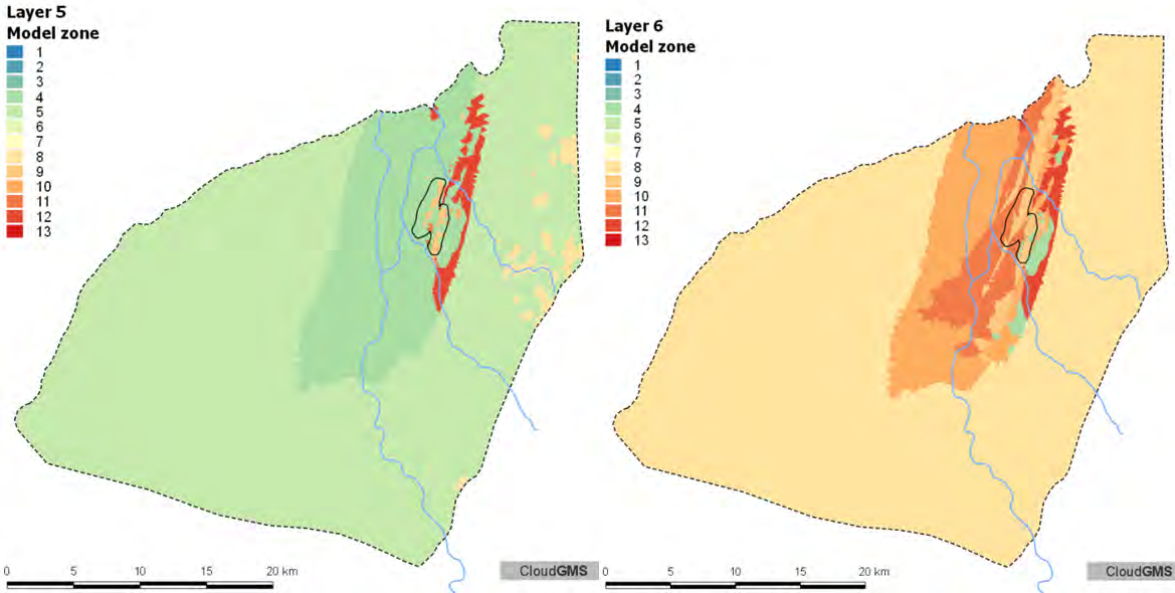


Figure 4-6 Distribution of layer 5 and layer 6 parameter model zones.

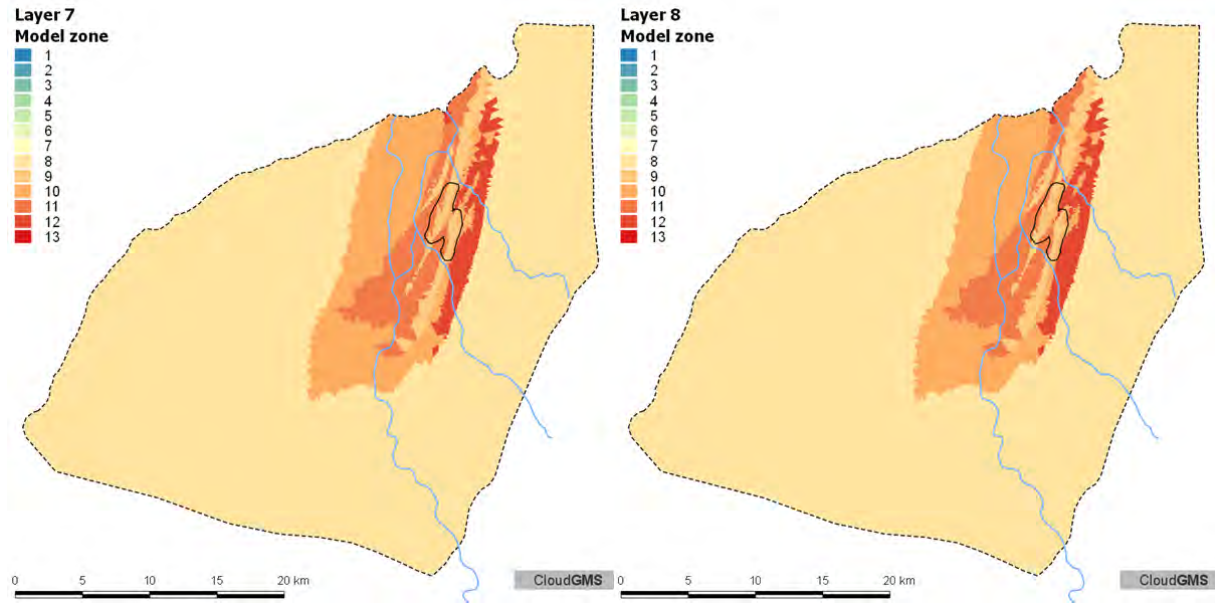


Figure 4-7 Distribution of layer 7 and layer 8 parameter model zones.

4.9 Boundary Conditions

4.9.1 Areal flux distributions (recharge and ET)

The recharge is applied to the model as a Parameter Expression using the In / outflow on top / bottom areal flux distribution.

The Parameter Expression is a user-defined expression linking the time- varying values of recharge to the In / outflow on top / bottom parameter, based on the dependencies of other parameters, in this case the recharge reference distribution, maximum evapotranspiration flux, extinction depth and reference distribution. Scaling factors are applied to the time- varying rainfall values using the recharge zones, which are attributed to the different soil types. Soils in this study have been defined using the surface geology (section 3.1) and the distribution of ET based on the LAI and vegetation mapping (section 2.11).

The ET function is determined using an estimate of the potential evaporation rate, an estimate of root depth or depth of capillary rise where vegetation is absent and the extent of persistent vegetation discussed in section 2.11.

$$ExtDep = \begin{cases} rd6, & ED.LAI = 6 \\ rd5, & ED.LAI = 5 \\ rd4, & ED.LAI = 4 \\ rd3, & ED.LAI = 3 \\ rd2, & ED.LAI = 2 \\ rd1, & ED.LAI = 1 \\ 0, & ED.LAI = 0 \end{cases}$$

$$ET = TS.Evap * \begin{cases} -0.001, & Head \geq ED.Surface \\ -0.001 * \left(1 - \frac{ED.Surface - Head}{ExtDep}\right), & (Ed.Surface - Head) < ExtDep \\ 0, & Otherwise \end{cases}$$

$$Leakage = \begin{cases} TS.tsf, & ED.Leak = 6 \\ TS.coarse.ore, & ED.Leak = 5 \\ TS.Raw.water, & ED.Leak = 4 \\ TS.SE.waste, & ED.Leak = 3 \\ TS.Nth.heave, & ED.Leak = 2 \\ TS.NE.waste, & ED.Leak = 1 \end{cases}$$

$$Rech = TS.Rainfall * \begin{cases} rech5, & ED.Rech = 5 \\ rech4, & ED.Rech = 4 \\ rech3, & ED.Rech = 3 \\ rech2, & ED.Rech = 2 \\ rech1, & ED.Rech = 1 \\ 0, & ED.Rech = 0 \end{cases}$$

$$Qp = Rech + ET + Leakage$$

where

Qp is the net flux applied to the upper surface of the element (coincident with the water table)

ET is the flux removed from the upper surface of the element

Rech is the flux added to the upper surface of the element

TS.Rainfall is the measured rainfall derived from the SILO Data Drill

TS.Evap is the evaporation data derived from the SILO Data Drill

Head is the groundwater elevation calculated during the simulation.

ED.Surface is the elemental distribution of reference ground elevation

ED.Rech is the recharge elemental distribution

ED.LAI is the elemental distribution of leaf area index used as a proxy for vegetation root depth.

fac1-fac3 are the scaling factors applied to the rainfall to account for losses in the unsaturated zone, these are determined during calibration.

rd1-rd6 are the root depths for each of the LAI zones determined during calibration.

The recharge zone distribution and leaf area index distribution used in the In / out flow on top / bottom Parameter Expression are presented below in Figure 4-8.

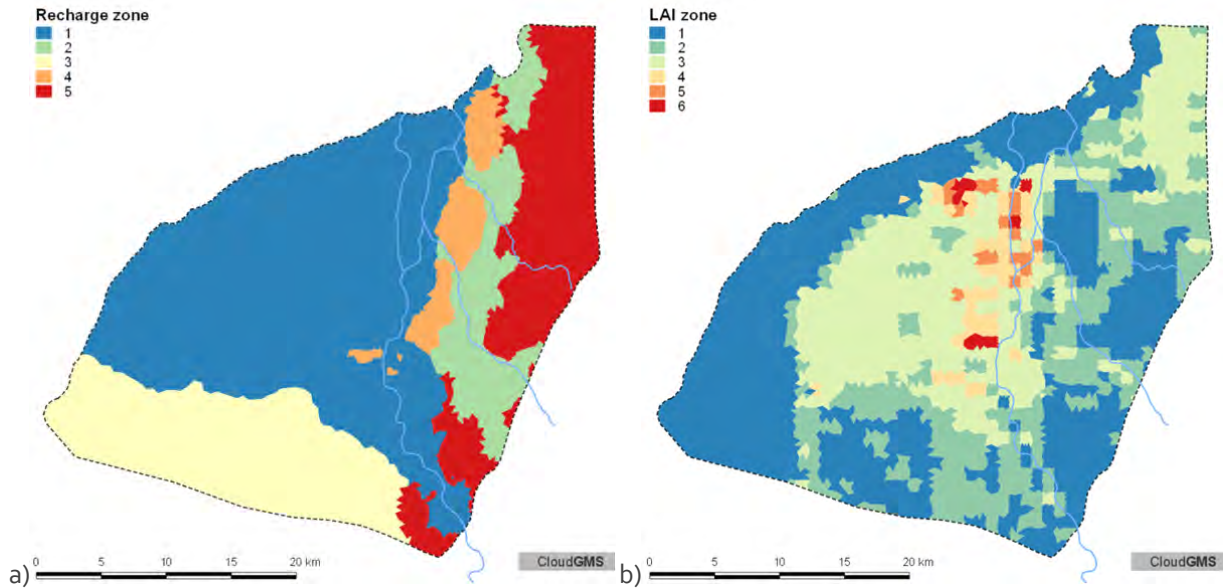


Figure 4-8 Reference distributions used in the In / out flow on top / bottom Parameter Expression a) recharge zones and b) leaf area index (LAI) zones.

4.9.2 Representation of the coast and tidal sections of rivers

The coastal boundary condition and the tidal sections of the rivers are represented with unconstrained specified head boundary conditions with the elevation set at a fresh water head value of equivalent to 0 mAHD of sea water. Lu, et al., 2014 provide a correction that should be applied to account for the fresh water discharging over the salt water interface.

4.9.3 Representation of non-tidal river features

Cauchy (Transfer) type boundary conditions are suitable to represent the surface water groundwater interaction processes (i.e. infiltration of surface water into the aquifer and exfiltration for water from the aquifer into surface water) where there may be an imperfect connection with a water body such as a river.

The transfer boundary conditions require a reference head and an elemental distribution of the transfer in / out rate material property, which defines the degree of connection between the model domain and the boundary condition. The transfer boundary conditions have been used to represent the following features:

- the main channels of the Fortescue River; and
- the channels of Edwards Creek and Du Boulay Creek.

The transfer boundary conditions have been applied to slice 1 & 2, the reference head was determined from the SRTM and the transfer in / out rate determined through calibration.

To simulate the ephemeral nature of the river flows the transfer boundary condition also has the capability to constrain the minimum and maximum flow [m^3/d]. The flow constraint was used to simulate the ephemeral nature of the recharge from the rivers in the area, limiting the periods of recharge to river flows. During periods of river flow the maximum flow was set to a flux determined through calibration. During periods of no-flow the maximum flow constraint was set to 0 m^3/d .

Conceptually the river recharge is a function of river flow duration and infiltration rate through the bed of the river.

The infiltration rate is controlled by the transfer boundary maximum inflow constraint, and the flow duration is a function of the flow in the river. The upper limit on flux represents the maximum infiltration rate through the floor of the river and was determined through calibration.

The river recharge is also a function of river flow duration. Flow duration was calculated by assuming a threshold for river discharge (as measured at the gauging station) below which no recharge occurs.

TSPROC (Doherty, 2008) was used to process the Fortescue River flow record to replace discharge values over a specified threshold with maximum inflow rate representing the infiltration rate through the bottom of the river channel.

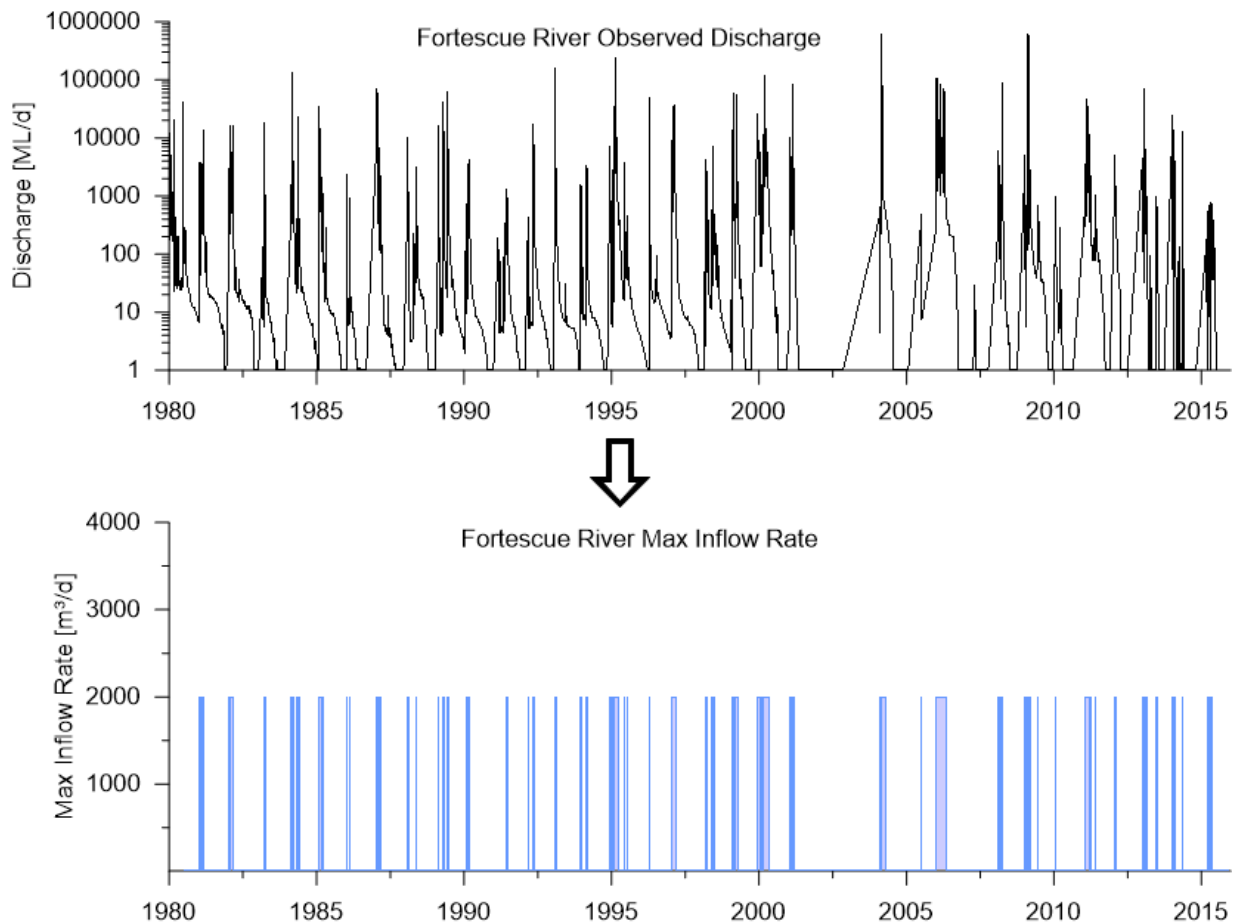


Figure 4-9 Transformation of Fortescue River discharge to flow duration and maximum infiltration rate used to simulate river recharge.

4.9.4 Representation of production bores

As indicated in section 2.7.1, there were 22 dewatering production bores operating in the project area. Through the mesh generation code, it has been possible to incorporate all pumping bores into the mesh at their surveyed locations with local refinement.

The pumping from the dewatering production bores are represented by well BCs assigned at specified nodes in the model domain. A well boundary condition applies a pre-defined extraction or injection to a

single node or to a group of nodes. The historic pumping record for each of the bores was used to specify the pumping rate (refer to section 2.7.1). The pumping bores were applied to the model using an IFM module called IfmAssignWells (CloudGMS, 2016) and the locations are presented below in Figure 4-10.

4.9.5 Representation of the pit during mining

The Dirchlet (specified hydraulic-head) boundary condition applies a pre-defined hydraulic head to a node. Instead of calculating hydraulic head as a simulation result, at these nodes the head is given by the boundary condition value. This can lead to an inflow into the model when neighboring nodes have a lower potential, or to an outflow from the model when there is a gradient from the neighboring nodes towards the boundary condition.

Head boundary conditions are applied in cases where the hydraulic potential is known in advance. This can be the case for example for surface water bodies with a perfect connection to groundwater (surface water level equals groundwater level), for pump sumps where a constant level is kept for dewatering purposes, or for seepage faces (in combination with a flow constraint).

A seepage face can discharge groundwater from the model domain, but no inflow to the model domain can occur.

The implication of using seepage face boundary conditions to represent the pit is that the inflow to the pit is a predicted output of the modelling, and the predictions of inflow are obtained from the model-calculated fluxes at the seepage face boundaries.

Dewatering of the pit excavation is simulated using seepage face boundary conditions that are activated sequentially in time, corresponding to the planned progression of the pit-levels over the life of mine.

The seepage face requires a reference elevation, which in this case has been determined from the pit shell elevations described in section 2.8. The full series of the pit shell development is available in Appendix D. The locations of the seepage face boundary conditions are presented below in Figure 4-10.

4.9.6 Representation of the pit post mining

Following the end of mining inflows to the pit void will no longer be actively removed. At this time evaporation is the only process removing inflows to the pit void.

After mining has ceased, groundwater levels recover and the pit void is filled from the pit base upwards via groundwater inflows and a lake will form in the pit void provided inflows exceed evaporation from the large surface area of the potential pit void lake.

This process is simulated by deactivating the seepage face boundary conditions and assigning an increased vertical / horizontal permeability 2 to 3 orders of magnitude greater than the host rock (1m/d) and a storage coefficient equal to 1.

Evaporation from the surface of the lake is represented by an outflow boundary condition that is active only if the calculated water table elevation in the pit-lake zone is above the elevation of the bottom of the pit void. Thus, evaporation from the lake occurs at a prescribed rate (determined by the average daily evaporation rate and a pan to lake coefficient) only when the lake contains water, and is otherwise zero.

Table 8 Summary of nodal boundary conditions invoked in the groundwater model.

Feature	Boundary condition	Value	Constraint	Value
Coast and tidal sections of the rivers	Dirchlet (specified head)	0.5 mAHD	-	-

SINO EXPANSION LIFE OF MINE GROUNDWATER MODEL
GROUNDWATER MODEL DESIGN

Mining activities	Dirchlet (seepage face)	Pit shell elevation	Minimum flow	0 m ³ /d
Post mining pit void lake	Evaporation	0 mm/d 0.65 pan to 0.85 pan	-	-
River	Cauchy	Ground elevation	Maximum flow Minimum flow	Timeseries 0 m ³ /d
Dewatering bore	Well	Variable m ³ /d	-	Timeseries

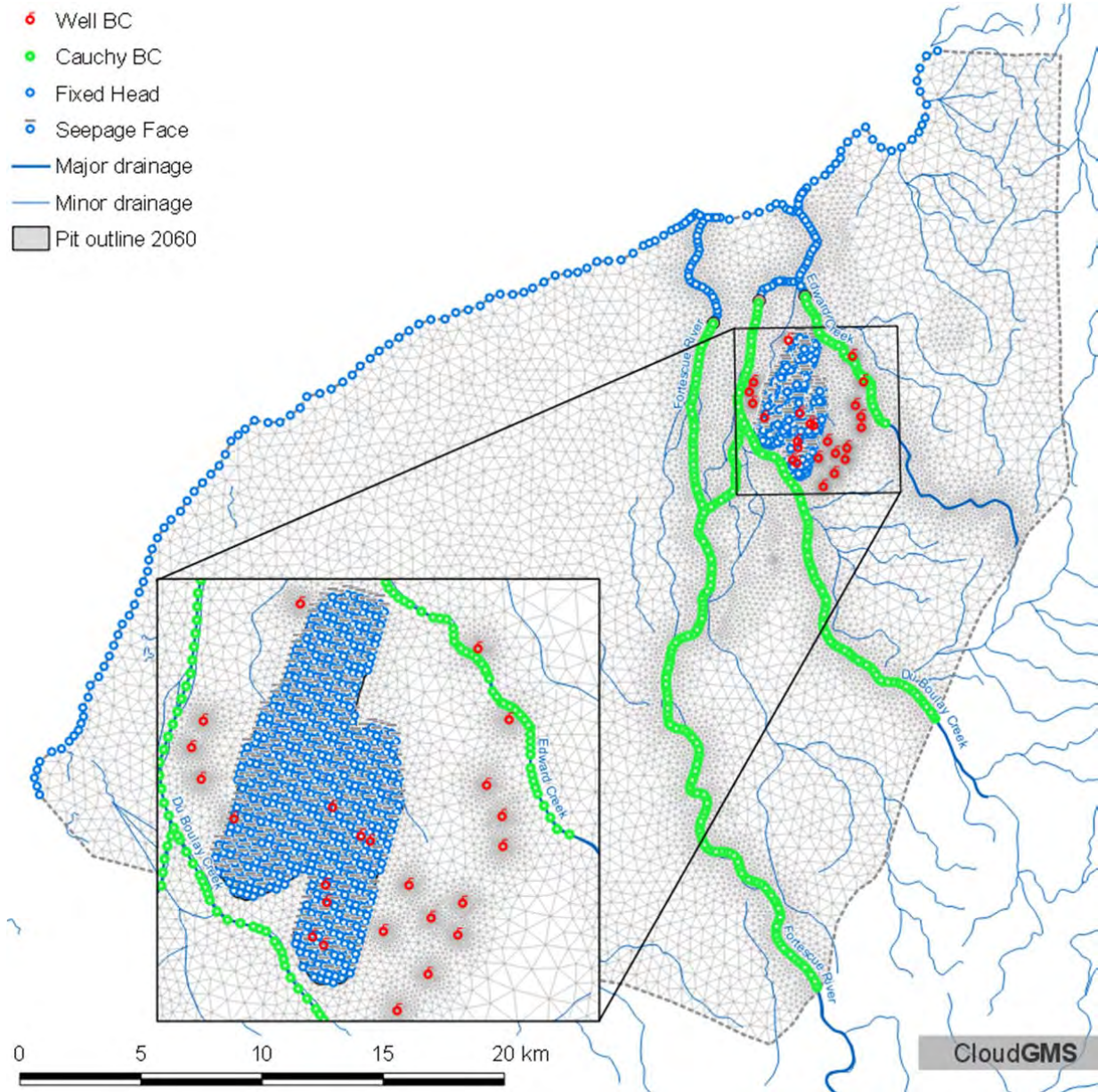


Figure 4-10 Locations of nodal boundary conditions.

5 Calibration and sensitivity analysis

5.1 Introduction

The calibration method relies on observed data showing a response to the groundwater stresses, preferably of known magnitude. Although they have associated uncertainties, the rate of sump and borefield pumping is known and the elevation of the pit through time is also known. However, as with the previous modelling campaigns, the calibration dataset used in this study is constrained by the following two items:

- The pit is currently relatively shallow and is predominantly excavated within the weathered material; and
- The production bores achieve a relatively high yield, but the majority of this groundwater most likely came from the upper section of the bore where it intercepts the weathered rocks (which have a higher permeability and storage than the deeper fresh rocks).

As with the SWS (2013a) study, this means that by far the most significant stress to the system to date has been restricted to the weathered material. This therefore presents an opportunity to calibrate the hydraulic parameters of the weathered material, but a limited opportunity to calibrate the parameters of the fresh rock beneath.

The simulated vertical extent of the weathered material has been taken from the CPM block model and the more recent mapping of the weathering and fracture depths. Any deficiencies in this dataset will therefore influence the effectiveness of the calibration and the future predictions. This is significant because the weathered and fractured material is likely to present the greatest inflow of groundwater to the open pit, and the predictions of inflow are dependent on both the lateral and vertical extent of this HSU and its parameters.

Based on the discussion above then, the initial hydraulic parameters assigned to the fresh rock have been based on the results of previous studies. Initial parameters for the alluvium and conglomerate were taken directly from the MWH (2010) model. Initial parameters for the fresh rock in the mine area were taken from the injection test modelling (SWS, 2013a).

5.2 Calibration strategy

The calibration was conducted in two stages:

- Stage 1 calibrated the parameters associated with the aquifers of the superficial sediments and inputs such as recharge (including river infiltration) and evapotranspiration; and
- Stage 2 calibrated the weathered and fresh rock parameters in the vicinity of the mine using the stresses from the bore dewatering and sump abstraction volumes.

The reason for the two staged approach was related to the time required for the 15 layer model to run. Running the 15 layer model for the full 35 year history match period required approximately 2 hours to complete, however, a 5 layered model over the 35 year history match period required just 30 minutes to complete. Therefore, to undertake the calibration of the superficial sediments, where the influence of the underlying formations has limited impact on the results and the detailed layering used to represent the dipping Hamersley Group was not required, a simplified model was employed where the unweathered formations were combined into a single unit to reduce the model layers from 15 to 5.

5.2.1 Automatic parameter estimation

The automatic parameter estimation code PEST (Doherty, 2010) was utilised to determine the updates to the hydraulic parameters in the groundwater model, and adjust inputs such as the scaling factors for the recharge zones and leakage features.

PEST has the capacity to incorporate all observations during the parameter estimation process including vertical gradients evident in the VWP data. The use of PEST and its associated utilities also allows for a more rigorous investigation of parameter uncertainty on model forecasts.

5.2.2 Stage 1 simulation period

The stage 1 calibration involved running the model from 01/01/1983 – 01/01/2015 and history matching undertaken to the observed groundwater levels in the superficial sediments within the model domain. This included the bores installed by DoW and the bores installed by CPM between Du Boulay creek and the western margin of the west pit (Global Groundwater, 2010).

5.2.3 Stage 2 simulation period

The stage 2 calibration involved running the model for the period that the dewatering infrastructure in and around the mine has been operating 01/01/2008 – 01/07/2016. History matching was undertaken for all the available observed groundwater levels within the model domain and the monthly pit abstraction volumes.

5.3 Stage 1 adjustable parameters

5.3.1 Distributed recharge and evapotranspiration parameters

The method for applying areal flux distributions associated with direct recharge from rainfall and evapotranspiration are presented in section 4.9.1. The parameters adjusted during the Stage 1 calibration process were:

- Recharge scaling factor (rech1 – rech5);
- Root depth (rdo – rd6)

5.3.2 River infiltration parameters

The flow record for the Fortescue River was utilised in the calibration via a methodology consistent with the proposed recharge mechanism detailed in section 3.6.1 and section 4.9.3. Conceptually the river recharge is a function of river flow duration and infiltration rate through the bed of the river and occurs when river flows reach a threshold flow rate, after which recharge is primarily determined by flow duration (above the threshold) and infiltration rate to the aquifer.

The river infiltration is applied to the three major drainage features using the observed Fortescue River flow discharge timeseries processed using the PEST utility TSPROC (Time Series Processor). The flow threshold value and replacement infiltration rate value were determined using PEST during Stage 1 of the calibration process and the adjustable parameters used to determine the inflow from the river are:

- The flow duration determined by a flow threshold (thresh1 – thresh3); and

- The infiltration rate through the river bed represented by the transfer boundary upper flow constraint (maxflow₁ – maxflow₃).

The flow duration and infiltration value were determined by generating new time series from the historic flow record using the PEST surface water time series processing utility TSPROC. The SERIES_CLEAN processing block was used to replace flow values above a specified threshold flow value with a constant value representing the transfer boundary condition flow constraint. Flow values below the threshold were replaced with a 0, resulting in no recharge during these times. The final river calibration parameters are summarised below in Table 11.

5.3.3 Hydraulic parameters

The following model hydraulic parameters have been calibrated by adjusting them to improve the match between observed and simulated groundwater level, water balance components and pit inflows (sump abstraction) observations:

- hydraulic conductivity;
- unconfined specific yield (drain / fillable porosity);
- confined specific storage; and
- transfer rate in

Material parameter distributions in the model were assigned using the utility PLPROC (Doherty, 2015).

Stage 1 the hydrostratigraphic units within the superficial aquifer system were assigned using 7 zones corresponding to HSUs 1, 2, 3, 6 & 7.

The hydraulic conductivity of the unweathered basement rocks was set to 0.005 m/d. The weathered basement rocks were set to 1 m/d. The final hydraulic parameters are summarised below in Table 13.

5.4 Stage 1 calibration targets

5.4.1 Groundwater levels

The following sets of groundwater level observations were used in the calibration:

- Standpipe piezometers in the alluvial sediments; and
- Standpipe piezometers in the alluvial sediments in the mine area.

5.4.2 Alluvial water budget

The estimated water budget components discussed in section 3.7 were used as targets for the recharge to the alluvial aquifer due to rainfall infiltration and flows in the Fortescue River.

5.5 Stage 1 calibration results

5.5.1 Final parameters

The final parameters used to determine the river inflow timeseries are presented below in Table 9, Table 11 and Table 11.

The recharge scaling factors (and equivalent percent of rainfall) for the applied to the recharge zones are presented in Table 9. The rainfall timeseries is input into the model as a mm/d rate and to convert to the units used by the model of m/d, the rainfall rate is multiplied by 0.001. The scaling factor is adjusted to a percentage of rainfall by multiplying by 1000.

The root depth assigned to each LAI zone are presented in Table 10.

The TSPROC parameters used to process the Fortescue River flow record to a timeseries of infiltration along the river is presented below in Table 11.

Table 9 Recharge scaling factors used in the final calibrated model.

Zone	Value	%
rech1	1.00E-04	0.1
rech2	1.00E-06	0.001
rech3	1.00E-05	0.01
rech4	1.00E-06	0.001
rech5	1.00E-05	0.01

Table 10 Final root depth assigned to leaf area index zones.

Parameter	Value	Unit
rd0	0.5	m
rd1	1.5	m
rd2	3.58	m
rd3	6.03	m
rd4	11.32	m
rd5	6.45	m
rd6	9.78	m

Table 11 Final TSPROC parameters used to process the Fortescue River flows to modelled inflows from the river.

Parameter	Value	Unit
Thresh1	400	ML/d
Thresh2	550	ML/d
Thresh3	250	ML/d
Maxflow1	2000	m ³ /d
Maxflow2	200	m ³ /d
Maxflow3	90	m ³ /d

The final hydraulic parameters determined for the superficial sediments are presented below in Table 12. The hydraulic parameters are consistent with the estimated hydraulic parameters presented by Commander and Global Groundwater (2010) and the previous modelling studies.

Table 12 Final stage 1 hydraulic parameters of the superficial sediments.

Formation	HSU	K _{xy} [m/d]	K _z [m/d]	S _y [-]	S _s [-]	Transfer In [1/d]
Alluvium	1	90	9	0.08	0.0001	2.02
Clay	3	1	0.1	0.01	0.0001	2.02
Tertiary	6	0.1	0.01	0.01	0.0001	2.02
Cretaceous	7	10	1.0	0.02	0.0001	2.02

5.5.2 Groundwater levels

The groundwater levels for the bores with records spanning the total period of simulation (1983 – 2016) are presented in Appendix E.

5.6 Stage 2 adjustable parameters

During the Stage 2 calibration the material distributions were generated using a combination of zones based on hydrostratigraphic units (HSUs) discussed in section 3.5. The weathered Hamersley Group was assigned using a zone corresponding to HSU 4 and the weathered Fortescue Group was assigned using the zone corresponding to HSU 5.

The groundwater level response to the pumping indicates that the weathered zone of the Hamersley Group (HSU 4) has the greatest variability. To reflect this variability the hydraulic parameters distributions in the vicinity of the pit (where time series observations are available) were generated using pilot points. Pilot points were defined near pumping bores and in areas where it was considered that the hydraulic parameters may be different. A total of 50 pilot points were used to describe the hydraulic properties for the weathered basement rocks (HSU 4) in the pit area.

The zonal distribution for layer 4 is presented below in Figure 5-1. The distribution of pilot points used to describe the hydraulic conductivity of the weathered zone (HSU 4) is also presented.

Each of the hydrostratigraphic units representing the unweathered basement (HSU 8, 9, 10, 11 & 12) were assigned using an individual zone for each unit.

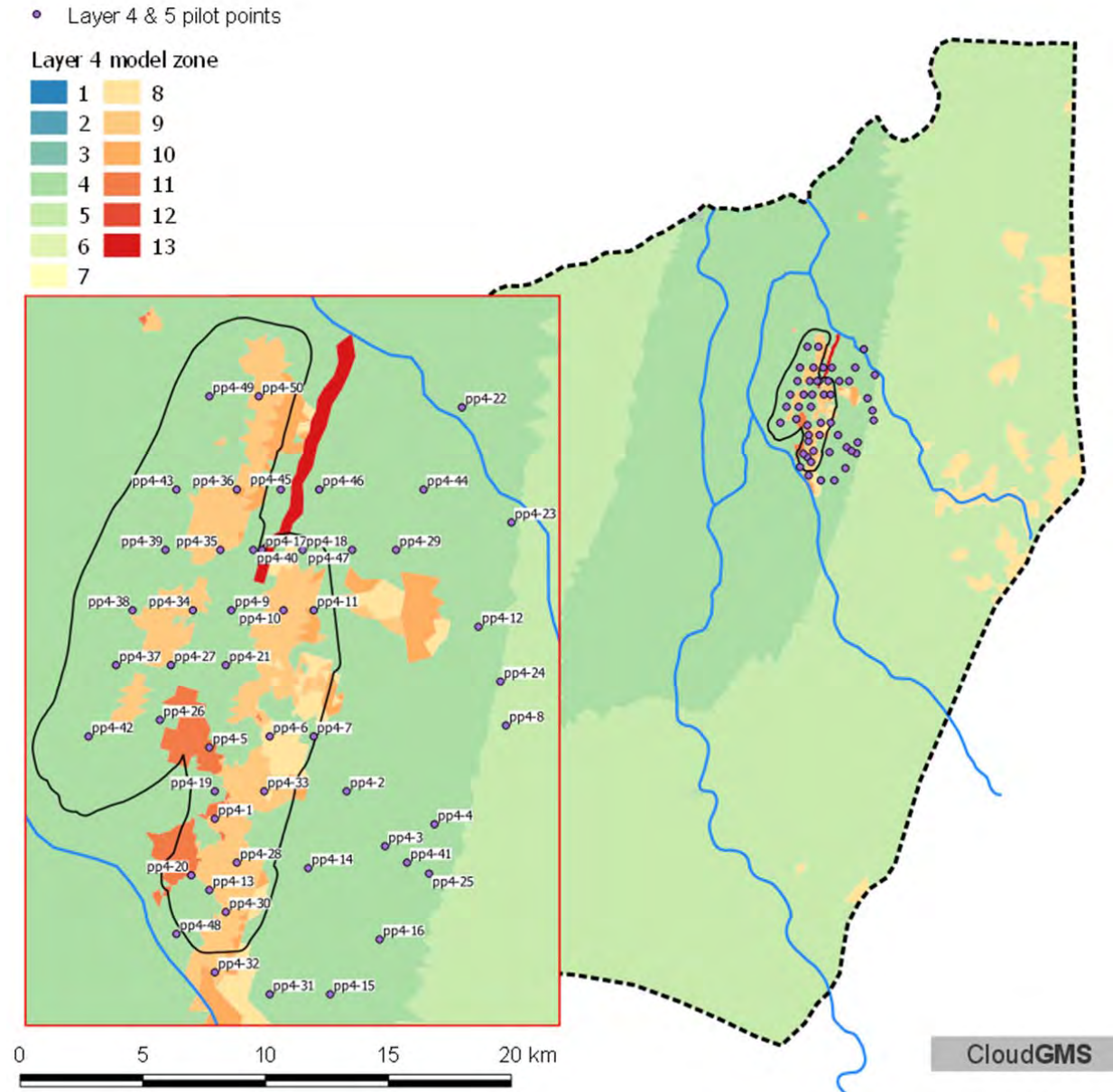


Figure 5-1 Location of pilot points used to describe the hydraulic conductivity and specific yield distributions for HSU 4 (layer 4). Model zones correspond to HSUs described in section .

5.7 Stage 2 calibration targets

5.7.1 Groundwater levels

The following sets of groundwater level observations were used in the calibration:

- Standpipe piezometers in the alluvial sediments;
- Standpipe piezometers in the mine area; and
- Pressure data from the vibrating wire piezometers.

5.7.2 Sump inflows / abstraction rates

Pit inflows can be separated into the northern and southern pit domains. The sump abstraction data was reported for the 4 main areas of abstraction; sumps 01 & 04, sump 02 and sump 03 in the southern pit domain and sumps 05, 06, 07, 08 & 09 in the northern pit domain.

Despite the uncertainties associated with the sump abstraction numbers (i.e. the exact proportion from groundwater, surface water and recirculation) it was found that a reasonable history match could be obtained, especially when the recirculation of water was incorporated into the model via the leakage features described in 2.6.

5.7.3 Leakage rates

The leakage rates for the SE waste dump, NE waste dump and North Heave were based on an estimate of the leakage area and conversion of the respective monthly sump abstraction rate to an areal application rate in m/d.

The leakage rates for the raw water pond and coarse ore stockpile have been estimated using trial and error based on an estimate of the leakage area and matching the simulated to the observed groundwater level rises in bores adjacent to each facility.

Leakage was then applied to the model as an areal flux using a Parameter Expression to calculate the In/outflow on top/bottom with the rates used in the Parameter Expression adjusted during calibration.

5.8 Stage 2 calibration results

The results presented are for the history match period (January 2008 – July 2016) used during calibration.

5.8.1 Parameter distributions

The calibration process involved adjusting the hydraulic conductivity of the elements representing the alluvium and weathered material in layers 1 – 4. Overall the final hydraulic conductivity distribution was consistent with the distribution from the SWS (2013a) model. However, there is a major difference in the area in the north of the current East pit associated with NE Fault-1, where the hydraulic conductivity was increased 10 fold (100 m/d) to reproduce the observed pit inflows at Sump 05, Sump06, Sump07 & Sump 08).

Layer 1 is generally above the water table in the pit area and as such has little effect on the groundwater inflows to the pit. However, in the areas underlying the leakage features, mounding resulted, requiring adjustment to the hydraulic conductivity to prevent the groundwater level from increasing above ground level. Discharge rates to the NE waste dump were found to be considerably greater than the capacity of the expected low hydraulic conductivity of the weathered material that it is situated over. Given that there is no apparent surficial ponding of the discharged water, it is interpreted that the overlying surficial formations or the weathered Dales Gorge Member have a higher hydraulic conductivity than the weathered material to the south and the faulting evident in the area of the NE waste dump (refer to Figure 3-3 in section 3.3.3). The exact flow path is currently unknown, and the localised increases in permeability associated with faulting have been modelled using more extensive higher permeability zones in HSU4.

The range of hydraulic parameters in the re-calibrated model are presented in Table 13.

SINO EXPANSION LIFE OF MINE GROUNDWATER MODEL
GROUNDWATER CALIBRATION AND SENSITIVITY

Table 13 Hydraulic conductivity ranges used in the current study.

Units	Kh / Kv	Sy [-]	S [m ⁻¹]
Calibrated in Stage 1 of this study (Layers 1 - 3)			
Alluvium – mine area	10.0 / 1.0	0.08	1.00E-04
Alluvium – central region	90.0 / 9.0	0.08	1.00E-04
Alluvium – west region	1.0 / 0.1	0.08	1.00E-04
Traella limestone	0.1 / 0.01	0.02	1.00E-06
Yarraloola conglomerate	10.0 / 1.0	0.05	1.00E-04
Calibrated in Stage 2 of this study (Layers 4 - 15)			
Kh = Kv			
Weathered zone - regional	1.0 / 0.1	0.08	1.00E-05
Weathered zone - northwest	2.0 / 0.2	0.08	1.00E-05
Weathered zone – northeast layer 1	5.0 / 0.5	0.08	1.00E-05
Weathered zone – northeast	0.75 / 0.075	0.08	1.00E-05
Weathered zone - central	0.08 / 0.008	0.04	1.00E-05
Weathered zone – south and southeast	0.01 / 0.001	0.04	1.00E-05
Weathered zone – NE Fault-1 zone	100.0 / 100.0	0.02	1.00E-05
Mt Sylvia shale	0.0001	0.01	1.00E-06
Weeli Wolli formation / yandicoogina shale	0.0003	0.01	5.74E-07
Joffre member	0.01	0.01	9.86E-07
Whaleback shale / dales gorge member	0.001	0.01	1.00E-07
Mt McRae shale	0.0001	0.01	1.00E-06
Fortescue Group (undifferentiated)	0.005	0.01	9.92E-07

5.8.2 History match pit inflows / abstraction rates

Predicted monthly inflows expressed as kL/d for the various pit sumps are presented below graphically in Figure 5-2 – Figure 5-5 (all are presented to a consistent scale). The inflows to the various reporting areas are consistent with the observed inflows, with generally good agreement between magnitude and trends for all four areas considered.

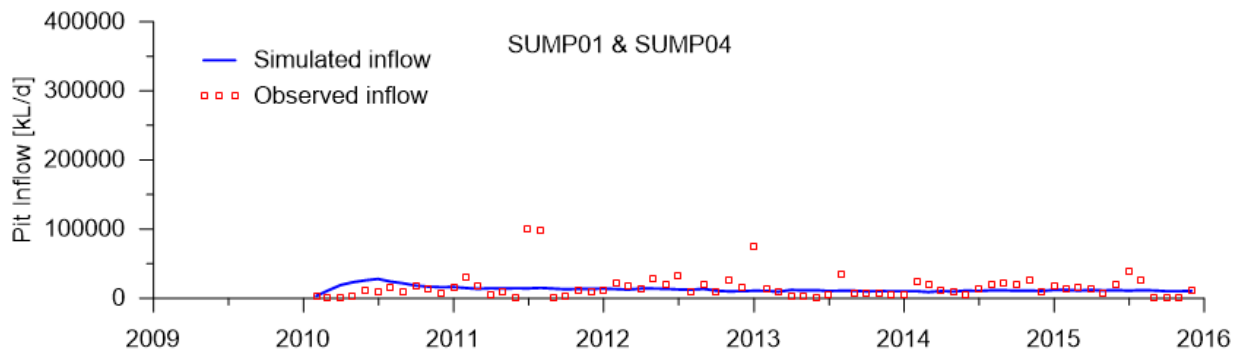


Figure 5-2 Pit inflows for Sump01 & Sump04 calculated from the calibrated model.

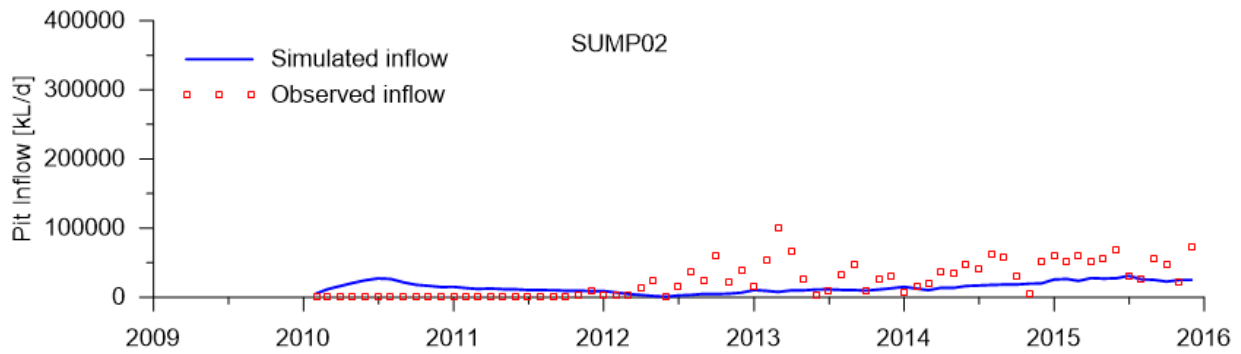


Figure 5-3 Pit inflows for Sump02 calculated from the calibrated model.

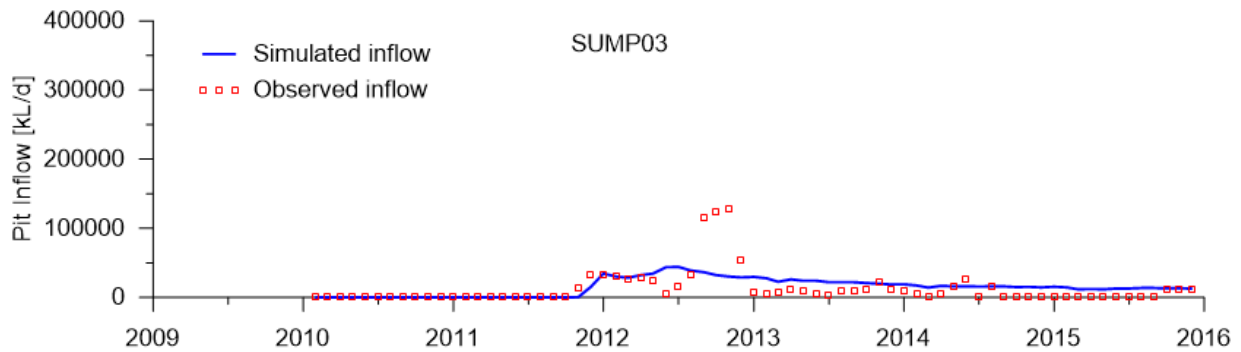


Figure 5-4 Pit inflows for Sump03 calculated from the calibrated model.

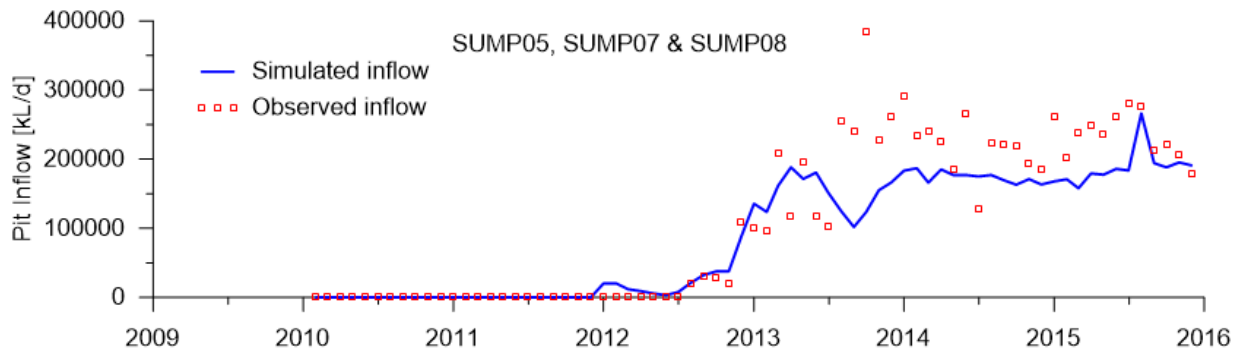


Figure 5-5 Pit inflows for Sump05, Sump07 & Sump08 calculated from the calibrated model.

5.9 History match groundwater levels

The simulated and observed groundwater levels for all the observation sites in the model domain are presented in Appendix E. The vibrating wire piezometer data are presented in Appendix F. Generally the modelled groundwater levels are consistent with the observed levels and trends.

To provide feedback about the performance of the calibration process the groundwater observation sites were categorized into observation groups based on sites location and type. PEST provides performance statistics relating to the modelled vs measured fit, the performance of each of the observation groups are presented in Appendix G.

Overall the root means square of all observations was 10 metres, it should be noted that this value is biased to the observations in the dewatering bores, where the misfit of individual observation was around 100 metres. It is expected that the misfit between groundwater levels and dewatering bores is related to

**SINO EXPANSION LIFE OF MINE GROUNDWATER MODEL
GROUNDWATER CALIBRATION AND SENSITIVITY**

attempting to model highly variable single point measurements taken at monthly intervals within a pumped bore using pumping rates averaged over monthly intervals.

The RMS error (reported as "Standard error" by PEST) for the superficial sediments is generally less than 1 metre with RMS errors of less than 3 metres for the observation group s_alluv. All standard errors are reported in Appendix G.

5.10 Groundwater contours

Regional groundwater contours were extracted from the model for timestep at 42370d, which correspond with dates 01/01/2016 and are presented below in Figure 5-6.

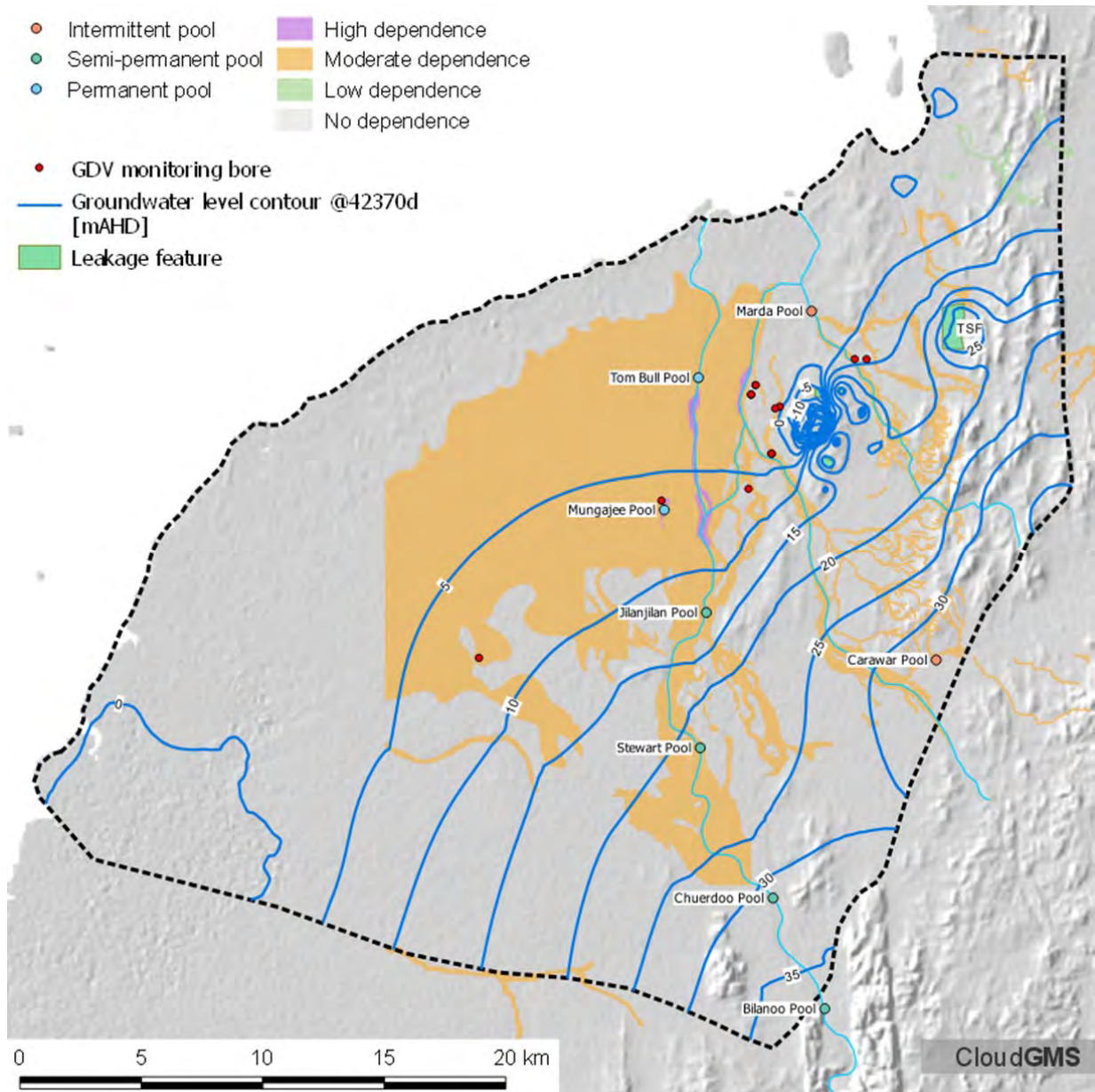


Figure 5-6 Groundwater contours at 42370d (01/01/2016) showing mounding beneath the leakage features represented in the model including the TSF to the northeast of the pit.

5.11 Historic water budget

The water balance closure for the entire model domain is presented below as total volumes and average annual volumes in Table 14.

The in \out flow components for the entire model domain are presented below in Figure 5-7 and as annual volumes in Appendix H.

The estimated inflow from the lower Fortescue in 1984-85 was estimated at 22 GL and the average annual recharge (assumed to be for the period 1983-1993) was estimated at 11 GL (Commander, 1993). The model compares favourably with these figures, with river recharge for the year 1984-85 was estimated at 18 GL and the average annual river recharge for the period 1983 – 1993 at around 10 GL.

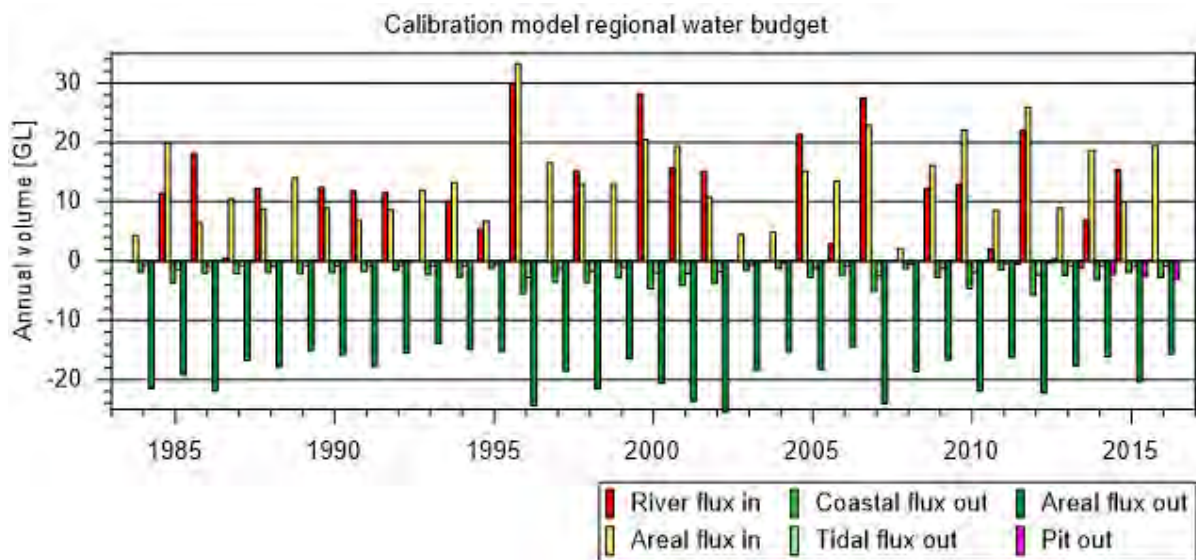


Figure 5-7 Model domain in / out flow water balance components.

It should also be noted that some years show quite high recharge due to rainfall (areal flux in), with no or minimal river recharge (for example 1989, 1993, 1997 and 2006) indicating that the river gauging station may not have been operating during these periods. Having said this, it should also be noted that the rainfall recharge is scaled from SILO data drill data and that localised rainfall events may generate higher than expected recharge. However, having said this, generally for the larger events the rainfall recharge and river recharge appear to track each other. Therefore, the model is possibly underestimating the inflows due to river recharge.

Storage capture and release are almost the same, suggesting that the system is in dynamic equilibrium. The baseline distributed sink term is approximately 20 GL/yr.

Model domain in \out fluxes presented above in Figure 5-7 for the period 01/01/1983 to 01/01/2016 are presented in Appendix G.

SINO EXPANSION LIFE OF MINE GROUNDWATER MODEL
GROUNDWATER CALIBRATION AND SENSITIVITY

Table 14 Calibrated model total water budget for the period 01/01/1983 to 01/01/2016.

Component	Out m ³	In m ³	Out GL/yr	In GL/yr
Specified head BC	-1.58E+08	1.07E+07	-4.80	0.32
Specified flux BC	0	0	0.00	0.00
Transfer BC	-1.41E+03	3.42E+08	0.00	10.36
Wells	-5.71E+06	0	-0.17	0.00
Distributed sink (-) / source (+)	-6.46E+08	4.44E+08	-19.59	13.46
Storage capture (-) / release (+)	-6.64E+08	6.75E+08	-20.12	20.47
Total	-1.47E+09	1.47E+09	-44.69	44.61
Imbalance %	-0.17			

5.12 Sensitivity

Sensitivity is the variation in the value of one of more output variables (such as hydraulic heads) due to changes in the value of one or more inputs to a groundwater flow model (such as hydraulic properties or boundary conditions). Sensitivity analysis is a procedure for quantifying the response of a model's output to an incremental variation in model parameters, stresses, and boundary conditions.

Parameter sensitivities are calculated by PEST during determination of the Jacobian matrix. PEST calculates the composite sensitivity of each adjustable parameter as the magnitude of the vector comprising the weighted column of the Jacobian matrix corresponding to that parameter, divided by the number of observations (Doherty, 2016). Composite sensitivities of the objective function to changes in each of the parameters for each of the observation groups are presented below. The observation groups used to determine the composite sensitivities were separated into the following observation groups:

- Monitoring bores within the footprint of the 2060 East and West Pits
 - east_pit
 - west_pit
- Monitoring bores outside the footprint of the 2060 East and West Pits
 - e_mine
 - n_mine
 - s_mine
- Dewatering monitoring bores
 - e_dewater – dewatering bores located to the east of the pit
 - ne_dewater – dewatering bores located to the northeast of the pit
 - pit_dewater – dewatering bores located within the current pit
 - s_dewater – dewatering bores located to the south of the pit
 - se_dewater – dewatering bores located to the southeast of the pit
- Alluvial bores
 - fcp (DoW monitoring bores installed in the superficial sediments)
 - e_alluv (CPM monitoring bores installed in the superficial sediments)
 - n_alluv (CPM monitoring bores installed in the superficial sediments)
 - s_alluv (CPM monitoring bores installed in the superficial sediments)

**SINO EXPANSION LIFE OF MINE GROUNDWATER MODEL
GROUNDWATER CALIBRATION AND SENSITIVITY**

- TSF monitoring bores (tsf)
- Bores external to the mine infrastructure (ex_mine)

The locations of the observation groups are presented below in Figure 5-8.

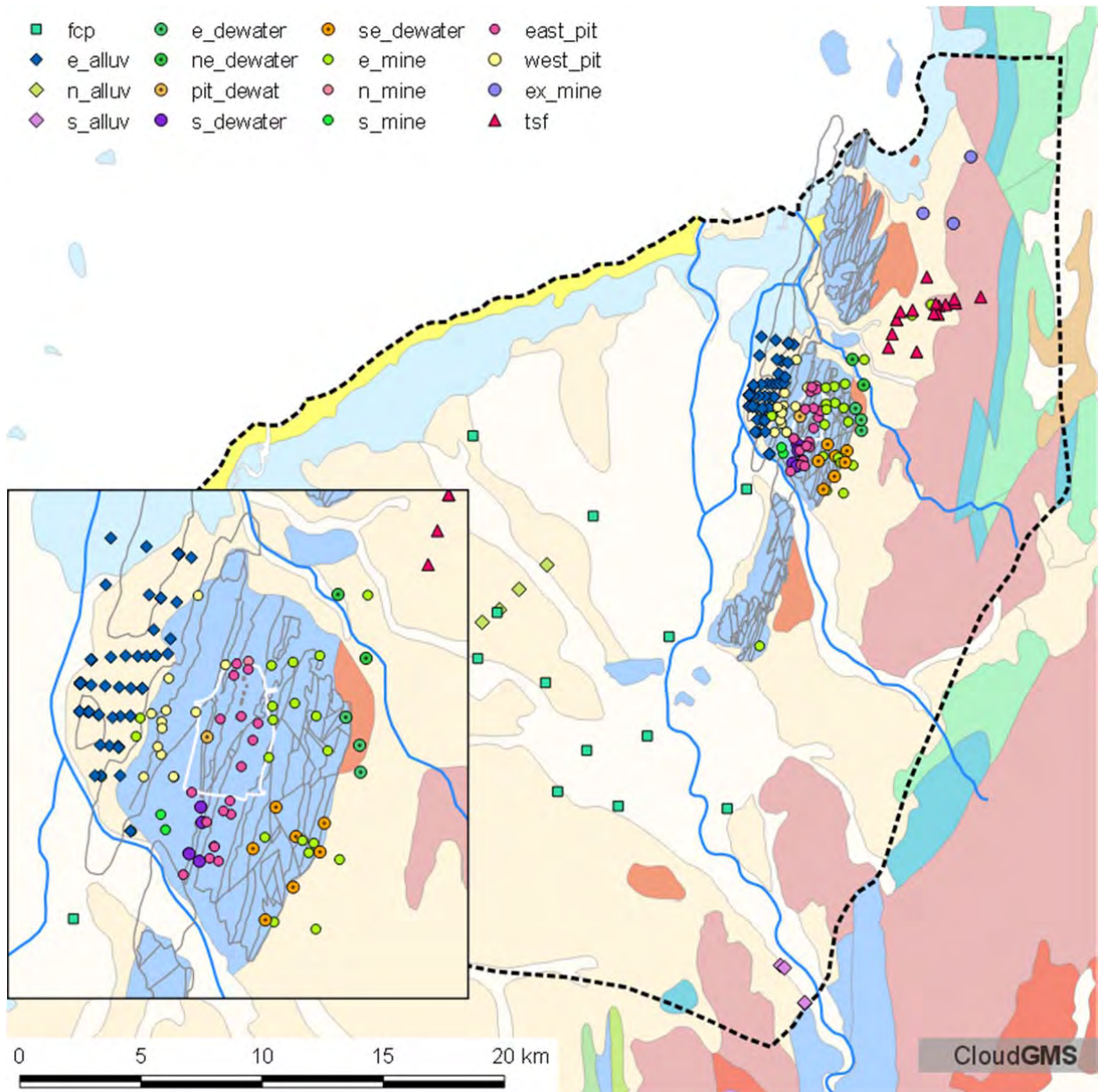


Figure 5-8 Monitoring bore observation groups used to assess the effectiveness of the calibration process.

Sensitivity analysis was conducted on the Stage 2 model to examine how the calibrated parameters affected the groundwater levels and pit inflows.

The hydraulic conductivity, specific yield and compressible storage parameters for selected pilot points and each of the HSUs were adjusted and the changes to the objective function were assessed to determine parameter sensitivity. The results of this analysis are presented below in Figure 5-9, Figure 5-10 and Figure 5-11.

SINO EXPANSION LIFE OF MINE GROUNDWATER MODEL

GROUNDWATER CALIBRATION AND SENSITIVITY

The scale of the composite sensitivity is different for each graph and as such the results for each of the observation groups presented should be considered individually as they pertain to a different objective function component base value (refer to Appendix G).

Two groups of pilot points were adjusted kxy₄₋₂₆ tied to pilot points in the centre of the 2060 West Pit and kxy₄₋₃₇ tied to pilot points along the contact between the superficial sediments and the weathered Hamersley Group to examine the effect of adjusting hydraulic parameters in these areas on the available observations. Generally adjusting these parameters had no appreciable impact on the objective function indicating that the information in the available observation data provides limited constraints on the hydraulic parameters in this area. A conclusion from this study is that further work is conducted along the western margin of the West Pit to reduce this uncertainty.

Parameters with the following prefixes were considered in the sensitivity analysis:

- 'fac' are recharge timeseries scaling factors;
- 'kxy' are hydraulic conductivity of each HSU zone;
- 'kxy₄₋' are hydraulic conductivity pilot points for HSU 4;
- 'sy₄₋₋' are specific yield pilot points for HSU 4;
- 'ss' are specific storage for each HSU zone; and
- 'trans₁' are transfer in / out for the model domain.

The locations of pilot points for hydraulic conductivity, specific yield and are shown above in Figure 5-1.

The results suggest that the available observation data contains limited information about many of the adjustable parameters considered given that many of the parameters are beyond the footprint of the pit. The effects of stresses associated with either dewatering or development of the pit have not propagated far beyond the immediate area of impact.

SINO EXPANSION LIFE OF MINE GROUNDWATER MODEL
GROUNDWATER CALIBRATION AND SENSITIVITY

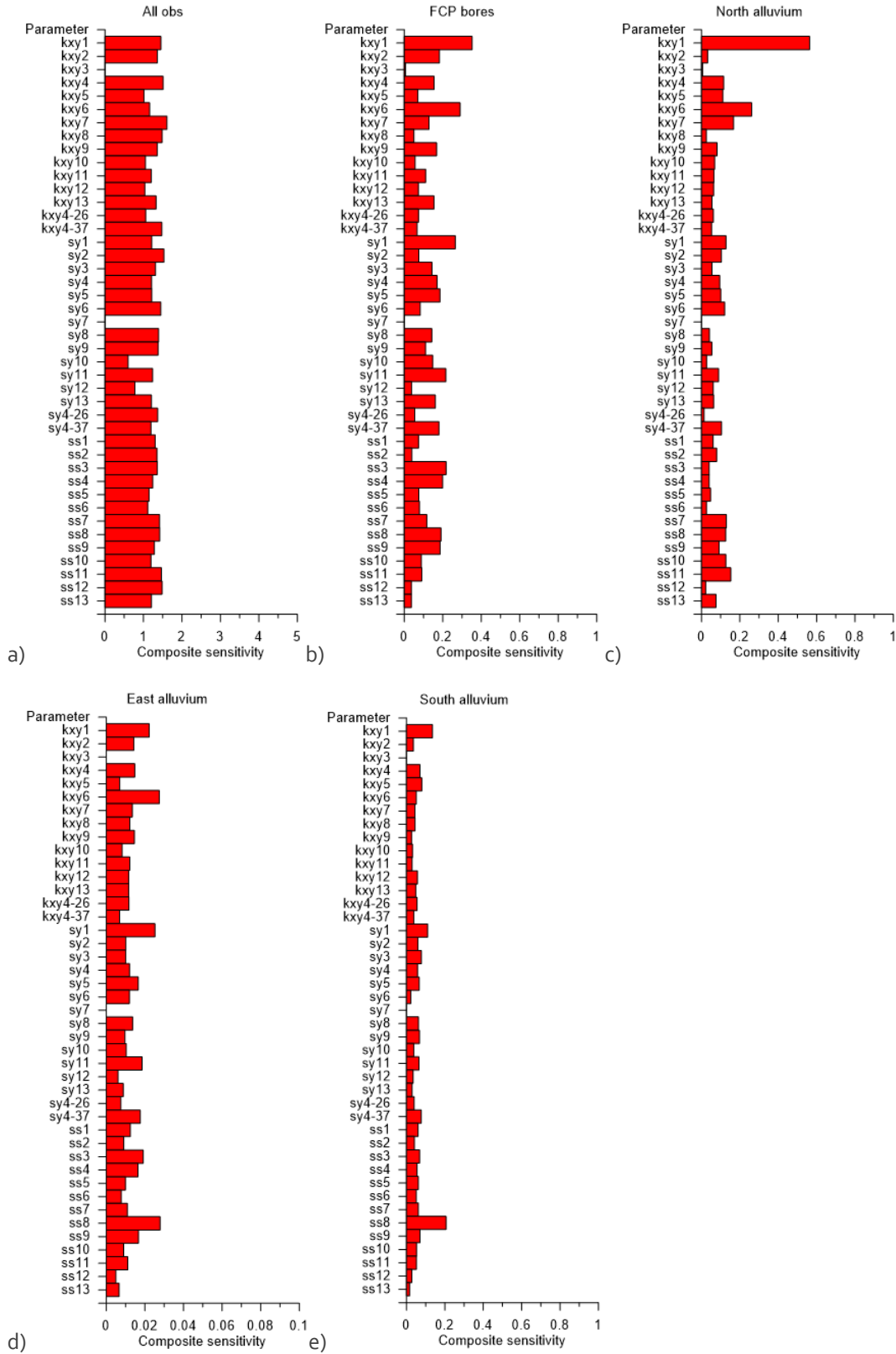


Figure 5-9 Sensitivities of observation groups to parameter variations for observation groups a) All obs bores, b) FCP bores, c) North alluvium, d) East alluvium and e) South alluvium

SINO EXPANSION LIFE OF MINE GROUNDWATER MODEL
GROUNDWATER CALIBRATION AND SENSITIVITY

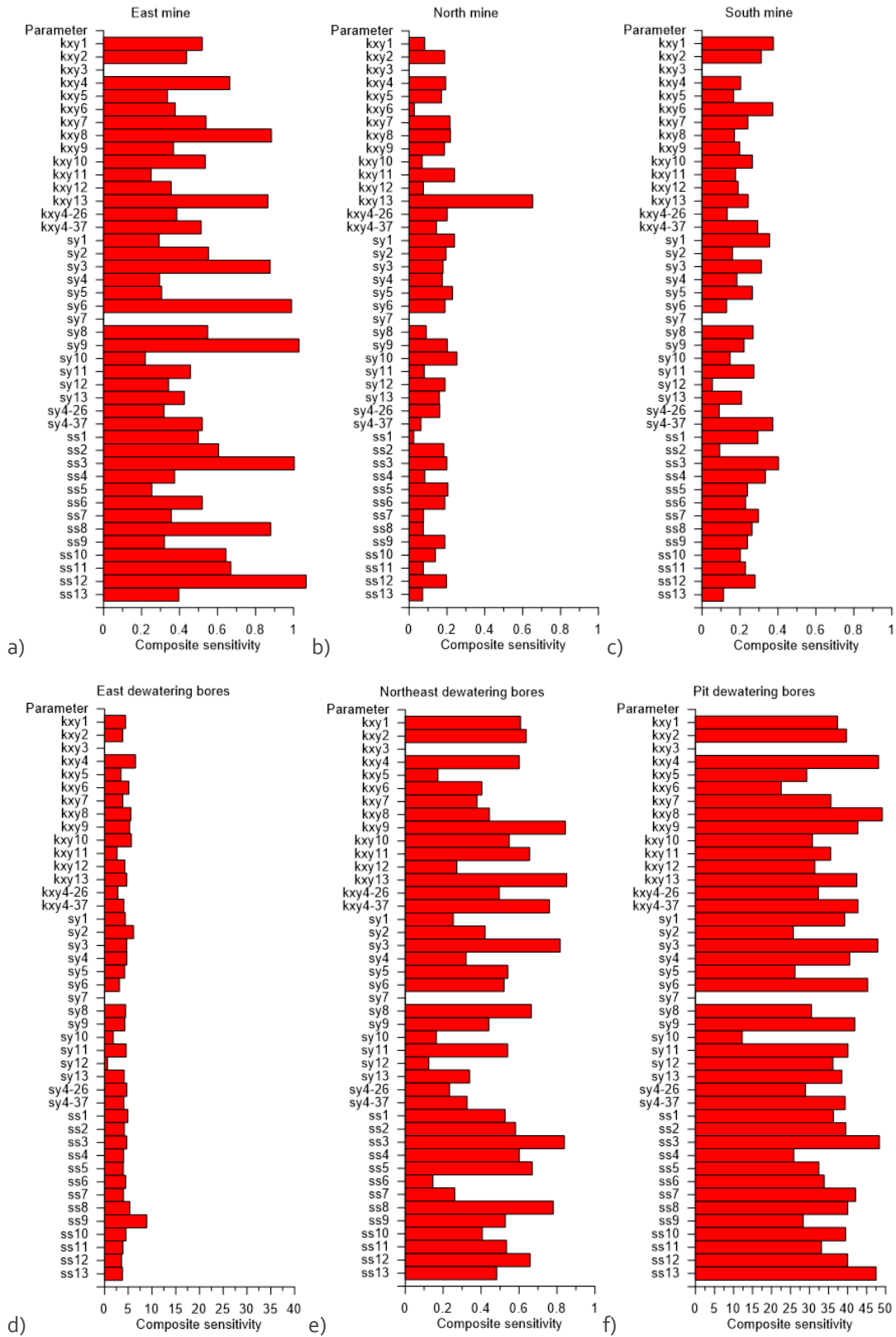


Figure 5-10 Sensitivities of observation groups to parameter variations for observation groups a) East_mine, b) North_mine, c) South mine, d) East dewatering bores, e) Northeast dewatering bores, and f) Pit dewatering bores.

SINO EXPANSION LIFE OF MINE GROUNDWATER MODEL
GROUNDWATER CALIBRATION AND SENSITIVITY

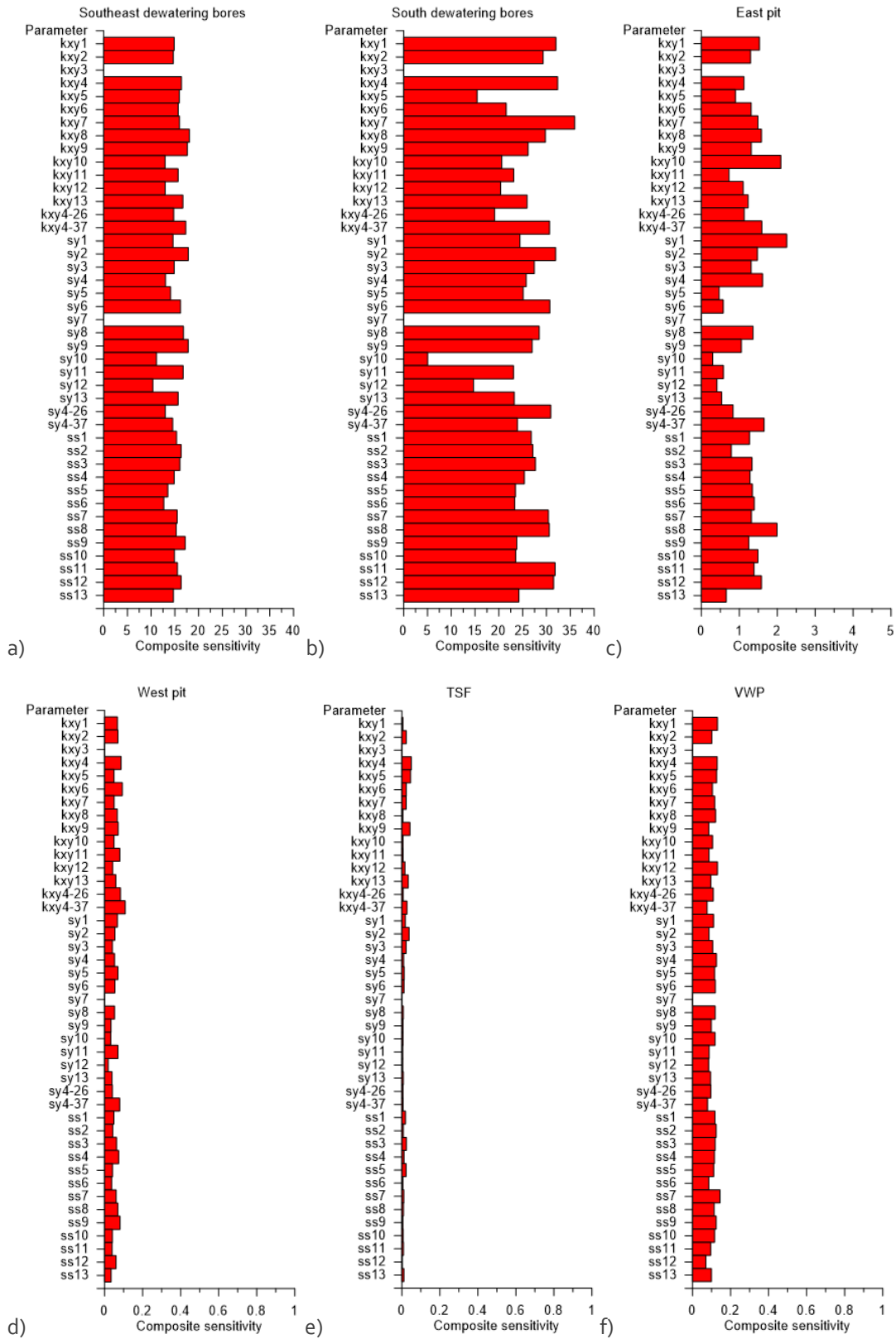


Figure 5-11 Sensitivities of observation groups to parameter variations for observation groups a) Southeast dewatering bores, b) South dewatering bores, c) East pit, d) West pit, e) TSF, and f) VWP

5.13 Summary calibration & sensitivity

Although the calibrated model provides reasonable matches to the available observation data, the majority of the available data only provides information relating to the weathered material in the vicinity of the pit, and often within the footprint of the final 2060 pit shell.

The limited sensitivity of observation groups to changes in the hydraulic parameters of the weathered rocks of the Hamersley Group for the area along the western margin of the West Pit suggests that the available information is insufficient to constrain the parameters in this area.

Although a number of parameters deviated significantly from their preferred value during calibration, particularly the area underlying NE Waste Dump, the impact of these parameters is unlikely to have a bearing on the impacts to the groundwater resources within the superficial sediment aquifers to the west (for reasons outlined below).

The groundwater levels in the superficial sediments, which comprise the aquifers sustaining the GDVs and pools in the region, generally reflect the natural stresses (ie recharge and discharge processes). The hydraulic parameters such as specific yield have been constrained by the groundwater level response and the estimated recharge to the superficial aquifer system, therefore, the derived hydraulic parameters are biased by the assumptions used to estimate these values.

To overcome the limited information available from the current datasets uncertainty analysis has been undertaken for the LoM forecast and the cumulative impact LoM scenarios (section 7). The uncertainty analysis has been conducted with an emphasis on the hydraulic properties of the weathered rocks of the Hamersley Group along the western margin of the West Pit to examine the impacts of assuming similar hydraulic parameters as observed in the majority of the current pit area.

6 Sino Iron Expansion forecast life of mine and post closure impacts

6.1 Introduction

The LoM and post closure impacts of the Sino Iron Continuation Project mine have been modelled using the calibrated model as a basis with two scenarios considered.

- Life of mine impacts for the period of mining from 2016 – 2060; and
- Post closure mine impacts scenario assuming all sources associated with mining activities cease after 2060.

The results for the LoM and pit lake models are presented as timeseries groundwater levels and as final groundwater level contours. The possible long term impacts to the groundwater quality in the vicinity of the Sino Iron pit have been investigated using stream line analysis (section 6.5) on the final timestep of each model.

6.1.1 Description of life of mine (LoM) forecast scenario

The LoM forecast scenario was designed to investigate the effect of the pit development on groundwater flow dynamics in the area. The following assumptions were made in predictive model runs:

- The model was run for a forecast period of 44 years from the end of the calibration period (01/07/2016) to the projected end date of the mine (01/01/2060).
- Pit shell elevations were applied to the model as per section 2.8;
- Groundwater dewatering is via sumps in accordance with current operations. No groundwater dewatering occurs from production bores;
- Groundwater recirculation and leakage features that have occurred historically as a result of the inability to take water away from the pit area (detailed in Section 2.6) have been excluded (ie pit sump water is assumed to be transferred away from the vicinity of the pit);
- All model parameters were taken from the calibrated model;
- Initial conditions were taken from the final heads of the calibrated model corresponding to 42370d (01/01/2016);
- The time series of river inflows in the calibration model were repeated to obtain the 44 year time series used to calculate river recharge for the forecast model; and
- Time series climatic inputs were replaced by the long term average rainfall and evaporation rates for the period 1983-2016 (this was done to reduce runtimes).

6.1.2 Description of the post closure pit-lake impacts scenario

The post closure impacts scenario was based on the life of mine scenario with the following additional assumptions / settings:

- Initial heads were taken from the final timestep of the LoM scenario (58441d or 01/01/2060);

- The post closure model runs for an additional 100 years with the final timestep ending at 94965d (01/01/2160);
- Removing the seepage face boundary conditions representing the pit; and
- Hydraulic parameters within the pit void were replaced with parameters representative of a free water body (ie hydraulic conductivity 2 orders of magnitude greater than the host rocks 1 m/d and drain / fillable porosity of 1).

The intermittent nature of the flows in the Fortescue River meant that a steady state model of the system was not deemed appropriate to assess the post closure impacts. The model was run to an approximate dynamic equilibrium identified by levelling of the groundwater levels in the superficial aquifer.

6.2 LoM and post closure pit lake results using calibrated model

6.2.1 Reporting areas for pit inflows during LoM

The pit inflow results are presented in terms of the following inflow areas:

- Total pit
- East Pit
- West Pit and
- Alluvial intersection with West Pit

The distribution of nodes used to generate the inflow budgets are presented below in Figure 6-1.

SINO EXPANSION LIFE OF MINE GROUNDWATER MODEL
GROUNDWATER LOM AND POST CLOSURE FORECASTS

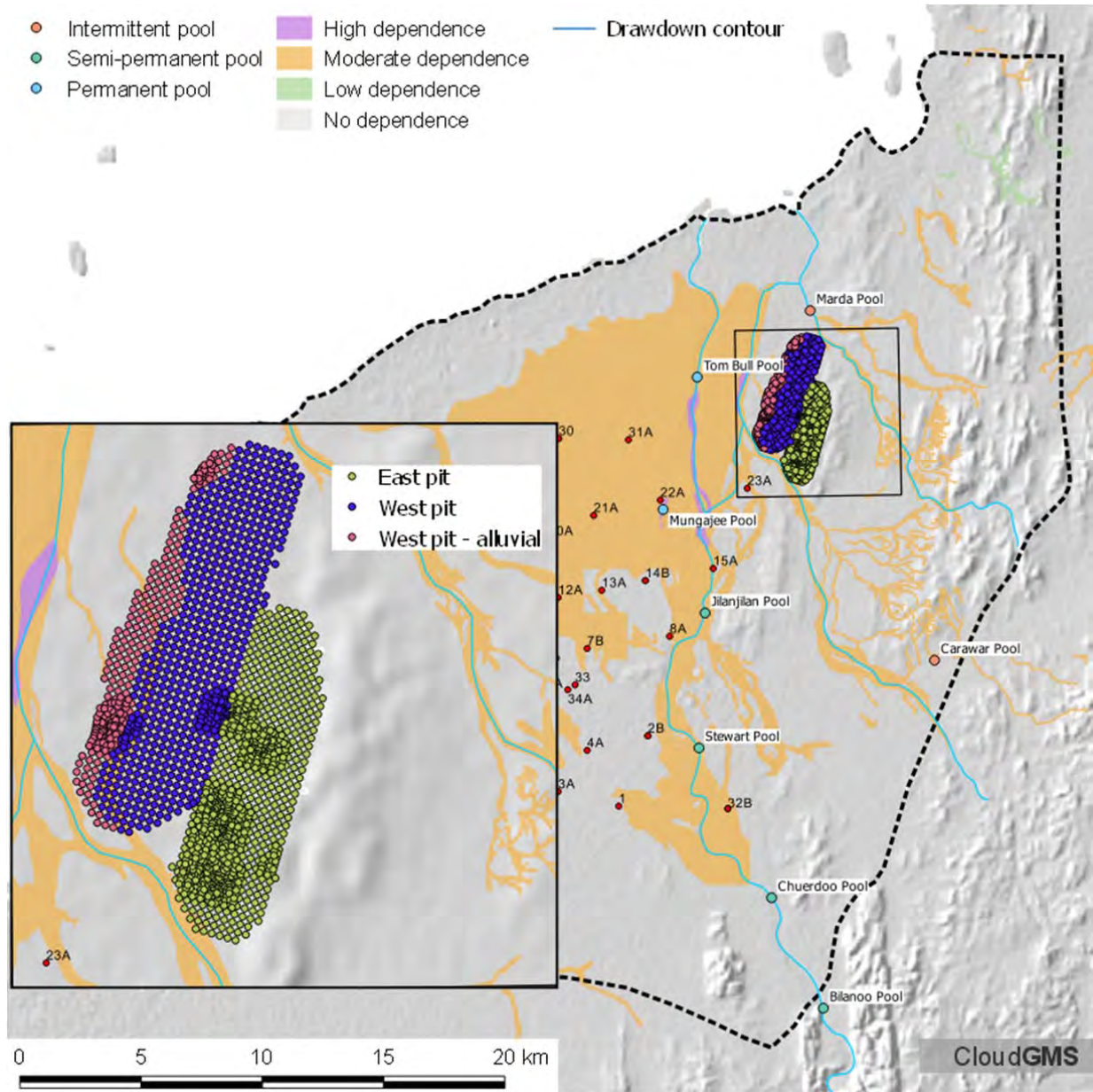


Figure 6-1 Nodes used to calculate pit inflows presented in the following plots and the locations of significant sites considered to examine impacts to groundwater levels.

6.2.2 Pit inflows during LoM

The pit inflows estimated by the calibrated groundwater model during the LoM are presented below in Figure 6-2, where a) is the total inflows to the pit, b) is the inflows to the West Pit; c) is the inflows to the East Pit; and d) is the contribution to the West Pit from the area where the pit intersects the superficial sediments (referred to as West Pit – alluvial).

**SINO EXPANSION LIFE OF MINE GROUNDWATER MODEL
GROUNDWATER LOM AND POST CLOSURE FORECASTS**

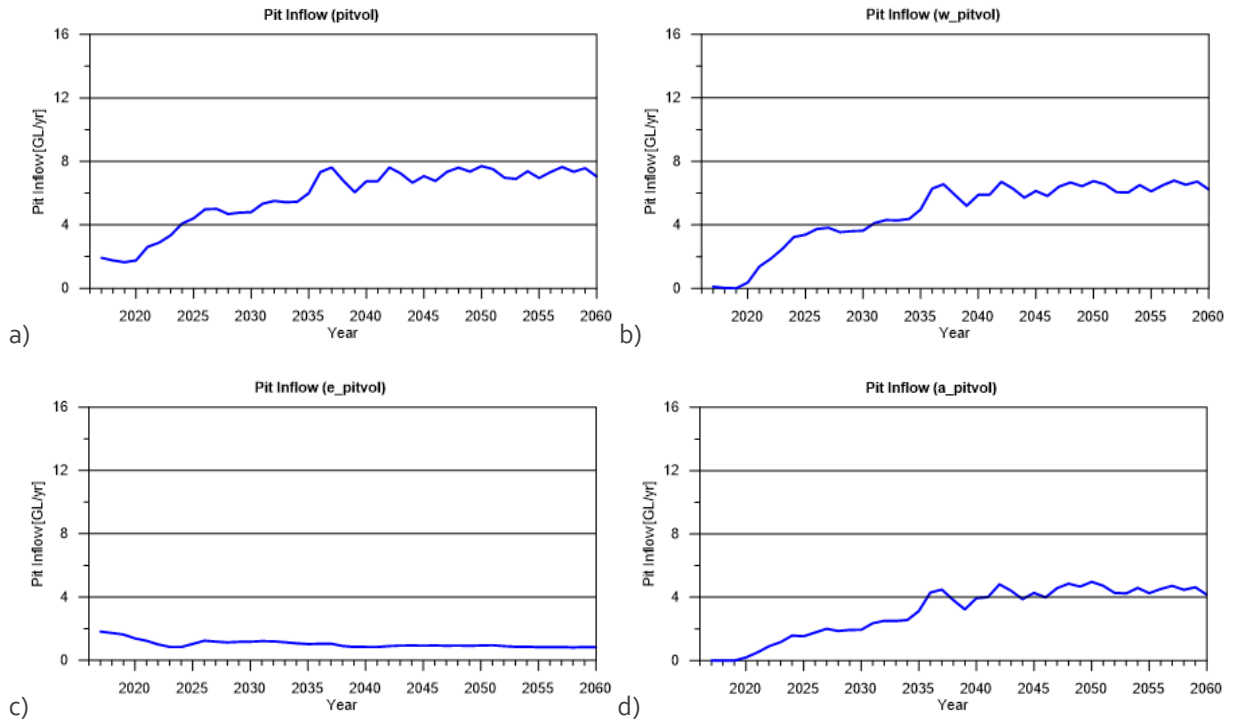


Figure 6-2 Calculated inflows for a) the total pit b) the West Pit c) the East Pit and d) the area where the pit intersects the superficial sediments. The inflow presented for the superficial sediments are also included in the West Pit volumes.

The corresponding total inflows to the Sino Iron pits are presented below in Table 15.

Table 15 Annual total inflows to the Sino Iron pit.

Year	Inflow [GL/yr]	Year	Inflow [GL/yr]
2017	-1.93	2039	-6.06
2018	-1.75	2040	-6.74
2019	-1.64	2041	-6.75
2020	-1.75	2042	-7.61
2021	-2.61	2043	-7.23
2022	-2.87	2044	-6.65
2023	-3.33	2045	-7.07
2024	-4.08	2046	-6.76
2025	-4.42	2047	-7.33
2026	-4.98	2048	-7.61
2027	-5.01	2049	-7.36
2028	-4.68	2050	-7.70
2029	-4.77	2051	-7.50
2030	-4.80	2052	-6.97
2031	-5.33	2053	-6.90
2032	-5.51	2054	-7.38
2033	-5.43	2055	-6.95
2034	-5.45	2056	-7.33
2035	-6.00	2057	-7.64
2036	-7.33	2058	-7.35
2037	-7.61	2059	-7.57
2038	-6.78	2060	-7.05

6.2.3 Groundwater level impacts at regional reference monitoring bores

Groundwater level hydrographs at the regional groundwater dependent vegetation (GDV) reference monitoring sites FCP10A, FCP22A and FCP23A are presented below in Figure 6-3 a, b & c respectively.

Groundwater levels for the monitoring bores outside of the footprint of the Sino Iron pits are also presented in Appendix I.

The locations of the regional monitoring sites and the permanent pools are presented above in Figure 2-24 (section 2.11.6). Groundwater levels respond as expected with sites closer to the pit showing the greatest drawdown and the sites further from the pit showing less impact.

FCP10A is located at approximately 15 km to the south west of the Sino Iron pits. The groundwater levels at FCP10A shows minimal impact, with a subtle decline in groundwater levels over the 144 year period modelled.

FCP22A is located approximately 4.8 km to the south west of the Sino Iron pits adjacent to Mungajee Pool. The groundwater levels at FCP22A show similar response to those presented for Mungajee Pool (see below). Groundwater levels show maximum declines of approximately 2 metres and appear to reach dynamic equilibrium at this level after approximately 2080.

FCP23A shows a gradual decline by approximately 3-4 metres during the LoM. The groundwater levels continue to decline following post closure and appear to reach dynamic equilibrium at a level of 4-5 metres below initial levels for the duration of the post closure scenario starting at 2080. The current trigger value at this site is 4.20 mAHD, and it is likely that this value will be consistently exceeded by 2040.

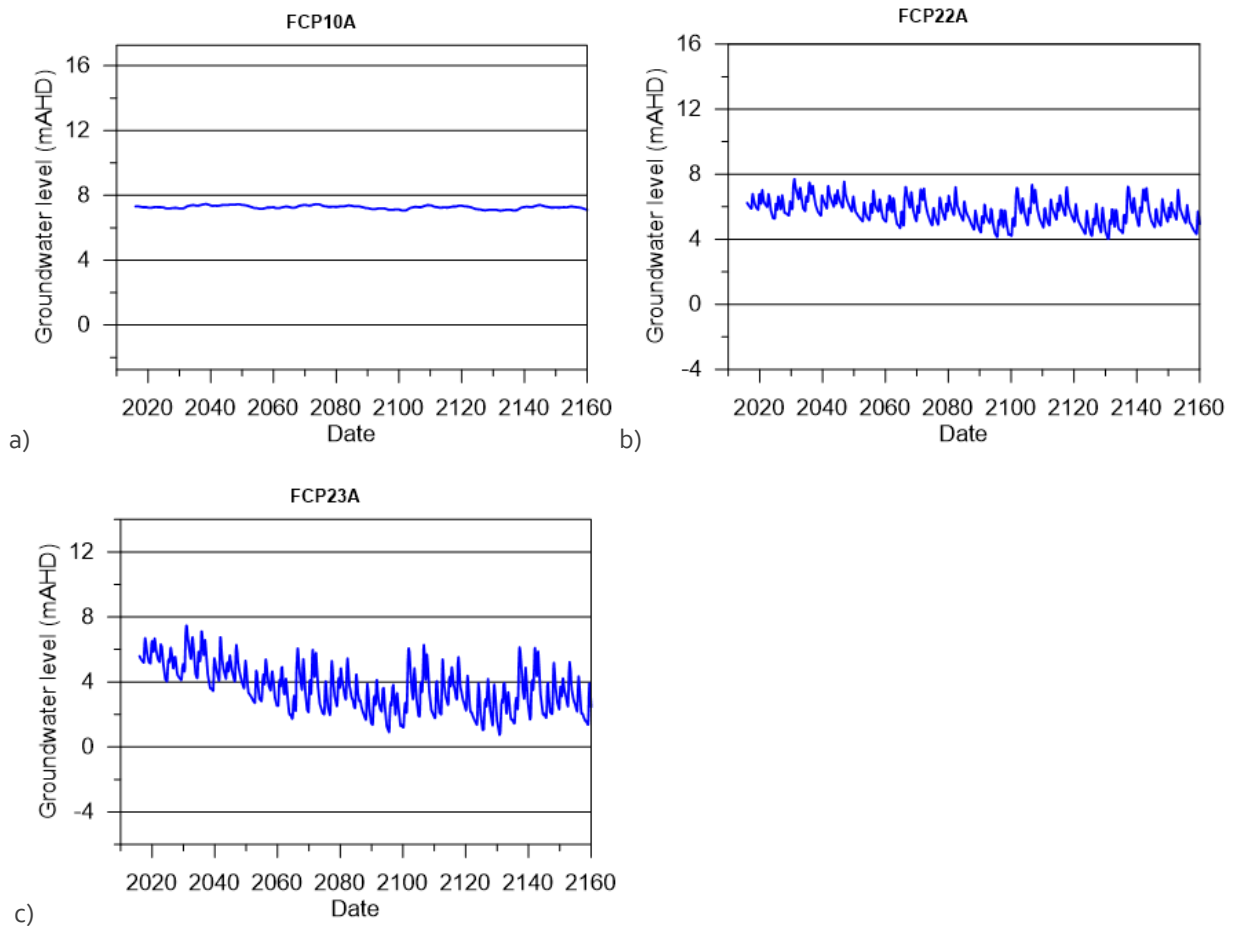


Figure 6-3 Groundwater level response over the modelled LoM and post closure periods at regional reference monitoring sites a) FCP10A b) FCP22A and c) FCP23A.

6.2.4 Groundwater level impacts at groundwater dependent vegetation (GDV) monitoring bores

Groundwater level hydrographs have been generated at selected monitoring sites 07RC149, 07RC156 are presented below in Figure 6-4 a & b and sites 09AC490 and 09AC534 in Figure 6-5 a & b.

A sub-set was selected due to the clustered nature of some of the monitoring sites with several sites providing the same response. It is considered that the sites presented are representative of the sites identified above in Table 2. The locations of the regional monitoring sites and the permanent pools are presented above in Figure 2-24 (section 2.11.6).

Groundwater levels for the monitoring bores outside of the footprint of the Sino Iron pits are also presented in Appendix I.

07RC149

The groundwater levels at 07RC149 show a decline in groundwater levels of approximately 10 metres over the 144 year period modelled. 07RC149 is a zone 2 GDV monitoring site and has a trigger 3 standard deviations below the baseline mean ($\mu= 4.20$ mAHD; $\sigma = 1.0$ m). This trigger is exceeded by the end of mining and continues to be exceeded following post closure. The 10 metre decline in groundwater levels occurs over a period of approximately 80 years, which results in a 0.125 metres per year rate of decline. At

these rates of decline it may be possible that GDV would be capable of adapting to the changes to the groundwater regime.

07RC156

07RC156 shows a decline by nearly 12 metres below the initial level during the LoM, however, it recovers following mine closure to approximately 8 metres below the initial water level and appears to reach dynamic equilibrium at this level soon after closure of the pit for the duration of the post closure scenario. 07RC156 is a zone 1 GDV monitoring site and has a trigger 2 standard deviations below the baseline mean ($\mu = 6.00$ mAHD; $\sigma = 1.0$ m). This trigger is exceeded by mid 2020 and continues to be exceeded for the duration of mining and the post closure.

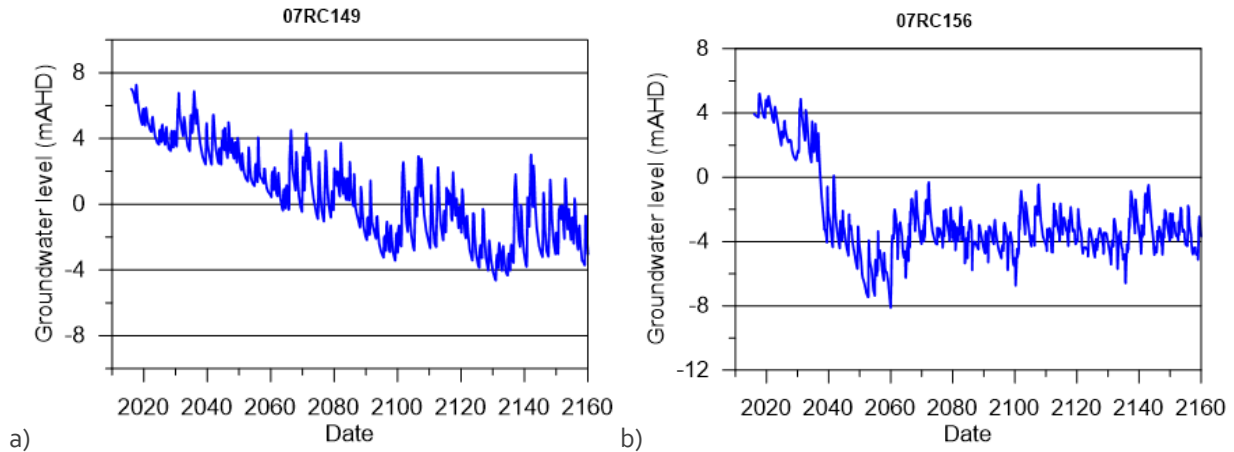


Figure 6-4 Representative GDV monitoring sites around the Sino Iron pit a) 07RC149 and b) 07RC156.

07AC490 and 07AC534

09AC490 and 09AC534 show declines of nearly 6 metres below the initial level during the LoM and appears to reach dynamic equilibrium at this level soon after closure of the pit for the duration of the post closure scenario. 09AC490 is a zone 1 GDV monitoring site and has a trigger 2 standard deviations below the baseline mean ($\mu = 2.70$ mAHD; $\sigma = 1.1$ m). 09AC534 is a zone 1 GDV monitoring site and has a trigger 2 standard deviations below the baseline mean ($\mu = 2.10$ mAHD; $\sigma = 0.7$ m). These triggers are exceeded by mid 2020 and continue to be exceeded for the duration of mining and the post closure. The 6 metre decline in groundwater levels occur over a period of approximately 30 -40 years, which results in a rate of decline of between 0.2 to 0.15 metres per year. At these rates of decline it may be possible that GDV would be capable of adapting to the changes to the groundwater regime.

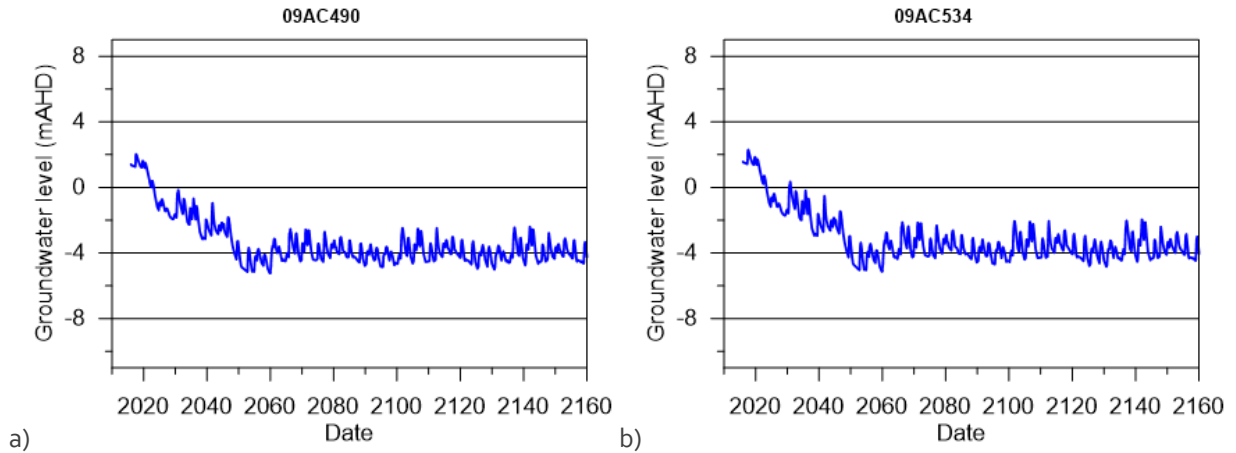


Figure 6-5 Representative GDV monitoring sites around the Sino Iron pit a) 09AC490 and b) 09AC534.

6.2.5 Groundwater level impacts at identified permanent pools

The groundwater levels at the permanent pools identified in the study area Mungajee Pool and Tom Bull Pool are presented below in Figure 6-6 a & b respectively.

The locations of the regional monitoring sites and the permanent pools are presented above in Figure 2-24 (section 2.11.6).

The maximum groundwater level decline at Mungajee Pool is approximately 1-2 metres.

The groundwater level response at Tom Bull Pool is approximately 1-2 metres below the initial groundwater levels. Although the groundwater level decline is limited by the influence of the tidal section of the river, streamline analysis (refer below to section 8.5) suggests that poorer quality groundwater associated with the tidal flats is unlikely to migrate towards Tom Bull Pool.

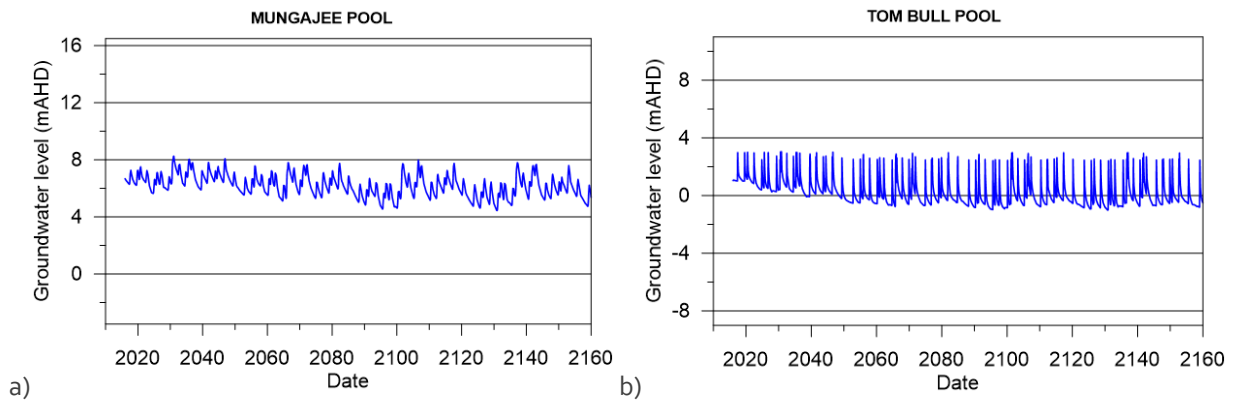


Figure 6-6 Groundwater level response over the modelled LoM and post closure periods at permanent pool sites at a) Mungajee Pool and b) Tom Bull Pool.

6.2.6 Final groundwater drawdown contours

Groundwater drawdown contours at the end of mining 58441d (01/01/2060) using the calibrated parameters are presented below in Figure 6-7. The contours have been generated at 0.5 m, 1 m, 5 m and then at 10 metre intervals. The contours provide an overview of the extent of groundwater impacts at the end of

SINO EXPANSION LIFE OF MINE GROUNDWATER MODEL
GROUNDWATER LOM AND POST CLOSURE FORECASTS

mining. To provide context, they have been plotted over the mapped groundwater dependent vegetation classes, the locations of pools and key monitoring sites.

Tom Bull Pool show declines of between 1 – 5 metres and Mungajee Pool shows less than 1 metre drawdown.

The detailed assessment of groundwater level response at the majority of groundwater dependent vegetation (GDV) monitoring bores (discussed above in section 6.2.3) show groundwater drawdowns of between 5 – 10 metres due to their proximity to the pit.

SINO EXPANSION LIFE OF MINE GROUNDWATER MODEL
GROUNDWATER LOM AND POST CLOSURE FORECASTS

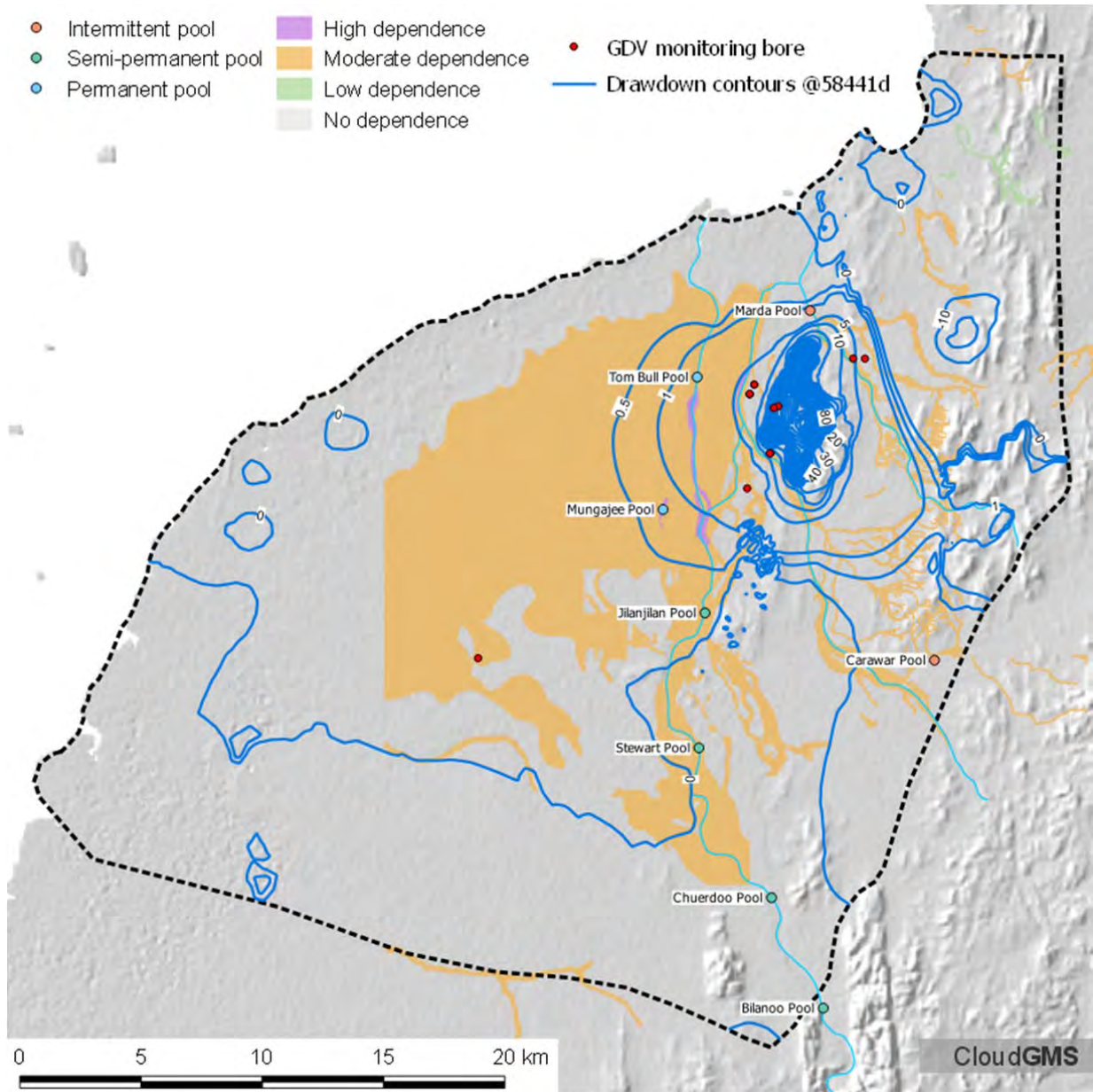


Figure 6-7 Groundwater drawdown contours at the end of mining at 58441d (01/01/2060).

6.3 Water balances

6.3.1 LoM regional water balance

The in / out flows water balance components have been extracted from the model to demonstrate the impacts of the Sino Iron mine on the water resources within the study area. The water balance closure for the entire model domain is presented below as total volumes for the period of the model run and average annual volumes in Table 16. The individual in/out flow components are presented in Appendix J.

SINO EXPANSION LIFE OF MINE GROUNDWATER MODEL
GROUNDWATER LOM AND POST CLOSURE FORECASTS

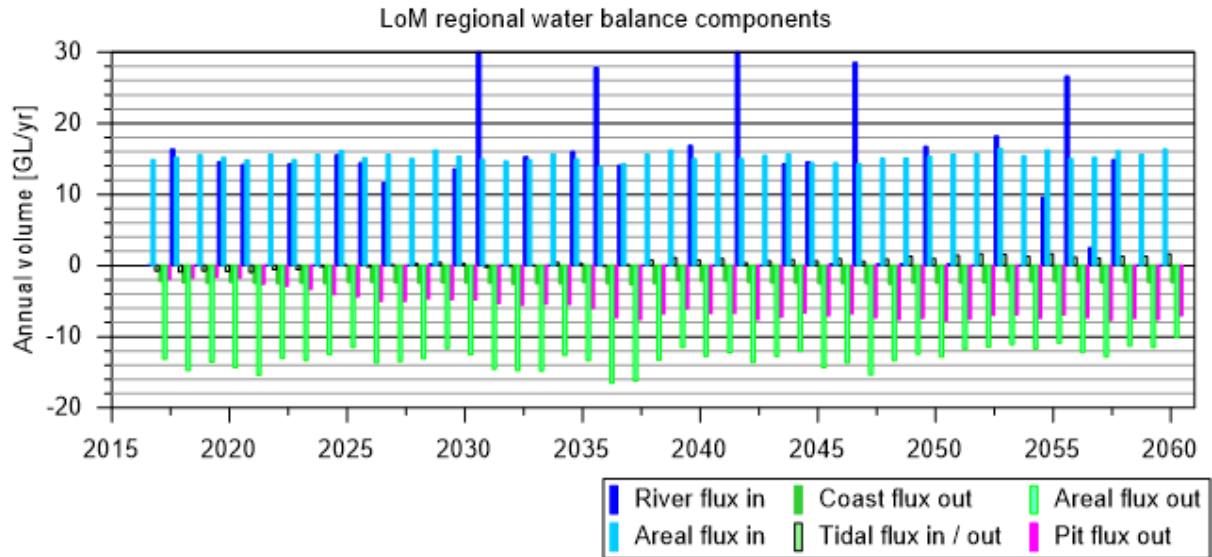


Figure 6-8 LoM (2016 – 2060) annual in / out flow water balance components in GL for the entire model domain.

Note the river flux in for 2030 (45 GL) and 2042 (39 GL) have been clipped to provide a consistent output. The actual fluxes are presented in Appendix J.

It should also be noted that the rainfall has been set to the average annual rainfall, this is reflected in the relatively constant Area Flux In component. The evaporation rate driving the ET fluxes has also been set at the average annual rate, however, there is greater variability in the Areal Flux Out component as this component is also related to the watertable levels.

The tidal boundary switches from net outflow (approx. -0.8 GL/yr) to a net inflow boundary (approx. 1.5 GL/yr) by about year 2025. Areal flux out (representing ET processes in the model) show a declining trend from approximately 2035, suggesting that much of the water removed from the pit is sourced from storage.

Table 16 LoM total water budget for the period 01/01/2016 to 01/01/2060.

Component	Out	In	Out	In
	m ³	m ³	GL/yr	GL/yr
Specified head BC	-3.89E+08	4.69E+07	-8.83	1.07
Specified flux BC	0	0	0.00	0.00
Transfer BC	-2.12E+03	4.27E+08	0.00	9.70
Wells	0	0	0.00	0.00
Distributed sink (-) / source (+)	-7.22E+08	6.44E+08	-16.42	14.63
Storage capture (-) / release (+)	-7.42E+08	7.35E+08	-16.86	16.70
Total	-1.85E+09	1.85E+09	-42.11	42.10
Imbalance %	0.062			

6.3.2 Comparison of LoM water budgets to natural conditions (2016 – 2060)

To provide an easier assessment of the changes to the water budgets presented in the previous section a 'natural' scenario was run where all stresses associated with mining activities were removed to provide a base case for comparison. The results for the LoM phase of mining are presented below in Table 17.

- The specified head boundary conditions, representing the coast and tidal sections of the rivers and the abstraction from the pit, show an outflow of -7.8 GL/yr, which is an increase in the net outflow of approximately -3.9 GL/yr from the natural outflow of -3.9 GL/yr. However, this includes outflows from the pit which over the LoM averages 5.8 GL/yr (refer Appendix J). This means that the pit induces a net inflow (ie combination of decreased outflow and increased inflow) of 1.9 GL/yr at the coast and tidal sections of the river (predominantly at along the tidal sections of the rivers).
- There is a slight increase in inflows from the transfer boundary conditions, representing the non-tidal sections of the rivers. This is due to the reduced groundwater levels around the pit providing additional storage for recharge from the rivers.
- The distributed in / out flow components show a net decrease in outflow, a result of a reduction in evapotranspiration due to the groundwater levels around the pits declining below the root depths used in the evapotranspiration function.

Table 17 Comparison of LoM period 2016 - 2060

Component	LoM 2016 - 2060			Natural 2016-2060			Change
	Out	In	Diff	Out	In	Diff	
	[GL/yr]	[GL/yr]	[GL/yr]	[GL/yr]	[GL/yr]	[GL/yr]	[GL/yr]
Specified head BC	-8.83	1.07	-7.76	-4.16	0.31	-3.85	-3.92
Specified flux BC	0.00	0.00	0.00	0.00	0.00	0.00	0.00
Transfer BC	0.00	9.70	9.70	0.00	9.37	9.37	0.33
Wells	0.00	0.00	0.00	0.00	0.00	0.00	0.00
Distributed sink (-) / source (+)	-16.42	14.63	-1.78	-17.90	12.66	-5.25	3.46
Storage release (-) / capture (+)	-16.86	16.70	-0.15	-12.72	12.31	-0.41	0.26
Total	-42.11	42.10	0.00	-34.78	34.64	-0.14	

6.3.3 Post closure water balance

The in / out flows water balance components have been extracted from the model to demonstrate the impacts of the Sino Iron mine on the water resources within the study area and are presented graphically in Figure 6-9. The water balance closure for the entire model domain is presented below as total volumes and average annual volumes in Table 18.

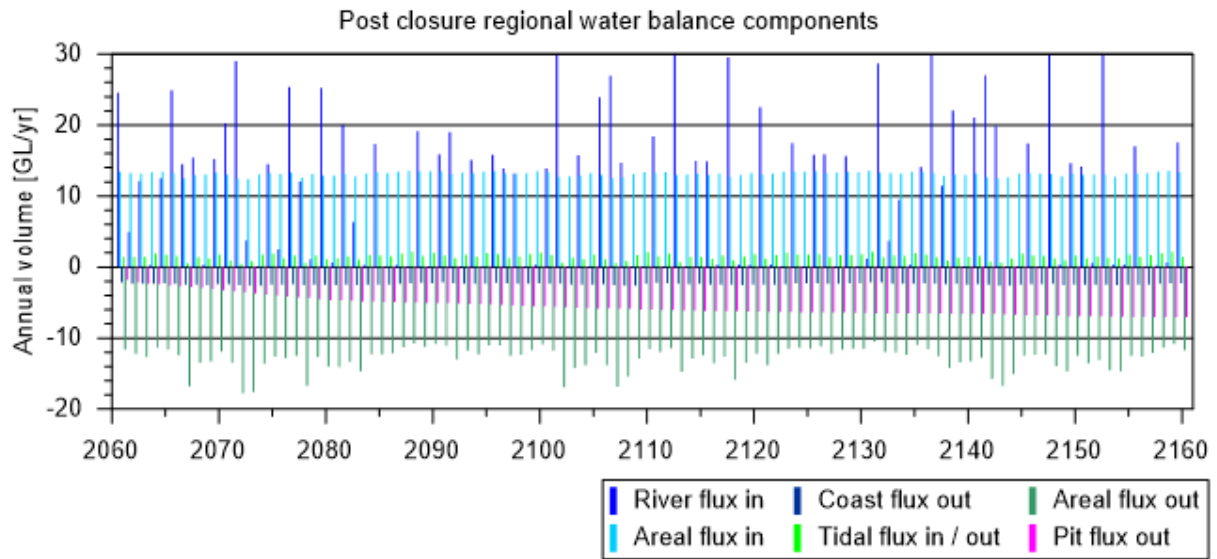


Figure 6-9 Post closure in / out flow water balance components for the model domain annual volumes are presented in Appendix J.

Table 18 Total water budget for the 100 year period from 01/01/2060 to 01/01/2160.

Component	Out	In	Out	In
	m ³	m ³	GL/yr	GL/yr
Specified head BC	-2.78E+08	1.85E+08	-2.78	1.85
Specified flux BC	0	0	0.00	0.00
Transfer BC	-6.14E+03	1.10E+09	0.00	10.97
Wells	0	0	0.00	0.00
Distributed sink (-) / source (+)	-2.00E+09	1.31E+09	-20.05	13.13
Storage capture (-) / release (+)	-1.92E+09	1.58E+09	-19.16	15.80
Total	-4.20E+09	4.17E+09	-42.00	41.75
Imbalance %	0.59			

6.3.4 Comparison of post closure water budgets to natural conditions

To provide an easier assessment of the changes to the water budgets presented in the previous sections a 'natural' scenario was run where all stresses associated with mining activities were removed. The results for the post closure phase are presented below in Table 19. Observations made from the comparison of the water balances are summarised as:

- The specified head boundary conditions, representing the coast and tidal sections of the rivers, show a change from net outflow of approximately -3.9 GL/yr to a net outflow of -0.9 GL/yr a reduction in outflow of 3 GL/yr. This is the result of 3 GL/yr being induced into the model domain along the tidal sections of the rivers.
- There is a net increase in inflows from the transfer boundary conditions, representing the non-tidal sections of the river, of approximately 1.1 GL/yr. This is interpreted to be as a result of the reduced groundwater levels around the pit providing additional storage for recharge from the river.

**SINO EXPANSION LIFE OF MINE GROUNDWATER MODEL
GROUNDWATER LOM AND POST CLOSURE FORECASTS**

- The distributed in / out flow components show a net increase in outflow, this is mostly due to the evaporation from the surface of the pit-lakes. Total evaporative loss from the Sino Iron pit averages 5.6 GL/yr (refer Appendix J) resulting in a reduction in ET of approximately 4.1 GL/yr from -18.6 GL/yr to -14.5 GL/yr.
- Storage capture / release shows that water is captured into storage (infill of the pit void) at a rate of approximately 3.4 GL/yr. The different volumes reported for the capture / storage values indicate that the model has not yet stabilised. This is supported by the discussion below regarding the pit-lake water levels after 100 years of recovery.

Table 19 Comparison of post closure period 2060 - 2160

Component	Post closure 2060 - 2160			Natural 2060-2160			Change
	Out [GL/yr]	In [GL/yr]	Diff [GL/yr]	Out [GL/yr]	In [GL/yr]	Diff [GL/yr]	
Specified head BC	-2.78	1.85	-0.93	-4.24	0.29	-3.94	3.01
Specified flux BC	0.00	0.00	0.00	0.00	0.00	0.00	0.00
Transfer BC	0.00	10.97	10.97	0.00	9.85	9.85	1.11
Wells	0.00	0.00	0.00	0.00	0.00	0.00	0.00
Distributed sink (-) / source (+)	-20.05	13.13	-6.92	-18.59	12.58	-6.00	-0.92
Storage release (-) / capture (+)	-19.16	15.80	-3.36	-12.89	12.85	-0.04	-3.32
Total	-42.00	41.75	-0.25	-35.71	35.58	-0.14	

6.4 Post closure pit-lake levels

Terminal discharge of regional groundwater flow at the pit lake has implications for long-term water quality in the lake, as this is the process by which salt lakes have formed in the region over millennia.

The rate of evaporative flux from the post closure pit-lake depends on the area of the open water surface and the rate of evaporation from the water surface. It follows that the evaporative discharge from the pit lake affects groundwater gradients surrounding the lake.

If the steady-state pit lake elevation stabilises below the surrounding pre-mining groundwater level, the pit lake becomes a terminal sink, with no water released into the environment through seepage into the groundwater system. However, if the final pit lake elevation reaches the surrounding pre-mining groundwater level, the pit lake becomes a through-flow system with water being released to the environment through groundwater seepage, with potential water quality effects (e.g. increased salinity dependent on the evaporative discharge).

Management of local surface and groundwaters through entrainment toward an evaporative terminal pit lake may provide a best-case scenario for protection of regional water resources required by typical mine closure time scales of hundreds to thousands of years (McCullough, et al., 2012).

The water quality of evaporative sink lakes is expected to show increases in various concentrations (notably salinity in the Pilbara) over time through accumulation of solutes introduced through groundwater inflows, surface catchment run-off and direct rainfall to the developing lake surface. The deterioration of water quality over time through evaporation and the consequent entrapment of solutes, although not desirable in itself, indicates that the pit lake is functioning as it should as an evaporative 'terminal' sink and protecting the surrounding environment (McCullough, et al., 2012).

The relationship between open water surface area and rate of evaporation has been included into the model using the following methodology (outlined previously in section 4.9.6):

- The cessation of active mining is represented by deactivating the seepage face (dewatering) boundary conditions in the pit allowing post-mining inflows from the surrounding rocks to drain to the pit void; and
- Assigning an enhanced vertical and horizontal permeability and porosity (1) to represent the pit void material properties.
- Assigning evaporation from any pit-lake that forms in the void.

6.4.1 Evaporation rates

It is common practice in water resource management for dams and reservoirs to estimate evaporation using nearby measurements of pan evaporation. Commonly, a pan coefficient is applied to measured pan evaporation rates to derive equivalent evaporation from the water storage of interest. Various studies have identified the limitations of this approach, however, it remains widely used because of its simplicity and moderate data requirements. Typically, a pan coefficient of 0.7 is used, although other studies showed that pan coefficients determined on an annual basis for water storages can have considerable variation across years (0.64–0.96) (McJannet et al, 2013) with values in the lower end of this range being more typical for saline lakes. It should also be noted that unlike typical lakes, evaporation from pit lakes is also influenced by shading by the pit walls and sheltering of the water surface from wind. Given the uncertainty associated with the pan to lake coefficient a range from 0.6 to 0.8 is considered in this study.

6.4.2 Pit lake water level vs surface area vs evaporative losses

The final pit lake water level can be determined using a simple water balance method and inflows to the pit estimated by the numerical model.

In the water balance method the planar area vs depth relationship was determined for the Sino Iron pits and the resulting evaporative flux was calculated assuming several pan to lake coefficients.

The expected clear trend that can be seen in the results is that a larger rate of evaporation from the lake leads to a lower pit lake level resulting in larger long-term drawdown of hydraulic head within the pit zone. Conversely, a smaller rate of evaporation from the pit lake results in a higher lake level resulting in smaller long-term drawdown of hydraulic head within the pit zone. The situation for the Sino Iron pit is complicated by the divide between the West and East pits. The crest of the divide is at approximately -118 mAHD, therefore, if the water level in the pit is below -118 mAHD, then the water level will be different in each pit if the inflow to the pits is different. The separate pit relationships are presented below in Figure 6-10.

Assuming an inflow of approximately 0.7 GL/yr inflow to the East Pit and 6.8 GL/yr inflow to the West Pit (the pit inflow rate at the end of mine at 2060) the final water level in each of the pits are expected to be approximately -300 metres AHD in the East Pit and range from approximately -120 to -170 metres AHD in the West Pit depending on the assumed pan to lake coefficient. These values assume that the system has attained steady state.

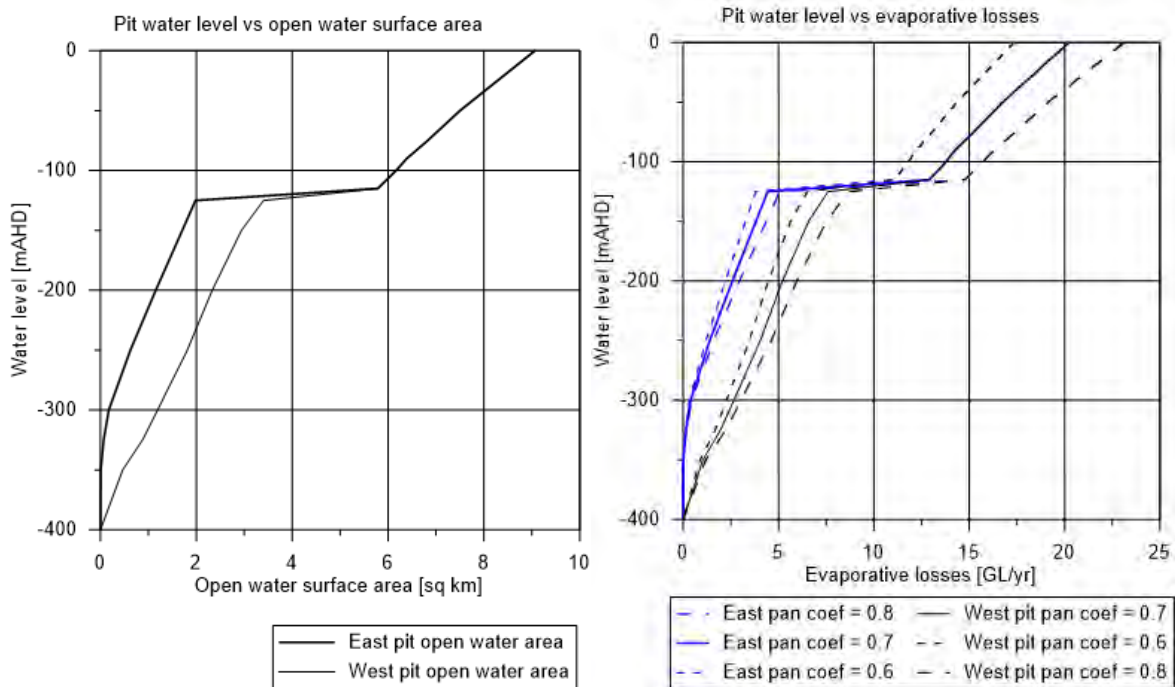


Figure 6-10 a) Pit area vs water elevation in the Sino pits based on the final pit void geometry and b) water elevation in the Sino pits vs the evaporative losses in GL/yr using a range of coefficients to convert pan evaporation into open body water evaporation.

6.4.3 Pit-lake water level after 100 years of recovery

The evolution and final level of the pit lake was assessed using the LoM model with the following adjustments:

- Removing the seepage face boundary conditions representing the pit, setting the pit void material properties and allowing evaporative discharge from the surface of an pit-lake that forms due to groundwater inflow;
- Time varying inputs, such as rainfall and evaporation were assigned long term average values for the period 1983-2016 (0.8053 mm/d and 8.74 mm/d respectively); and
- 100 years of river recharge inputs were taken from the predicted 35 year time series used in the calibration model and repeated as needed.

It was assumed that the extended version of the transient model attained quasi-steady state. The final groundwater level drawdown after 100 years of recovery are presented below in Figure 6-11.

SINO EXPANSION LIFE OF MINE GROUNDWATER MODEL
GROUNDWATER LOM AND POST CLOSURE FORECASTS

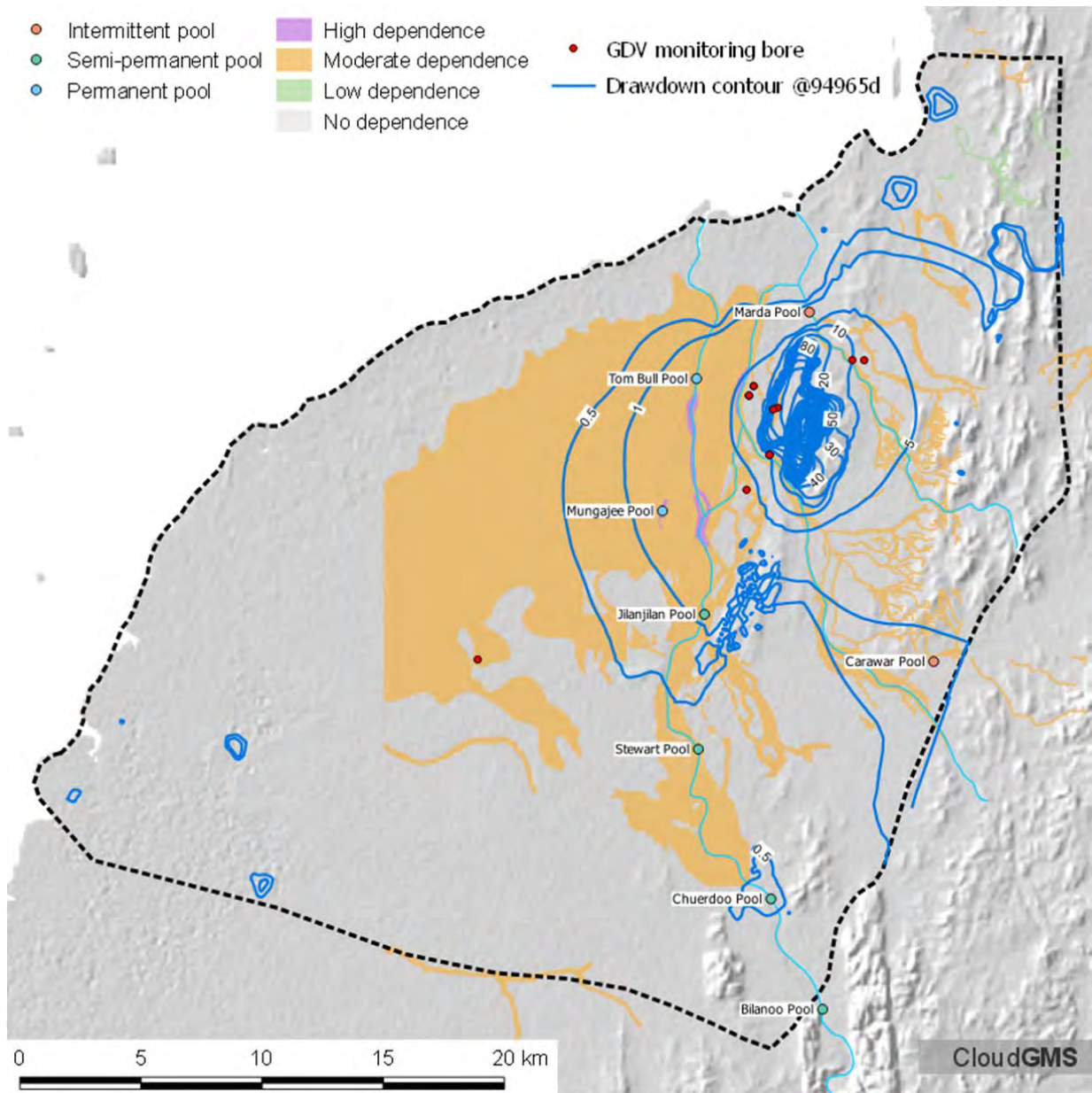


Figure 6-11 Drawdown contours (relative to groundwater levels prior to mining) for year 2160 or 100 years after cessation of mining.

The West Pit fills relatively rapidly due to groundwater inflows from the weathered material along the western margin of the pit, which is overlain by the superficial aquifer system. Using a pan coefficient of 0.7 the West Pit reaches a level of -160 to -170 mAHD after 100 years. The East Pit in contrast, recovers to a level of -300 to -310 mAHD, slightly lower than the level expected using the simple surface area vs flux analytical relationship described above with an inflow of 0.7 GL/yr (the East Pit inflow rate at the end of mining at 2060). The final pit-lake levels were:

- West Pit pit-lake level between -160 to -170 mAHD
- East Pit pit-lake level between -300 to -310 mAHD

The total flux due to evaporation at the end of the post closure model run reaches a maximum of 19400 kL/d or approximately 7.1 GL/yr. This is a slightly lower rate compared to the pit inflows at the end of

mining, which indicated pit inflows of the order of 7.5 GL/yr. The estimated pit lake level using the surface area vs evaporative flux relationship and the lower evaporative fluxes than at the end of mining suggest that in the vicinity of the pit, the inflows to the pit from the groundwater system, the evaporative fluxes and the pit water level have only reached a state of quasi-equilibrium after 100 years and full equilibrium would take much longer. However, further investigations into aquifer properties to the west of the pits is required in order to reduce crucial uncertainties before further hypothesis testing would be warranted.

6.5 Sino Iron groundwater quality impacts

The possible impacts on groundwater quality have been assessed using backward streamline analysis with reference to the water quality distribution presented in section 3.8 modified from Haig (2009).

Backward streamlines are determined by releasing a number of particles from seeding points (in this case the nodes within the pit), the particles move against the hydraulic gradient (upgradient) until exiting the model at an inflowing boundary (or ending up in a zone without significant flow velocity). In this way backward streamline tracks can be used to obtain a catchment area for boundary conditions or sink features. The use of streamlines assumes steady-state flow conditions.

Two scenarios were considered using the streamline analysis generated using the groundwater velocity flow field at:

- the end of mining (year 2060); and
- after 100 years of recovery in the pit lake (year 2160);

The results of the two scenarios are presented below in Figure 6-12 and Figure 6-13. The streamline length is 36500d (100 years).

An immediate observation from both scenarios is that the streamlines completely surround the Sino Iron pits, indicating that the pit is a sink at the end of mining and following development of the pit lake. It also appears that the poorer quality groundwater will not be drawn into areas of better groundwater quality. For example, although the saline and hypersaline groundwater to the north and northwest of the pit are drawn to the northern extent of the pit, the path line is through similar quality groundwater. Conversely, it is indicated that the groundwater quality in the vicinity of Tom Bull Pool will be the same, or slightly improved by the migration of better groundwater quality to the south and west.

Groundwater from all salinity categories (fresh to hyper saline) will be drawn into the final pit-lake. The resulting water quality residing in the pit lake will evolve to become hypersaline through evapoconcentration processes. To understand the evolution of the water quality in the pit-lake, a study similar to that completed for the Mount Goldsworthy pit-lake (Sivapalan, 2005) would be required, which is beyond the scope of the current study.

SINO EXPANSION LIFE OF MINE GROUNDWATER MODEL
GROUNDWATER LOM AND POST CLOSURE FORECASTS

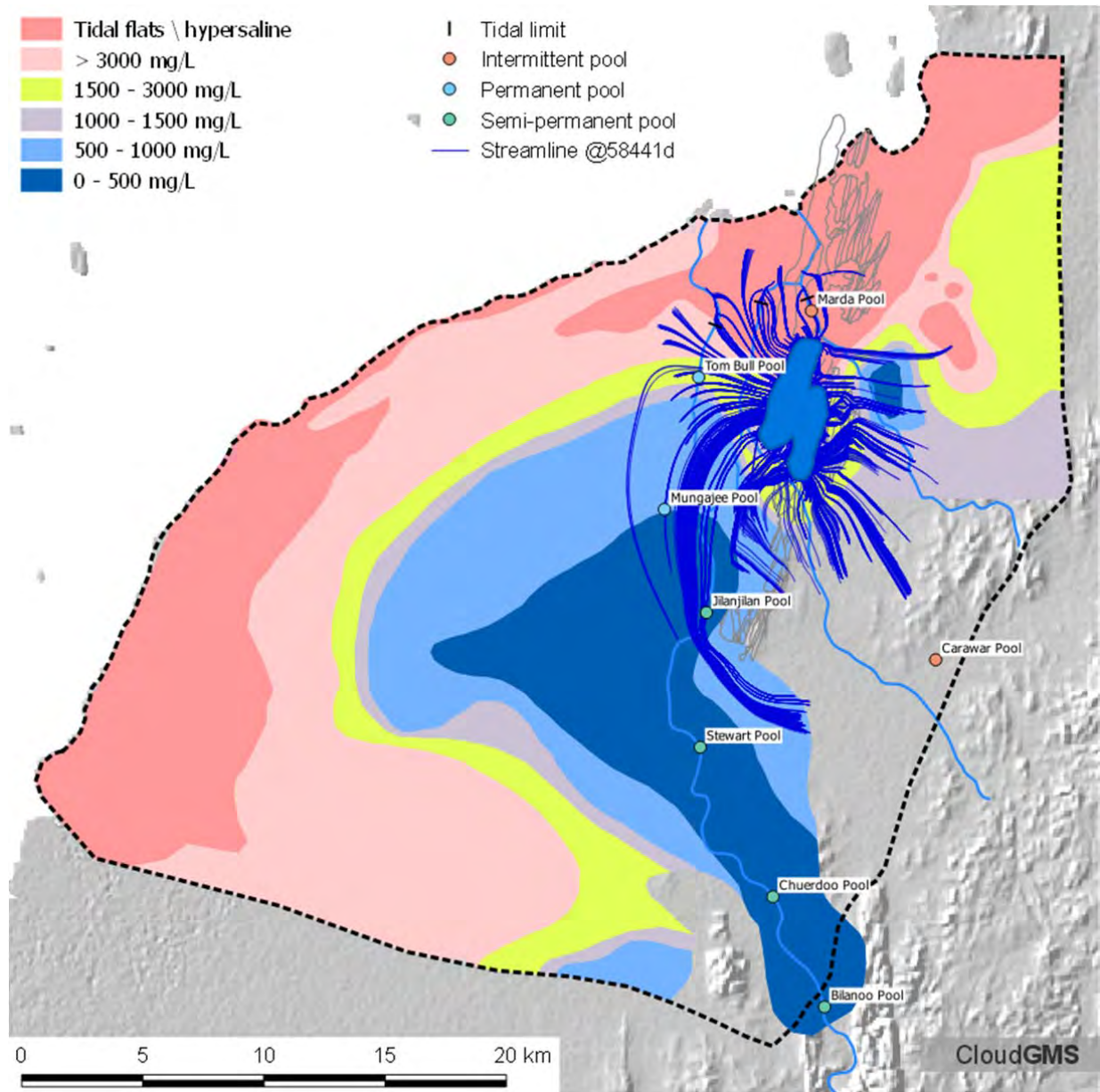


Figure 6-12 Backward streamlines indicating the source of groundwater entering the pit at the end of mining (2060).

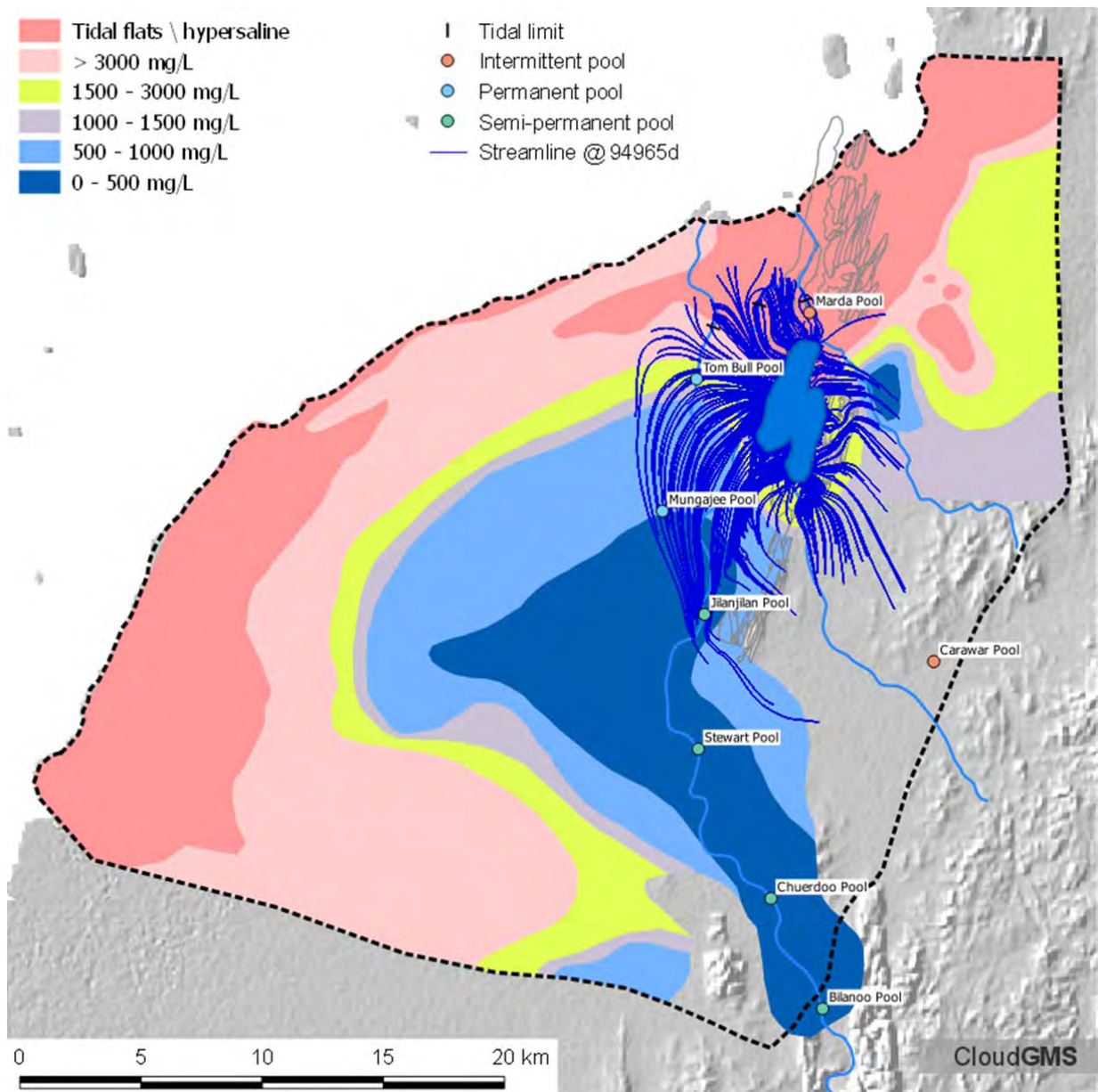


Figure 6-13 Backward streamlines indicating the source of groundwater entering the pit after 100 years of recovery following the end of mining (ie year 2160).

6.6 Impacts on existing users

The final groundwater drawdown contours at 94965 (2160) are presented below in Figure 6-14 with the locations of the existing stock wells in the study area. Drawdowns of between 1 – 5 metres are evident at Marda Well and Fortescue Bore, with Fortescue Bore expecting closer to 5 metres drawdown. All other wells in the study area are expected to shows drawdowns of less than 1 metre.

SINO EXPANSION LIFE OF MINE GROUNDWATER MODEL
GROUNDWATER LOM AND POST CLOSURE FORECASTS

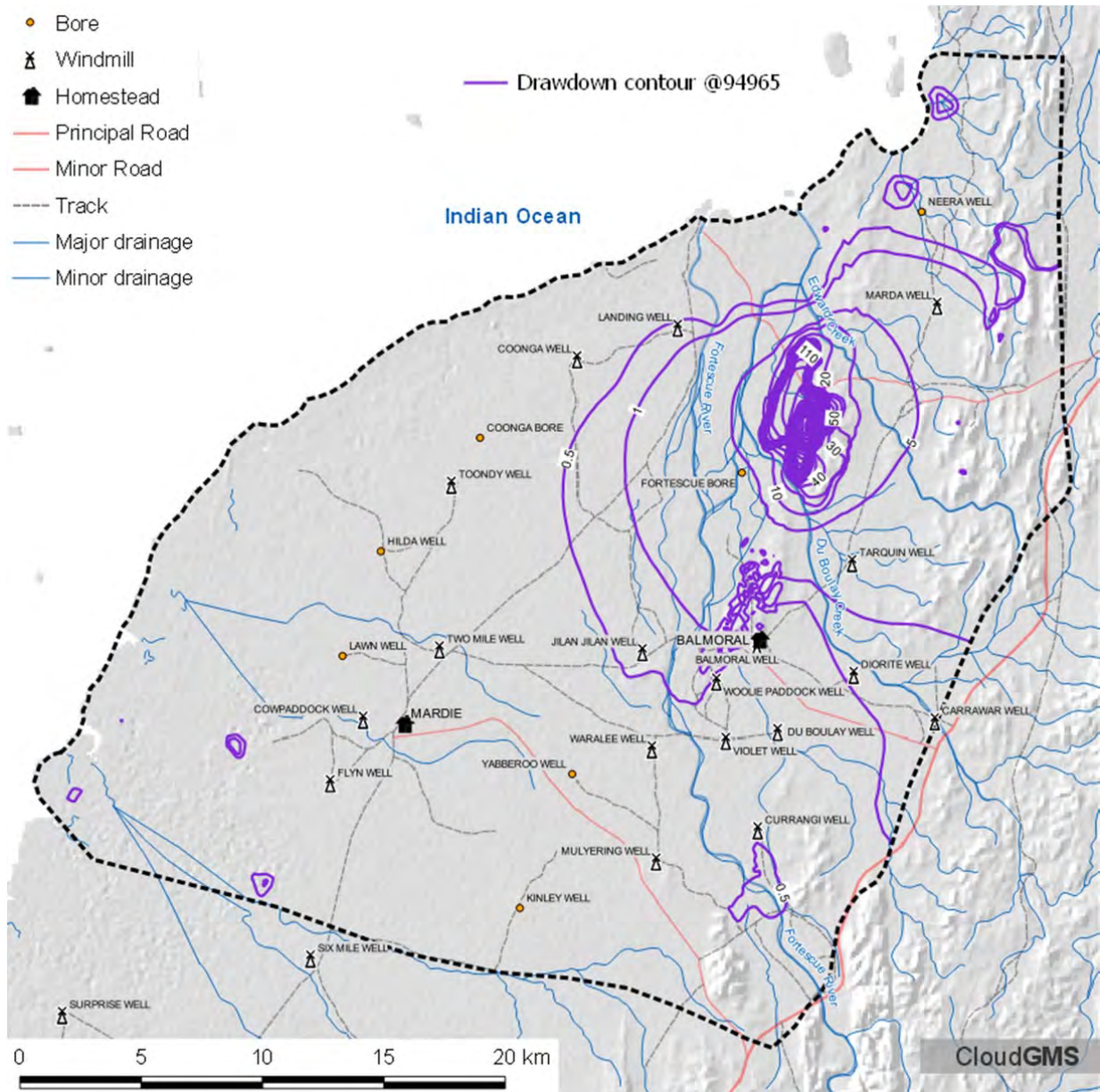


Figure 6-14 Comparison of groundwater drawdown contours at 94965d (2160) and the locations of wells used for pastoral activities.

7 LoM uncertainty analysis

7.1 Introduction

Uncertainty analysis builds upon, but is distinct from, sensitivity analysis. Whereas sensitivity simply evaluates how model outputs change in response to changes in model input, uncertainty analysis is a more encompassing assessment of the quality of model predictions.

To provide confidence in the results and examine some of the concerns regarding the level of connection between the superficial sediments and the pit, a suite of 100 random parameter sets were used in the model.

The parameter sets were generated using the PEST utility RANDPAR. Each parameter was centred on its calibrated value and the allowable range determined by a user supplied value for the standard deviation of the log transformed parameter value. The standard deviation value was chosen to provide a reasonable range in each parameter and generally providing values that spanned 2 orders of magnitude. The parameter probability distributions are presented in Appendix K.

The focus of the uncertainty analysis was to investigate the possible impacts if the pit model on the aquifers in the superficial, the uncertainty analysis was therefore simplified by removing the leakage features such as the TSF as discussed earlier in section 6.1.1.

Although the analysis is not exhaustive, it does provide insights to the areas where further work could reduce the uncertainty regarding the possible impacts on the groundwater resource within the superficial sediments of the Fortescue River floodplain.

The uncertainty analysis has only been completed for the LoM scenario. Uncertainty analysis of the post closure mining was considered inappropriate at this time, as the unconstrained variation of hydraulic parameters (particularly hydraulic conductivity) has been observed to result in an unstable model at the interface between the low permeability host rock and the much higher hydraulic conductivity of the simulated pit void. Further field investigations, testing and analysis is required to reduce the range in hydraulic parameters along the western margin of the West Pit, to allow modelling investigation of strategies to provide a robust model to simulate these conditions and enable examination of the post closure impacts. The uncertainty analysis conducted does provide insights into the areas where future work is warranted.

7.2 Life of mine (LoM) forecast results

The LoM models have been queried to generate outputs for selected metrics such as annual pit inflows, final drawdown contours, timeseries groundwater level changes at selected GDV monitoring sites and permanent pools identified in the study area. The results are presented for the suite of model realisations that have been considered using random parameter sets constrained to by the current understanding of hydraulic parameters in the area.

7.2.1 Total pit inflows

The simulated inflows to the pit for the period 01/07/2016 to 01/01/2060 are presented below in Figure 7-1. Using the median values the inflows show a steady increase from approximately 2 GL/yr (5500 kL/d) in 2018 to approximately 5 GL/yr in 2026. This steady increase coincides with the commencement of mining in the West Pit.

The median final pit inflows are approximately 8 GL/yr (22000 kL/d) with 50% of realisations (ie pit inflows between p25 and p75) showing a variation of ± 1.5 GL/yr or 18%.

Under all realisations the final pit inflows are greater than 4 GL/yr (11000 kL/d) with the majority of inflows from the West Pit along the western margin (see below).

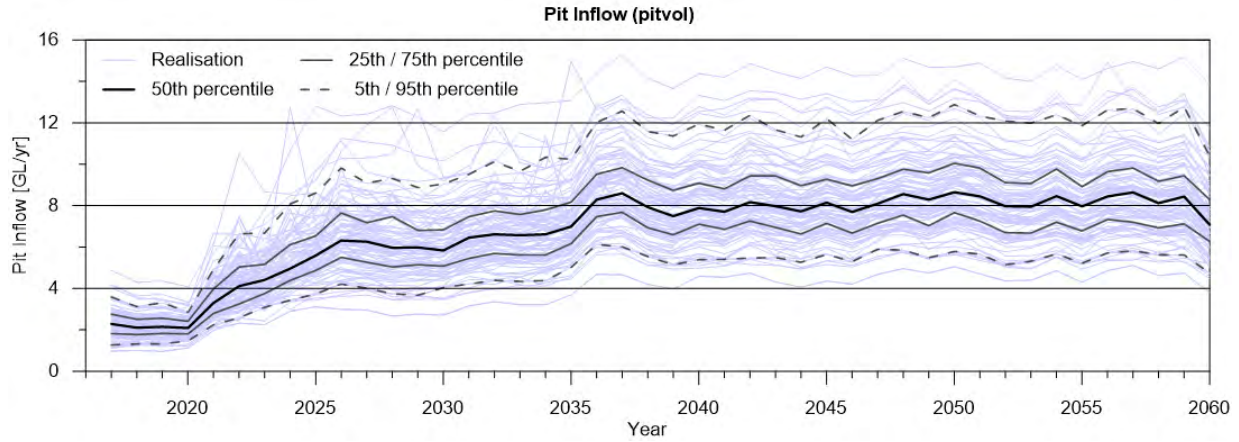


Figure 7-1 Total inflows to the Sino Iron pits showing variability from 100 parameter set realisations.

7.2.2 East pit inflows

The contribution of inflows to the pit from the East Pit area for the period 01/07/2016 to 01/01/2060 are presented below in Figure 7-2.

The inflows to the pit in this area account for all inflows to the total pit area up to 2019, after which the mining commences in the West Pit. Using the median or 50th percentile values the pit inflows in 2018 are approximately 2 GL/yr (5500 kL/d), which is equivalent to the current pit inflows at the end of 2016 assuming no re-circulation occurs from the leakage features especially the NE waste dump.

After 2020 the pit inflows gradually decline and the range of expected pit inflows is relatively constrained under the range of parameters considered and at least 95% of realisations forecast inflows of less than 4 GL/yr for the duration of mining and less than 2 GL/yr (5500 kL/d) from 2040.

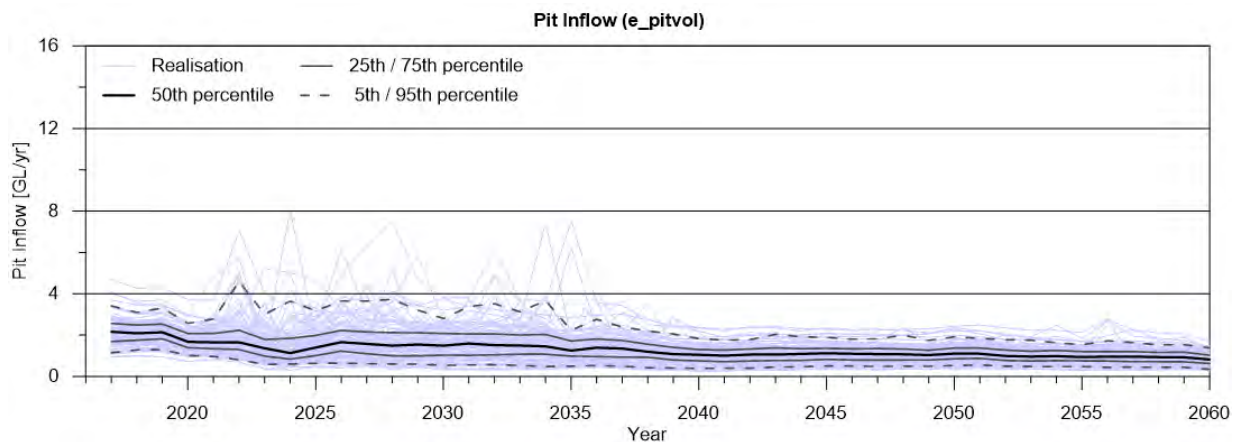


Figure 7-2 Contribution to pit inflows from the Sino Iron East Pit.

7.2.3 West pit inflows

The contribution of inflows to the pit from the West Pit area for the period 01/07/2016 to 01/01/2060 are presented below in Figure 7-3.

Inflows to the West pit commence between 2019-2020 as the pit intersects the water table in areas of weathered basement along the western margin of the East pit and the superficial sediments to the west. Using the median or 50th percentile values for the period 2025 – 2035, approximately 4GL/yr (11000 kL/d) inflows to the pit in this area, which accounts for approximately 60 – 70 % of inflows to the total pit area. The inflows to the pit increase by approximately 2 – 3 GL/yr for the period 2035 – 2060.

Pit inflows gradually increase and the lower range of expected pit inflows is relatively constrained under the range of parameters considered and at least 95% of realisations forecast inflows of greater than 3-4 GL/yr (11000 kL/d) for the period 2025 – 2035 and greater than 4 GL/yr for the period 2035 – 2060.

The upper 25th percentile of estimated inflows are associated with realisations that have relatively high weathered zone hydraulic conductivity values in the vicinity of the surface contact between the alluvial sediments and the outcropping Hamersley Group. This suggests that increased permeability associated with features such as faults may result in considerable increases in pit inflows.

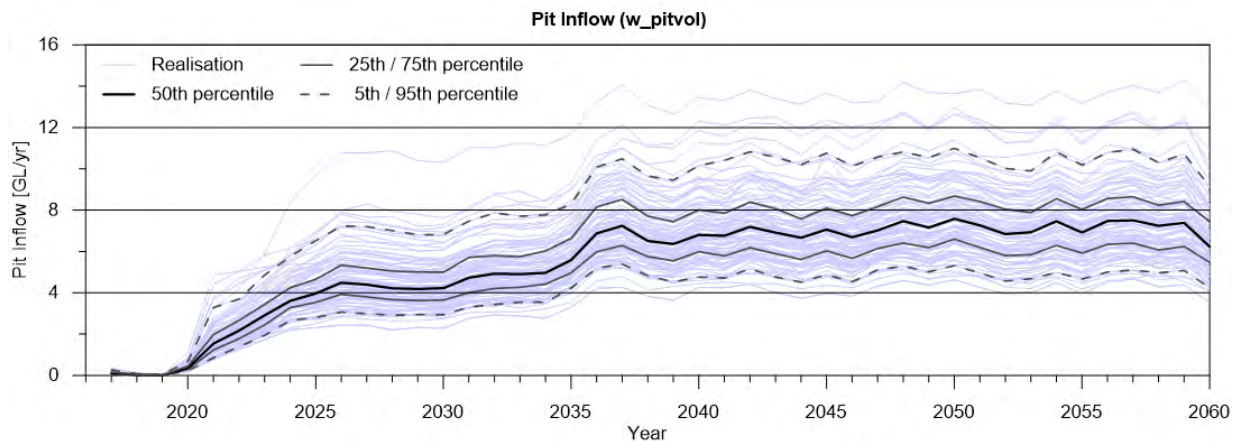


Figure 7-3 Contribution to pit inflows from the Sino Iron West Pit.

7.2.4 West pit inflows from the alluvial sediments

The contribution of inflows to the pit from the superficial sediments along the western margin of the West Pit area for the period 01/07/2016 to 01/01/2060 are presented below in Figure 7-4.

Inflows to the pit in this region commence between 2019-2020 as the pit intersects the superficial sediments to the west. Using the median or 50th percentile values, the inflows to the pit in this area are approximately 4 – 5 GL/yr (11000 – 13700 kL/d) and account for approximately 50% of inflows to the total pit area from 2035 – 2060.

Pit inflows gradually increase and the lower range of expected pit inflows is relatively constrained under the range of parameters considered and at least 95% of realisations forecast inflows of greater than 2 GL/yr (5500 kL/d) for the duration of mining.

As identified above, the upper 25th percentile of estimated inflows are associated with parameter sets with relatively high weathered zone hydraulic conductivity values in the vicinity of the surface contact between

SINO EXPANSION LIFE OF MINE GROUNDWATER MODEL
GROUNDWATER LOM UNCERTAINTY ANALYSIS

the alluvial sediments and the outcropping Hamersley Group. The values greater than approximately 8 GL/yr are associated with weathered zone hydraulic conductivities an order of magnitude high than the calibrated value.

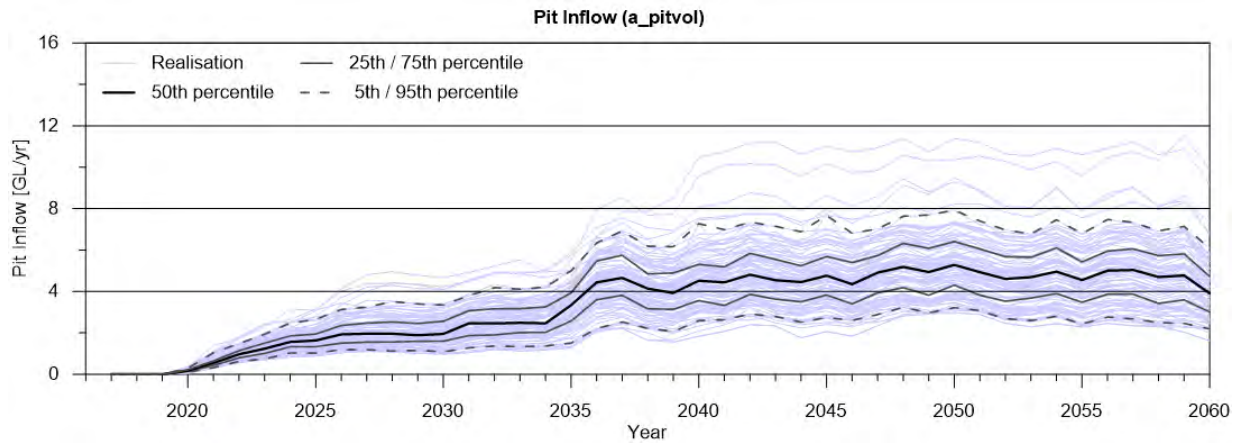


Figure 7-4 Contribution to pit inflows from the western edge of the Sino Iron West Pit associated with the alluvial sediments.

7.2.5 Groundwater dependent vegetation (GDV) monitoring sites

The monitoring sites considered for further assessment were taken from the Groundwater Dependent Vegetation Monitoring Plan (Astron, 2015) and are presented above in Table 2.

In addition to these monitoring sites, the 2 permanent pools (Tom Bull Pool & Mungajee Pool) have also been considered in the analysis.

Table 20 Monitoring sites identified by Astron (2015).

Zone	Active	Astron site number	Monitoring bores	Catchment
Reference	Current	8	FCP23A	Fortescue River
	Current	-	FCP10A	Fortescue River
1	Current	13	09AC489, 09AC490, 09AC534, 09AC537, 09AC539	Du Boulay Creek
	From 2018	5	07RC156, 09AC546, 09AC547	Du Boulay Creek
2	Current	2	07RC149, 07RC150	Du Boulay Creek
	Current	6	07RC151, 13DD732	Du Boulay Creek

Zone 1 trigger = 2 standard deviations below baseline mean

Zone 2 trigger = 3 standard deviations below baseline mean

7.2.6 Groundwater level impacts at regional reference monitoring bores

Groundwater level hydrographs have been generated at selected monitoring sites (FCP10A, FCP22A and FCP23A). The results are presented as a suite of groundwater level responses for each realisation and 5th, 25th, 50th, 75th and 95th percentile values marked.

FCP10A

FCP10a is an active regional reference monitoring site approximately 15 km from the Sino Iron pits. The groundwater levels at FCP10a are presented below in Figure 7-5. The results are consistent with the results

SINO EXPANSION LIFE OF MINE GROUNDWATER MODEL
GROUNDWATER LOM UNCERTAINTY ANALYSIS

from the calibrated model presented above. The realisations that show the greatest drawdown are associated with parameter sets where the superficial sediments have relatively high values, with the Yaraloola Conglomerate 2-3 times the calibrated value and the alluvial gravels 40-80% greater than the calibrated value.

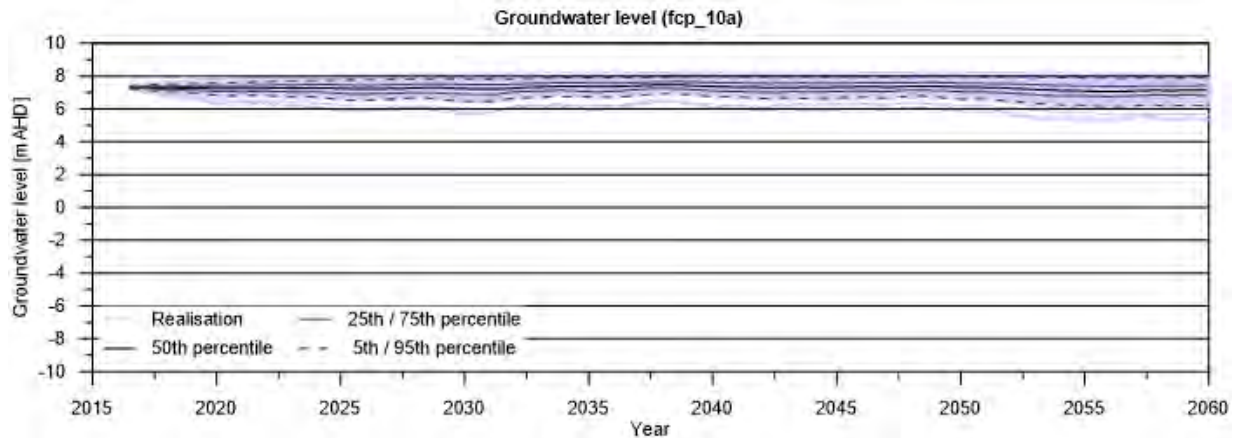


Figure 7-5 Groundwater level variability at monitoring bore FCP10A located approximately 15km to the southwest of the Sino Iron pits.

FCP22A

FCP22A is an additional regional reference monitoring site approximately 4.8 km from the Sino Iron pits. The groundwater levels at FCP22A are presented below in Figure 7-6. The groundwater level response shows declines of approximately 2-3 metres over the life of the mine under all realisations considered.

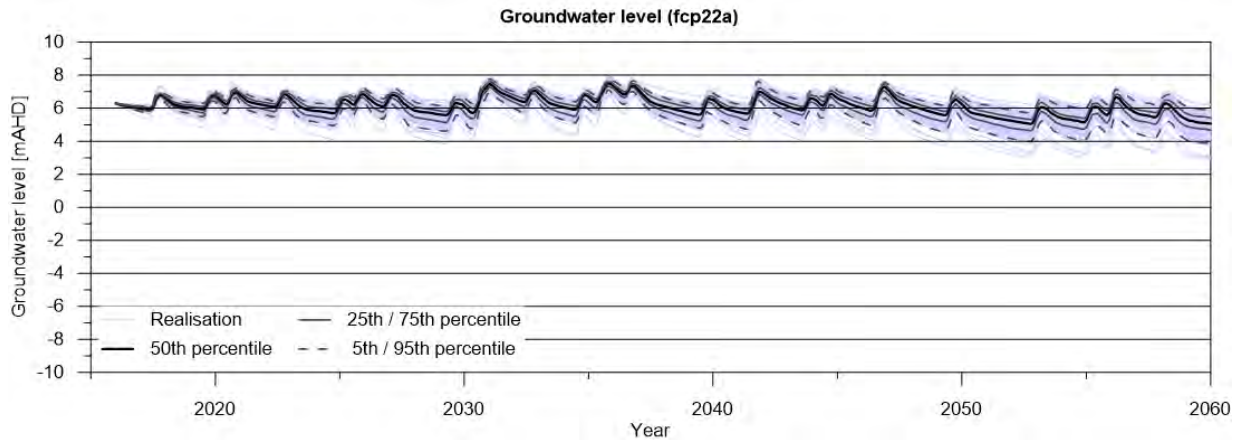


Figure 7-6 Groundwater level variability at monitoring bore FCP22A located approximately 4.8km to the southwest of the Sino Iron pits.

FCP23A

FCP23A is an active regional reference monitoring site approximately 2 km from the Sino Iron pits. The groundwater levels at FCP23A are presented below in Figure 7-7. The groundwater level response shows considerable declines of greater than 2 metres over the life of the mine under all realisations considered.

The current trigger value for this site is 2 standard deviations below the baseline mean ($\mu = 6.98$ mAHD; $\sigma = 0.92$ m refer to Appendix A). The median decline in groundwater levels 3 – 4 metres over the life of the mine, with declines of greater than 7 metres observed in 5 percent of realisations.

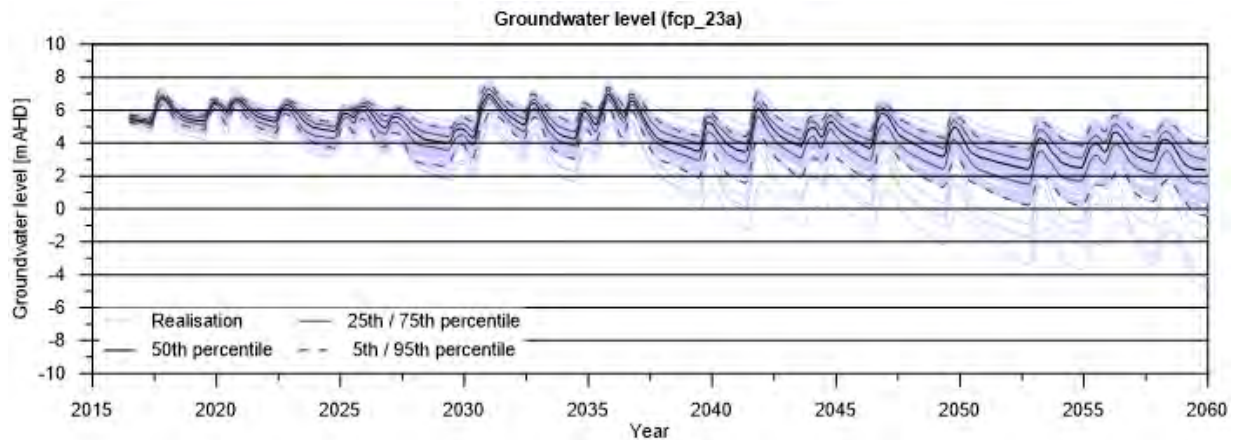


Figure 7-7 Groundwater level variability at monitoring bore FCP23A located approximately 2km to the southwest of the Sino Iron pits.

7.2.7 Groundwater level impacts at groundwater dependent vegetation (GDV) monitoring bores

Groundwater level hydrographs have been generated at selected monitoring sites (07RC149, 07RC156, 09AC490 and 09AC534). A sub-set was selected due to the clustered nature of some of the monitoring sites and several sites providing the same response. It is considered that the sites are representative of the GDV sites identified above in Table 2. The results are presented as a suite of groundwater level responses for each realisation and 5th, 25th, 50th, 75th and 95th percentile values marked.

07RC149

The groundwater levels at 07RC149 shows a decline in groundwater levels of approximately 10 metres over the 144 year period modelled. 07RC149 is a zone 2 GDV monitoring site and has a trigger that is 3 standard deviations below the baseline mean ($\mu = 4.20$ mAHD; $\sigma = 1.0$ m refer to Appendix A). This trigger is exceeded by the end of mining and continues to be exceeded post closure.

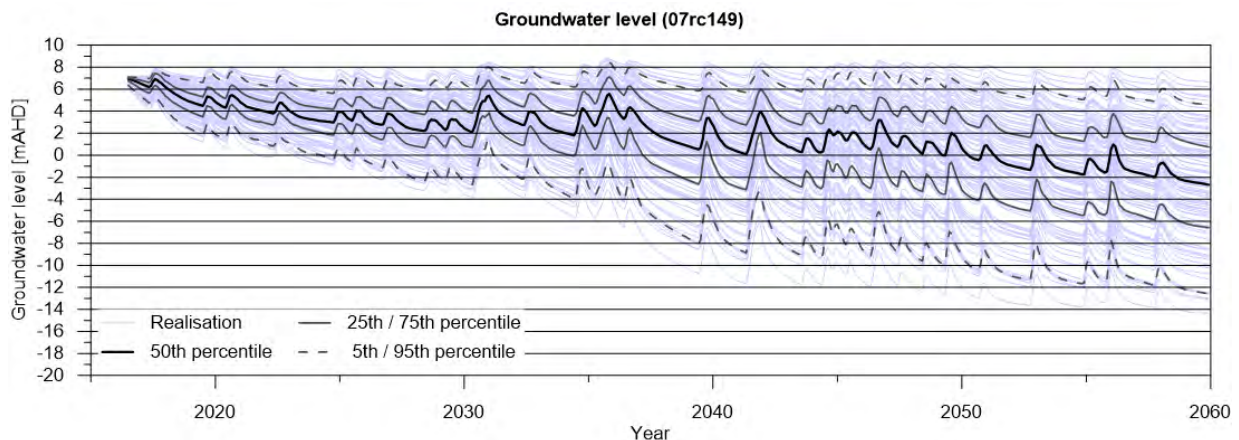


Figure 7-8 Groundwater level variability at monitoring bore 09RC149 located approximately 750 metres to the west of the Sino Iron pits.

07RC156

07RC156 shows a decline by nearly 12 metres below the initial level during the LoM, however, it recovers following mine closure to approximately 8 metres below the initial water level and appears to reach

SINO EXPANSION LIFE OF MINE GROUNDWATER MODEL
GROUNDWATER LOM UNCERTAINTY ANALYSIS

dynamic equilibrium at this level soon after closure of the pit for the duration of the post closure scenario. 07RC156 is a zone 1 GDV monitoring site and has a trigger that is 2 standard deviations below the baseline mean ($\mu= 6.00$ mAHD; $\sigma = 1.0$ m refer to Appendix A). This trigger is exceeded by mid 2020 and continues to be exceeded for the duration of mining and the post closure.

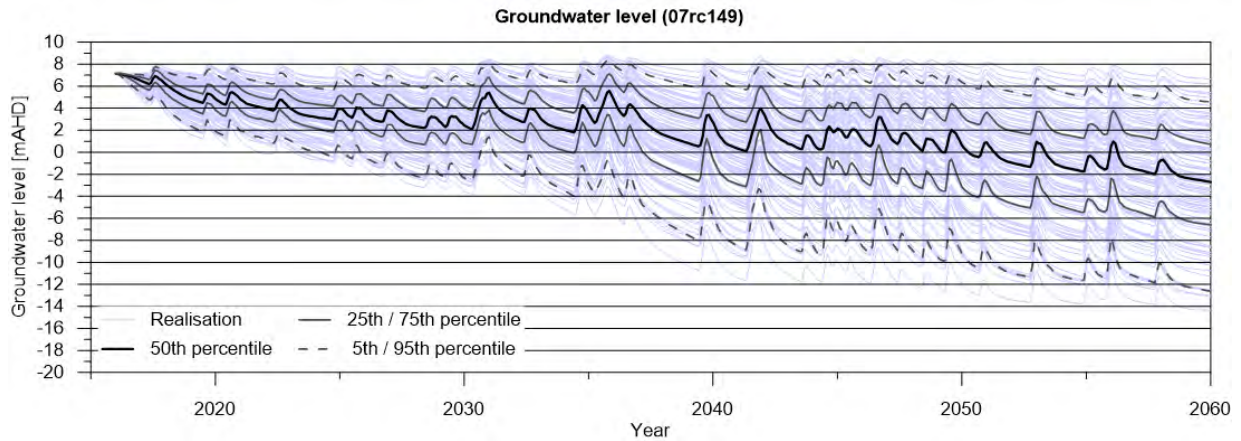


Figure 7-9 Groundwater level variability at monitoring bore 07RC156 located approximately 750 metres to the west of the Sino Iron pits.

09AC490 and 09AC534

09AC490 and 09AC534 are active Zone 1 reference monitoring site along the western margin of the West Pit and are constructed in the superficial sediments. The groundwater levels at 09AC490 and 09AC534 are presented below in Figure 7-10 and Figure 7-11 respectively.

The groundwater level response shows considerable decline ($>5 - 6$ metres) over the life of the mine under all realisations considered. The median drawdown at 09AC490 is approximately 7 – 8 metres. The median decline in groundwater level is greater than the 2 standard deviations from the mean identified as a trigger value ($\mu= 2.70$ mAHD; $\sigma = 1.08$ m refer to Appendix A). The median drawdown at 09AC534 is approximately 7 – 8 metres. The median decline in groundwater level is greater than the 2 standard deviations from the mean identified as a trigger value ($\mu= 2.1$ mAHD; $\sigma = 0.7$ m refer to Appendix A).

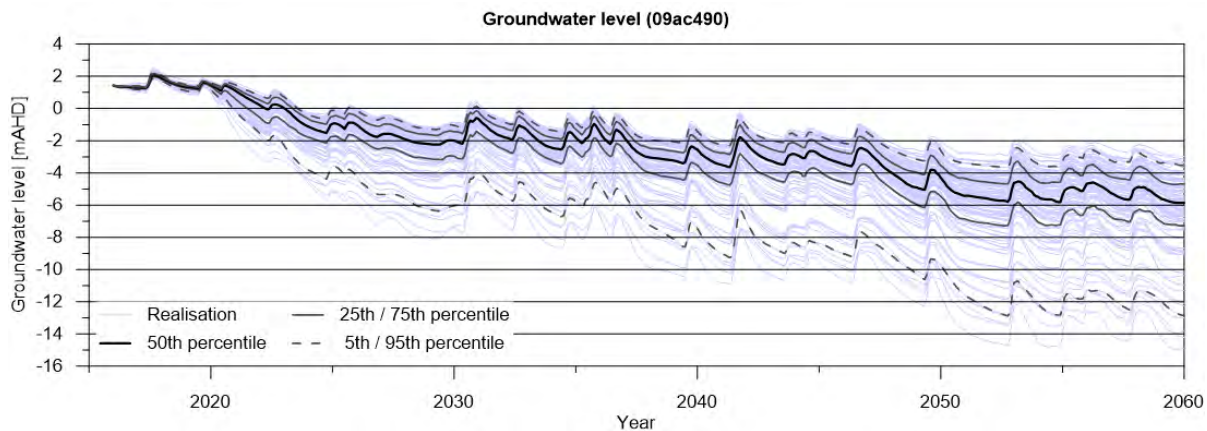


Figure 7-10 Groundwater level variability at monitoring bore 09AC490 located approximately 750 metres to the west of the Sino Iron pits.

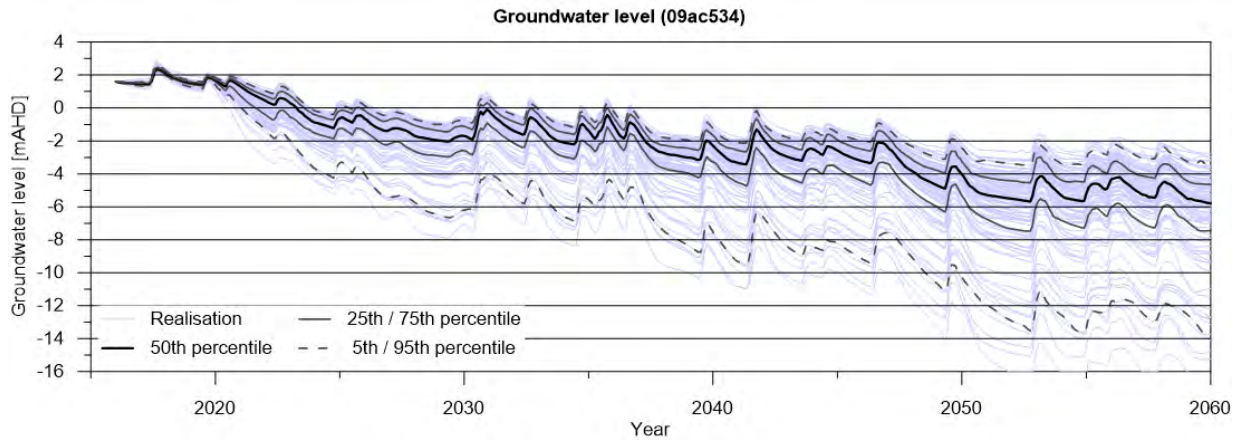


Figure 7-11 Groundwater level variability at monitoring bore 09AC534 located approximately 750 metres to the west of the Sino Iron pits.

7.2.8 Groundwater level impacts at permanent pools

Mungajee Pool

The groundwater levels at Mungajee pool are presented below in Figure 7-12. The maximum impact is predicted to be between 2 – 3 metres over the life of the mine for 95 percent of the realisations considered. Median declines are between 1 – 2 metres (0.2 – 0.05 metres per year). At these rates of decline it would be expected that GDV would be capable of adapting to the changes to the groundwater regime.

Maximum drawdown occurs when the parameter values of the weathered zone in the southwest corner of the West Pit are high in conjunction with high hydraulic conductivity in the superficial sediments.

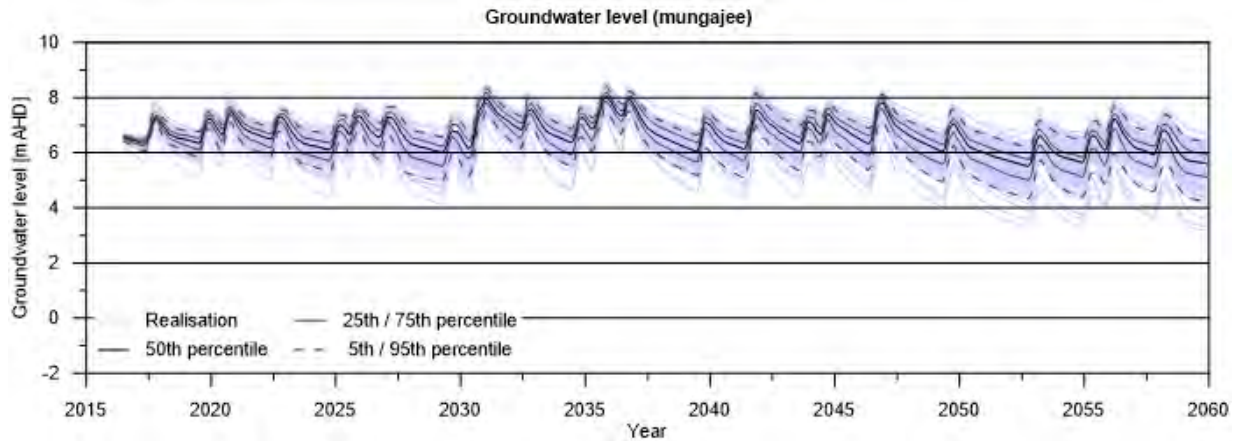


Figure 7-12 Groundwater level variability at Mungajee Pool located approximately 5km to the southwest of the Sino Iron pits.

Tom Bull Pool

The groundwater levels at Tom Bull pool are presented below in Figure 7-13. The maximum impact are predicted to be approximately 3 metres over the life of the mine for 95 percent of the realisations considered. Median declines are approximately 2 metres (0.05 metres per year). At this rate of decline it would be expected that GDV would be capable of adapting to the changes to the groundwater regime.

SINO EXPANSION LIFE OF MINE GROUNDWATER MODEL
GROUNDWATER LOM UNCERTAINTY ANALYSIS

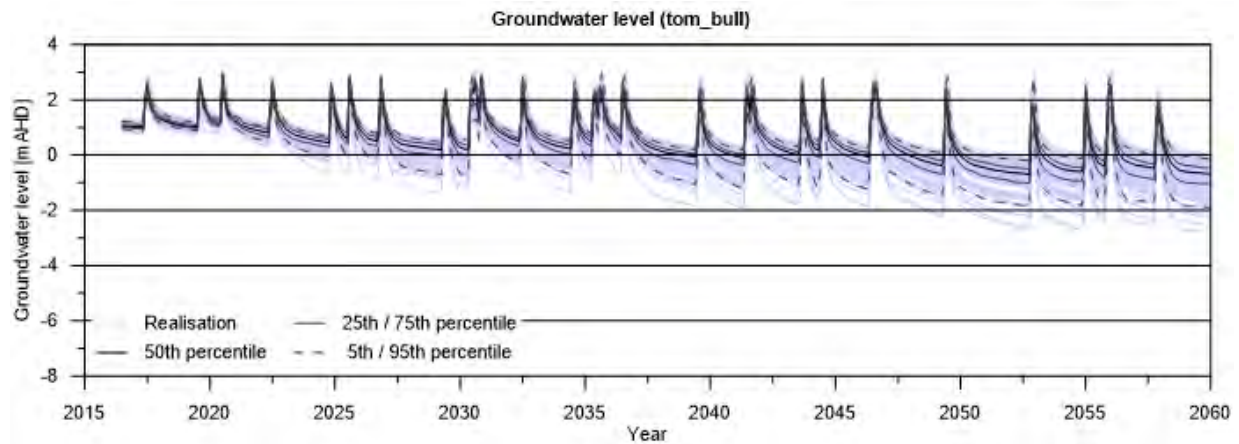


Figure 7-13 Groundwater level variability at the permanent pool Tom Bull Pool located approximately 3km to the west of the Sino Iron pits.

Conceptually both Mungajee Pool and Tom Bull Pool are considered to be permanent due to the connection to the groundwater in the superficial sediments aquifer (refer to section 2.11.1). However, as identified the proximity to the river mouth indicates Tom Bull Pool may be tidally influenced.

The uncertainty analysis indicates that the groundwater will decline by at least 1 metre at Mungajee Pool and by at least 2 – 3 metres at Tom Bull Pool, it is therefore recommended that works be conducted to a) confirm the relationship between the pools and the groundwater, and b) establish monitoring sites between the pools and the Sino Iron pit to identify impacts. Data that could be used to assess the connection between the pools and the groundwater include:

- Water quality parameters during the end of dry season, prior to surface water flows.
- Survey the pool levels for comparison with groundwater level data.
- Installation of loggers to monitor the water levels in the pools.
- Bathymetric survey of the pools.

Collection of some of this data was attempted in early 2017, however, localised rains and resulting surface water flows precluded the collection of site specific data.

Groundwater trigger levels for further action and impact management will continue to be assessed as part of the adaptive management framework incorporated into the Groundwater Dependent Vegetation Monitoring Plan.

8 Cumulative impacts scenario

8.1 Cumulative impact scenario description

This section investigates the possible cumulative impacts if the Sino Iron mine and the additional 3 proposed mines were developed in the area.

The cumulative impact scenario considered includes:

- parameters determined for the calibrated Sino Iron mine;
- initial heads determined from the calibrated model;
- the 4 pits developed as per the schedules detailed below; and
- the Balmoral South borefield.

The locations of the pits and the Balmoral South borefield are presented below in Figure 8-1. The Mineralogy and Balmoral South pits are projected to commence in 2022 and the Austeel pit in 2024. The mine schedules for the four mines planned for the Balmoral deposit are presented below in Table 21. The schedules have been simplified from the schedules presented by Aquaterra (2009). It has been assumed that the three additional pits cease mining at the same time in 2038.

The Balmoral South borefield operates for the 24 year life of the mine and is located in the superficial sediments to the southwest of the Sino Iron project. The pumping rate for each bore was set at 822 kL/d assuming a 6 GL/yr (16438 kL/d) allocation limit and 20 production bores.

The cumulative impact scenario is consistent with the Sino Iron LoM assessment commencing at 01/07/2016 (42370d) and uses the final calibrated heads as the initial conditions.

The shorter mine life of the 3 other pits, that is 2022 - 2038 for the Austeel, Balmoral South and Mineralogy projects compared with 2016 – 2060 for the Sino Iron project, and the alteration of material properties in the pit voids meant that it was necessary to run the model over the LoM for two separate periods (2016 – 2038 and 2038 – 2060).

SINO EXPANSION LIFE OF MINE GROUNDWATER MODEL
GROUNDWATER CUMULATIVE IMPACT FORECASTS

Table 21 Cumulative impacts mining schedule showing maximum depth of pit.

	Year	Mineralogy Iron	Sino Iron Expansion		Balmoral South	Austeel
			West Pit	East Pit		
0	2010			-35		
2	2012			-35		
4	2014			-35		
6	2016			-65		
8	2018			-100		
10	2020		-52	-143		
12	2022	-38	-126	-143	-20	
14	2024	-86	-200	-135	-68	-62
16	2026	-134	-234	-165	-140	-110
18	2028	-182	-234	-165	-224	-158
20	2030	-266	-234	-205	-240	-242
24	2034	-328	-234	-205	-250	-266
28	2038	-389	-234	-205	-260	-290
30	2040	-389	-290	-205	-260	-290
35	2045	-389	-290	-355	-260	-290
40	2050	-389	-290	-355	-260	-290
45	2055	-389	-397	-355	-260	-290
50	2060	-389	-397	-355	-260	-290

The final pit shell elevations and contours are presented below in Figure 8-1.

SINO EXPANSION LIFE OF MINE GROUNDWATER MODEL
GROUNDWATER CUMULATIVE IMPACT FORECASTS

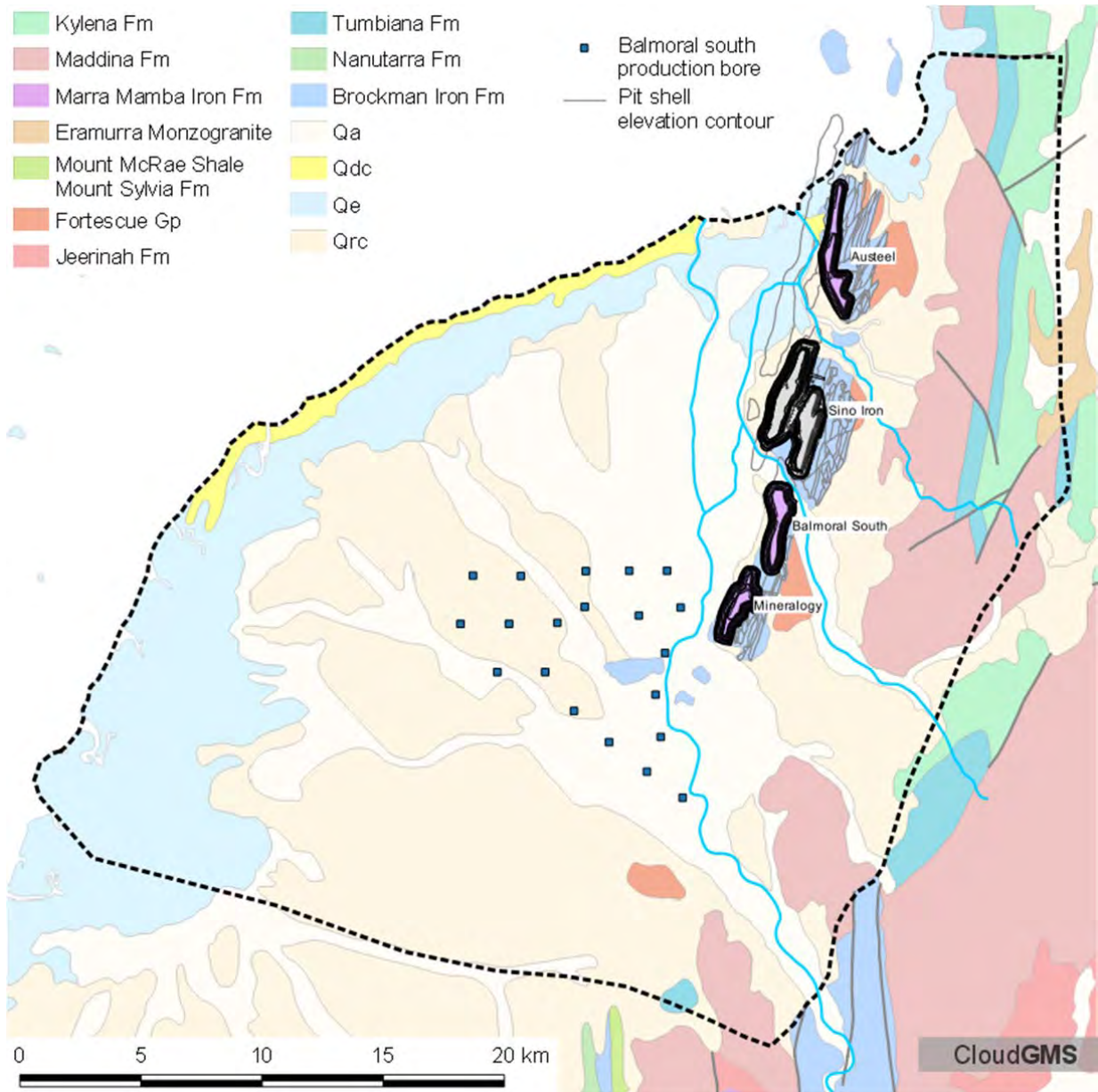


Figure 8-1 Locations of the proposed Austeel, Balmoral South and Mineralogy pits and the Balmoral South borefield.

8.1.1 Limitations

It should be remembered that the geometry utilised in the cumulative impact model have not been optimised for the three (3) other mine sites. That is the geometry of the interface between the surficial sediments and the weathered basement rocks has not been resolved with the same detail as in the vicinity of the Sino Iron pit. The hydraulic parameters are also not constrained by the available information.

8.2 Pits and borefield cumulative impacts

8.2.1 Pit inflows during LoM

The pit inflow results are presented in terms of the following inflow areas:

- Austeel pit
- Balmoral south pit
- Mineralogy pit; and
- Sino Iron pits

The pit inflows estimated by the calibrated groundwater model during the LoM are presented below in Figure 6-2. Figure 6-2 a) the total inflows to the Austeel pit, b) inflows to the Balmoral South pit; c) inflows to the Mineralogy pit; and d) the contribution to the Sino Iron pit. The final pit inflow to the Sino Iron pits is approximately 1 GL/yr less than that forecast by the Sino Iron LoM scenario. This is interpreted to be due to interception of groundwater from the adjacent pits.

The abrupt initial increase in inflows to the additional pits (Austeel, Balmoral South and Mineralogy) is due to the method of applying the development of these pits in the model. As indicated in section 2.8.3, the pits have been applied using the final pit void as a basis and using the elevation identified in the mining schedule to determine the base of the pit shell, that is the pit uses the full pit footprint and develops downwards. This is in contrast to the Sino Iron pits, which develops gradually in time, both vertically and laterally, and as a result generates more gradual increases in the inflows.

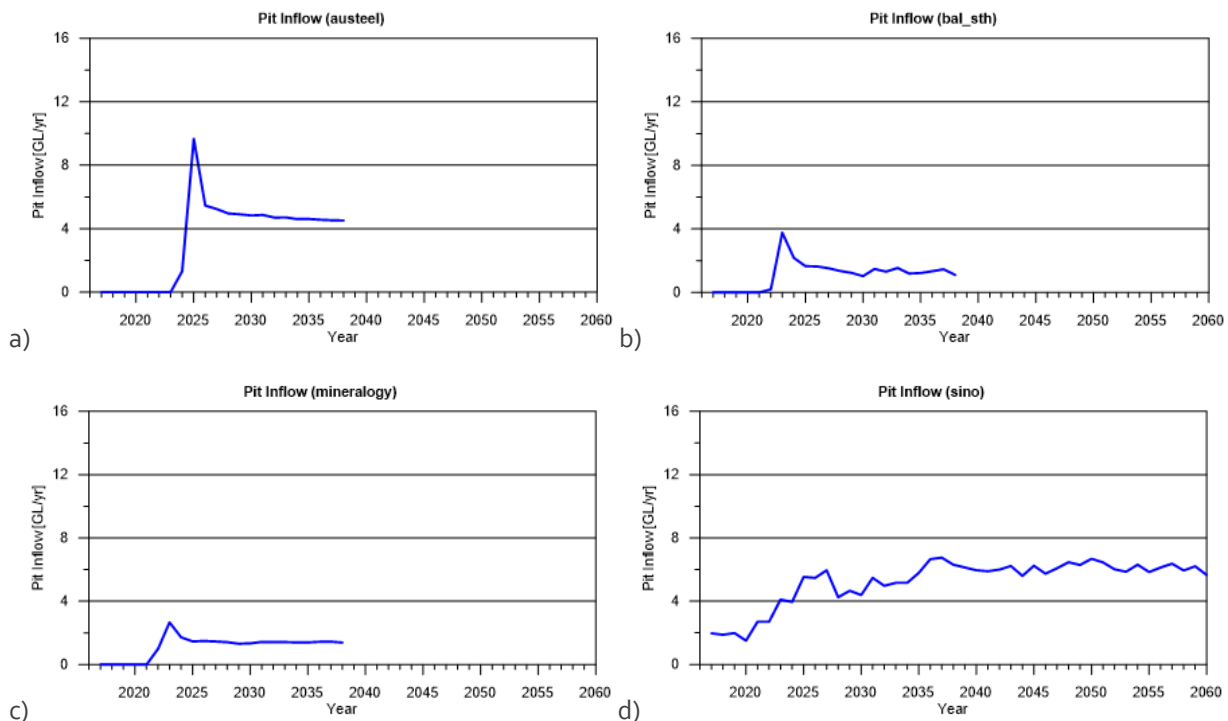


Figure 8-2 Cumulative impact calculated inflows for a) the Austeel pit b) the Balmoral South pit c) the Mineralogy pit and d) the Sino Iron pit.

The annual inflows to the pits are presented below in Table 22.

SINO EXPANSION LIFE OF MINE GROUNDWATER MODEL
GROUNDWATER CUMULATIVE IMPACT FORECASTS

Table 22 Annual pit inflows to the pits considered in the cumulative impact assessment.

Date	Sino [GL/yr]	Austeel [GL/yr]	Bal_sth [GL/yr]	Mineral [GL/yr]	Date	Sino [GL/yr]	Austeel [GL/yr]	Bal_sth [GL/yr]	Mineral [GL/yr]
01/01/2017	-1.95	0.00	0.00	0.00	01/01/2039	-5.61	-4.68	-0.99	-1.31
01/01/2018	-1.71	0.00	0.00	0.00	01/01/2040	-6.10	-1.59	-1.32	-0.56
01/01/2019	-1.62	0.00	0.00	0.00	01/01/2041	-6.17	-2.04	-1.44	-0.69
01/01/2020	-1.43	0.00	0.00	0.00	01/01/2042	-6.62	-2.38	-1.47	-0.78
01/01/2021	-2.22	0.00	0.00	0.00	01/01/2043	-6.45	-2.51	-1.57	-0.95
01/01/2022	-2.67	0.00	-0.32	-1.69	01/01/2044	-6.07	-2.76	-1.69	-0.98
01/01/2023	-3.72	0.00	-5.43	-4.22	01/01/2045	-6.34	-2.93	-1.72	-1.02
01/01/2024	-4.04	-0.95	-2.67	-2.10	01/01/2046	-5.99	-3.19	-1.76	-1.10
01/01/2025	-4.23	-10.98	-1.91	-1.72	01/01/2047	-6.35	-3.22	-1.78	-1.12
01/01/2026	-4.66	-5.79	-1.72	-1.58	01/01/2048	-6.76	-3.22	-1.76	-1.15
01/01/2027	-4.49	-5.51	-1.57	-1.54	01/01/2049	-6.57	-3.22	-1.76	-1.19
01/01/2028	-4.36	-5.21	-1.39	-1.47	01/01/2050	-7.00	-3.30	-1.73	-1.21
01/01/2029	-4.30	-5.19	-1.24	-1.36	01/01/2051	-6.92	-3.33	-1.71	-1.24
01/01/2030	-4.36	-5.14	-1.13	-1.33	01/01/2052	-6.57	-3.38	-1.67	-1.27
01/01/2031	-5.00	-4.99	-1.31	-1.42	01/01/2053	-6.13	-3.39	-1.64	-1.27
01/01/2032	-5.14	-4.85	-1.29	-1.40	01/01/2054	-6.61	-3.39	-1.58	-1.24
01/01/2033	-4.89	-4.85	-1.44	-1.33	01/01/2055	-6.27	-3.41	-1.56	-1.23
01/01/2034	-5.15	-4.73	-1.33	-1.37	01/01/2056	-6.47	-3.47	-1.54	-1.24
01/01/2035	-5.44	-4.81	-1.49	-1.33	01/01/2057	-6.83	-3.51	-1.46	-1.24
01/01/2036	-6.59	-4.65	-1.31	-1.33	01/01/2058	-6.60	-3.49	-1.43	-1.23
01/01/2037	-7.05	-4.70	-1.72	-1.40	01/01/2059	-6.56	-3.55	-1.41	-1.23
01/01/2038	-6.31	-4.76	-1.20	-1.39	01/01/2060	-6.37	-3.57	-1.38	-1.23

The groundwater drawdown contours at 2038, which corresponds to the end of mining for the three pits (Austeel, Balmoral South and Mineralogy) and the Balmoral South borefield, are presented below in Figure 8-3.

Drawdowns of between 1 – 5 metres are generated in the vicinity of the Balmoral South borefield (Figure 8-3). The groundwater level at the regional baseline monitoring bore FCP10A, which is on the western edge of the borefield, shows drawdowns of 2 – 3 metres (refer below to Figure 8-6).

SINO EXPANSION LIFE OF MINE GROUNDWATER MODEL
GROUNDWATER CUMULATIVE IMPACT FORECASTS

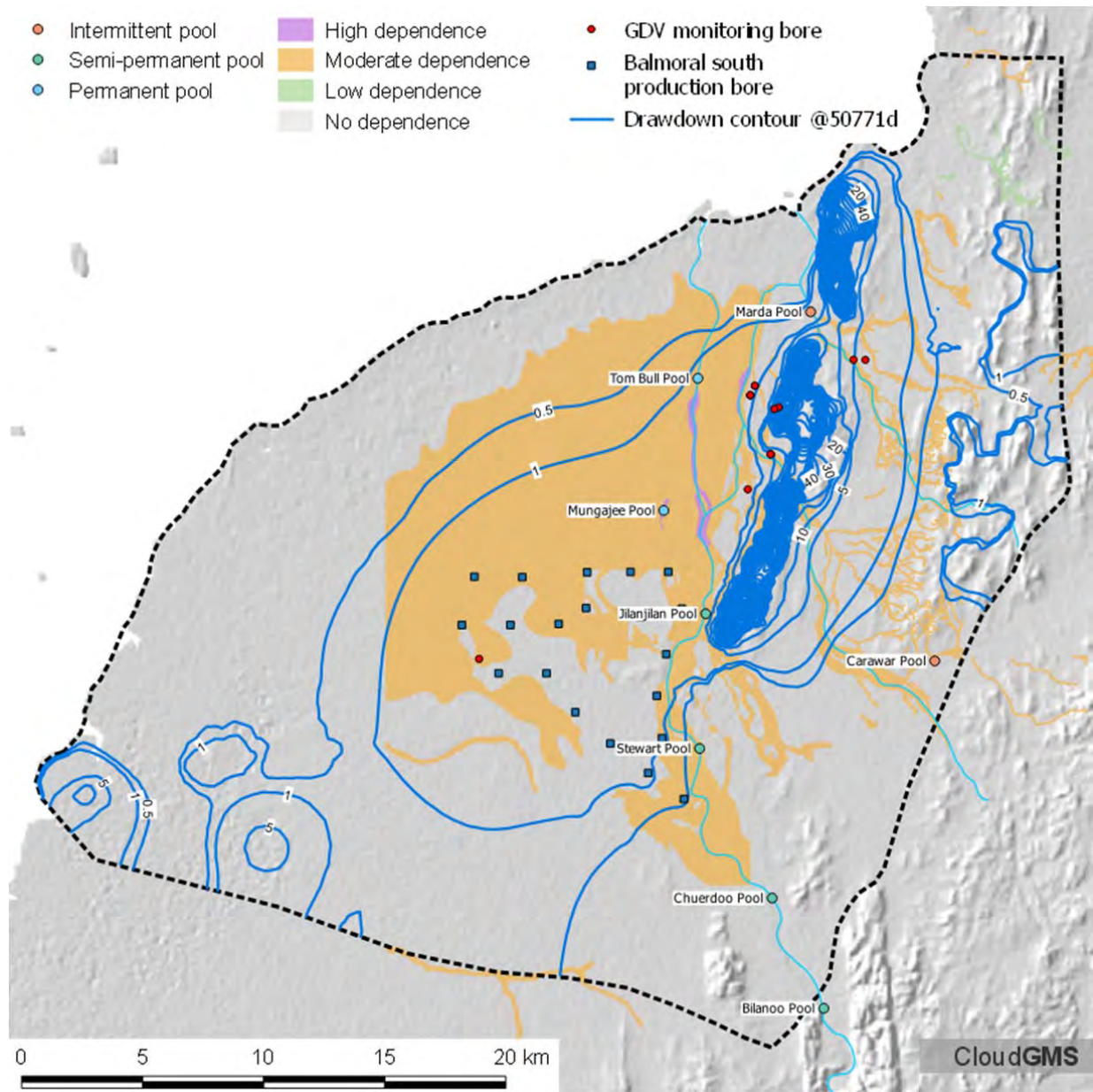


Figure 8-3 Drawdown at the end of mining 50771d (year 2038) showing the impacts of the Balmoral South borefield.

SINO EXPANSION LIFE OF MINE GROUNDWATER MODEL
GROUNDWATER CUMULATIVE IMPACT FORECASTS

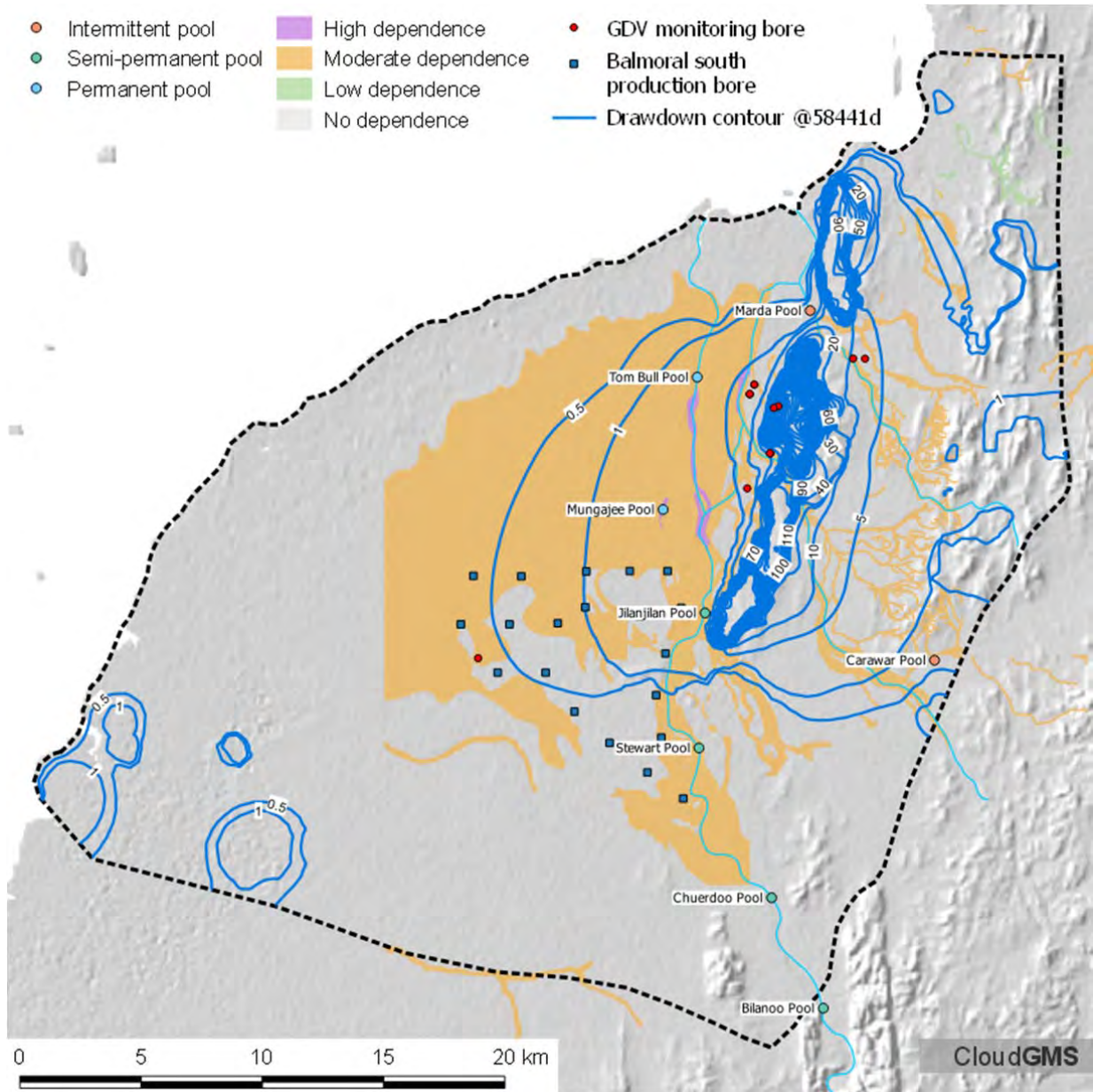


Figure 8-4 Drawdown contours at 58441d (year 2060) showing recovery of the groundwater levels in the vicinity of the Balmoral South borefield.

8.3 Final pit lake cumulative impacts

8.3.1 Groundwater contours

The cumulative impact LoM and pit lake model was run to the same final timestep as the Sino Iron LoM and pit lake model (94965d). The final groundwater level contours at 94965d (year 2160) are presented below in Figure 8-5.

SINO EXPANSION LIFE OF MINE GROUNDWATER MODEL
GROUNDWATER CUMULATIVE IMPACT FORECASTS

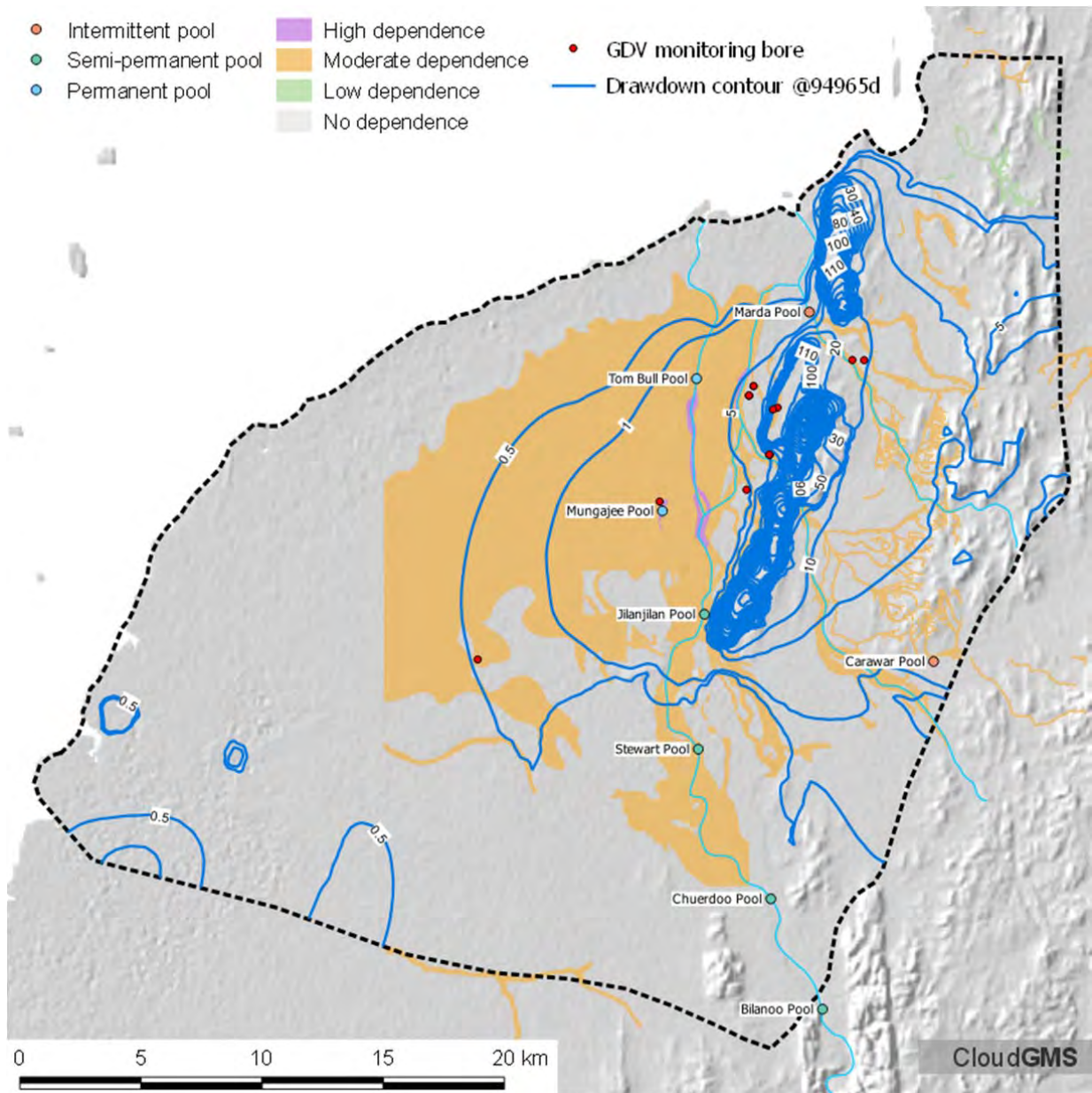


Figure 8-5 Drawdown contours at 94965d (year 2160).

The final water level in the Sino Iron pit lake is comparable with the post closure scenario discussed previously in section 6.4. Considerable inflows from the tidal sections of the rivers are induced

The final levels in the various pit lakes after 100 years of recovery are:

- Austeel is between -170 to -180 mAHD;
- Balmoral South is between -230 to -240;
- Mineralogy is between -240 to -250 mAHD;
- Sino Iron East Pit is between -310 and -320 mAHD; and
- Sino Iron West Pit is between -120 and -130 mAHD

The pit-lake water levels in the cumulative impact scenario, like the Sino Iron scenario, did not reach full equilibrium and it is expected several hundred years would be required to reach full equilibrium.

However, further investigations into aquifer properties to the west of the pits is required in order to reduce crucial uncertainties before further hypothesis testing would be warranted.

8.3.2 Groundwater level impacts at reference monitoring bores

Groundwater levels have been extracted from the cumulative impact scenario at the regional reference sites (FCP10A, FCP22A and FCP23A) and are presented below in the following sections. Groundwater levels for the monitoring bores outside of the footprint of the Sino Iron pits are also presented in Appendix L.

The groundwater levels at all sites considered appear to reach a state of dynamic equilibrium at approximately 2080.

FCP10A

The cumulative impact response at FCP10a is consistent with the LoM response, however, for the period that the Balmoral South borefield is operational (2022 – 2038), groundwater levels are seen to decline approximately 2-3 metres. Following mine closure, they recover to nearly pre-pumping levels.

FCP22A

Groundwater levels at FCP22A show a similar trend to the LoM and post closure scenarios, however, they stabilise at approximately 1-2 metres below those established during the LoM and post closure scenarios.

FCP23A

Groundwater levels at FCP23A show a similar trend to the LoM and post closure scenarios presented in section 6.2.3, however, they stabilise at approximately 2 metres below those established during the LoM and post closure scenarios. FCP23A has a trigger value of 4.2 mAHD, under the cumulative scenario. This value is exceeded by mid 2020 and groundwater continue to decline after this time and stabilise at between 4-5 metres below the current trigger value.

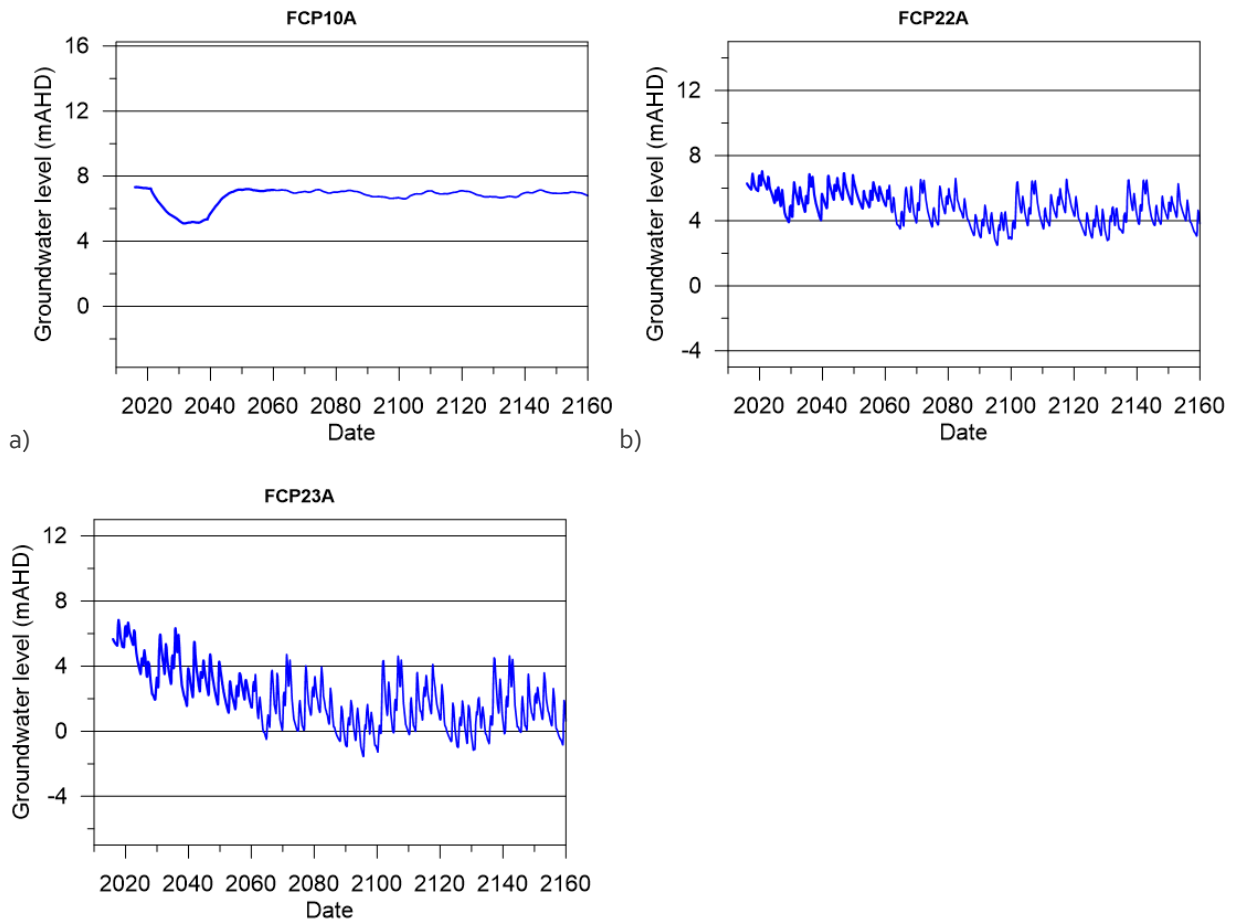


Figure 8-6 Groundwater level response at regional baseline bores a) FCP10A, b) FCP22A and c) FCP23A.

Selected Groundwater Dependent Vegetation (GDV) monitoring bores

Groundwater level hydrographs at the groundwater dependent vegetation monitoring sites (07RC149, 07RC156, 09AC490 and 09AC534) are presented below in Figure 8-8 a & b and Figure 8-8 a & b.

07RC149

The groundwater levels at 07RC149, which is a zone 2 GDV monitoring site, show a decline in groundwater levels of approximately 10 metres at the end of mining (2060), after which they stabilise for the rest of the 144 year period modelled. The final drawdown is greater than the trigger value for 07RC149 determined as 3 standard deviations from the mean ($\mu = 5.60$ mAHd; $\sigma = 1.0$ m refer Appendix A).

07RC156

The groundwater levels at 07RC156, which is a zone 1 GDV monitoring site, show a decline by nearly 12 metres below the initial level during the LoM, however, it recovers following mine closure (2060) to approximately 10 metres below the initial water level and appears to reach dynamic equilibrium at this level soon after closure of the pit for the duration of the post closure scenario. The final decline in groundwater level is greater than the 2 standard deviations from the mean identified as a trigger value ($\mu = 6.00$ mAHd; $\sigma = 1.0$ m refer Appendix A).

**SINO EXPANSION LIFE OF MINE GROUNDWATER MODEL
GROUNDWATER CUMULATIVE IMPACT FORECASTS**

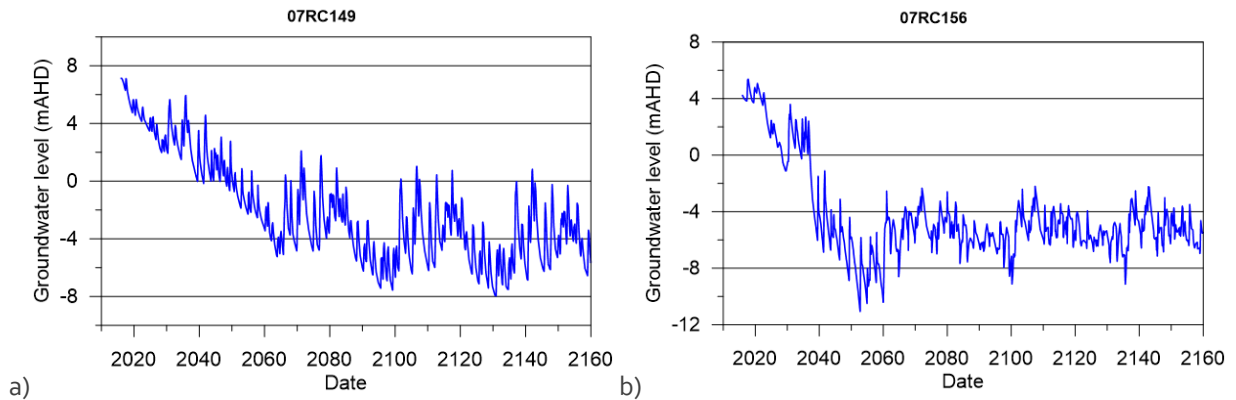


Figure 8-7 Representative GDV monitoring sites around the Sino Iron pit a) 07RC149 and b) 07RC156.

09AC490 and 09AC534

09AC490 and 09AC534 are active Zone 1 reference monitoring sites along the western margin of the West Pit and are constructed in the superficial sediments. The sites are representative of the groundwater level changes at the GDV site 13 (Astron, 2015). The groundwater levels at 09AC490 and 09AC534 are presented below in Figure 8-8 a & b respectively.

The groundwater levels at 09AC490 and 09AC534 at the end of mining is approximately 7 metres, after which it stabilises for the rest of the period modelled.

The final decline in groundwater level at both sites is greater than the 2 standard deviations from the mean identified as a trigger values (09AC490 $\mu= 2.70$ mAHd; $\sigma = 1.1$ m and 09AC534 $\mu= 2.10$ mAHd; $\sigma = 0.7$ m refer Appendix A). However, the triggers are not reached until approximately 2025. The rate of decline in groundwater levels is relatively slow at between 0.23 and 0.18 metres per year and as discussed in section 2.11.2 there may be capacity for the GDV at these sites to adapt to this rate of decline in groundwater levels.

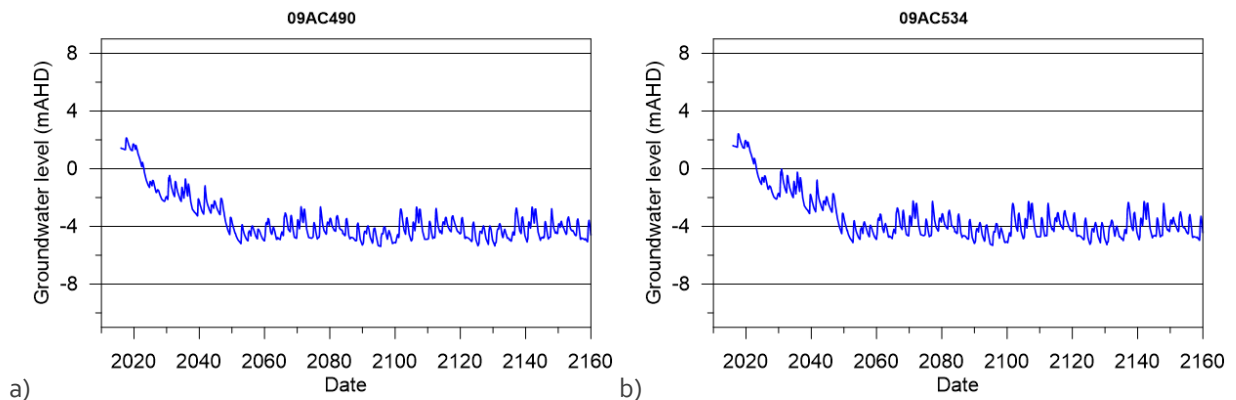


Figure 8-8 Representative GDV monitoring sites around the Sino Iron pit a) 09AC490 and b) 09AC534.

Groundwater levels at permanent pools

The groundwater level decline in response to the cumulative impact scenario at Mungajee Pool and Tom Bull Pool are presented below in Figure 8-9 a & b respectively.

SINO EXPANSION LIFE OF MINE GROUNDWATER MODEL
GROUNDWATER CUMULATIVE IMPACT FORECASTS

The maximum groundwater level decline at Mungajee Pool is approximately 3 metres, which is 1 – 2 metres greater than the LoM response. The greater impact is due to the influence of the additional pits to the southeast of the pool.

The groundwater level response at Tom Bull Pool is approximately 0.2 metres below the impacts estimated for the LoM scenario. The similar response at Tom Bull is due to its distance from the additional projects to the south east and the proximity to the tidal sections of the Fortescue River. Although the groundwater level decline is limited by the influence of the tidal section of the river, streamline analysis (refer below to section 8.5) suggests that poorer quality groundwater associated with the tidal flats is unlikely to migrate towards Tom Bull Pool.

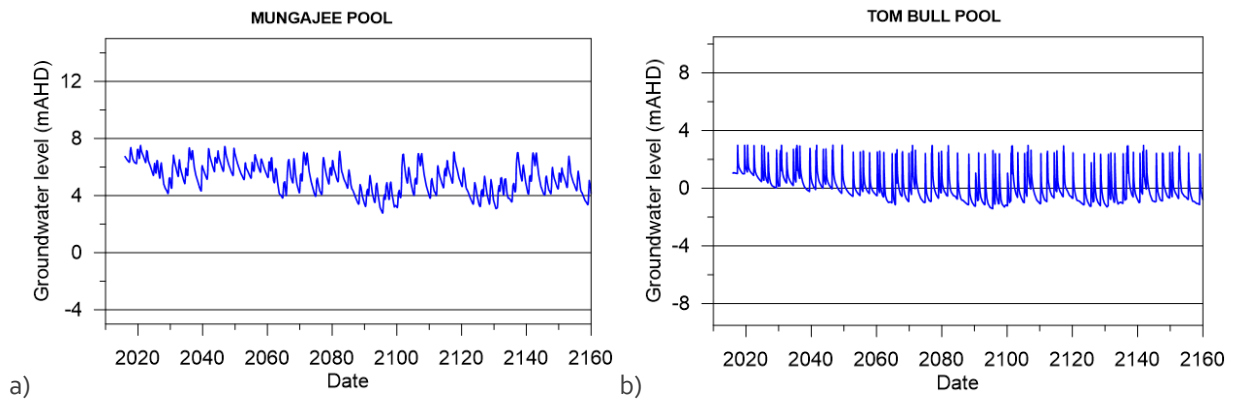


Figure 8-9 Groundwater level response at regional baseline bores a) Mungajee Pool and b) Tom Bull Pool.

8.4 Cumulative impact water balances

8.4.1 LoM water balance

The cumulative impact model has been queried to provide regional water balance components and are presented in Figure 8-10. The components presented are consistent with the water balance components presented for the LoM model noting the inclusion of the Balmoral South borefield. To improve readability the individual pit fluxes have been combined into a total pit flux. The components of the total pit flux are presented in a separate graphic refer to Figure 8-11.

The values used in the plot above are presented in Appendix M.

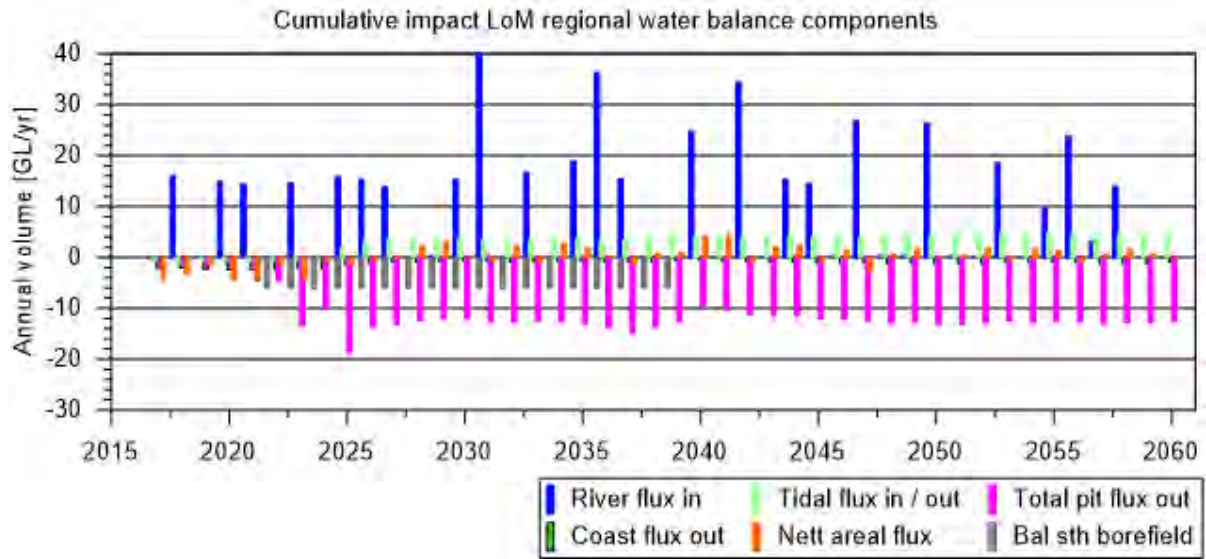


Figure 8-10 Cumulative impact regional water budget components with the inflows to the individual pits combined as a total pit flux value.

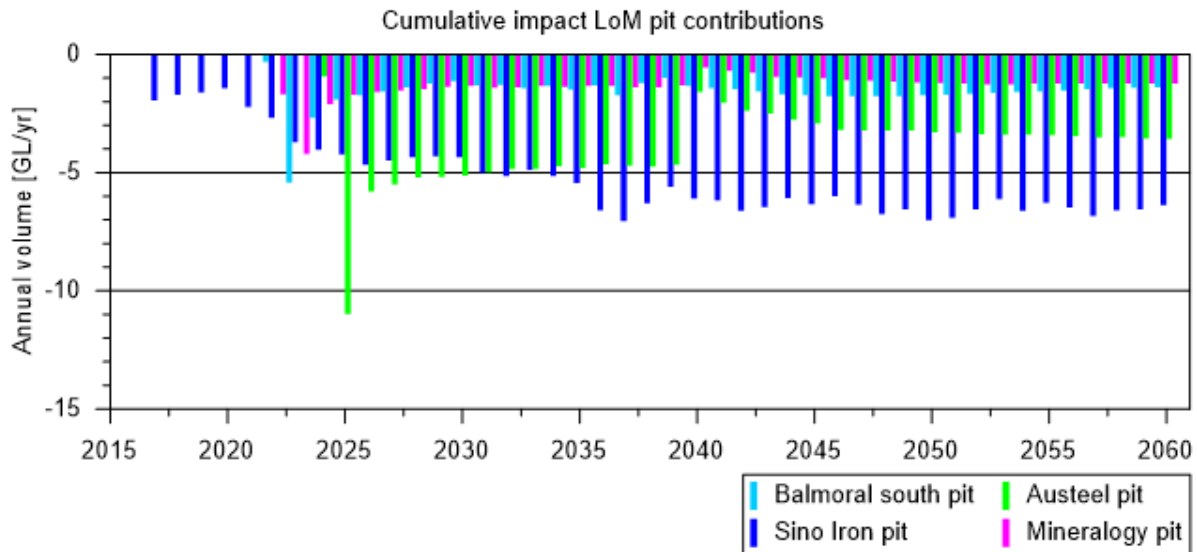


Figure 8-11 LoM contributions to the total pit inflow component of the regional water budget. The flows reported for the Austeel, Balmoral South and Mineralogy pits after 2038 are due to the evaporative flux from the surface of the pit lake.

8.4.2 Cumulative impact LoM water balances

The water balances closures for the 2 model runs that comprise the cumulative LoM impacts are presented below in Table 23 and Table 24.

SINO EXPANSION LIFE OF MINE GROUNDWATER MODEL
GROUNDWATER CUMULATIVE IMPACT FORECASTS

Table 23 Total water budget for the period 01/01/2016 to 01/01/2038.

Component	Out	In	Out	In
	m ³	m ³	GL/yr	GL/yr
Specified head BC	-3.00E+08	7.77E+07	-13.62	3.53
Specified flux BC	0	0	0.00	0.00
Transfer BC	2.11E+03	2.53E+08	0.00	11.50
Wells	-1.08E+08	0	-4.91	0.00
Distributed sink (-) / source (+)	-3.25E+08	3.10E+08	-14.78	14.09
Storage release (-) / capture (+)	-4.30E+08	5.20E+08	-19.53	23.61
Total	-1.16E+09	1.16E+09	-52.85	52.73
Imbalance %	0.22			

Table 24 Total water budget for the period 01/01/2039 to 01/01/2060.

Component	Out	In	Out	In
	m ³	m ³	GL/yr	GL/yr
Specified head BC	-1.91E+08	1.26E+08	-8.66	5.71
Specified flux BC	0.00E+00	0.00E+00	0.00	0.00
Transfer BC	0.00E+00	2.13E+08	0.00	9.70
Wells	0.00E+00	0.00E+00	0.00	0.00
Distributed sink (-) / source (+)	-3.85E+08	2.83E+08	-17.50	12.86
Storage capture (-) / release (+)	-4.07E+08	3.59E+08	-18.52	16.33
Total	-1.73E+06		-44.68	44.60
Imbalance %	0.18			

8.4.3 Comparison of cumulative impact LoM water budgets to natural conditions

To provide an easier assessment of the changes to the water budgets presented in the previous sections a 'natural' scenario was run where all stresses associated with mining activities were removed.

The cumulative LoM impact scenario was separated into two model runs; one run to simulate the development of the pits, the second run involved converting the pits to pit voids and continuing the development of the Sino Iron pit to end of life at 2060. The results for the cumulative impact LoM phase of mining therefore are presented for the period 2016 – 2038 below in Table 25 and for the period 2038 – 2060 in Table 26.

Comparison for period 2016 – 2038

The following observations were made regarding the water balance for the cumulative impacts for the LoM for the period 2016 – 2038:

- The specified head boundary conditions, representing the coast and tidal sections of the rivers and the abstraction from the pits, show an increase in the net outflow of approximately -6.1 GL/yr from a net outflow ('difference') outflow of -4.0 GL/yr. from the "natural" run to a net outflow (difference) of 10.1 GL/yr for the LoM run). However, the increase in net outflow includes outflows from the pits which over the period considered averages -12.7 GL/yr (refer to Appendix M). This means that the pits induces a net inflow of -6.6 GL/yr at the coast and tidal sections of the river.

SINO EXPANSION LIFE OF MINE GROUNDWATER MODEL
GROUNDWATER CUMULATIVE IMPACT FORECASTS

- There is a slight increase in inflows of 1.1 GL/yr from the transfer boundary conditions, representing the non-tidal sections of the rivers. This is due to the reduced groundwater levels around the pit providing additional storage for recharge from the rivers.
- The distributed in / out flow components show a net decrease in outflow of 4.7 GL/yr, this is a result of a reduction in evapotranspiration due to the groundwater levels around the pits declining below the root depths used in the evapotranspiration function.

Table 25 Comparison of cumulative impacts for the period 2016 – 2038.

Component	Cum impact Lom 2016 – 2038			Natural 2016 – 2038			Change
	Out	In	Diff	Out	In	Diff	
	[GL/yr]	[GL/yr]	[GL/yr]	[GL/yr]	[GL/yr]	[GL/yr]	[GL/yr]
Specified head BC	-13.62	3.53	-10.09	-4.33	0.33	-4.00	-6.09
Specified flux BC	0.00	0.00	0.00	0.00	0.00	0.00	0.00
Transfer BC	0.00	11.50	11.50	0.00	10.42	10.42	1.08
Wells	-4.91	0.00	-4.91	0.00	0.00	0.00	-4.91
Distributed sink (-) / source (+)	-14.78	14.09	-0.70	-18.67	13.24	-5.43	4.73
Storage release (-) / capture (+)	-19.53	23.61	4.08	-14.29	13.14	-1.15	5.23
Total	-52.85	52.73	-0.12	-37.29	37.14	-0.15	

Comparison for period 2038 – 2060

The following observations were made regarding the water balance for the cumulative impacts for the LoM for the period 2038 – 2060:

- The specified head boundary conditions, representing the coast and tidal sections of the rivers and the continuing abstraction from the Sino Iron pit, show a net inflow of 0.8 GL/yr from an outflow of -3.7 GL/yr. However, this includes outflows from the Sino Iron pit which over the period considered averages -6.4 GL/yr (refer to Appendix M). This means that the pits induce a net inflow of -7.2 GL/yr at the coast and tidal sections of the river.
- There is a slight increase in inflows of 1.39 GL/yr from the transfer boundary conditions, representing the non-tidal sections of the rivers. This is due to the reduced groundwater levels around the pit providing additional storage for recharge from the rivers.
- The distributed in / out flow components show a net increase in inflow of 0.4 GL/yr, however, the outflow value includes evaporative losses from the developing pit-lakes. The combined evaporative fluxes from these pit-lakes averages is -5.8 GL/yr. This results in a reduction in evapotranspiration of approximately 5.4 GL/yr. The reduction in evapotranspiration is due to the groundwater levels around the pits declining below the root depths used in the evapotranspiration function.
- Storage capture / release shows water is captured into storage (infill of the pit voids) at a rate of approximately -2.5 GL/yr.
- The different volumes reported for the storage release / capture values indicate that the model has not yet stabilised. This is supported by the discussion below regarding the pit-lake water levels after 100 years of recovery.

SINO EXPANSION LIFE OF MINE GROUNDWATER MODEL
GROUNDWATER CUMULATIVE IMPACT FORECASTS

Table 26 Comparison of cumulative impacts for the period 2038 – 2060.

Component	Cum impact Lom 2038 – 2060			Natural 2038 – 2060			Change
	Out	In	Diff	Out	In	Diff	
	[GL/yr]	[GL/yr]	[GL/yr]	[GL/yr]	[GL/yr]	[GL/yr]	[GL/yr]
Specified head BC	-8.66	5.71	-2.95	-3.99	0.29	-3.70	0.75
Specified flux BC	0.00	0.00	0.00	0.00	0.00	0.00	0.00
Transfer BC	0.00	9.70	9.70	0.00	8.31	8.31	1.39
Wells	0.00	0.00	0.00	0.00	0.00	0.00	0.00
Distributed sink (-) / source (+)	-17.50	12.86	-4.64	-17.14	12.07	-5.07	0.43
Storage release (-) / capture (+)	-18.52	16.33	-2.19	-11.16	11.48	0.32	-2.51
Total	-44.68	44.60	-0.08	-32.28	32.15	-0.14	

8.4.4 Cumulative impact post closure water balance

The in / out flow components for the post closure scenario are presented below in Figure 8-12. The total pit flux out is the evaporative loss from the surface water of the four pit lakes and stabilises at approximately 14 – 15 GL/yr.

The flow into the model domain from the coastal boundary reduces from approximately 10 GL/yr to 3 – 4 GL/yr. The inflows to the model domain from the tidal sections of the rivers is relatively constant at approximately 4-5 GL/yr. Similarly the areal fluxes out of the model domain remain relatively constant at 11-12 GL/yr. Therefore, the losses due to evaporation are met by the flows induced into the model domain from the coast and tidal portions of the rivers.

A consistent outcome from the water balance results is that the inflows to the pits increases and stabilises at a value similar to the maximum inflow observed during the LoM.

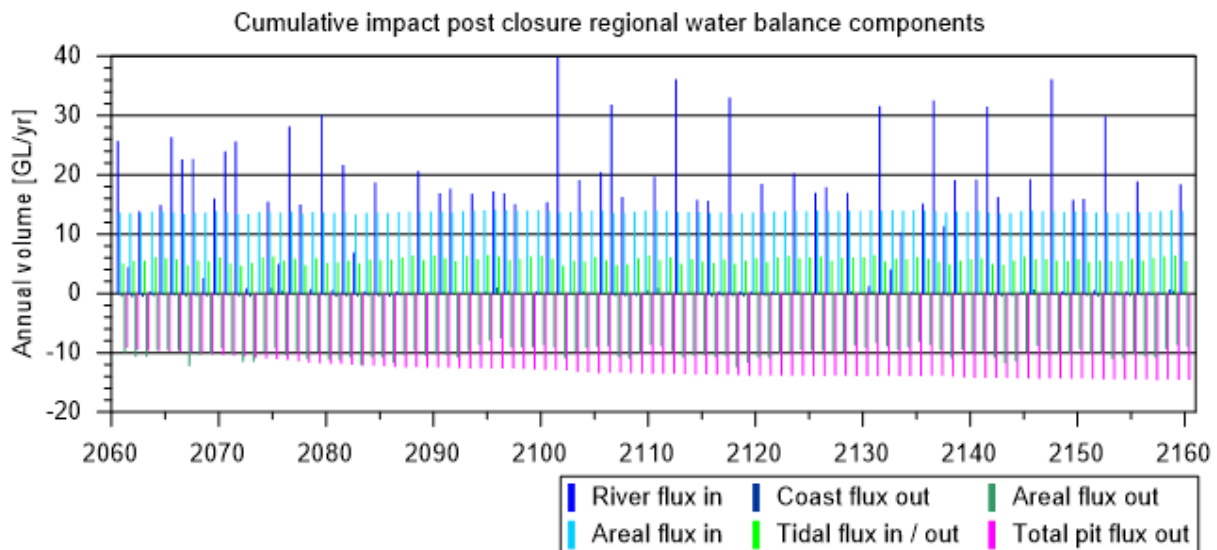


Figure 8-12 Cumulative impact post closure in / out flow water balance components for the model domain.

The water balance closure for the cumulative impact post closure pit lake model run is presented below in Table 27.

SINO EXPANSION LIFE OF MINE GROUNDWATER MODEL
GROUNDWATER CUMULATIVE IMPACT FORECASTS

Table 27 Cumulative impact post closure total water budget for the period 01/01/2060 to 01/01/2160.

Component	Out m ³	In m ³	Out GL/yr	In GL/yr
Specified head BC	-2.36E+08	7.90E+08	-2.36	7.90
Specified flux BC	0.00E+00	0.00E+00	0.00	0.00
Transfer BC	-1.25E+04	1.17E+09	0.00	11.74
Wells	0.00E+00	0.00E+00	0.00	0.00
Distributed sink (-) / source (+)	-2.65E+09	1.36E+09	-26.54	13.60
Storage release (-) / capture (+)	-2.58E+09	2.12E+09	-25.79	21.17
Total	-5.47E+09	5.44E+09	-54.69	54.41
Imbalance %	0.51			

8.4.5 Comparison of cumulative impact post closure water budgets to natural conditions

The results for the post closure phase of mining for the period 2060 – 2160 are presented below in Table 28. Observations made from the comparison of the water balances are summarised as:

- The specified head boundary conditions, representing the coast and tidal sections of the rivers, show a change from net outflow of approximately -3.9 GL/yr to a net inflow of 5.5 GL/yr a change of 9.4 GL/yr. This is a significant change to the water balance equating to approximately 25% of the total inflows under the natural scenario.
- The major component of the inflows is associated with the evaporative flux from the Austeel pit, which averages around 5.1 GL/yr and this demand is met directly with inflows from the tidal sections of the river and the coast, which are 200 and 400 metres from the edges of the pit respectively.
- There is a net increase in inflows from the transfer boundary conditions, representing the non-tidal sections of the river, as the reduced groundwater levels around the pits provide additional storage for recharge from the river.
- The distributed in / out flow components show a net increase in outflow, this is mostly due to the evaporation from the surface of the pit-lakes. Total evaporative loss from the pits averages 13 GL/yr (refer to Appendix M) resulting in a reduction in ET of approximately 5.1 GL/yr from -18.6 GL/yr to -13.5 GL/yr.
- Storage release / capture shows water is captured into storage (infill of the pit void) at a rate of approximately 4.6 GL/yr. The different volumes reported for the capture / storage values indicate that the model has not yet stabilised. This is supported by the discussion below regarding the pit-lake water levels after 100 years of recovery.

SINO EXPANSION LIFE OF MINE GROUNDWATER MODEL
GROUNDWATER CUMULATIVE IMPACT FORECASTS

Table 28 Comparison of cumulative impacts for the post closure period 2060 - 2160

Component	Cum impact Lom 2060 - 2160			Natural 2060 - 2160			Change
	Out	In	Diff	Out	In	Diff	
	[GL/yr]	[GL/yr]	[GL/yr]	[GL/yr]	[GL/yr]	[GL/yr]	[GL/yr]
Specified head BC	-2.36	7.90	5.54	-4.24	0.29	-3.94	9.48
Specified flux BC	0.00	0.00	0.00	0.00	0.00	0.00	0.00
Transfer BC	0.00	11.74	11.74	0.00	9.85	9.85	1.89
Wells	0.00	0.00	0.00	0.00	0.00	0.00	0.00
Distributed sink (-) / source (+)	-26.54	13.60	-12.93	-18.59	12.58	-6.00	-6.93
Storage release (-) / capture (+)	-25.79	21.17	-4.62	-12.89	12.85	-0.04	-4.58
Total	-54.69	54.41	-0.28	-35.71	35.58	-0.14	

8.5 Cumulative groundwater quality impacts

The possible cumulative impacts on groundwater quality have been assessed using backward streamline analysis with reference to the water quality distribution presented in section 3.8 modified from Haig (2009).

Streamline analysis generated using the groundwater velocity flow field has been completed for a single scenario at the end of the post closure run after 100 years of recovery in the pit lake (year 2160);

The results of the scenario are presented below in Figure 8-13. The streamline length is 36500d (100 years).

An immediate observation of the results is that the streamlines still completely surround the Sino Iron pits, indicating that the pit is a sink at the end of mining and following development of the pit lake. It also appears that the poorer quality groundwater will not be drawn into areas of better groundwater quality. For example, although the saline and hypersaline groundwater to the north and northwest of the pit are drawn to the northern extent of the pit, the path line is through similar quality groundwater. Conversely, it is indicated that the groundwater quality in the vicinity of Tom Bull Pool will be the same, or slightly improved by the migration of better groundwater quality from the south and west.

Groundwater from all salinity categories (fresh to hyper saline) will be drawn into the final Sino Iron pit-lake. The resulting water quality residing in the pit-lake will evolve to eventually become hypersaline through evapoconcentration processes. To understand the evolution of the water quality in the pit-lake, a study similar to that completed for the Mount Goldsworthy pit-lake (Sivapalan, 2005) would be required, which is beyond the scope of the current study.

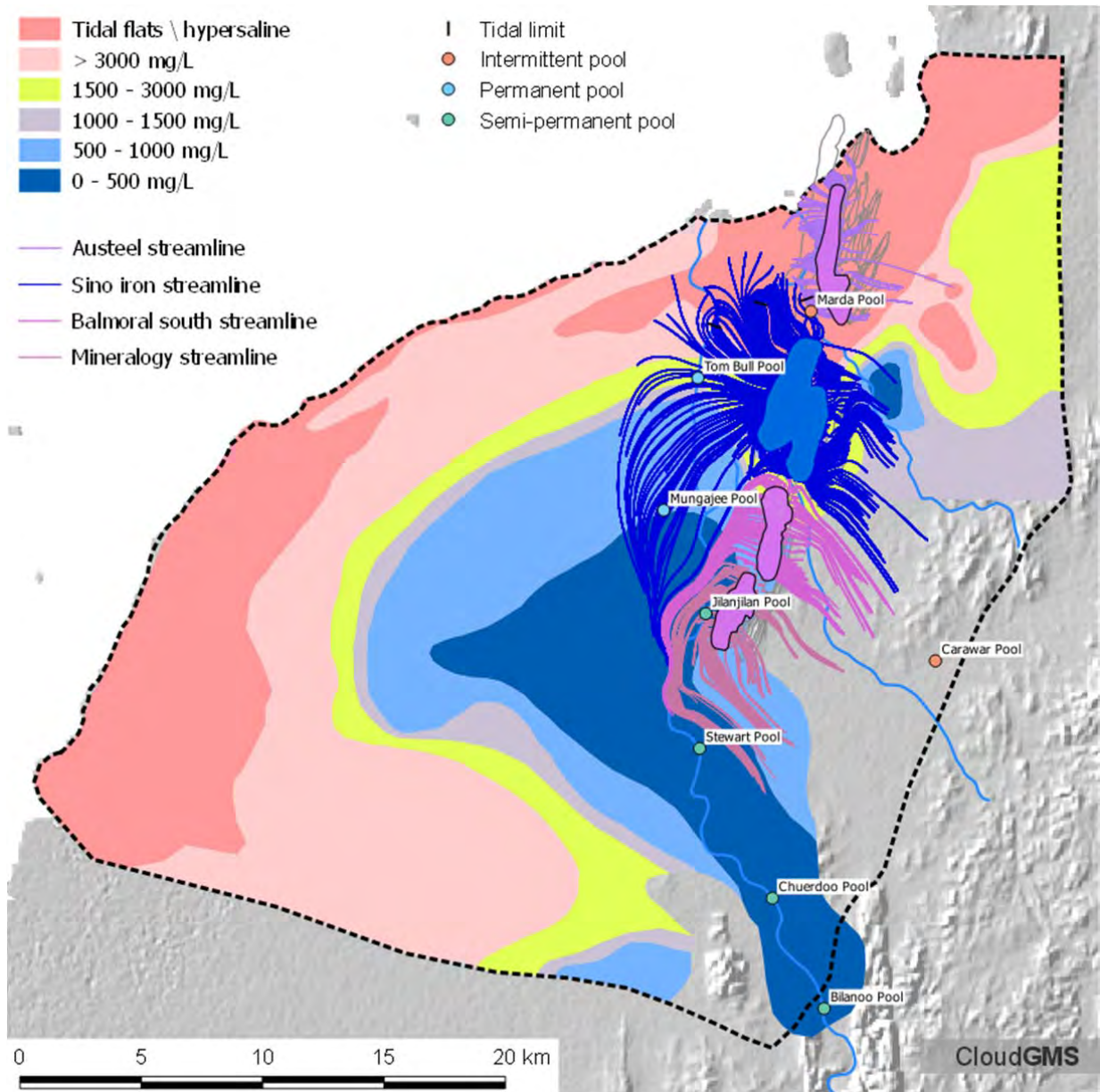


Figure 8-13 Backward streamlines indicating the source of groundwater entering the pits after 100 years of recovery following the end of mining 94965d (year 2160).

8.6 Impacts on existing users

The groundwater drawdown contours for the cumulative impact scenario at 94965d (year 2160) are presented below in Figure 6-14 with the locations of the existing stock wells in the study area. The drawdown impacts are appreciably greater than the Sino Iron scenario.

Jillan Jillan Well can expect drawdowns of greater than 1 metre. Drawdowns of approximately 5 metres are evident at Marda Well, and Fortescue Bore. Balmoral Well at the Balmoral Homestead and Tarquin Well show drawdowns of greater than 5 metres. All other wells in the study area are expected to show drawdowns of less than 1 metre.

SINO EXPANSION LIFE OF MINE GROUNDWATER MODEL
GROUNDWATER CUMULATIVE IMPACT FORECASTS

Depending on the construction of the wells, it is possible that drawdowns of greater than 5 metres may have a significant impact on the available drawdown and therefore the yield of the bore. The streamline analysis discussed previously indicates that water quality changes are unlikely to occur.

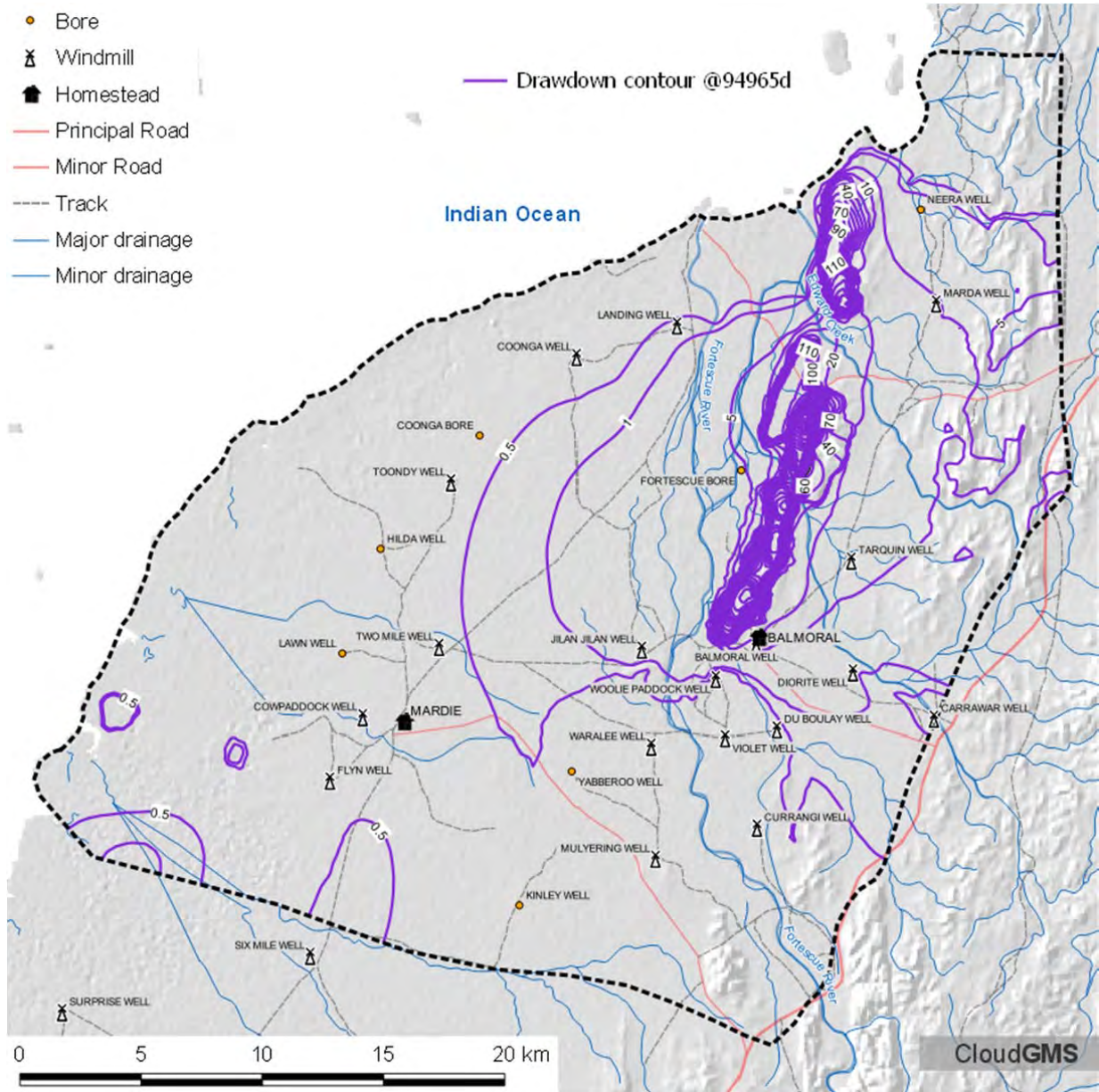


Figure 8-14 Comparison of groundwater drawdown contours at 94965d (2160) and the locations of wells used for pastoral activities.

8.7 Cumulative impact uncertainty analysis

8.7.1 Pit inflows

The trends in the total pit inflows for the cumulative impact scenario is similar to the LoM inflows, although the median inflow is slightly lower by about 25% from 8 GL/yr to 6 GL/yr. It is interpreted that this is due to the interception of groundwater by the adjacent pits.

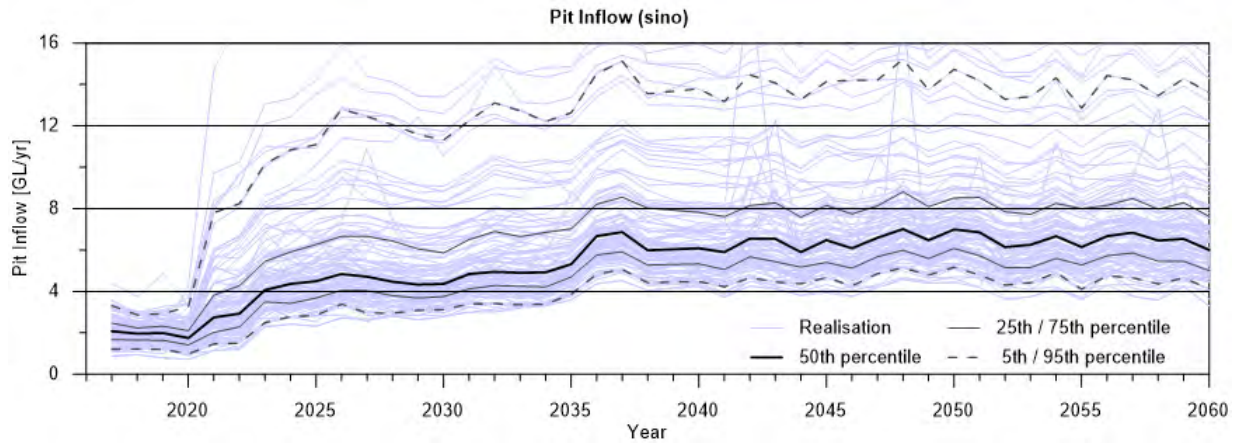


Figure 8-15 Cumulative impacts estimated inflows to the Sino Iron pit (LoM 2016 – 2060).

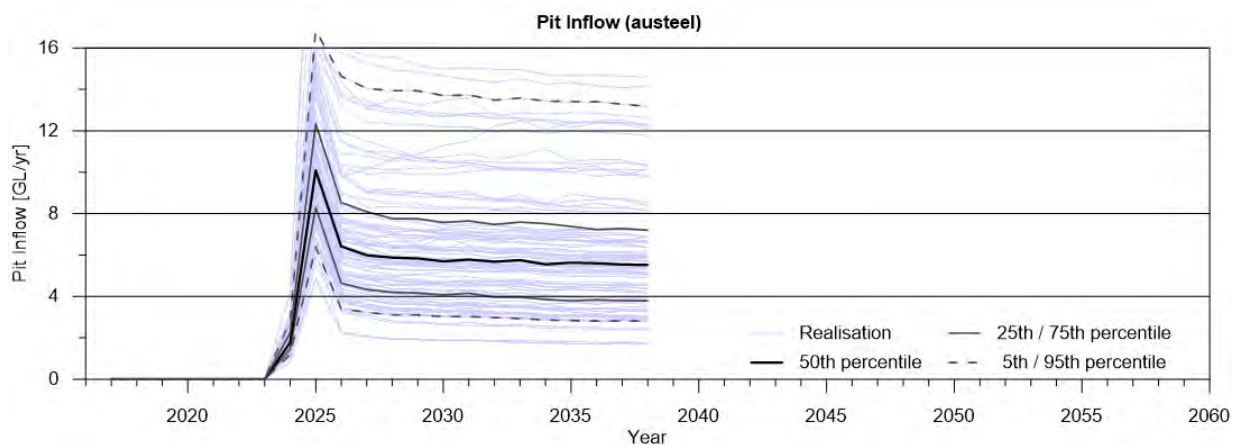


Figure 8-16 Cumulative impacts estimated inflows to the Austeel pit (LoM 2024 – 2038).

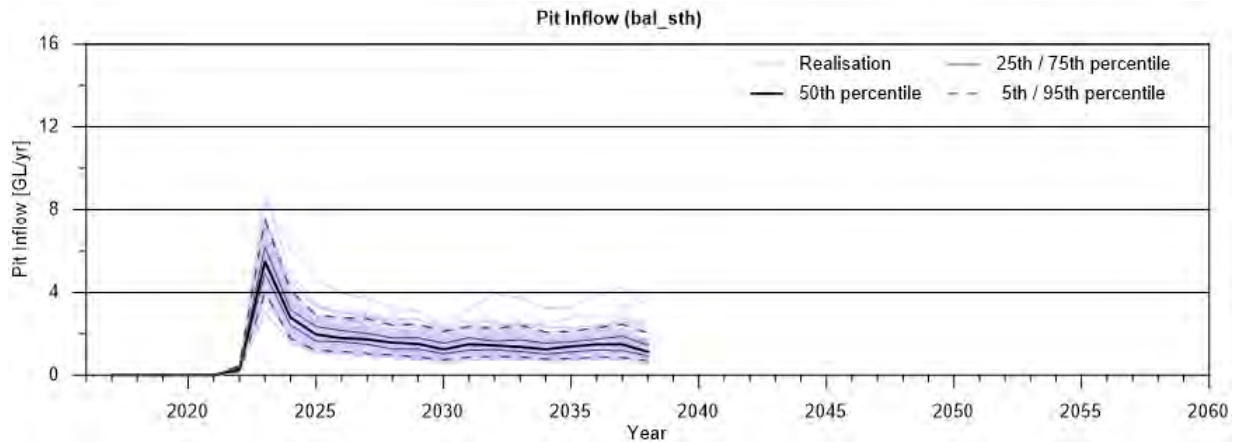


Figure 8-17 Cumulative impacts estimated inflows to the Balmoral South pit (LoM 2022 – 2038).

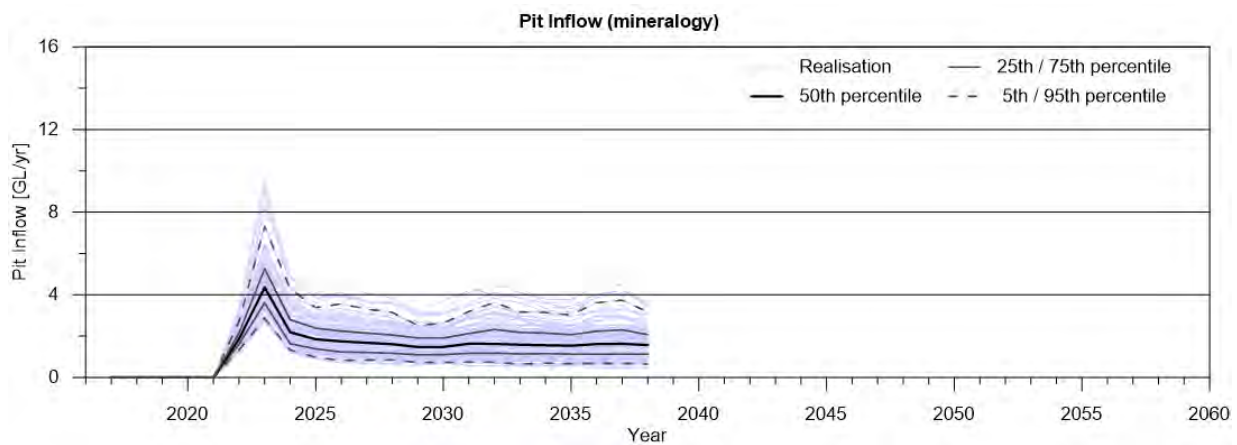


Figure 8-18 Cumulative impacts estimated inflows to the Mineralogy pit (LoM 2022 – 2038).

The uncertainty analysis conducted on the cumulative impacts model shows similar outcomes to the Sino Iron LoM model, however, there is a much narrower range of predicted inflows at the Balmoral South and Mineralogy Pits compared to the Sino Iron pit. It would be expected that similar pit inflows would be expected, and this indicates the importance of the relationship between the contact between the superficial sediments and the weathered Hamersley Group and the proximity of the pit shell to this contact.

8.7.2 Groundwater level hydrograph at GDV monitoring bores

Groundwater level hydrographs have been generated at selected monitoring sites (07RC149, 07RC150, 07RC156, 09AC490, 09AC537, FCP10A and FCP23A). A sub-set was selected due to the clustered nature of some of the monitoring sites several provide the same response and the sites presented are considered representative of the sites identified above in Table 20. The results are presented as a suite of groundwater level responses for each realisation and 5th, 25th, 50th, 75th and 95th percentile values marked.

Groundwater levels respond as expected with sites closer to the pit showing the greatest drawdown and the sites further from the pit showing less impact.

FCP10A

FCP10a is an active regional reference monitoring site located at approximately 15 km to the south west of the Sino Iron pits. The groundwater levels at FCP10a are presented below in Figure 8-19a. The current trigger value for this site is 2 standard deviations below the baseline mean ($\mu= 6.98$ mAHD; $\sigma = 0.92$ m).

SINO EXPANSION LIFE OF MINE GROUNDWATER MODEL
GROUNDWATER CUMULATIVE IMPACT FORECASTS

FCPA22A

FCP22A is located at approximately 4.8 km to the south west of the Sino Iron pits. The site is located near Mungajee pool and has been selected for future monitoring to assess its connection with the groundwater in the superficial sediments aquifer. The response is consistent with the results at Mungajee Pool.

FCP23A

FCP23A is an active regional reference monitoring site located at approximately 2 km to the south west of the Sino Iron pits. The groundwater levels at FCP23A are presented below in Figure 8-19b.

The current trigger value for this site is 2 standard deviations below the baseline mean ($\mu = 6.98$ mAHD; $\sigma = 0.92$ m).

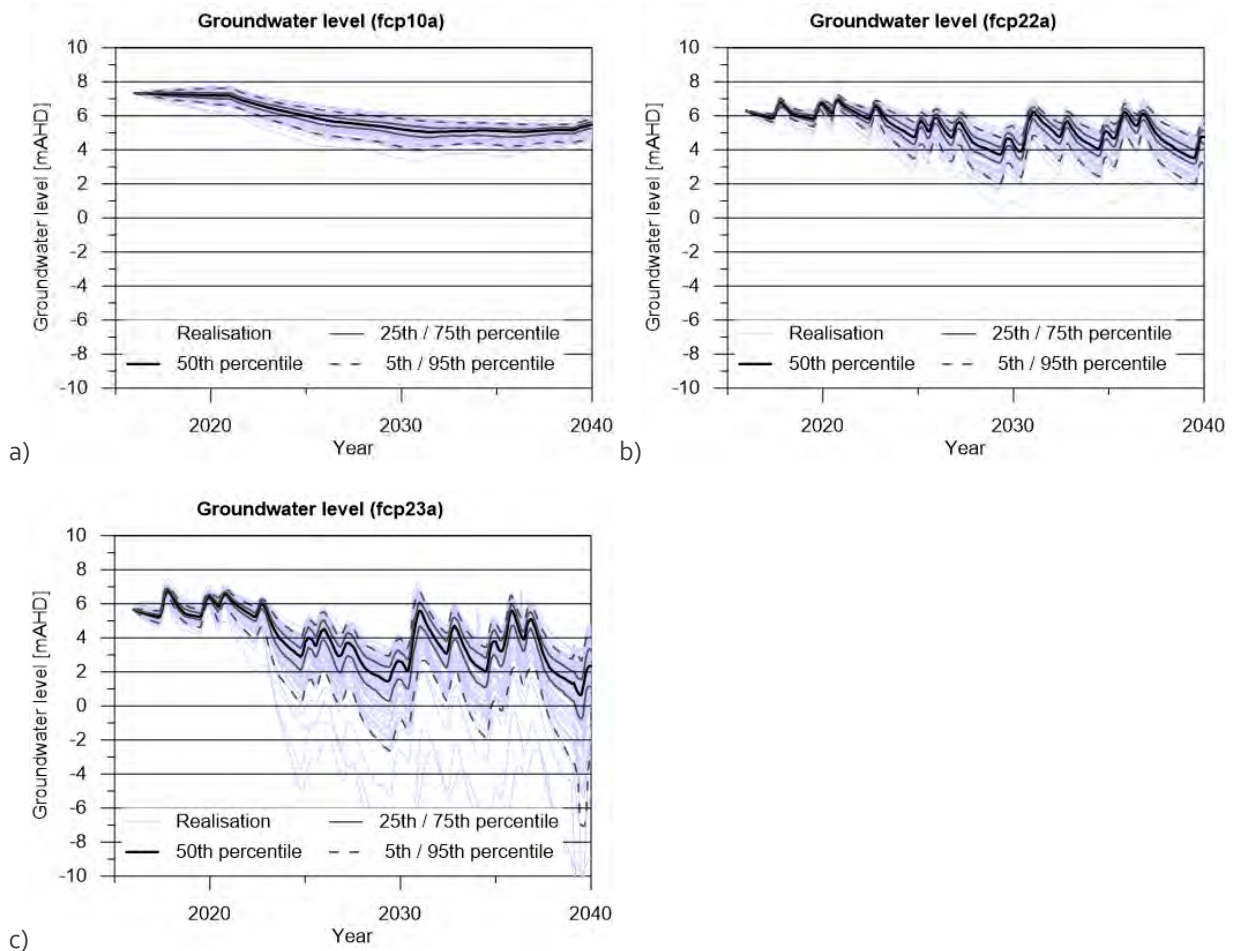


Figure 8-19 Groundwater level variability at monitoring bores a) FCP10A located approximately 15 km to the southwest of the Sino Iron pits, b) FCP22A located approximately 4.8 km to the southwest of the Sino Iron pits and c) FCP23A located approximately 2km to the southwest of the Sino Iron pits.

07RC149

07RC149 is an active Zone 1 reference monitoring site along the western margin of the West Pit and is constructed in the superficial sediments. The groundwater levels at 07RC149 are presented below in Figure 8-20a.

The response calculated at 07RC149 is related to the hydraulic conductivity at pilot point kxy4-22.

09AC490 and 09AC534

09AC490 and 09AC534 are active Zone 1 reference monitoring site along the western margin of the West Pit and is constructed in the superficial sediments. These sites are representative of the groundwater level changes at the GDV site 13 (Astron, 2015). The groundwater levels at 09AC490 are presented below in Figure 8-20c.

The median drawdown at 09AC490 at the end of mining is approximately 3 – 4 metres. The final decline in groundwater level is greater than the 2 standard deviations from the mean identified as a trigger value ($\mu=2.70$ mAHD; $\sigma = 1.08$ m). However, the trigger is not reached until approximately 2025.

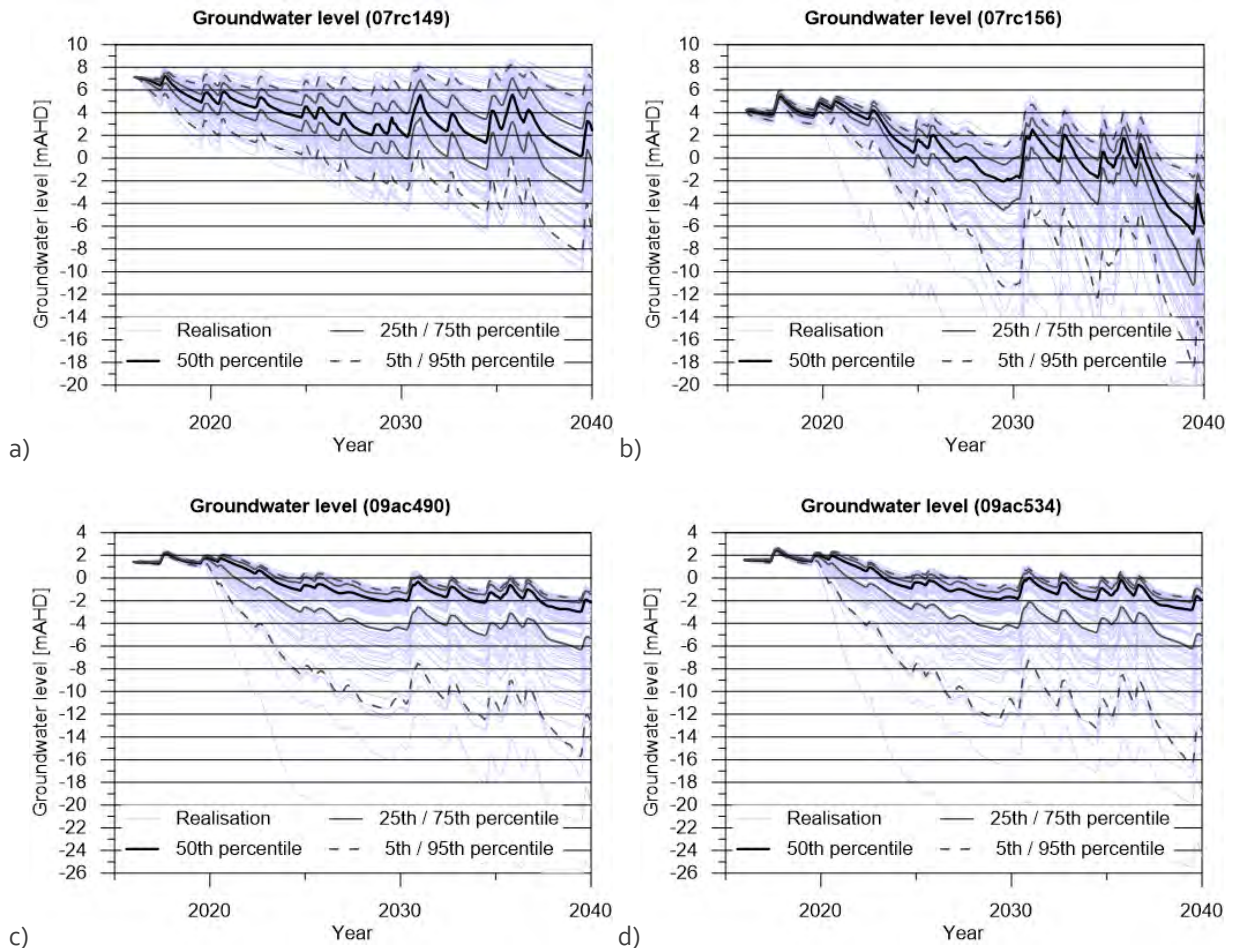


Figure 8-20 Groundwater level variability at monitoring bores a) 07RC149, b) 07RC156, c) 09AC490 located approximately 750 m to the west of the Sino Iron pits and d) 09AC534 located approximately 750 m to the west of the western margin of the Sino Iron pit.

8.7.3 Groundwater level response at permanent pools

The variability in the groundwater levels at the 2 permanent pools (Mungajee and Tom Bull) in response to the different parameter sets applied to the cumulative impact scenario are presented below in Figure 8-21. The results are discussed in the following sections.

Mungajee Pool

The groundwater levels at Mungajee pool are presented below in Figure 8-21a.

Maximum drawdown occurs when the weathered zone along the western margin of the West Pit is high in conjunction with high hydraulic conductivity in the superficial sediments.

Tom Bull Pool

The groundwater levels at Tom Bull pool are presented below in Figure 8-21b.

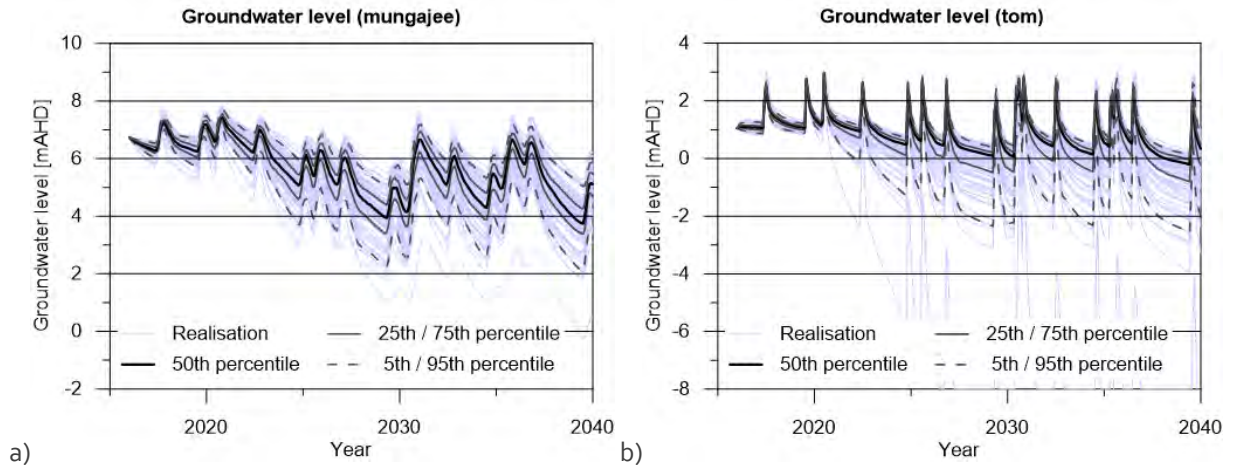


Figure 8-21 Groundwater level variability at the permanent pools a) Mungajee Pool located approximately 5km to the southwest of the Sino Iron pits and b) Tom Bull Pool located approximately 3km to the west of the Sino Iron pits.

Mungajee Pool and Tom Bull Pool are considered to be permanent due to persistence in satellite Conceptually both Mungajee Pool and Tom Bull Pool are considered to be permanent due to the connection to the groundwater in the superficial sediments aquifer (refer to section 2.11.1). However, the proximity to the river mouth indicates Tom Bull Pool may be tidally influenced.

The uncertainty analysis indicates that the groundwater will decline by at least 2 metres at Mungajee Pool and by at least 2-3 metres at Tom Bull Pool, it is therefore recommended that works be conducted to a) confirm the relationship between the pools and the groundwater, and b) establish monitoring sites between the pools and the Sino Iron pit to identify impacts. Data that could be used for such assessments include:

- Water quality parameters during the end of dry season, prior to surface water flows.
- Survey the pool levels for comparison with groundwater level data.
- Installation of loggers to monitor the water levels in the pools.
- Bathymetric survey of the pools.

Collection of some of this data was attempted in early 2017, however, localised rains and resulting surface water flows precluded the collection of site specific data.

9 Conclusions

The numerical groundwater flow model for the Sino Iron project has been developed and calibrated using all available data. The calibrated model has then been used to determine impacts under two scenarios:

- LoM and post closure pit lake considering only the development of the Sino Iron pits; and
- LoM and post closure pit lake development considering the Sino Iron pits and the additional proposed Mineralogy Project pits and Balmoral South borefield.

9.1 Calibration

The combination of groundwater levels and fluxes provided a reasonable calibration dataset for the mining period, although the most significant stress to the system to date has been restricted to the weathered basement material. The updates to the hydraulic parameters are therefore primarily associated with the weathered material, and presented a limited opportunity to calibrate the parameters of the fresh rock beneath or the areas to the west in the footprint of the West Pit. Sensitivity analysis conducted at the completion of the calibration process indicates that this is indeed the case. The calibration process identified:

- A discrete zone of increased secondary permeability associated with structural features such as faults are the source of large groundwater inflows in the northern pit domain (sump 05, 07 & 08); and
- The calibration dataset does not contain sufficient information to constrain the hydraulic properties of the material to the west of the current pit extent, particularly the weathered material separating the superficial sediments of the Fortescue floodplain to the west and the western margin of the future West Pit.

To investigate the importance of the weathered material in the modelled outcomes an uncertainty analysis was conducted. The uncertainty analysis confirmed that the weathered material along the western margin of the West Pit influences forecast inflows to the pit and the magnitude of the drawdown within the superficial sediment aquifer.

9.2 Sino Iron LoM and post closure scenario

9.2.1 Pit inflows

The inflows to the Sino Iron pits during the calibrated LoM model parameters is estimated at approximately 7.5 GL/yr and the post closure flux from the final pit lake surface is also expected to be approximately 7.5 GL/yr. This is approximately 20% of the overall water budget and a significant component of the overall recharge to groundwater systems in the study area. Examination of the results from the uncertainty analysis indicates median final pit inflows of 8 GL/yr (22000 kL/d) with 50% of realisations (ie pit inflows between p25 and p75) showing a variation of ± 1.5 GL/yr or 18%.

Under all realisations the final pit inflows are greater than 4 GL/yr (11000 kL/d) with the majority of inflows from the West Pit along the western margin.

Inflows to the West pit commence between 2019-2020 as the pit intersects the water table in areas of weathered basement along the western margin of the East pit and the superficial sediments to the west. Using the median or 50th percentile values for the period 2025 – 2035, approximately 4GL/yr inflows to the

CONCLUSIONS

pit in this area, which accounts for approximately 60 – 70 % of inflows to the total pit area. The inflows to the pit increase by approximately 2 – 3 GL/yr for the period 2035 – 2060.

Inflows to the West pit gradually increase with time and the lower range of expected pit inflows is relatively constrained under the range of parameters considered and at least 95% of realisations forecast inflows of greater than 3-4 GL/yr for the period 2025 – 2035 and greater than 4 GL/yr for the period 2035 – 2060.

The upper 25th percentile of estimated inflows are associated with realisations that have relatively high weathered zone hydraulic conductivity values in the vicinity of the surface contact between the alluvial sediments and the outcropping Hamersley Group. This suggests that increased permeability associated with features such as faults may result in considerable increases in pit inflows.

The inflows to the East pit account for all inflows to the total pit area up to 2019, after which the mining commences in the West Pit. Using the median or 50th percentile values the East pit inflows in 2018 are approximately 2 GL/yr (5500 kL/d), which is equivalent to the current pit inflows at the end of 2016 assuming no re-circulation occurs from the leakage features especially the NE waste dump.

After 2020 the inflows to the East pit gradually decline and the range of expected pit inflows is relatively constrained under the range of parameters considered and at least 95% of realisations forecast inflows of less than 4 GL/yr for the duration of mining and less than 2 GL/yr (5500 kL/d) from 2040.

9.2.2 Water balance

To provide an easier assessment of the changes to the water budgets determined for each scenario were compared to a 'natural' scenario where all stresses associated with mining activities were removed.

Based on water budget analysis the removal of water from the Sino Iron pit over the life of mine results in drawdown of the surrounding water table and consequently a reduction in evapotranspiration by approximately 1.5 GL/yr. It also results in an increase in flows from the coast and tidal sections of the river by approximately 1.9 GL/yr to account for the out flows from the model.

The post closure water balance indicates that drawdown due to the pit-lake inflows induces an inflow of 3 GL/yr along the tidal sections of the rivers. Evapotranspiration shows a reduction of approximately 5.1 GL/yr from 18.6 GL/yr in the natural scenario to 14.5 GL/yr. The reduction in evapotranspiration is due to the groundwater levels around the pits declining below the root depths used in the evapotranspiration function.

Storage changes shows water is captured into storage (infill of the pit void) at a rate of approximately 3.4 GL/yr. The different volumes reported for the storage release / capture values indicate that the model has not yet stabilised. This is supported by the discussion below regarding the pit-lake water levels after 100 years of recovery.

9.2.3 Post closure pit water levels

The West Pit fills relatively rapidly due to groundwater inflows from the weathered material along the western margin of the pit, which is in connection with the superficial aquifer system. Using a pan coefficient of 0.7 the West Pit reaches a level of -160 to -170 mAHD after 100 years of recovery. The East Pit in contrast, recovers to a level of -300 to -310 mAHD. The elevation predicted by the numerical groundwater model is slightly less than the level expected using the surface area vs flux analytical relationship described above using an inflow of 0.7 GL/yr (the East Pit inflow rate at the end of mining at 2060).

The total flux due to evaporation at the end of the post closure model run reaches a maximum of 19400 kL/d or approximately 7.1 GL/yr. This is a slightly lower rate compared to the pit inflows at the end of mining, which indicated pit inflows of the order of 7.5 GL/yr. The estimated pit lake level using the surface

CONCLUSIONS

area vs evaporative flux relationship and the lower evaporative fluxes than at the end of mining suggest that in the vicinity of the pit, the inflows to the pit from the groundwater system, the evaporative fluxes and the pit water level have not reached a state of equilibrium after 100 years. Unfortunately time constraints prevented running the model to test this hypothesis, and in any case, further investigations into aquifer properties to the west of the pits is required in order to reduce crucial uncertainties before further hypothesis testing would be warranted.

9.2.4 Impacts on groundwater dependent vegetation

Close to the pit at the GDV monitoring sites considered, the groundwater levels are likely to decline by between 5 and 10 metres depending on their proximity to the pits. However, the rate of groundwater decline at the sites considered is expected to be less than 0.2 metres per year. Under these rates of groundwater level decline it may be possible for affected GDV to adapt to the changes. The rate of groundwater level decline in the superficial sediment aquifers can be managed through pit shell optimisation.

9.2.5 Suitability of groundwater level triggers

The current groundwater level triggers used to assess impacts to GDV monitoring sites are based on deviation from mean historic values by either 2 or 3 times the observed variation (standard deviation) seen in the available groundwater level record. These triggers appear to be suitable in the short term until approximately 2020 – 2025. After this time the estimated impacts are expected to exceed these triggers.

The groundwater trigger levels used for further action and impact management will continue to be assessed as part of the adaptive management framework incorporated into the Groundwater Dependent Vegetation Monitoring Plan.

9.2.6 Water quality impacts

Streamline analysis conducted for the Sino Iron scenario indicate that the pits are completely surrounded by streamlines towards the Sino Iron pits, indicating that the final pit voids will become terminal sinks following development of the pit lake. Groundwater from all salinity categories (fresh to hyper saline) will be drawn into the final Sino Iron pit-lake. The resulting water quality residing in the pit-lake will evolve to eventually become hypersaline through evapoconcentration processes. To understand the evolution of the water quality in the pit-lake, a study similar to that completed for the Mount Goldsworthy pit-lake (Sivapalan, 2005) would be required, which is beyond the scope of the current study.

It also appears that the poorer quality groundwater will not be drawn into areas of better groundwater quality. For example, although the saline and hypersaline groundwater to the north and northwest of the Sino Iron pit are drawn to the northern extent of the pit, the path line is through similar quality groundwater. Similarly, it is indicated that the groundwater quality in the vicinity of Tom Bull Pool will be the same, or slightly improved by the migration of better groundwater quality from the south and west. The water quality at Mungajee is expected to be unaffected.

9.2.7 Impacts to existing users

Drawdowns of between 1 – 5 metres are evident at Marda Well and Fortescue Bore, with Fortescue Bore expecting closer to 5 metres drawdown. All other wells in the study area are expected to show drawdowns of less than 1 metre.

Depending on the construction of the wells, it is possible that drawdowns of greater than 5 metres may have a significant impact on the available drawdown and therefore the yield of the bore. The streamline

CONCLUSIONS

analysis discussed previously indicates that adverse water quality changes at the pastoral wells are unlikely to occur.

9.3 Cumulative scenario

9.3.1 Cumulative scenario pit inflows

There is an appreciable difference in both the extent of the groundwater level response and the forecast pit inflows at the Balmoral South and Mineralogy sites compared to the Sino Iron site. The Sino Pit shows groundwater level drawdowns extending into the superficial sediments compared to the drawdowns associated with the Balmoral South and Mineralogy pits. Inflows to the Sino Pit are approximately 3 times that of the Balmoral South and Mineralogy pits.

The difference in response is attributed to the differing geometry of the contact between the superficial sediments and the underlying weathered Hamersley Group and the degree to which the pit intersects the superficial sediments.

The uncertainty analysis conducted on the cumulative impacts model shows similar outcomes to the Sino Iron model, however, the much narrower range of predicted inflows at the Balmoral South and Mineralogy Pits compared to the Sino Iron pit again identifying the importance of the relationship between the contact between the superficial sediments and the weathered Hamersley Group and the proximity of the pit shell to this contact.

9.3.2 Cumulative scenario impacts post closure pit water levels

Using a pan coefficient of 0.7 the Sino Iron West Pit reaches a level of -170 to -180 mAHD after 100 years of recovery. The Sino Iron East Pit in contrast, recovers to a level of -320 to -330 mAHD, slightly lower than the level expected using the surface area vs flux analytical relationship using an inflow of 0.7 GL/yr (the East Pit inflow rate at the end of mining at 2060).

The estimated Sino Iron pit-lake levels using the surface area vs evaporative flux relationship and the inflows to the pit from the groundwater system, the evaporative fluxes and the pit water level have not reached a state of equilibrium after 100 years. Unfortunately time constraints prevented running the model to test this hypothesis.

The pit-lake water levels predicted in the additional pits considered in the cumulative impact scenario after 122 years recovery are:

- Austeel between -180 to -190 mAHD
- Balmoral South between -240 to -250 mAHD
- Mineralogy between -240 to -250 mAHD

9.3.3 Cumulative scenario impacts on groundwater dependent vegetation

Close to the Sino Iron pit at the GDV monitoring sites considered, the groundwater levels are likely to decline by between 5 and 10 metres depending on their proximity to the pits. However, the rate of groundwater decline at the sites considered is expected to be less than 0.2 metres per year. Under these rates of groundwater level decline it may be possible for affected GDV to adapt to the changes. The rate of groundwater level decline in the superficial sediment aquifers can be managed through pit shell optimisation.

9.3.4 Suitability of groundwater level triggers under cumulative impact conditions

The current groundwater level triggers used to assess impacts to GDV monitoring sites are based on deviation from mean historic values by either 2 or 3 times the observed variation (standard deviation) seen in the available groundwater level record. These triggers appear to be suitable in the short term until approximately 2020 – 2025. After this time the estimated impacts are expected to exceed these triggers.

The groundwater trigger levels used for further action and impact management will continue to be assessed as part of the adaptive management framework incorporated into the Groundwater Dependent Vegetation Monitoring Plan.

9.3.5 Cumulative scenario water quality impacts

Streamline analysis conducted for the cumulative impact scenario indicate that the pits are completely surrounded by streamlines, indicating that the final pit voids will become terminal sinks following development of the pit-lakes.

As with the Sino Iron scenario, it also appears that the poorer quality groundwater will not be drawn into areas of better groundwater quality. For example, although the saline and hypersaline groundwater to the north and northwest of the Sino Iron pit are drawn to the northern extent of the pit, the path line is through similar quality groundwater. Similarly, it is indicated that the groundwater quality in the vicinity of Tom Bull Pool will be the same, or slightly improved by the migration of better groundwater quality from the south and west. The water quality at Mungajee is expected to be unaffected.

9.3.6 Cumulative scenario Impacts to existing users

The drawdown impacts are appreciably greater than the Sino Iron scenario, particularly to the north and south of the Sino Iron pits. Jillan Jillan Well can expect drawdowns of greater than 1 metre. Drawdowns of approximately 5 metres are evident at Marda Well, and Fortescue Bore. Balmoral Well at the Balmoral Homestead and Tarquin Well show drawdowns of greater than 5 metres. All other wells in the study area are expected to show drawdowns of less than 1 metre.

Depending on the construction of the wells, it is possible that drawdowns of greater than 5 metres may have a significant impact on the available drawdown and therefore the yield of the bore. The streamline analysis discussed previously indicates that water quality changes are unlikely to occur.

10 Recommendations

10.1 Reduction in uncertainty of hydraulic material properties

Aquifer tests are recommended to determine the permeability and storage coefficient of the weathered zone to the west of the West Pit. This information is expected to reduce the uncertainty in the degree of connection with the superficial sediment aquifer, constraining the range of likely impacts to the water resources of the superficial aquifer and improve forecasts of dewatering volumes.

To reduce the uncertainty in the material properties along the western margin of the West Pit, CPM are currently designing a hydrogeological drill program to address points raised by the DoW in response to the Mineralogy Expansion Proposal 2009.

The drill program will comprise approximately 40 investigation / monitoring wells and 6 test production wells scheduled to commence in mid 2017.

Program objectives include: refining the alluvial aquifer geometry in relation to the proposed west pit; locating test production wells to assess likely alluvial dewatering rates, hydraulic connection between the weathered bedrock and major structural faults to the alluvial system; and to refine and validate site specific hydraulic parameters used for modelling.

10.2 Confirmation of pool and groundwater connectivity

Conceptually both Mungajee Pool and Tom Bull Pool are considered to be permanent due to the connection to the groundwater in the superficial sediments aquifer (refer to section 2.11.1). However, the proximity to the river mouth indicates Tom Bull Pool may be tidally influenced.

The uncertainty analysis indicates that the groundwater will decline by at least 2 metres at Mungajee Pool and by at least 2-3 metres at Tom Bull Pool. It is therefore recommended that works be conducted to a) confirm the relationship between the pools and the groundwater, and b) establish monitoring sites between the pools and the existing sites along the western margin of the Sino Iron pit to identify impacts. Data that could be used to assess the degree of connection between the pools and the groundwater include:

- Water quality parameters during the end of dry season, prior to surface water flows.
- Survey the pool levels for comparison with groundwater level data.
- Installation of loggers to monitor the water levels in the pools.
- Bathymetric survey of the pools.

Collection of some of this data was attempted in early 2017, however, localised rains and resulting surface water flows precluded the collection of groundwater specific data.

10.3 Improvement in the definition of strata geometry and hydraulic material properties at other proposed projects

Proponents of the proposed mines to the north and south of the Sino Iron mine should undertake comprehensive investigations to determine the geometry of the superficial sediments and the underlying weathered formations, particularly where the pit shell is likely to intersect the superficial sediments. This

RECOMMENDATIONS

study has also highlighted the need to understand the hydraulic properties of the weathered formations at this contact.

11 References

- Anderson, M., Woessner, W. & Hunt, R., 2015. *Applied groundwater modeling simulation of flow and advective transport*. 2nd ed. San Diego: Academic Press.
- Aquaterra, 2009. *Mineralogy Expansion Project*, Report: Aquaterra Pty Ltd for Mineralogy Pty Ltd.
- ARANZ Geo Ltd, 2017. *Leapfrog Hydro v 2.6 3D Geological Modelling Software*. [Online] Available at: <http://www.leapfrog3d.com/products/leapfrog-hydro/capabilities> [Accessed 26 January 2017].
- Barnett, B. et al., 2012. *Australian groundwater modelling guidelines*, Waterlines report 82: National Water Commission, Canberra.
- Burrows, W. & Doherty, J., 2015. Efficient calibration/uncertainty analysis using paired complex/simple models. *Ground Water*, 53(4), pp. 531-541.
- CloudGMS, 2016. *2015 update to Sino pit dewatering groundwater model ver 1.0*, Memorandum prepared for Citic Pacific Mining, CloudGMS: Adelaide.
- Commander, D. P., 1989. *Fortescue River Coastal Plain bore completion reports*, Western Australia Geological Survey Hydrogeological Report No 1989/13: Unpublished.
- Commander, D. P., 1993. *Hydrogeology of the Fortescue River Alluvium*, Western Australia Geological Survey Report No 1993/14: Unpublished.
- CPMM, 2014. *Weathering Profile around the Sino Iron Pit – Drilling photo analysis*, s.l.: Unpublished memo.
- Department of Water, 2009. *Pilbara pool mapping*, corporate GIS layer, Department of Water, Government of Western Australia, Perth.
- Department of Water, 2011. *Lower Fortescue groundwater allocation limit report Method used to set an allocation limit and licensing rules for the Lower Fortescue alluvial aquifer*, Government of Western Australia: s.n.
- DHI-WASY, 2015. *FEFLOW User Help*, s.l.: DHI-WASY.
- Diersch, H. J., 2015. *FEFLOW Finite Element Modeling of Flow, Mass and Heat Transport in Porous and Fractured Media*, Heidelberg: Springer.
- Doherty, J., 2008. *PEST Surface Water Utilities*, Watermark Numerical Computing: Brisbane.
- Doherty, J., 2010. *PEST Model Independent Parameter Estimation User Manual*, Brisbane: Watermark Numerical Computing.
- Doherty, J., 2016. *Model-Independent Parameter Estimation User Manual Part I: PEST, SENSAN and Global Optimisers*, Brisbane: Watermark Numerical Computing.
- Doherty, J., 2016. *PEST Model-Independent Parameter Estimation User Manual Part I: PEST Software*. 6th ed. Brisbane: Watermark Numerical Computing.
- Doherty, J., Hunt, R. & Tonkin, M., 2010. *Approaches to Highly Parameterized Inversion: A Guide to Using PEST for Model-Parameter and Predictive-Uncertainty Analysis*. Reston, Virginia: U.S. Geological Survey Scientific Investigations Report 2010-5211, 71 p.
- Global Groundwater Pty Ltd, 2010. *Sino Iron Project – Cape Preston Western Superficial Deposits 2009 Investigation, Drilling and Testing Report*, Perth: Unpublished report to CPM.
- Global Groundwater, 2010. *Sino Iron Project – Cape Preston Western Superficial Deposits 2009 Investigation, Drilling and Testing Report*, Perth: Unpublished report to CPM.
- Haig, T., 2009. *The Pilbara coast water study*, Hydrogeological record series, Report HG34: Department of Water, Perth.
- Hatton, T. & Evans, R., 1998. *Dependence of ecosystems on groundwater and its significance to Australia. Land and Water Resources Research and Development Corporation (Australia), Occasional Paper No. 12/98*, Canberra: ACT.
- Hickman, A. H. & Strong, C. A., 1998. *Structures in the Cape Preston area, northwest Pilbara Craton / new evidence for a convergent margin*, Department of Mines and Energy: Perth.

REFERENCES

- Hickman, A. H. & Strong, C. A., 2003. *Dampier – Barrow Island, W.A. (2nd Edition): Western Australia Geological Survey, 1:250 000 Geological Series Explanatory Notes*, Western Australia Geological Survey: Perth.
- Loomes, R., 2010. *2010 Lower Fortescue River: ecological values and issues, Environmental water report series, report no. 15*, Department of Water, Government of Western Australia: Perth.
- Lu, C., Werner, A. D., Simmons, C. T. & Luo, J., 2014. A Correction on Coastal Heads for Groundwater Flow Models. *Ground Water*, 53(1).
- McCullough, C. D. et al., 2012. *Pit lakes as evaporative 'terminal' sinks: an approach to best available practice mine closure..* International Mine Water Association, s.n.
- MWH, 2010a. *Numerical Groundwater Model for the Lower Fortescue River Catchment*, Report prepared for Dept of Water: Perth.
- MWH, 2010b. *Sino Iron Project Mine Dewatering Model*, Unpublished report prepared for CPM: Perth.
- Pfautsch, S., Dodson, W., Madden, S. & Adams, M. A., 2014. Assessing the impact of large-scale water table modifications on riparian trees: a case study from Australia. *Ecohydrology*, 8(4), pp. 642-651.
- Shewchuk, 2005. *TRIANGLE: a two-dimensional quality mesh generator and Delaunay triangulator.*, Berkley: University of California, Computer Science Division.
- Sivapalan, M., 2005. *Modelling the Evolution of Mount Goldsworthy Pit Lake*, University of Western Australia: Perth.
- Stratagen, 2013. *Cape Preston Iron Ore Development High level review of cumulative impacts*, Report: Citic Pacific Mining.
- SWS, 2013a. *Sino - Citic Pacific Mining update to dewatering model*, Memorandum prepared for Citic Pacific Mining: Perth.
- SWS, 2013b. *Sino - Citic Pacific Mining update to dewatering model (Dewatering Bore Addendum)*, Memorandum prepared for Citic Pacific Mining: Perth.
- Tweed, S. O., LeBlanc, M., Webb, J. A. & Lubczynski, M. W., 2007. Remote sensing and GIS for mapping groundwater recharge and discharge areas in salinity prone catchments, southeastern Australia. *Hydrogeology Journal*, Volume 15, pp. pp75-96.

12 Document history and version control

VERSION	DATE RELEASED	APPROVED BY	BRIEF DESCRIPTION
0.1	14/09/2016	AK	Draft containing available data and conceptualisation.
0.2	20/01/2017	AK	Draft final report including all sections with incomplete results / discussion
0.3	30/01/2017	AK	Draft final report including all sections with results / discussion and incorporating CPM comments from LD.

- Appendix A. Summary of observation bores
- Appendix B. Sino Iron dewatering bores
- Appendix C. **Geological sections through superficial sediments**
- Appendix D. **Pit shell elevations**
- Appendix E. **Calibrated standpipe groundwater levels**
- Appendix F. **Calibrated vibrating wire piezometers pore pressures**
- Appendix G. **Groundwater level observation group calibration statistics**
- Appendix H. **Calibrated model water balances (1983 – 2016)**
- Appendix I. **LoM and post closure forecast groundwater levels**
- Appendix J. **LoM and post closure forecast water balance components**
- Appendix K. **Hydraulic parameter histograms used in uncertainty analysis**
- Appendix L. **Cumulative impact LoM and post closure forecast groundwater levels**
- Appendix M. Cumulative impact LoM and post closure water balances

SINO EXPANSION LIFE OF MINE GROUNDWATER MODEL

APPENDIX A Summary of observation bores

Appendix A Summary of observation bores.

Regional observation bores installed during the GSWA 1983-1985 investigations.

Site	Easting	Northing	Start Date	End Date	Ave SWL [mAHD]	Std Dev [m]	Site	Easting	Northing	Start Date	End Date	Ave SWL [mAHD]	Std Dev [m]
CAMP	398938	7658855	23/11/1983	26/03/1991	10.15	0.61	FCP17A	393938	7661755	24/08/1983	25/03/1991	2.21	0.32
FCP1A	402938	7653155	06/07/1983	12/05/2016	19.86	0.78	FCP18A	395165	7663987	25/08/1983	25/03/1991	2.29	0.28
FCP2A	404138	7656055	26/07/1983	10/04/2013	18.75	1.38	FCP19A	397538	7664055	05/08/1983	26/03/1991	4.08	0.28
FCP2B	404138	7656055	22/07/1983	12/05/2016	18.13	1.43	FCP20A	400047	7664189	08/08/1983	26/03/1991	4.94	0.25
FCP3A	400438	7653755	07/07/1983	10/04/2013	16.04	0.71	FCP21A	401905	7665140	11/08/1983	28/02/2012	5.47	0.55
FCP4A	401638	7655455	12/07/1983	12/05/2016	16.08	0.88	FCP22A	404653	7665769	10/08/1983	25/03/1991	6.39	1.19
FCP5A	398238	7656455	11/07/1983	27/03/1991	9.63	0.36	FCP23A	408238	7666255	27/07/1983	20/05/2016	7.00	0.90
FCP6A	399938	7658255	24/08/1983	12/05/2016	11.60	0.60	FCP24N	397638	7666155	26/08/1983	25/03/1991	2.49	0.24
FCP7B	401638	7659655	30/08/1983	26/03/1991	11.48	0.52	FCP25A	391038	7658455	03/08/1984	14/02/1991	1.03	0.40
FCP8A	405038	7660155	17/07/1983	12/05/2016	14.75	1.80	FCP26A	390738	7661655	02/08/1984	14/02/1991	1.30	0.72
FCP9A	395738	7657055	26/07/1983	14/02/1991	5.27	0.29	FCP27A	392338	7664055	31/07/1984	14/02/1991	0.11	0.40
FCP10A	397138	7659255	03/08/1983	21/05/2016	7.19	0.56	FCP28A	394138	7666155	30/07/1984	25/03/1991	0.71	0.36
FCP11A	397938	7661155	04/08/1983	12/05/2016	6.61	0.50	FCP29A	396938	7668455	30/07/1984	23/10/2014	1.69	0.35
FCP12A	400438	7661755	18/08/1983	26/03/1991	8.03	0.36	FCP30A	400466	7668312	20/07/1984	13/10/1988	1.28	0.72
FCP13A	402238	7662055	19/08/1983	26/03/1991	10.10	0.64	FCP31A	403338	7668255	16/07/1984	25/03/1991	2.95	0.61
FCP14A	404038	7662455	12/09/1983	26/03/1991	10.96	0.92	FCP32A	407438	7653055	28/06/1985	12/05/2016	24.66	1.65
FCP14B	404038	7662455	22/08/1983	26/03/1991	12.30	1.15	FCP32B	407438	7653055	04/07/1985	12/05/2016	24.42	1.72
FCP15A	406838	7662955	02/08/1983	26/03/1991	10.73	1.43	FCP33A	401138	7658155	06/06/1985	27/03/1991	12.54	1.15
FCP16B	393438	7659155	09/09/1983	14/02/1991	3.19	0.63	FCP34A	400838	7657955	25/06/1987	27/03/1991	13.17	0.46

Coordinates are in GDA94 MGA50

SINO EXPANSION LIFE OF MINE GROUNDWATER MODEL

APPENDIX A Summary of observation bores

Sino observation bores

Site	Easting	Northing	Start Date	End Date	Ave SWL [mAHD]	Std Dev [m]	Site	Easting	Northing	Start Date	End Date	Ave SWL [mAHD]	Std Dev [m]
06RC017	410749.3	7670451.3	22/09/2011	04/06/2016	-2.71	2.5	09AC553	409796.8	7670633.5	30/10/2009	16/05/2016	1.2	1.1
07NC255	415073.0	7673435.0	30/06/2010	16/08/2015	9.59	2.5	09AC554	409839.9	7670880.6	02/11/2009	16/05/2016	1.3	1.0
07NC256	415862.9	7673881.1	16/10/2009	18/06/2016	13.59	1.8	09DD448	409629.3	7669099.7	13/05/2014	16/05/2016	0.3	0.7
07NC260	411010.1	7668769.0	30/07/2008	30/07/2008	-18.24	0.0	09DD454	409767.2	7669697.8	16/09/2014	16/05/2016	1.1	0.6
07RC110	410561.1	7667452.3	12/04/2008	17/05/2016	2.79	3.5	09DD455	409695.3	7669511.2	30/04/2014	16/05/2016	0.4	0.7
07RC135	409897.9	7668598.5	16/05/2008	19/05/2016	1.31	2.3	09DD472	409271.5	7669268.2	21/06/2014	15/05/2016	2.0	0.4
07RC138	409596.0	7670598.9	12/04/2008	16/05/2016	1.67	1.0	09DD483	409702.0	7669401.8	13/04/2014	18/10/2015	1.4	0.5
07RC139	411399.3	7667601.1	12/04/2008	16/12/2008	12.08	0.2	09DD597	415264.6	7671926.2	21/09/2010	18/06/2016	13.5	1.6
07RC140	412248.7	7669602.9	10/05/2008	04/06/2016	5.65	2.2	09DD598	414095.8	7672109.6	21/09/2010	18/06/2016	6.5	0.8
07RC141	409099.9	7670599.9	16/05/2008	03/06/2016	0.69	1.0	09DD599	414248.5	7672667.8	21/09/2010	18/06/2016	8.1	0.8
07RC143	411911.6	7667620.1	12/04/2008	12/07/2012	-2.34	12.9	09DD600	414437.3	7673263.7	21/09/2010	18/06/2016	8.5	0.7
07RC144	410297.9	7671596.4	12/04/2008	08/05/2016	1.49	1.1	09DD601	414433.0	7673262.4	21/09/2010	18/06/2016	8.5	0.7
07RC147	412306.8	7670602.1	10/05/2008	26/01/2011	5.00	0.6	09DD602	414587.2	7673588.1	20/09/2010	18/06/2016	8.7	0.8
07RC148	412746.8	7669581.3	10/05/2008	04/06/2016	10.62	7.2	09DD603	415093.5	7673648.7	20/09/2010	18/06/2016	10.3	0.8
07RC149	412610.9	7671609.1	10/05/2008	17/05/2016	4.19	1.0	09DD604	417908.0	7674195.8	21/09/2010	18/05/2016	22.2	1.7
07RC150	413099.2	7671602.2	10/05/2008	15/05/2016	5.57	1.1	09NC397	410361.7	7667846.6	11/11/2009	08/05/2016	-50.3	30.6
07RC151	409339.9	7669572.0	12/04/2008	19/05/2016	2.17	0.9	09NC398	410438.8	7667854.6	13/10/2009	17/05/2016	-13.4	4.4
07RC153	408483.4	7669666.6	16/05/2008	19/05/2016	2.57	0.7	09NC411	409890.1	7668603.4	16/09/2009	19/05/2016	1.1	2.2
07RC154	409397.6	7668599.4	12/04/2008	19/05/2016	3.20	1.1	09NC412	412607.1	7671613.1	13/11/2009	08/05/2016	0.0	13.2
07RC155	408703.3	7668604.8	12/04/2008	10/05/2016	2.94	1.5	09NC414	413069.6	7670558.5	18/05/2009	08/05/2016	4.5	2.5
07RC156	409195.8	7667699.2	13/01/2008	15/05/2016	6.02	1.0	09NC422	423301.6	7678573.2	29/02/2012	05/05/2016	19.4	0.5
07RC170	410346.1	7668091.3	05/03/2008	29/09/2008	-11.26	12.4	09NC423	423169.1	7678894.9	29/02/2012	05/05/2016	18.3	0.4
07RC171	410125.5	7667340.3	01/04/2008	17/05/2016	-5.98	3.9	09NC424	423104.4	7678483.8	29/02/2012	29/02/2012	19.7	0.0
07RD116	410822.9	7668203.8	12/04/2008	10/08/2009	7.53	4.1	09NC425	422910.2	7678512.3	29/02/2012	29/02/2012	19.6	0.0
08AC283	408487.1	7669675.3	06/08/2009	15/05/2016	2.93	0.9	09NC426	415683.6	7675018.5	10/10/2009	08/05/2016	6.9	10.4

SINO EXPANSION LIFE OF MINE GROUNDWATER MODEL

APPENDIX A Summary of observation bores

Site	Easting	Northing	Start Date	End Date	Ave SWL [mAHD]	Std Dev [m]	Site	Easting	Northing	Start Date	End Date	Ave SWL [mAHD]	Std Dev [m]
08AC284	408480.3	7669669.9	20/05/2010	19/05/2016	2.43	0.7	09NC427	416777.7	7677227.2	19/06/2009	08/05/2016	3.0	4.7
08AC285	408691.7	7668617.9	01/12/2008	10/05/2016	3.87	0.7	09NC430	417500.5	7679984.7	16/10/2009	16/05/2016	6.3	1.2
08DD224	409687.1	7668966.0	29/04/2014	16/05/2016	1.51	0.8	09NC434	423907.2	7667956.0	13/05/2009	08/05/2016	43.9	6.3
08DD338	409811.9	7670227.0	16/09/2014	16/05/2016	0.24	0.4	09NC435	423493.2	7668071.0	16/05/2009	08/05/2016	7.0	27.3
08NC265	410341.2	7668101.7	31/07/2008	08/05/2016	-36.78	15.4	09NC436	423304.9	7668151.6	16/05/2009	08/05/2016	41.8	2.0
08NC266	410148.7	7667329.2	09/01/2009	17/05/2016	-12.17	19.0	09NC437	423220.6	7679075.3	29/02/2012	05/05/2016	18.4	0.4
08NC267	422618.2	7672585.9	01/05/2008	05/05/2016	33.04	0.7	09NC439	423597.1	7678075.4	29/02/2012	21/05/2016	17.8	4.7
08NC268	410445.7	7669257.3	01/11/2008	15/05/2011	-33.77	7.1	09NC491	408525.7	7670539.2	02/10/2009	03/06/2016	2.8	0.8
08NC273	411912.0	7667613.5	19/12/2008	17/05/2016	-19.18	44.2	09NC500	408494.3	7669673.4	11/09/2009	10/05/2016	3.1	1.9
08NC280	412735.9	7669584.1	24/08/2008	04/06/2016	-0.68	11.1	09NC508	408982.1	7669086.0	28/03/2010	10/05/2016	2.5	0.8
08NC306	408777.2	7659769.9	12/09/2008	13/02/2016	19.43	0.7	09NC533	409967.8	7672280.0	24/10/2009	20/05/2016	1.2	0.6
08NC361	411866.2	7666776.6	28/04/2009	01/09/2010	-29.57	5.2	09NC541	408351.2	7670145.0	30/10/2009	10/05/2016	2.1	0.6
08NC362	411201.7	7667413.6	09/11/2009	08/05/2016	-23.13	31.2	09NC563	412309.0	7667359.1	21/12/2009	17/02/2015	2.6	6.0
08NC363	411581.5	7668099.0	28/06/2009	08/05/2016	-0.90	9.8	09NC564	412208.1	7667503.8	21/12/2009	17/05/2016	4.3	4.9
08NC366	412380.8	7667834.0	25/04/2009	24/05/2013	-46.44	16.1	09NC565	412020.0	7667547.8	24/01/2010	17/05/2016	0.8	12.3
08NC368	410316.3	7667205.4	27/08/2010	17/05/2016	-5.68	1.9	09NC566	412124.5	7667346.0	20/12/2009	17/05/2016	-5.1	14.1
08NC379	410647.1	7645010.5	15/10/2009	21/05/2016	37.34	0.9	10NC573	422888.0	7667996.2	26/06/2010	08/05/2016	21.7	8.7
08NC380	410643.1	7645035.9	15/10/2009	14/07/2010	37.74	1.4	10NC575	421809.4	7669208.5	22/08/2010	17/05/2016	43.0	1.8
08NC382	409636.0	7646575.2	16/10/2009	21/05/2016	33.17	3.2	10NC576	423984.3	7667856.0	22/08/2010	17/05/2016	46.8	1.6
08NC383	409802.4	7646472.6	07/07/2009	21/05/2016	34.15	1.7	10NC577	423904.3	7667860.0	22/08/2010	17/05/2016	46.7	2.0
08NC630	397321.0	7660752.0	16/01/2013	21/05/2016	6.69	0.3	10NC578	423777.7	7668182.6	22/08/2010	17/05/2016	45.7	2.1
08NC631	398036.0	7661267.0	16/01/2013	21/05/2016	6.72	0.3	10NC579	423801.2	7668193.4	23/06/2010	08/05/2016	45.8	2.0
08NC632	398844.0	7662113.0	16/01/2013	21/05/2016	6.53	0.3	10NC581	423798.4	7669353.8	20/06/2010	08/05/2016	30.9	10.4
08NC633	399995.0	7663122.0	16/01/2013	21/05/2016	5.95	0.4	10NC583	411550.2	7666200.9	08/03/2011	19/05/2016	6.6	2.7
09AC487	409304.0	7670592.6	24/08/2009	15/05/2016	1.82	1.0	10NC584	412240.3	7666083.0	15/12/2010	17/05/2016	13.6	0.8
09AC488	408855.3	7670576.4	24/08/2009	23/05/2016	2.32	1.0	10NC585	412632.4	7667233.5	08/03/2011	17/05/2016	13.8	0.6
09AC489	408531.7	7670529.1	24/08/2009	15/05/2016	2.18	0.5	10NC586	412978.7	7668677.1	04/03/2010	08/05/2016	5.8	9.1

SINO EXPANSION LIFE OF MINE GROUNDWATER MODEL

APPENDIX A Summary of observation bores

Site	Easting	Northing	Start Date	End Date	Ave SWL [mAHD]	Std Dev [m]	Site	Easting	Northing	Start Date	End Date	Ave SWL [mAHD]	Std Dev [m]
09AC490	408532.8	7670537.5	24/08/2009	15/05/2016	2.70	1.1	10NC587	412964.3	7669120.9	29/09/2010	04/06/2016	3.0	11.6
09AC492	409012.4	7669601.0	05/09/2009	15/05/2016	2.27	1.1	10NC588	412308.9	7667359.1	29/09/2010	08/05/2016	3.9	6.5
09AC493	409184.3	7669604.5	31/08/2009	19/05/2016	2.37	0.6	10NC589	412437.4	7669031.2	10/03/2010	19/05/2016	7.5	6.7
09AC494	409177.7	7669603.6	01/09/2009	15/05/2016	1.97	0.9	10NC590	411406.5	7666236.1	29/09/2010	08/05/2016	-2.8	9.4
09AC495	408650.4	7669624.0	05/09/2009	15/05/2016	3.20	0.9	11DD708	410190.6	7668345.1	23/11/2013	04/06/2016	-19.2	0.6
09AC496	408657.8	7669625.7	05/09/2009	15/05/2016	2.33	0.7	11DD712	409757.8	7667725.4	19/03/2014	16/05/2016	0.7	4.6
09AC497	408337.0	7669681.1	24/08/2009	15/05/2016	3.30	0.9	12DD721	411129.5	7670510.1	28/04/2014	04/06/2016	-4.2	1.1
09AC498	408340.3	7669681.4	02/09/2009	23/05/2016	2.52	0.8	12DD722	411380.5	7668384.7	09/05/2016	11/06/2016	16.4	0.3
09AC501	409008.7	7668621.0	20/05/2010	15/05/2016	4.08	0.7	12DD727	410051.2	7666984.5	13/04/2014	17/05/2016	-5.3	0.3
09AC504	408593.6	7668618.3	20/05/2010	15/05/2016	4.07	0.7	12DD728	409679.3	7667976.4	28/10/2013	16/05/2016	1.5	0.6
09AC505	408980.1	7669089.0	18/12/2009	17/05/2016	2.11	0.7	12DD730	410260.1	7669669.4	23/11/2013	04/06/2016	-8.0	1.0
09AC506	408992.4	7669089.9	18/12/2009	17/05/2016	2.17	0.7	13DD732	409523.1	7669644.5	12/07/2014	16/05/2016	1.2	0.6
09AC507	408978.5	7669108.4	18/12/2009	15/05/2016	2.49	1.0	15AG733	416864.7	7673945.5	07/05/2015	18/06/2016	22.4	0.5
09AC510	408830.7	7669111.5	18/12/2009	10/05/2016	2.99	0.6	15AG734	416819.5	7674113.5	07/05/2015	03/09/2015	22.1	0.2
09AC511	409187.0	7670065.0	30/10/2009	15/05/2016	1.48	1.2	15AG735	416458.0	7673869.8	07/05/2015	03/06/2016	20.0	0.3
09AC512	409374.6	7670062.6	30/10/2009	20/05/2016	1.97	0.7	15AG737	416182.1	7673825.7	06/06/2015	06/06/2015	18.5	0.0
09AC513	409378.8	7670060.7	30/10/2009	20/05/2016	1.96	0.7	15AG738	416052.6	7673903.5	07/05/2015	18/06/2016	15.6	0.3
09AC514	408993.2	7670080.2	30/08/2009	15/05/2016	2.26	0.9	15AG739	416155.0	7673483.7	07/05/2015	10/03/2016	18.9	0.3
09AC516	408762.1	7670101.0	28/08/2009	23/05/2016	2.19	0.8	15AG740	415970.2	7673514.7	07/05/2015	07/10/2015	17.4	0.1
09AC523	408530.4	7670115.9	30/10/2009	20/05/2016	2.62	0.7	A06	411200.7	7669206.6	04/03/2007	08/08/2009	6.6	1.6
09AC524	409676.4	7671551.2	24/08/2009	20/05/2016	1.29	0.7	A13	411286.2	7669483.9	06/03/2007	11/08/2010	4.4	0.5
09AC525	409682.1	7671556.7	01/09/2009	16/05/2016	1.36	0.7	A16	411008.6	7669598.6	30/11/2008	18/07/2010	2.6	2.2
09AC526	409487.8	7671607.5	26/10/2009	20/05/2016	1.28	0.6	FCP10A	397138.0	7659255.0	27/10/2008	21/05/2016	7.4	0.6
09AC527	408771.0	7671774.5	24/08/2009	16/05/2016	1.69	0.3	FCP21A	401938.0	7665155.0	24/01/2011	28/02/2012	6.7	0.1
09AC528	409442.3	7672404.0	24/08/2009	15/05/2016	1.27	0.5	FCP23A	408177.0	7666340.0	06/08/2009	20/05/2016	7.0	0.9
09AC529	408854.6	7672545.5	05/09/2009	15/05/2016	2.18	0.6	M27	410839.4	7667981.8	20/03/2007	19/05/2016	10.5	2.8
09AC530	409968.0	7672288.0	24/08/2009	16/05/2016	1.36	0.6	PH25	410715.1	7668036.1	27/02/2007	17/05/2016	-5.7	13.3

SINO EXPANSION LIFE OF MINE GROUNDWATER MODEL

APPENDIX A Summary of observation bores

Site	Easting	Northing	Start Date	End Date	Ave SWL [mAHD]	Std Dev [m]	Site	Easting	Northing	Start Date	End Date	Ave SWL [mAHD]	Std Dev [m]
09AC531	409973.4	7672280.1	24/10/2009	16/05/2016	1.25	0.6	PH33	410662.8	7669554.9	06/03/2007	11/06/2010	1.0	2.4
09AC532	409988.7	7672280.1	24/10/2009	16/05/2016	1.15	0.6	W_MRWA_ SLK1033_ 5R200	423295.6	7671183.7	05/04/2009	05/05/2016	37.4	2.7
09AC534	408343.2	7670138.3	28/08/2009	15/05/2016	2.12	0.7	W_NEERA_ WELL	415529.0	7677649.0	16/10/2009	16/05/2016	2.7	0.4
09AC537	408344.6	7670145.9	30/10/2009	23/05/2016	2.82	0.7	W_Telstra_ Bore	426868.3	7671920.2	26/09/2013	05/05/2016	32.0	10.8
09AC538	408344.2	7670149.8	30/10/2009	15/05/2016	2.10	0.6	Y03	411866.0	7670494.8	10/05/2008	16/05/2011	4.5	0.9
09AC539	408355.4	7670140.9	30/10/2009	15/05/2016	2.13	0.7	Y04	411509.2	7670440.2	03/01/2008	04/06/2016	2.3	2.2
09AC540	408371.6	7670151.1	17/10/2009	15/05/2016	2.16	0.7	Y16	411892.0	7669815.2	10/05/2008	12/10/2009	5.5	0.3
09AC542	408681.5	7669125.1	30/10/2009	15/05/2016	2.82	0.7	Y17	411524.4	7669767.0	28/09/2008	12/06/2010	3.9	1.3
09AC543	409944.3	7671486.1	24/08/2009	16/05/2016	1.27	0.8	Y20	411533.5	7669540.8	20/03/2007	11/06/2010	4.6	0.5
09AC544	410184.6	7672222.5	19/08/2009	20/05/2016	1.47	0.6	Y29	411464.2	7668919.5	05/03/2004	30/05/2010	11.9	1.5
09AC545	409445.9	7670593.8	24/08/2009	15/05/2016	1.66	0.9	Z03	410887.6	7670275.4	27/02/2007	13/08/2011	2.7	0.9
09AC546	409179.6	7667705.0	30/10/2009	15/05/2016	5.78	0.9	Z04	411124.8	7670375.3	27/02/2007	23/08/2011	2.6	0.9
09AC547	409181.9	7667704.6	20/10/2009	15/05/2016	5.67	0.9	Z05	410935.9	7670468.4	10/05/2008	24/07/2011	2.6	0.6
09AC548	409600.5	7670603.6	27/10/2009	16/05/2016	1.37	0.9	Z07	410567.2	7667444.4	27/02/2007	17/05/2016	2.9	4.5
09AC549	408884.0	7669580.5	05/09/2009	23/05/2016	2.59	0.9	Z10	410486.7	7667253.2	04/03/2007	17/05/2016	5.2	2.5
09AC550	409565.0	7671028.8	30/10/2009	15/05/2016	1.36	0.8	Z11	410635.0	7667206.1	14/05/2008	20/05/2015	11.7	1.5

SINO EXPANSION LIFE OF MINE GROUNDWATER MODEL

APPENDIX B – Sino Iron dewatering bores

Production Bore ID	Area	Easting	Northing	Collar (mAHD)	Final depth (mbgl)	Status (Q2, 2016)	Start	End	Flow rate monthly average (L/s)*	Flow rate monthly maximum (L/s)	Purpose
07NC258		410867.8	7668829.7	35.2	105.0	Not equipped	Not operated		-	-	
08NC265	South of 15 yr pit rim	410341.0	7668102.0	22.7	111.0	Operating	May-08	May-16	3.1	8.5	Dewatering
08NC266	South of 15 yr pit rim	410149.0	7667329.0	18.4	113.0	Not equipped	Oct-08	Sep-09	1.7	2.4	Dewatering
08NC268	North pit	410446.0	7669258.0	19.4	100.1	Not equipped	May-08	Jul-11	4.9	7.3	Dewatering
08NC273	South East of pit	411912.0	7667613.0	41.6	171.0	Not equipped	Oct-08	Aug-10	2.2	3.6	Dewatering
08NC280	East of pit	412736.0	7669584.0	26.1	81.0	Not equipped	Aug-08	Feb-12	7.3	12.5	Dewatering
08NC361	South East of pit	411866.0	7666777.0	27.4	114.0	Not equipped	Apr-09	Sep-10	7.0	8.9	Dewatering
08NC362	East of pit	411201.0	7667414.0	36.3	160.6	Operating	Nov-09	May-15	5.6	9.0	Dewatering
08NC363	South East of pit	411570.0	7668107.0	40.9	84.2	Operating	Jun-09	May-15	1.9	7.8	Dewatering
08NC366	East of pit	412381.0	7667834.0	36.9	142.1	Operating	Apr-09	Apr-13	6.0	9.2	Dewatering
08NC368	South of 15 yr pit rim	410316.0	7667205.0	21.5	114.0	Not equipped	Not operated		-	-	
09NC397	South of 15 yr pit rim	410362.0	7667847.0	22.1	131.6	Operating	Nov-09	Apr-15	1.8	4.0	Dewatering
09NC412	North East of pit	412607.0	7671613.0	11.5	95.6	Operating	Oct-09	Nov-12	3.3	10.8	Dewatering
09NC414	North East of pit	413070.0	7670559.0	15.4	44.5	Not equipped	Oct-09	Aug-11	3.8	7.2	Dewatering
09NC491		408525.7	7670539.2	7.4	76.0		Oct-12	Jul-13			Production Yarraloola
09NC500		408494.3	7669673.4	9.8	64.0		Sep-12	Apr-13			Production Yarraloola
09NC508		408982.1	7669086.0	10.8	22.2		Apr-10	Apr-16			Production Alluvial
09NC533		409967.8	7672280.0	4.8	32.2	Not equipped	Not operated				Production Yarraloola
09NC541		408351.2	7670145.0	8.5	21.0		Jul-12	Oct-13			Production Alluvial
10NC586	East of pit	412979.0	7668677.0	29.0	97.6	Not	Aug-11	Dec-11	1.5	2.9	Dewatering

SINO EXPANSION LIFE OF MINE GROUNDWATER MODEL

APPENDIX B – Sino Iron dewatering bores

Production Bore ID	Area	Easting	Northing	Collar (mAHD)	Final depth (mbgl)	Status (Q2, 2016)	Start	End	Flow rate monthly average (L/s)*	Flow rate monthly maximum (L/s)	Purpose
						equipped					
10NC587	East of pit	412964.0	7669121.0	26.1	83.5	Operating	Sep-10	Jun-13	2.2	5.8	Dewatering
10NC588	South East of pit	412309.0	7667359.0	31.1	93.0	Operating	Sep-10	Jul-13	1.1	4.8	Dewatering
10NC590	South East of pit	411407.0	7666236.0	30.5	93.7	Operating	Dec-10	May-16	6.6	9.0	Dewatering

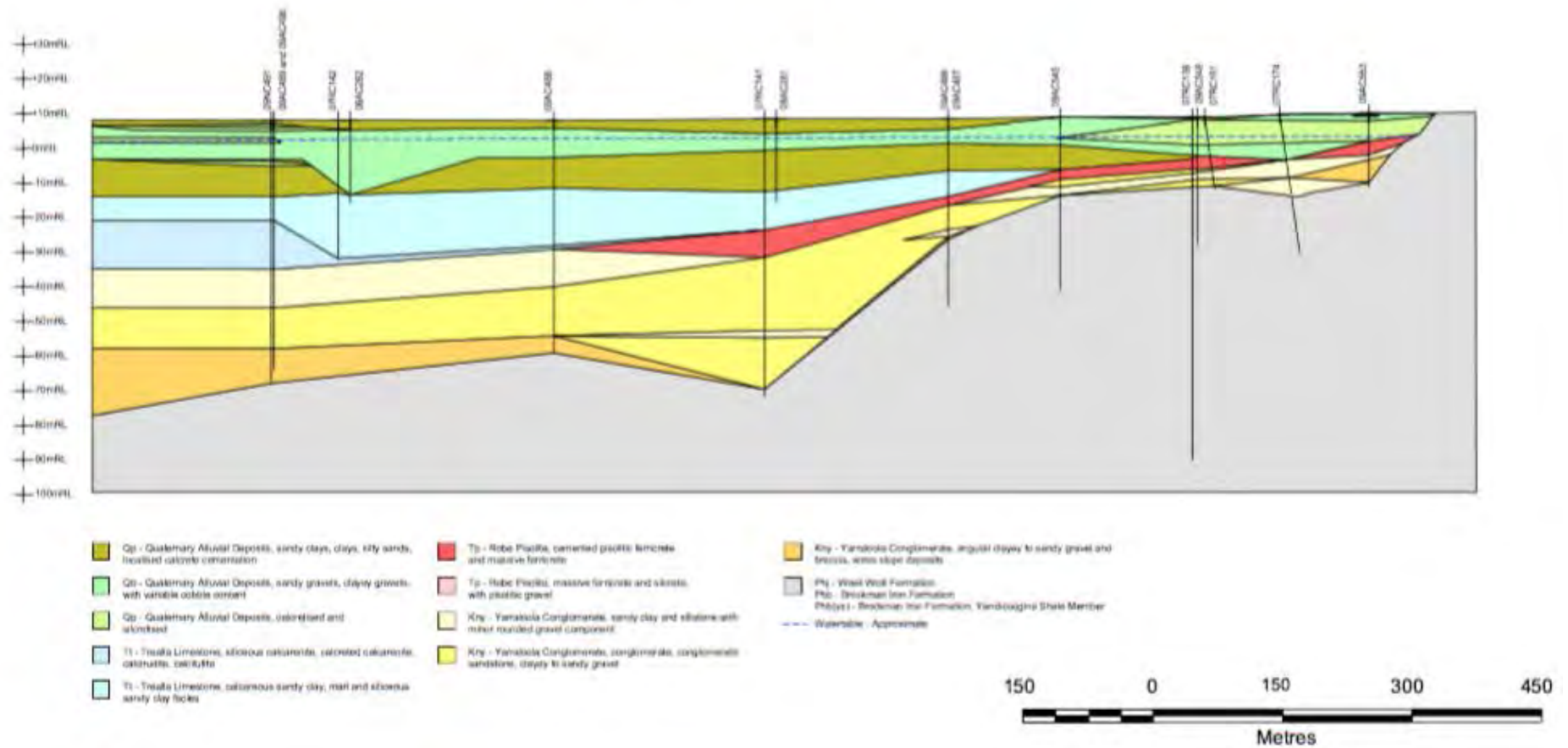
Coordinates are in GDA94 MGA50

SINO EXPANSION LIFE OF MINE GROUNDWATER MODEL
APPENDIX C - Geological sections through superficial sediments

408,327mE 7,670,519mN

409,913mE 7,670,674mN

Section A-A'



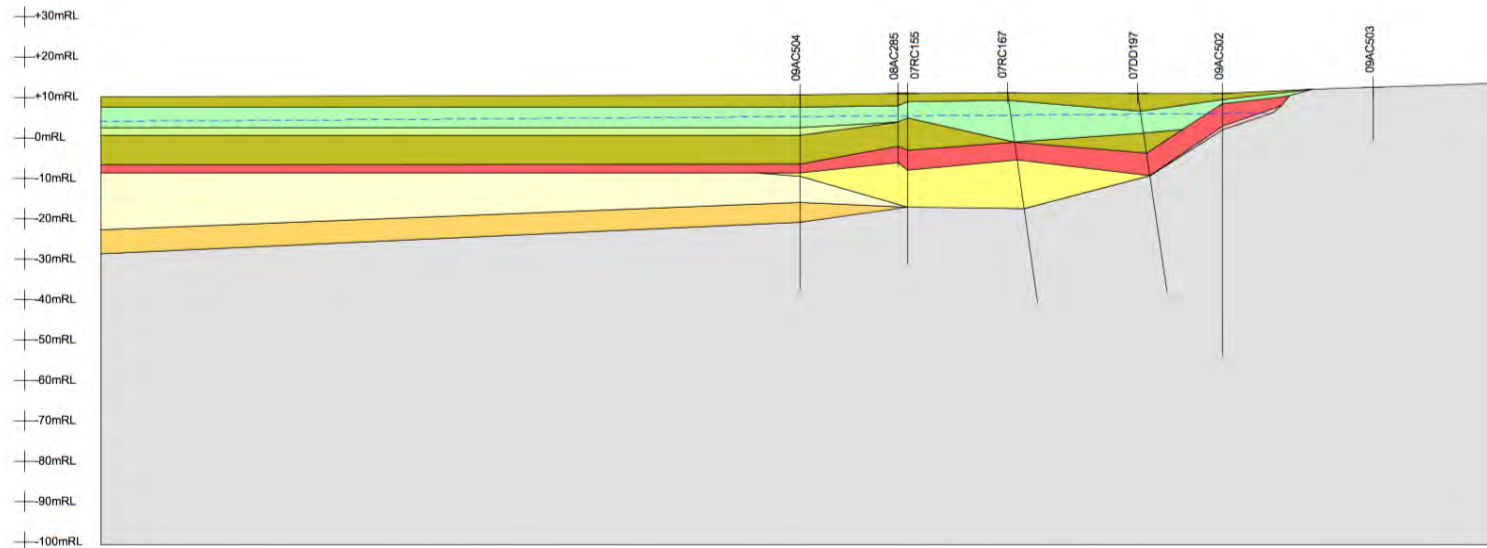
Section A-A' from Global Groundwater (2010)

SINO EXPANSION LIFE OF MINE GROUNDWATER MODEL
APPENDIX C - Geological sections through superficial sediments

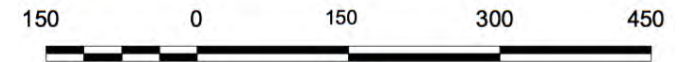
407,904mE 7,668,624mN

409,294mE 7,668,629mN

Section B-B'



- | | | |
|----------------------------------------------------------------------------------------------------|----------------------------------------------------------------------------------------------|-------------------------------------------------------------------------------------------------|
| Qp - Quaternary Alluvial Deposits, sandy clays, clays, silty sands, localised calcrete cementation | Tp - Robe Pisolite, cemented pisolitic ferricrete and massive ferricrete | Kny - Yarraloola Conglomerate, angular clayey to sandy gravel and breccia, scree slope deposits |
| Qb - Quaternary Alluvial Deposits, sandy gravels, clayey gravels, with variable cobble content | Tp - Robe Pisolite, massive ferricrete and silcrete, with pisolitic gravel | Phj - Weeli Woll Formation |
| Qp - Quaternary Alluvial Deposits, calcitised and silcretised | Kny - Yarraloola Conglomerate, sandy clay and siltstone with minor rounded gravel component | Phb - Brockman Iron Formation |
| Tl - Trealla Limestone, siliceous calcarenite, calcareted calcarenite, calcirudite, calcilutite | Kny - Yarraloola Conglomerate, conglomerate, conglomeratic sandstone, clayey to sandy gravel | Phb(ys) - Brockman Iron Formation, Yandicoogina Shale Member |
| Tl - Trealla Limestone, calcareous sandy clay, marl and siliceous sandy clay facies | | - - - - - Water table - Approximate |



Metres
 Horizontal Scale: 1:8,000
 4x Vertical Eggageration
 Coordinate Units - MGA GDA94 Z50

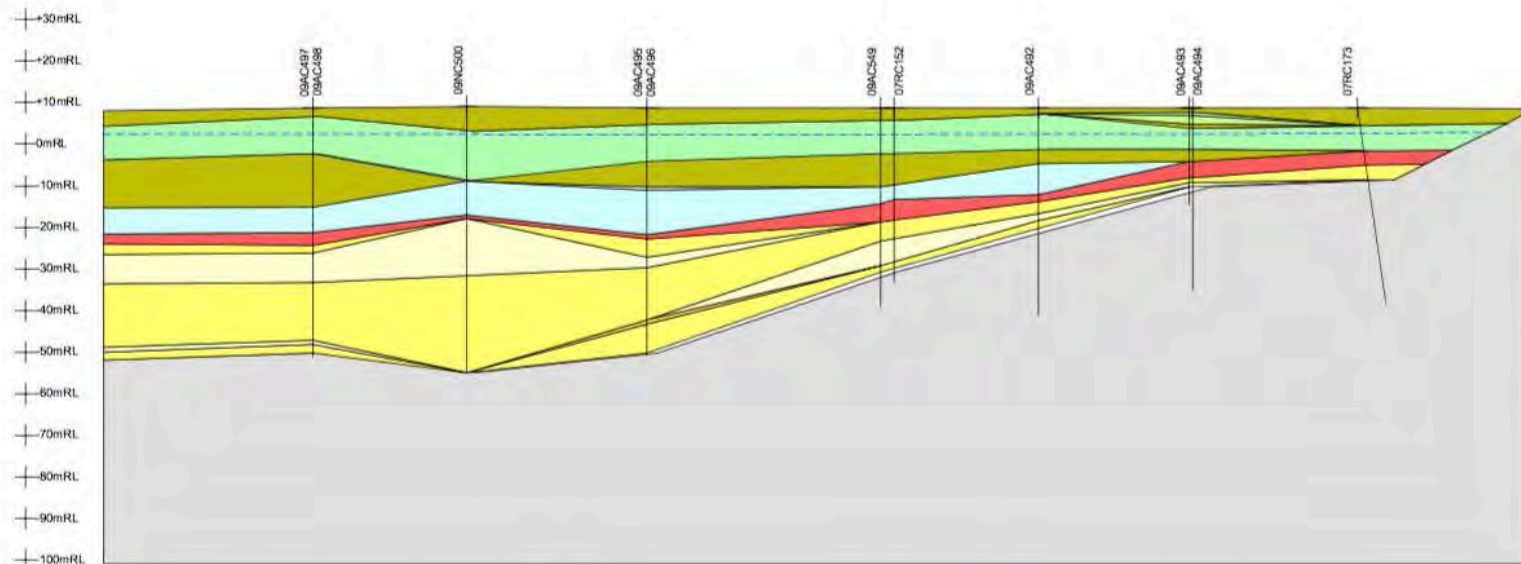
Section B-B' from Global Groundwater (2010)

SINO EXPANSION LIFE OF MINE GROUNDWATER MODEL
APPENDIX C - Geological sections through superficial sediments

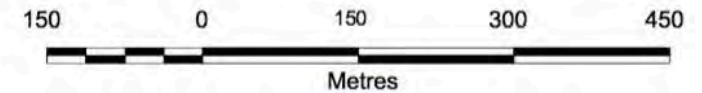
408,146mE 7,669,707mN

409,506mE 7,669,683mE

Section C-C'



- | | | |
|---------------------------------------------------------------------------------------------------------------------------------------------------------------------------------------------------------------------------------------------------------------------------------------------------------------------------------------------------------------------------------------------------------------------------------------------------------------------------------------------------------------------------------------------------------------------------------------------------------------------------------------------------------------------------------------------------------------------------------------------------------------------------------------------------------------------------------------------------------------------------------------------------------------------------------------------------------------------------------------------------------------------------------------------------------------------------------------------------------------------------------------------------------------------------------------------------------------------------------------------------------------------------------------|-----------------------------------------------------------------------------------------------------------------------------------------------------------------------------------------------------------------------------------------------------------------------------------------------------------------------------------------------------------------------------------------------------------------------------------------------------------------------------------------------------------------------------------------------------------------------------------------------------------------------------------------------------------------------------------------------------------------------------------------------------------------------------------------------------------------------------------------------------------------------------------------------------------------------------------------------------------------------------------------------------------------------|---------------------------------------------------------------------------------------------------------------------------------------------------------------------------------------------------------------------------------------------------------------------------------------------------------------------------------------------------------------------------------------------------------------------------------------------------------------------------------------------------------------------------------------------------------------------------------------------------------------------------------------------------------------------------------------------------------------------------------------------------------------------------------------------------------------------------------------------------------------------------------------------------------------------------------------------------------------------------------------------------------------------------------------------------------------|
| <ul style="list-style-type: none"> Qp - Quaternary Alluvial Deposits, sandy clays, clays, silty sands, localised calcareous cementation Qb - Quaternary Alluvial Deposits, sandy gravels, clayey gravels, with variable cobble content Qp - Quaternary Alluvial Deposits, calcareous and silicified T1 - Trealla Limestone, siliceous calcarenite, calcareous calcarenite, calcirudite, calcilutite T1 - Trealla Limestone, calcareous sandy clay, marl and siliceous sandy clay facies | <ul style="list-style-type: none"> Tp - Robe Pisolite, cemented pisolitic ferricrete and massive ferricrete Tp - Robe Pisolite, massive ferricrete and silcrete, with pisolitic gravel Kry - Yarraloola Conglomerate, sandy clay and siltstone with minor rounded gravel component Kry - Yarraloola Conglomerate, conglomerate, conglomeratic sandstone, clayey to sandy gravel | <ul style="list-style-type: none"> Kry - Yarraloola Conglomerate, angular clayey to sandy gravel and breccia, scree slope deposits Phj - Weall Woll Formation Phb - Brockman Iron Formation Phb(ye) - Brockman Iron Formation, Yandicoogina Shale Member Water table - Approximate |
|---------------------------------------------------------------------------------------------------------------------------------------------------------------------------------------------------------------------------------------------------------------------------------------------------------------------------------------------------------------------------------------------------------------------------------------------------------------------------------------------------------------------------------------------------------------------------------------------------------------------------------------------------------------------------------------------------------------------------------------------------------------------------------------------------------------------------------------------------------------------------------------------------------------------------------------------------------------------------------------------------------------------------------------------------------------------------------------------------------------------------------------------------------------------------------------------------------------------------------------------------------------------------------------|-----------------------------------------------------------------------------------------------------------------------------------------------------------------------------------------------------------------------------------------------------------------------------------------------------------------------------------------------------------------------------------------------------------------------------------------------------------------------------------------------------------------------------------------------------------------------------------------------------------------------------------------------------------------------------------------------------------------------------------------------------------------------------------------------------------------------------------------------------------------------------------------------------------------------------------------------------------------------------------------------------------------------|---------------------------------------------------------------------------------------------------------------------------------------------------------------------------------------------------------------------------------------------------------------------------------------------------------------------------------------------------------------------------------------------------------------------------------------------------------------------------------------------------------------------------------------------------------------------------------------------------------------------------------------------------------------------------------------------------------------------------------------------------------------------------------------------------------------------------------------------------------------------------------------------------------------------------------------------------------------------------------------------------------------------------------------------------------------|



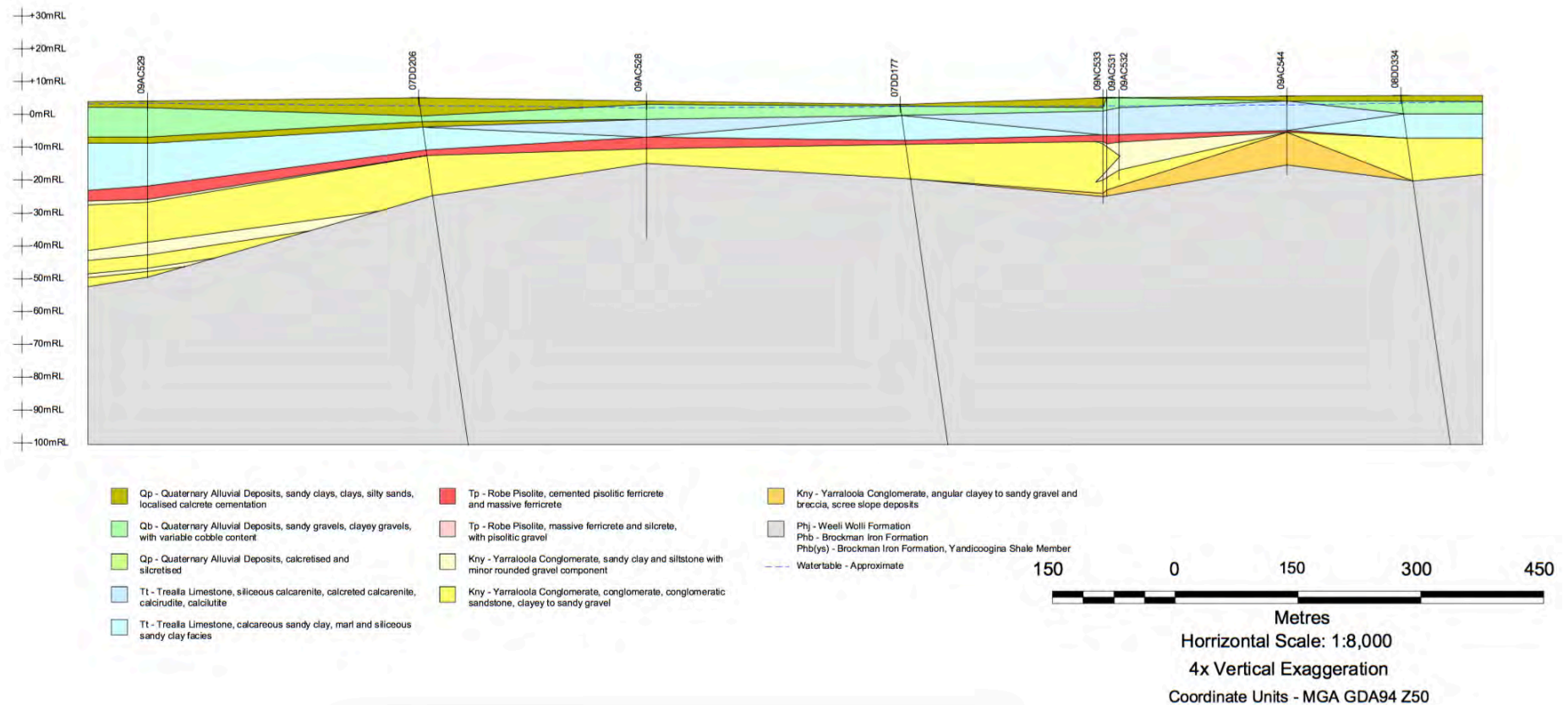
Section C-C' from Global Groundwater (2010)

SINO EXPANSION LIFE OF MINE GROUNDWATER MODEL
APPENDIX C - Geological sections through superficial sediments

408,790mE 7,672,578mN

410,412mE, 7,672,150mN

Section D-D'



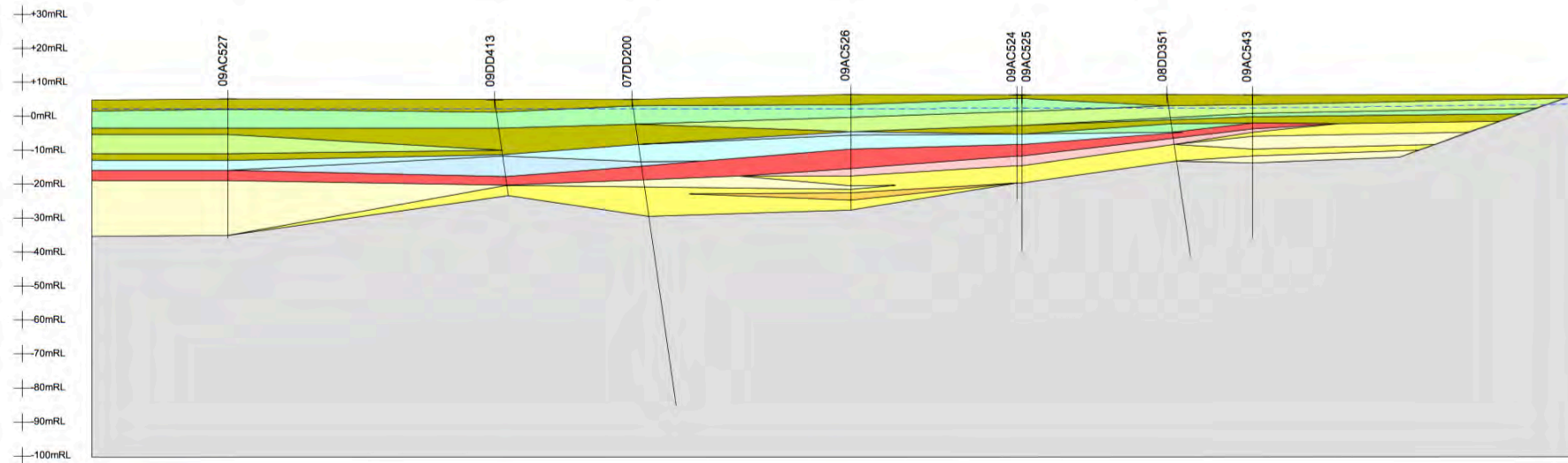
Section D-D' from Global Groundwater (2010)

SINO EXPANSION LIFE OF MINE GROUNDWATER MODEL
APPENDIX C - Geological sections through superficial sediments

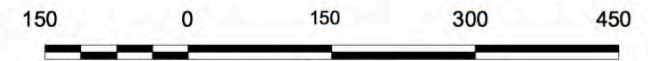
408,619mE 7,671,821mN

410,171mE 7,671,434mN

Section E-E'



- | | | |
|-------------------------------------------------------------------------------------------------------------------------------------------------------------------------------------------------------------------------------------------------------------------------------------------------------------------------------------------------------------------------------------------------------------------------------------------------------------------------------------------------------------------------------------------------------------------------------------------------------------------------------------------------------------------------------------------------------------------------------------------------------------------------------------------------------------------------------------------------------------------------------------------------------------------------------------------------------------------------------------------------------------------------------------------------------------------------------------------------------------------------------------------------------------------------------------------------------------------------------------------------------------------------------------------|-----------------------------------------------------------------------------------------------------------------------------------------------------------------------------------------------------------------------------------------------------------------------------------------------------------------------------------------------------------------------------------------------------------------------------------------------------------------------------------------------------------------------------------------------------------------------------------------------------------------------------------------------------------------------------------------------------------------------------------------------------------------------------------------------------------------------------------------------------------------------------------------------------------------------------------------------------------------------------------------------------------------------|----------------------------------------------------------------------------------------------------------------------------------------------------------------------------------------------------------------------------------------------------------------------------------------------------------------------------------------------------------------------------------------------------------------------------------------------------------------------------------------------------------------------------------------------------------------------------------------------------------------------------------------------------------------------------------------------------------------------------------------------------------------------------------------------------------------------------------------------------------------------------------------------------------------------------------------------------------------------------------------------------------------------------------------------------------------|
| <ul style="list-style-type: none"> Qp - Quaternary Alluvial Deposits, sandy clays, clays, silty sands, localised calcareous cementation Qb - Quaternary Alluvial Deposits, sandy gravels, clayey gravels, with variable cobble content Qp - Quaternary Alluvial Deposits, calcareous and silicified Tl - Tressalla Limestone, siliceous calcarenite, calcareous calcarenite, calcirudite, calcilutite Tl - Tressalla Limestone, calcareous sandy clay, marl and siliceous sandy clay facies | <ul style="list-style-type: none"> Tp - Robe Pisolite, cemented pisolitic ferricrete and massive ferricrete Tp - Robe Pisolite, massive ferricrete and silcrete, with pisolitic gravel Kry - Yarraloola Conglomerate, sandy clay and siltstone with minor rounded gravel component Kry - Yarraloola Conglomerate, conglomerate, conglomeratic sandstone, clayey to sandy gravel | <ul style="list-style-type: none"> Kry - Yarraloola Conglomerate, angular clayey to sandy gravel and breccia, scree slope deposits Phj - Weeli Welli Formation Phb - Brockman Iron Formation Phb(ys) - Brockman Iron Formation, Yandicoogina Shale Member Water table - Approximate |
|-------------------------------------------------------------------------------------------------------------------------------------------------------------------------------------------------------------------------------------------------------------------------------------------------------------------------------------------------------------------------------------------------------------------------------------------------------------------------------------------------------------------------------------------------------------------------------------------------------------------------------------------------------------------------------------------------------------------------------------------------------------------------------------------------------------------------------------------------------------------------------------------------------------------------------------------------------------------------------------------------------------------------------------------------------------------------------------------------------------------------------------------------------------------------------------------------------------------------------------------------------------------------------------------|-----------------------------------------------------------------------------------------------------------------------------------------------------------------------------------------------------------------------------------------------------------------------------------------------------------------------------------------------------------------------------------------------------------------------------------------------------------------------------------------------------------------------------------------------------------------------------------------------------------------------------------------------------------------------------------------------------------------------------------------------------------------------------------------------------------------------------------------------------------------------------------------------------------------------------------------------------------------------------------------------------------------------|----------------------------------------------------------------------------------------------------------------------------------------------------------------------------------------------------------------------------------------------------------------------------------------------------------------------------------------------------------------------------------------------------------------------------------------------------------------------------------------------------------------------------------------------------------------------------------------------------------------------------------------------------------------------------------------------------------------------------------------------------------------------------------------------------------------------------------------------------------------------------------------------------------------------------------------------------------------------------------------------------------------------------------------------------------------|



Metres
 Horizontal Scale: 1:8,000
 4x Vertical Exaggeration
 Coordinate Units - MGA GDA94 Z50

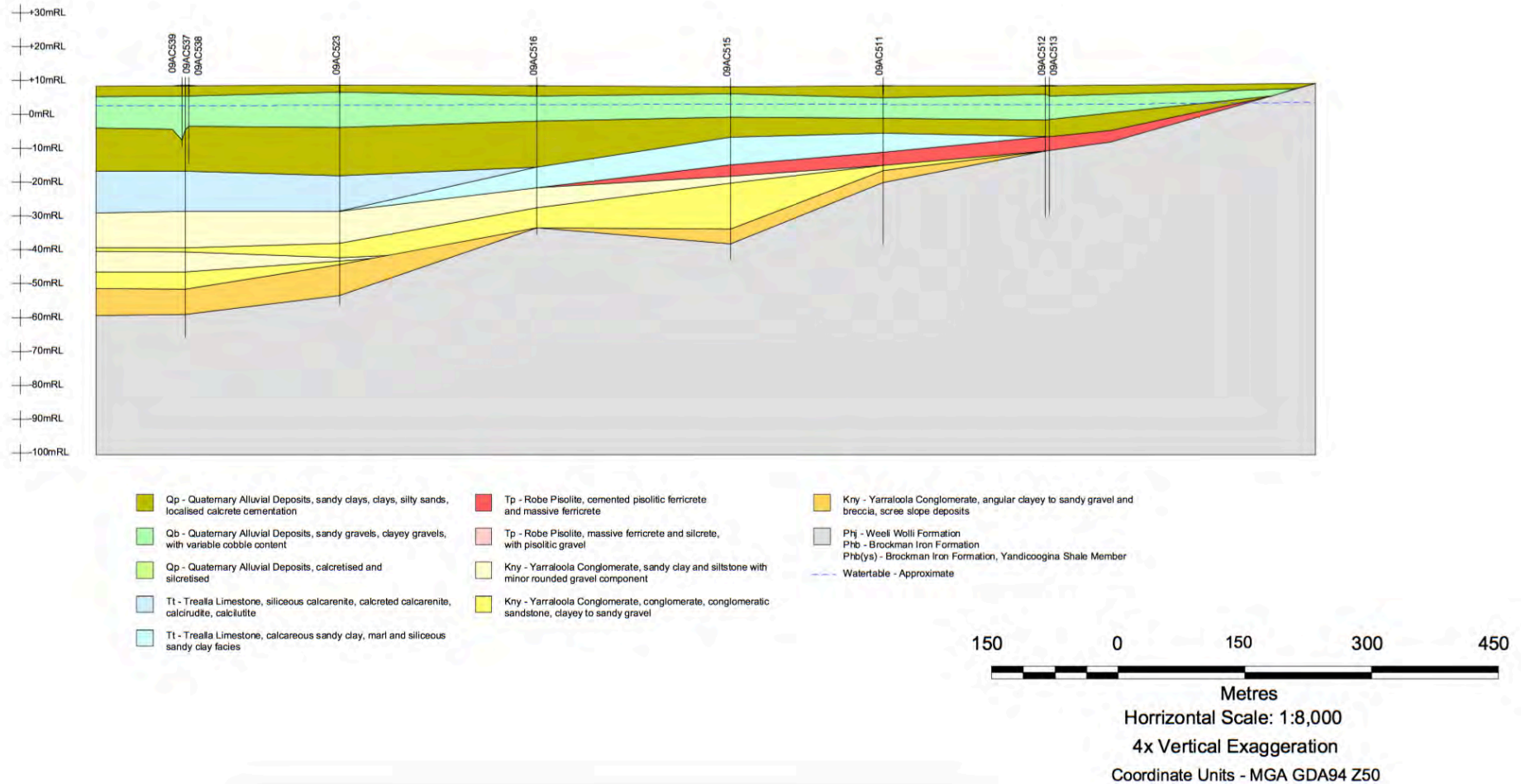
Section E-E' from Global Groundwater (2010)

SINO EXPANSION LIFE OF MINE GROUNDWATER MODEL
APPENDIX C - Geological sections through superficial sediments

408,247mE 7,670,159mN

409,697mE 7,670,016mN

Section G-G'



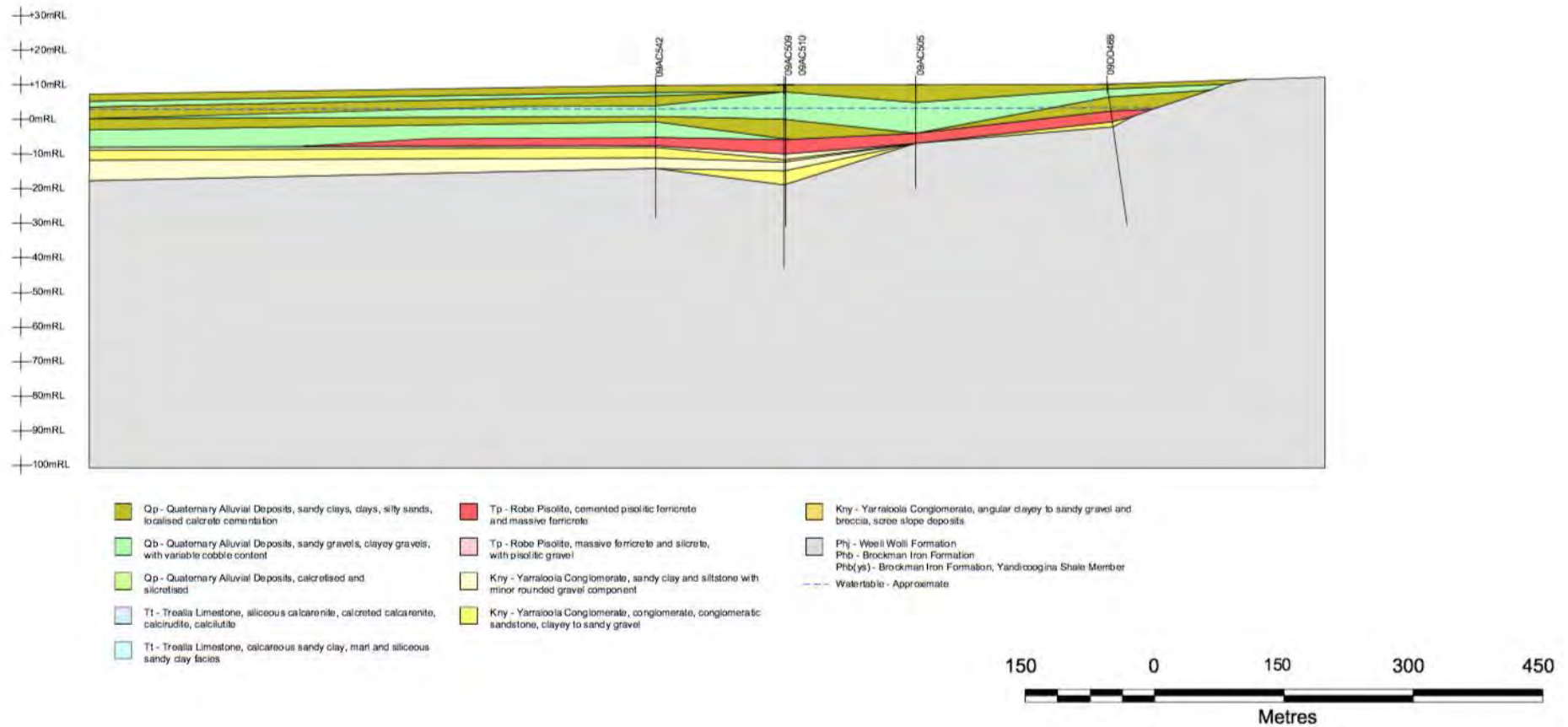
Section G-G' from Global Groundwater (2010)

SINO EXPANSION LIFE OF MINE GROUNDWATER MODEL
APPENDIX C - Geological sections through superficial sediments

408,525mE 7,669,132mN

409,449mE 7,669,038mN

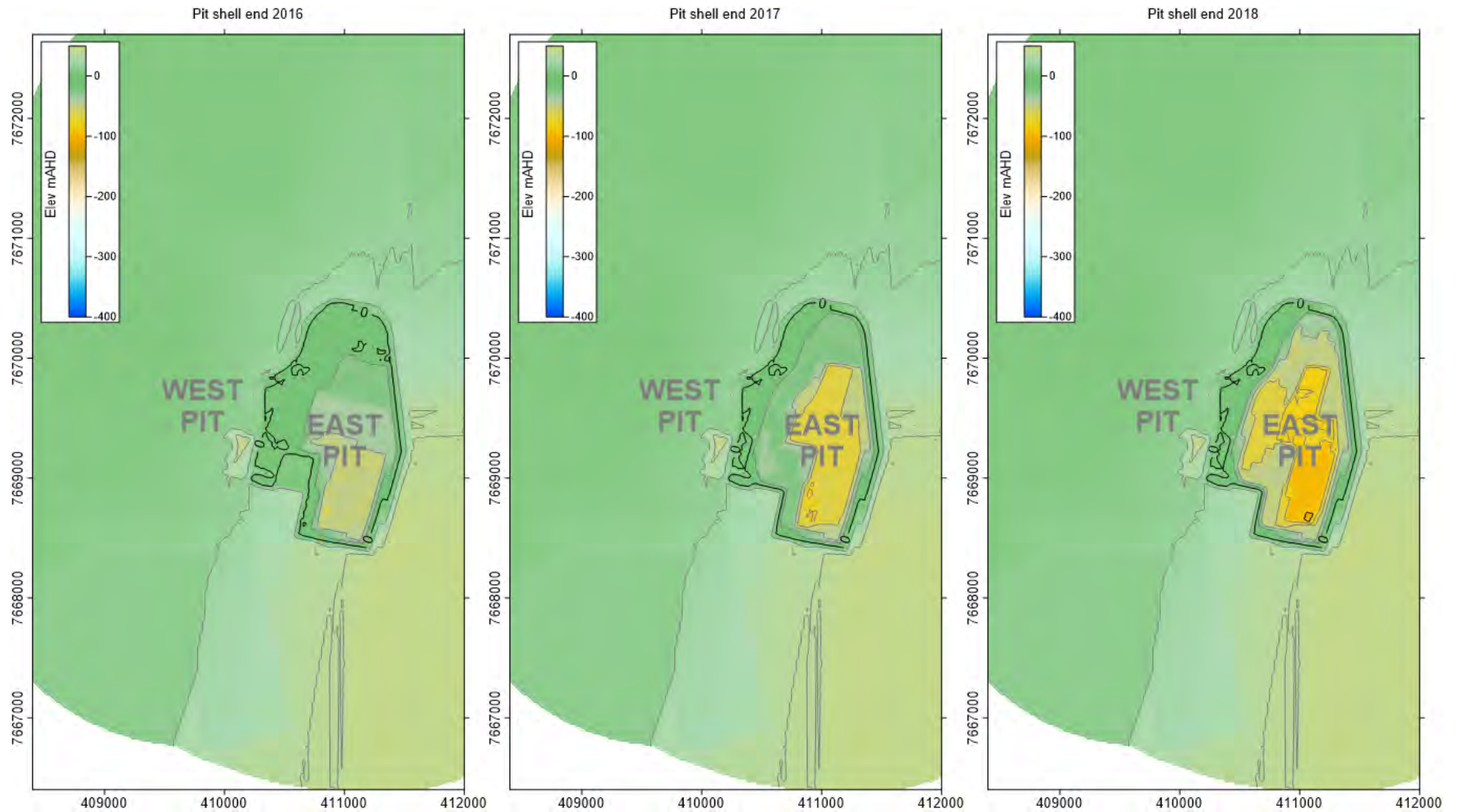
Section H-H'



Section H-H' from Global Groundwater (2010)

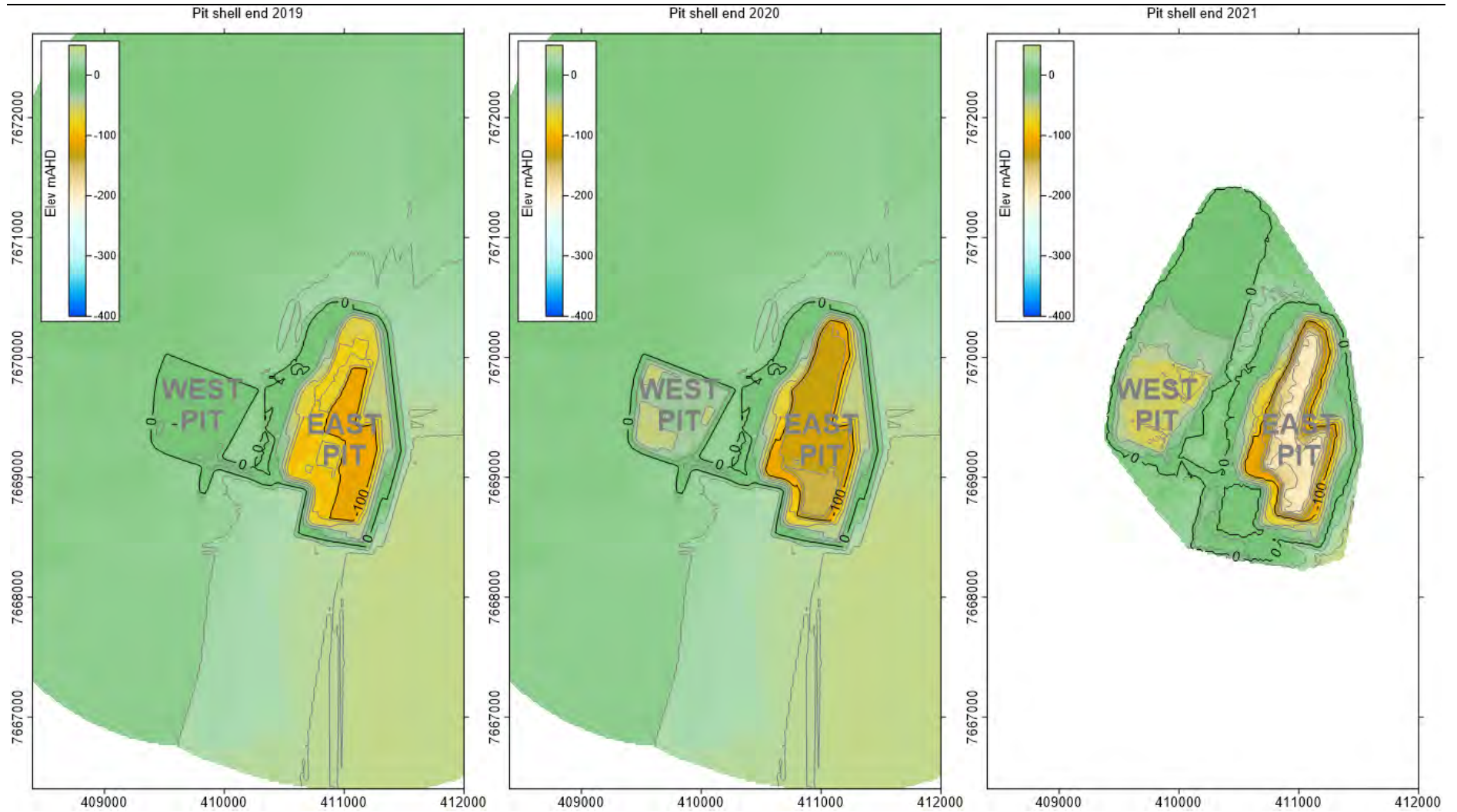
SINO EXPANSION LIFE OF MINE GROUNDWATER MODEL

APPENDIX D Pit shell elevations



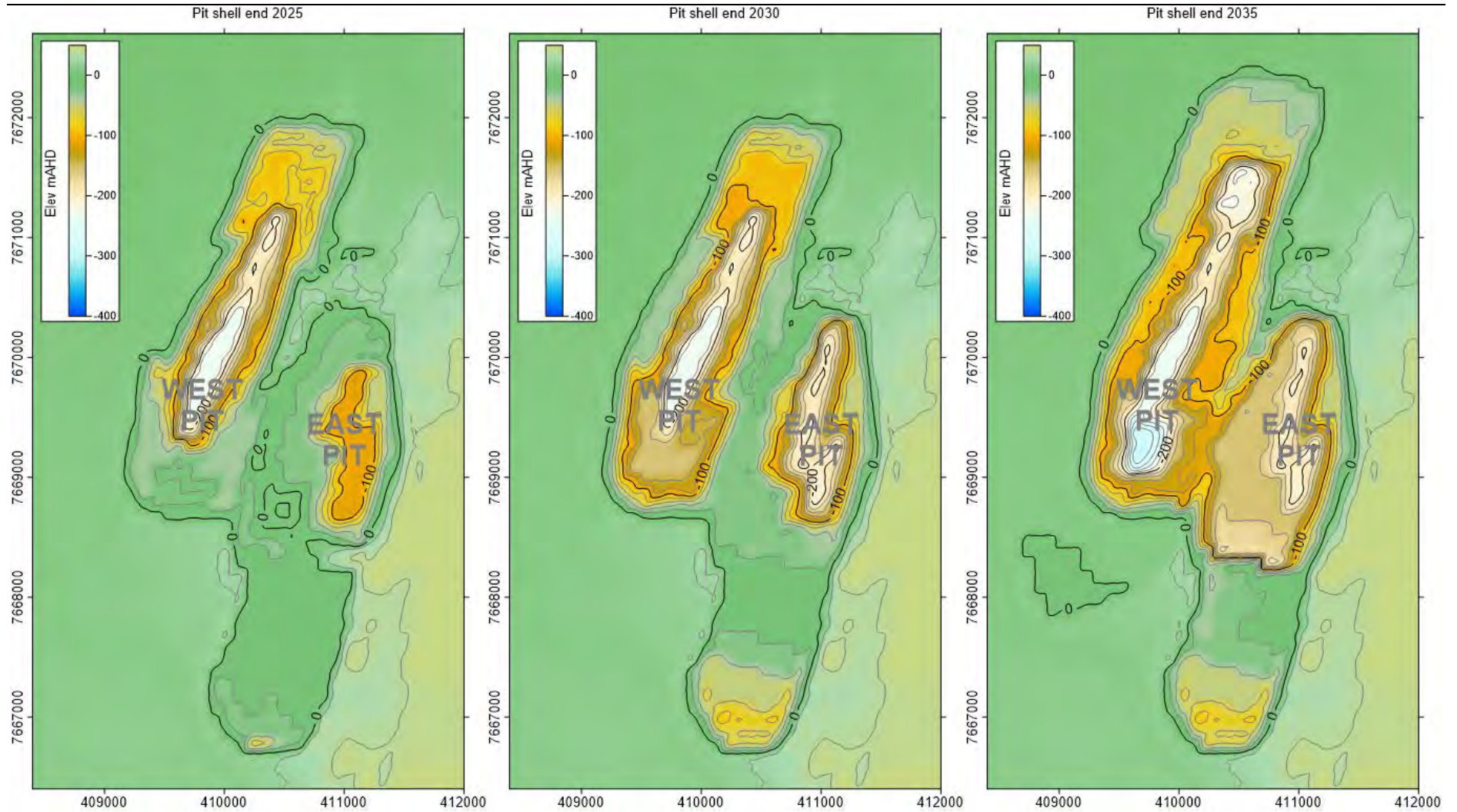
SINO EXPANSION LIFE OF MINE GROUNDWATER MODEL

APPENDIX D Pit shell elevations



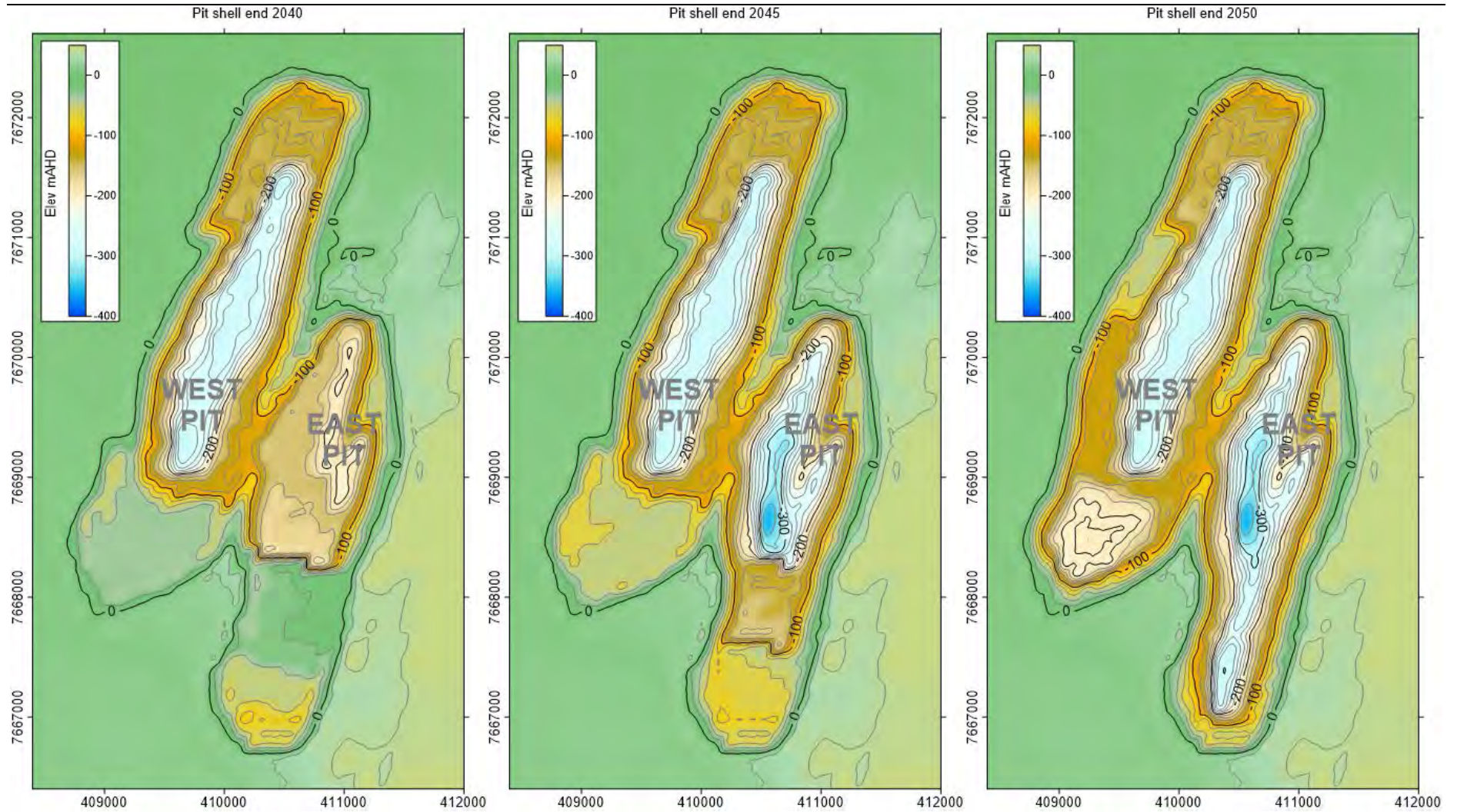
SINO EXPANSION LIFE OF MINE GROUNDWATER MODEL

APPENDIX D Pit shell elevations



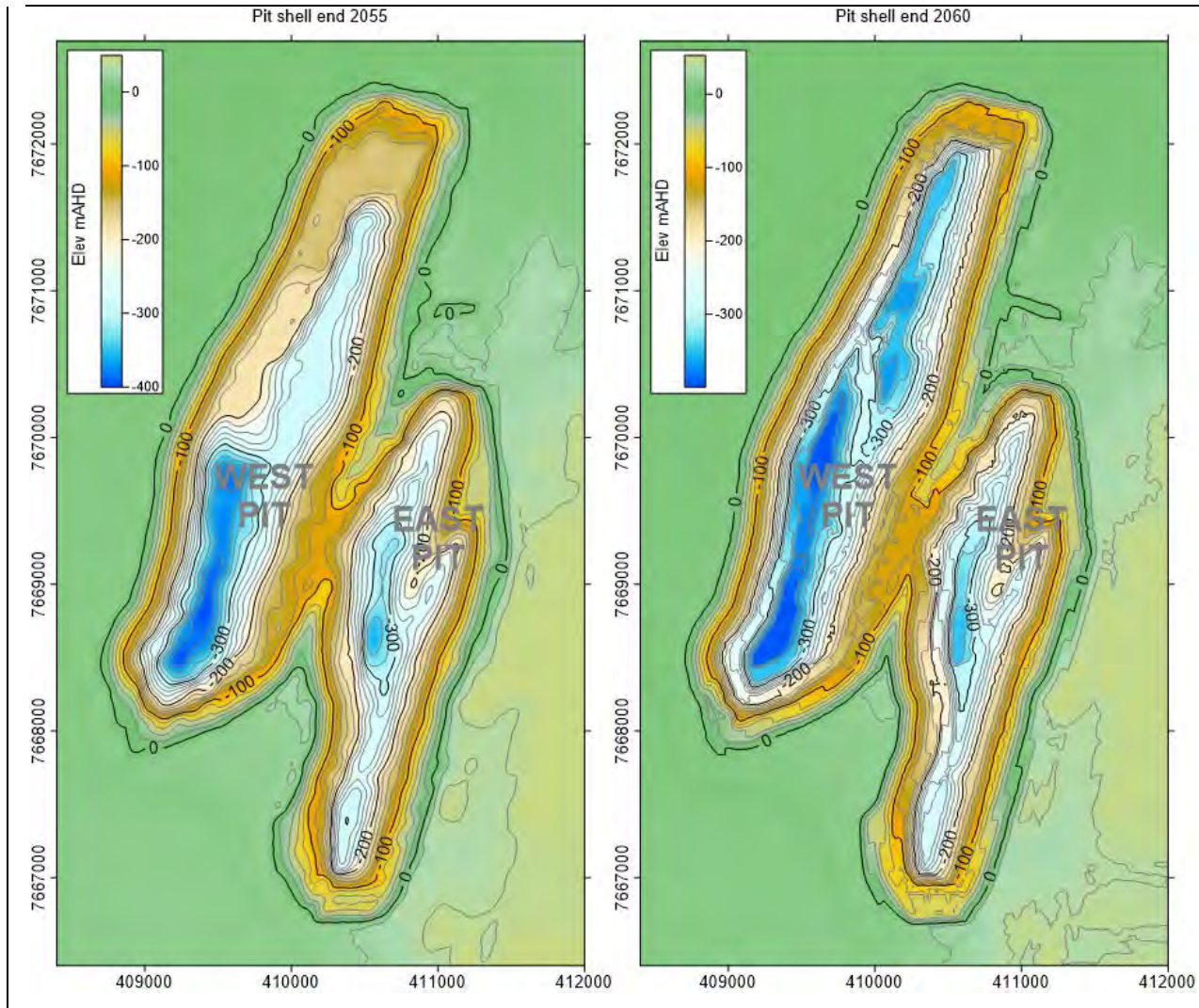
SINO EXPANSION LIFE OF MINE GROUNDWATER MODEL

APPENDIX D Pit shell elevations

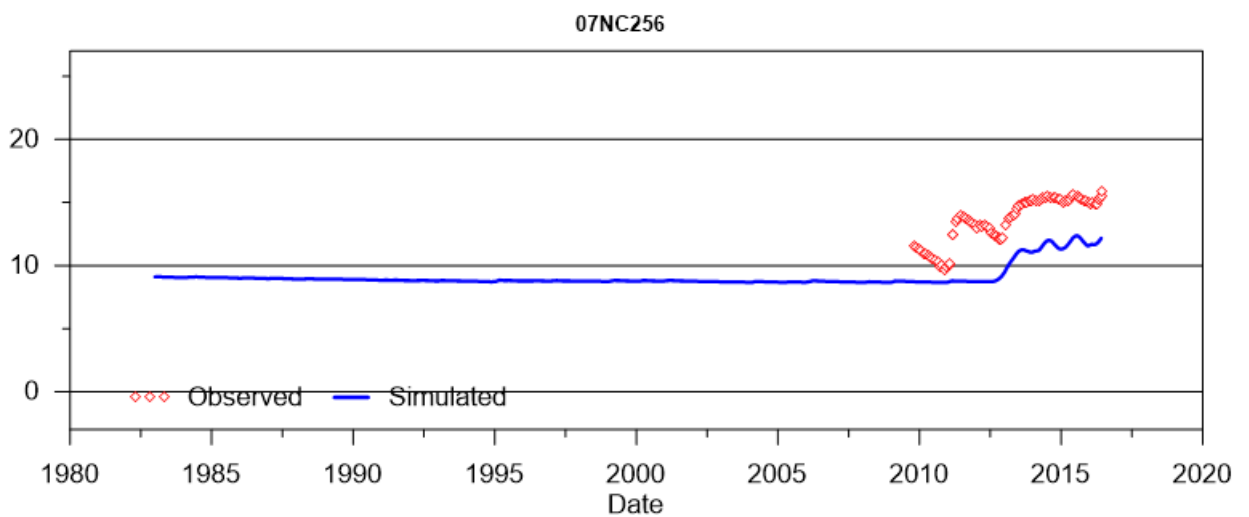
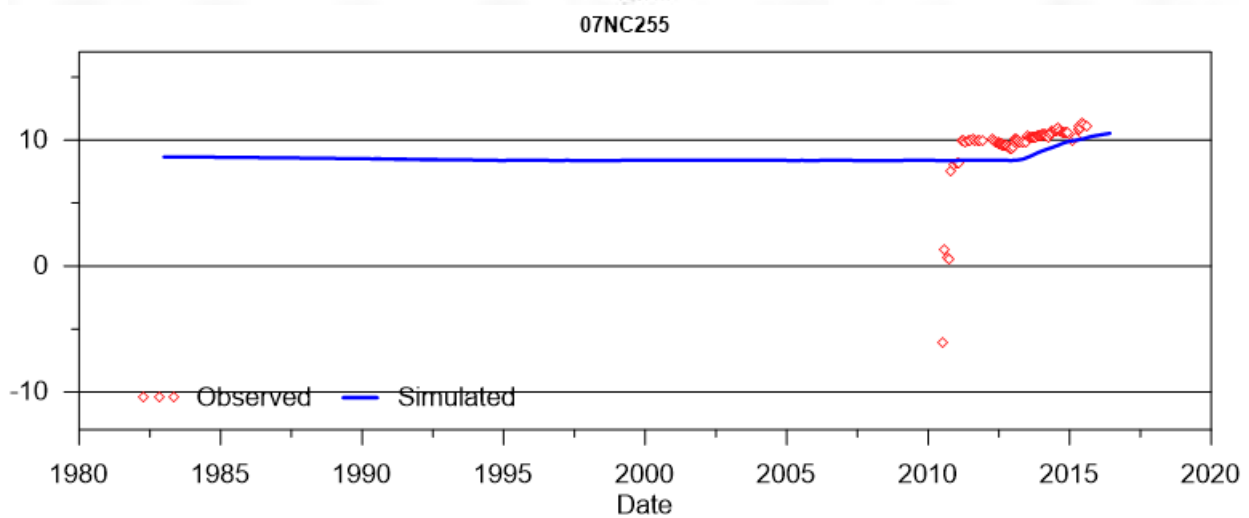
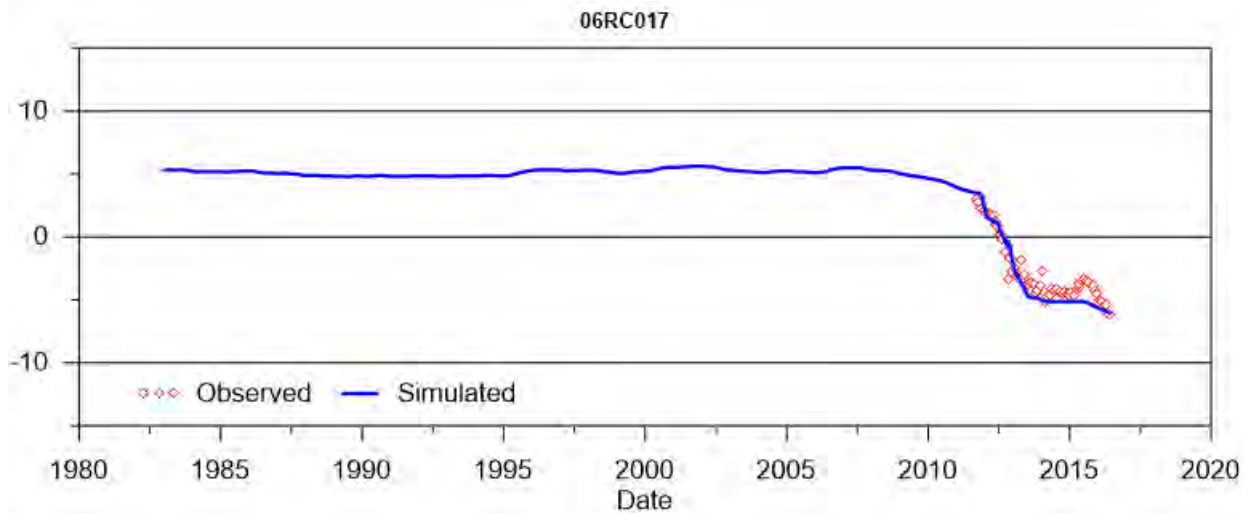


SINO EXPANSION LIFE OF MINE GROUNDWATER MODEL

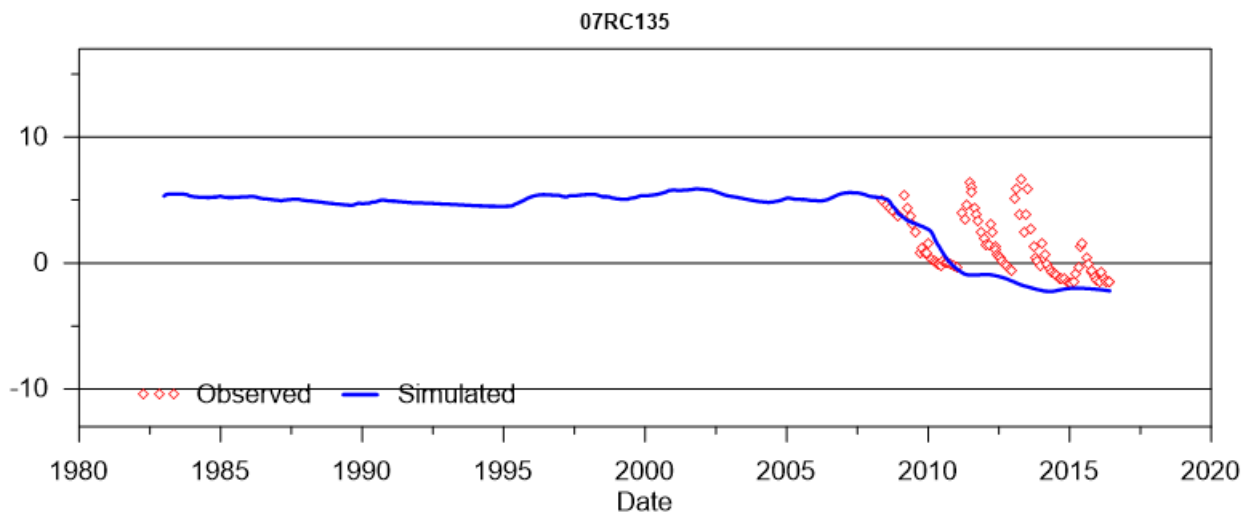
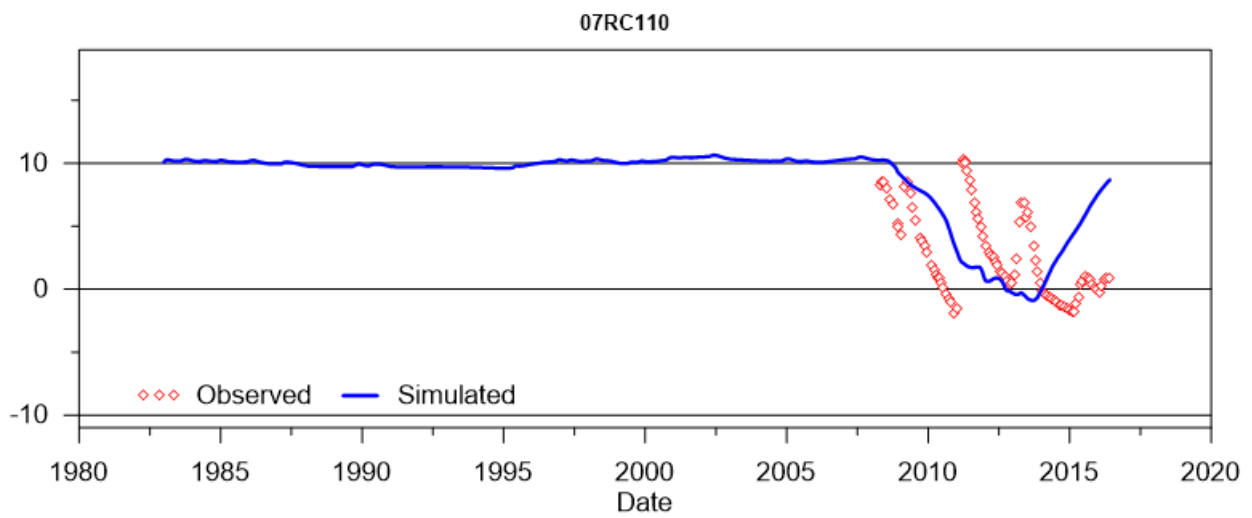
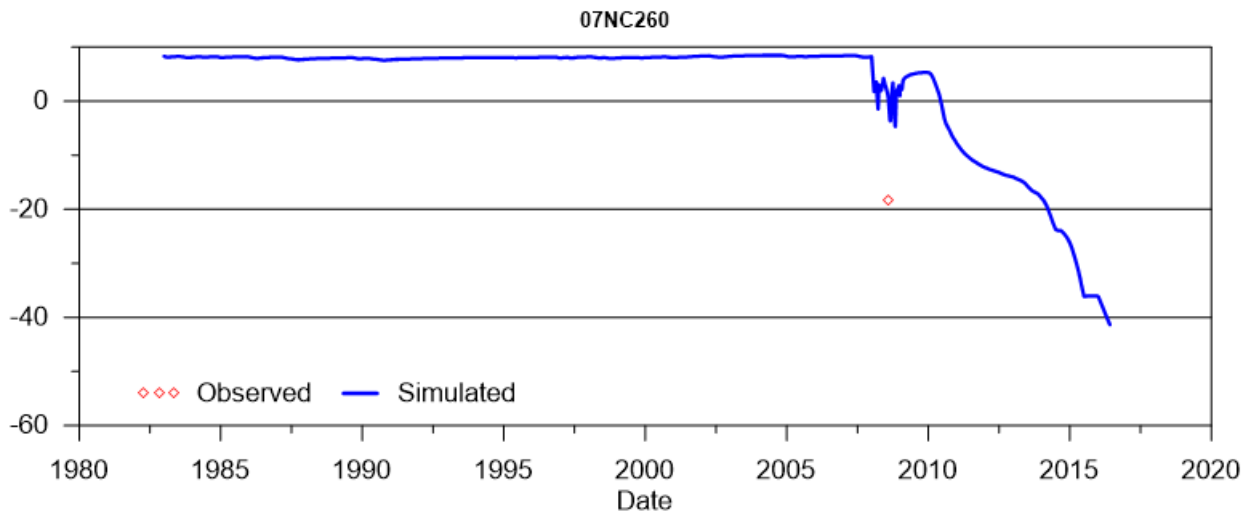
APPENDIX D Pit shell elevations



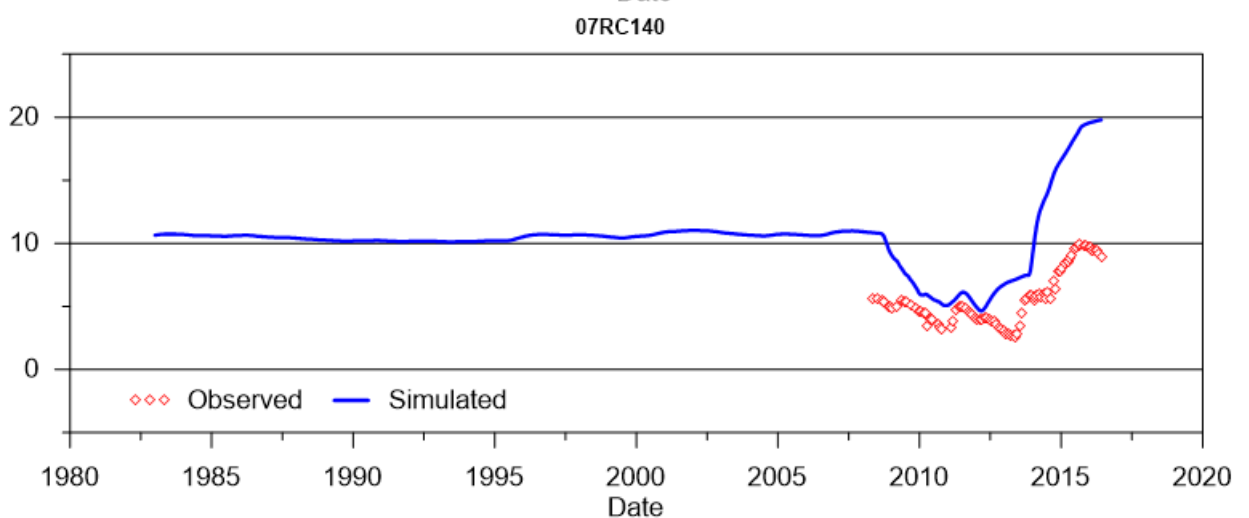
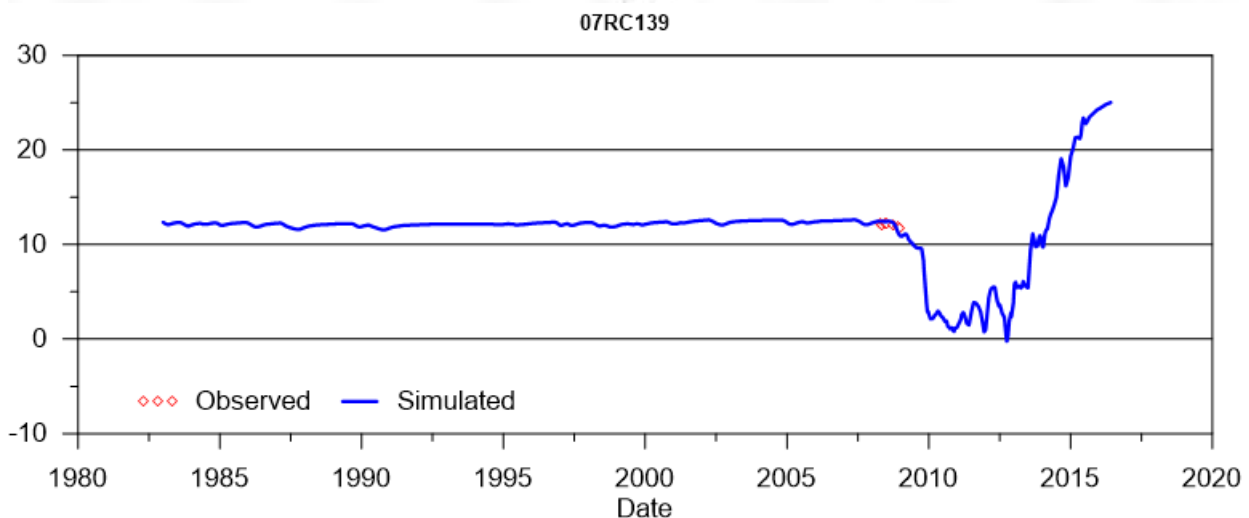
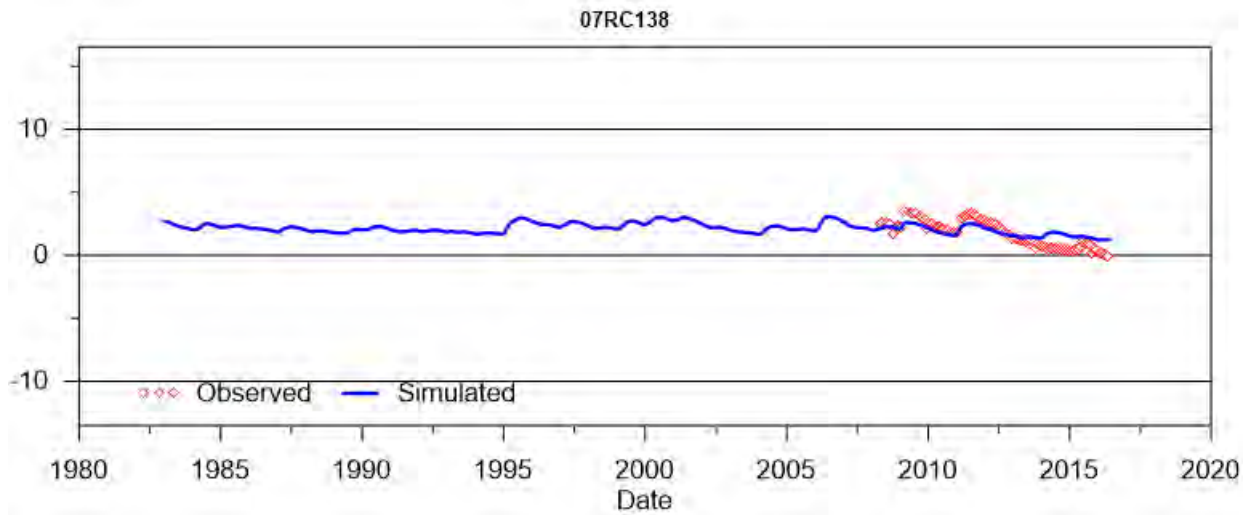
SINO EXPANSION LIFE OF MINE GROUNDWATER MODEL
APPENDIX E –Calibrated standpipe groundwater levels



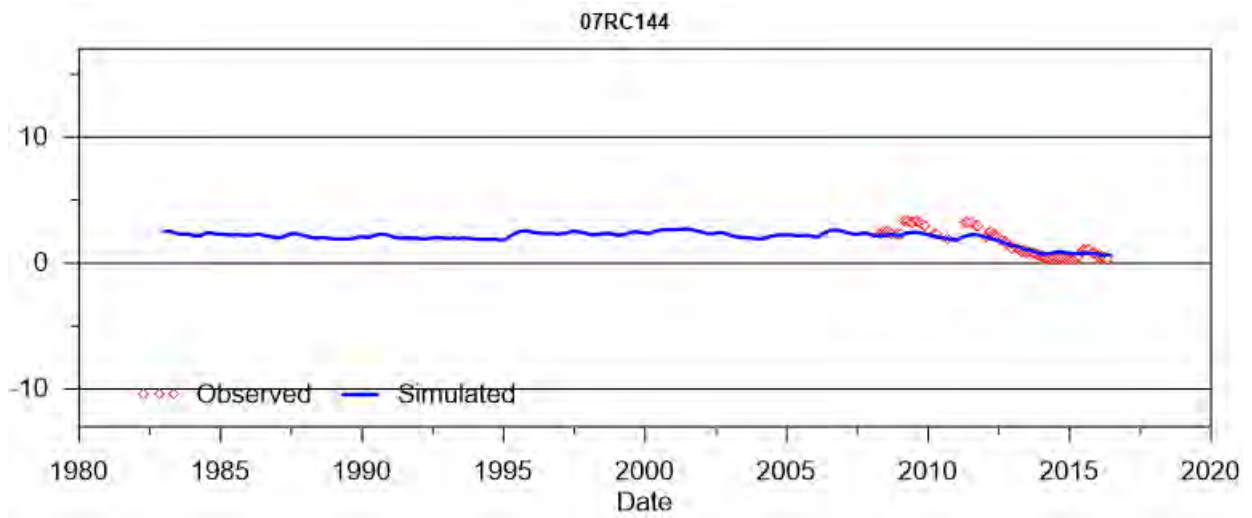
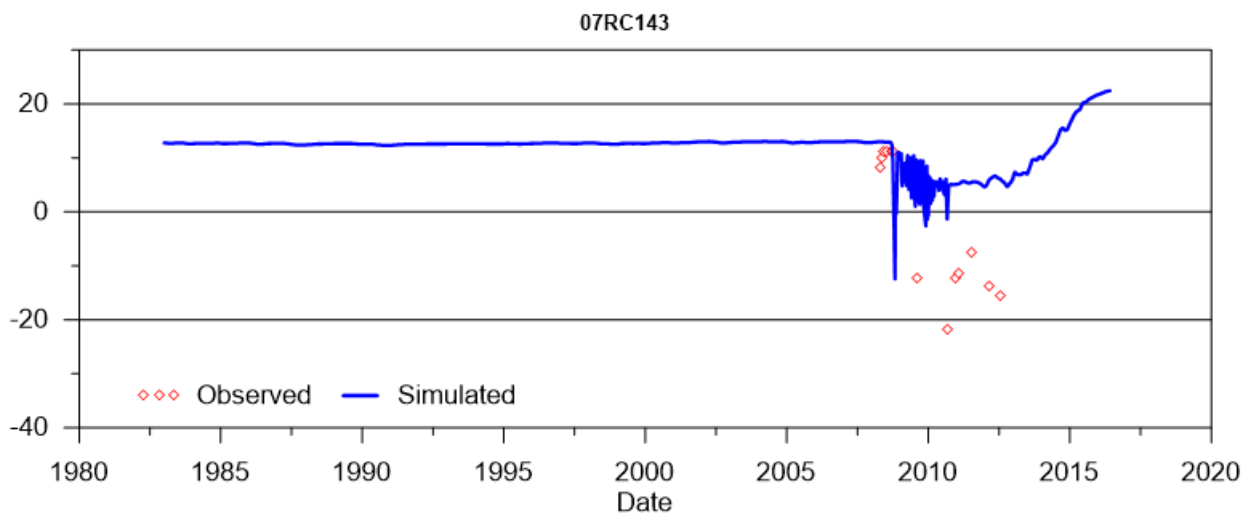
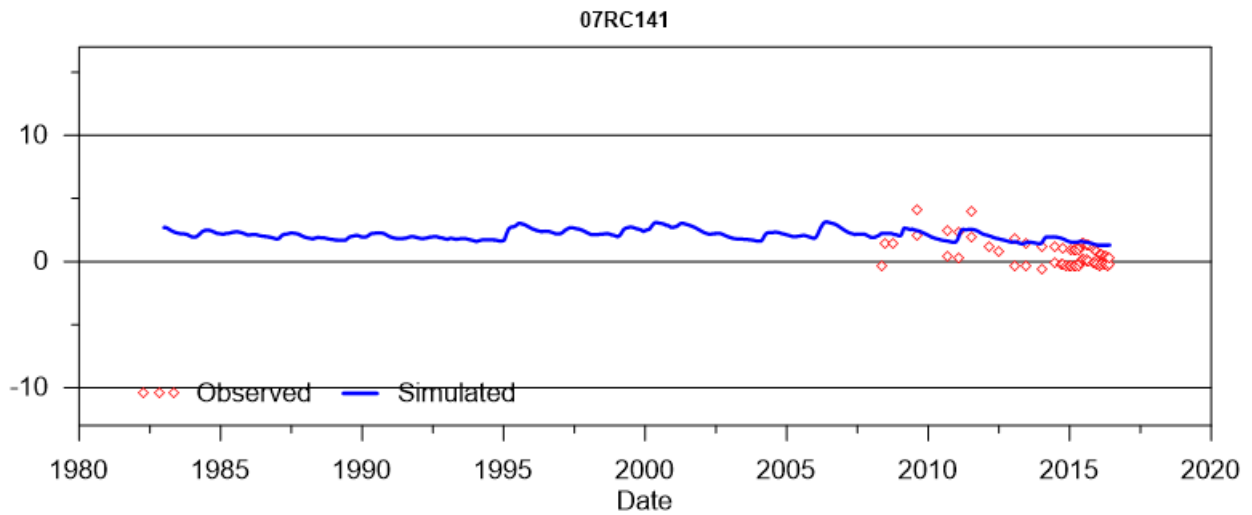
SINO EXPANSION LIFE OF MINE GROUNDWATER MODEL
APPENDIX E –Calibrated standpipe groundwater levels



SINO EXPANSION LIFE OF MINE GROUNDWATER MODEL
APPENDIX E –Calibrated standpipe groundwater levels

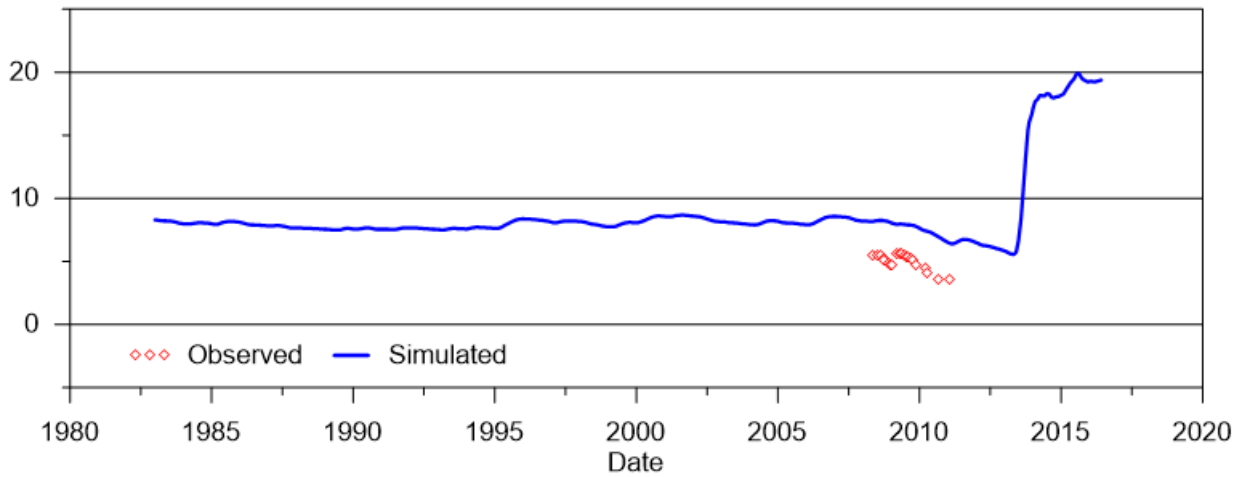


SINO EXPANSION LIFE OF MINE GROUNDWATER MODEL
APPENDIX E –Calibrated standpipe groundwater levels

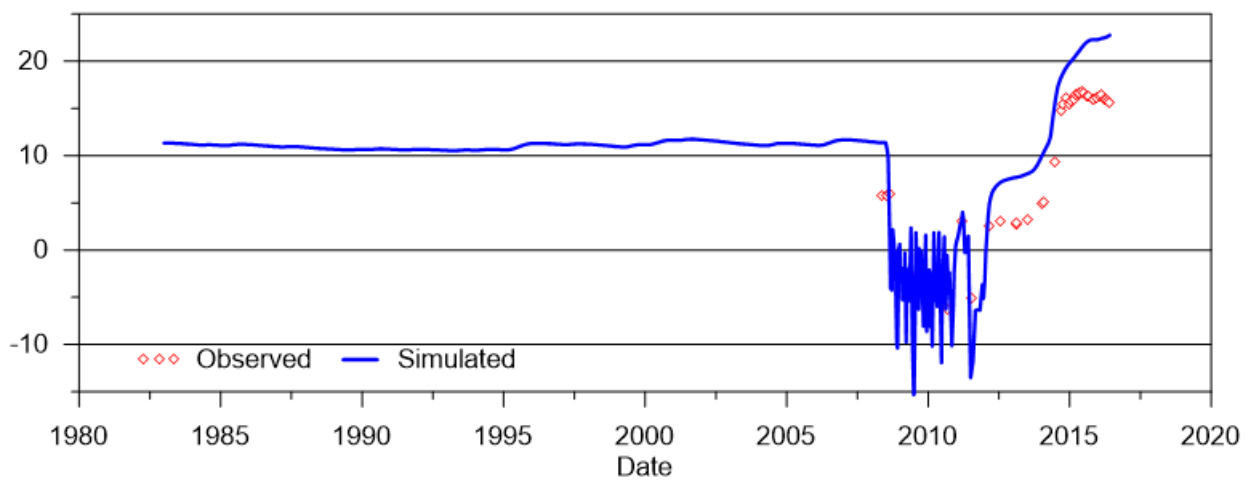


SINO EXPANSION LIFE OF MINE GROUNDWATER MODEL
APPENDIX E –Calibrated standpipe groundwater levels

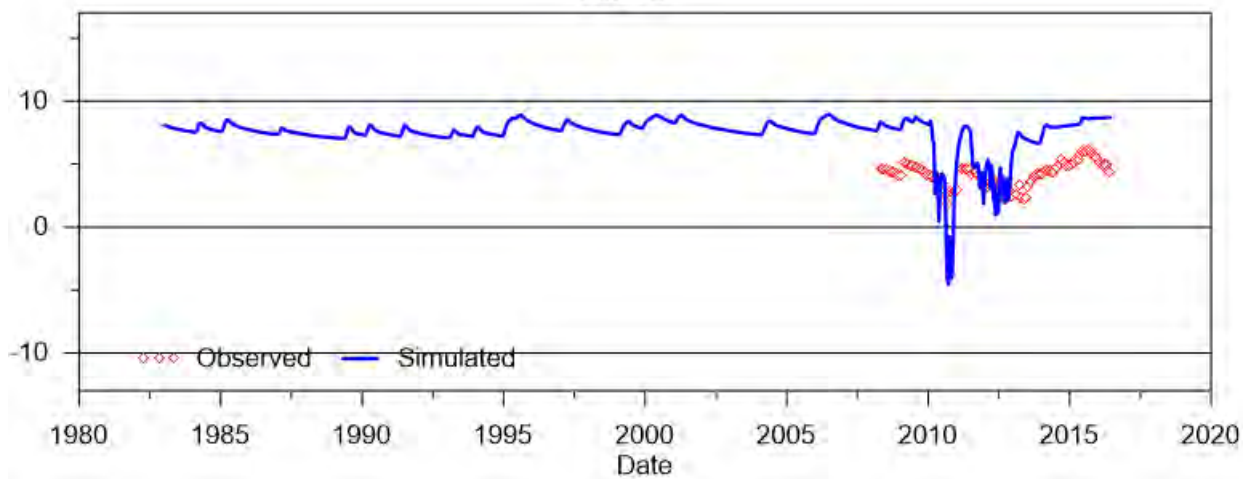
07RC147



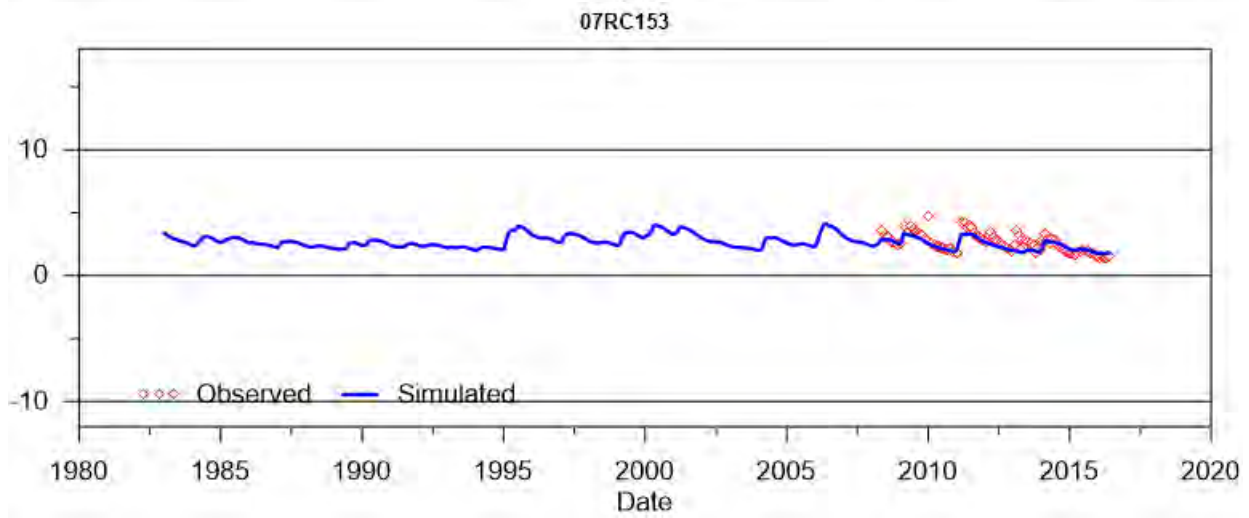
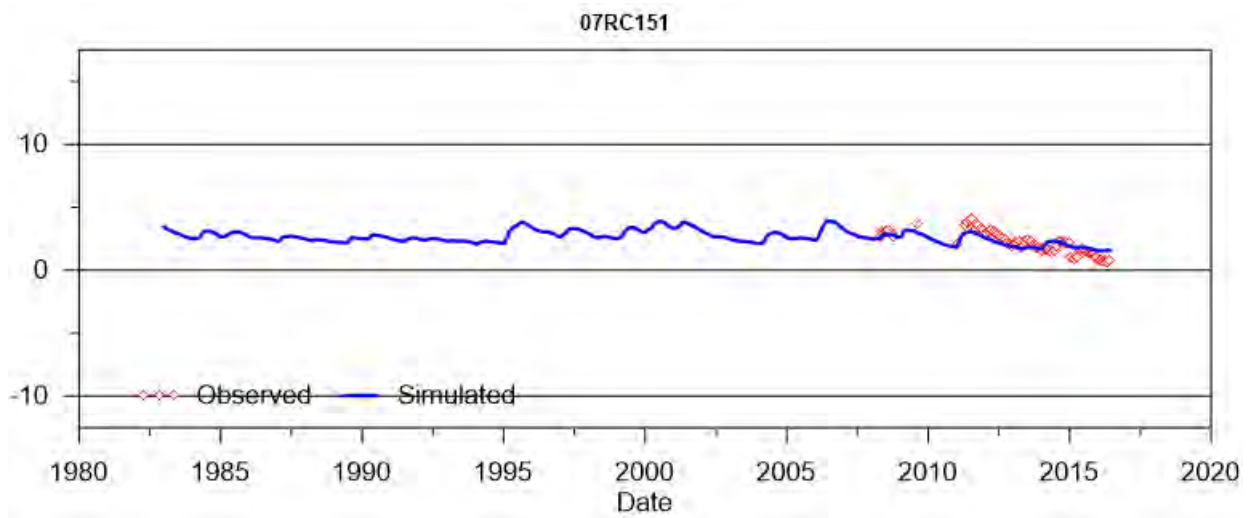
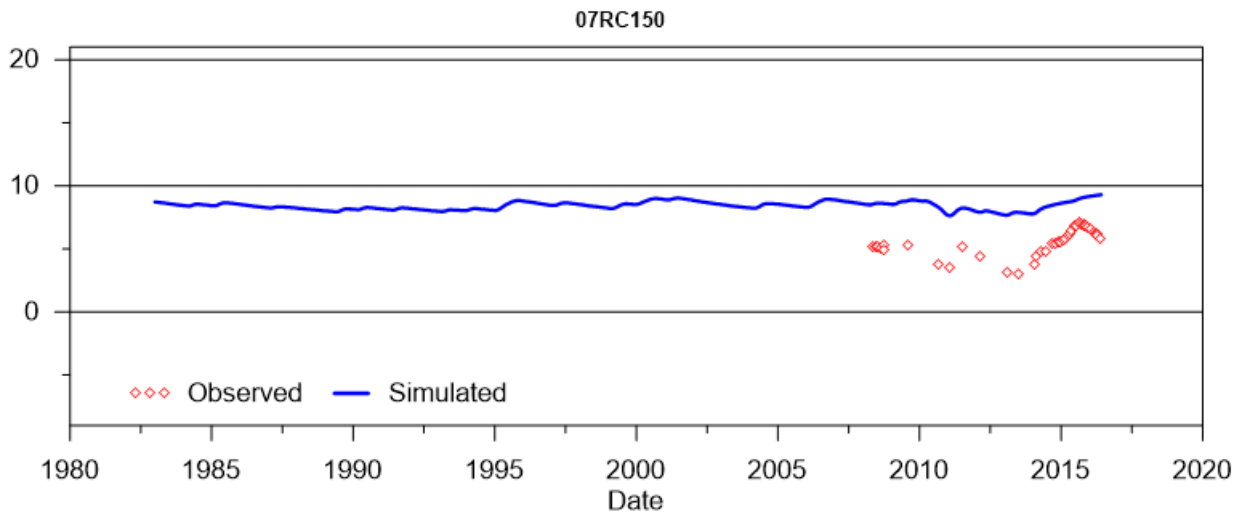
07RC148



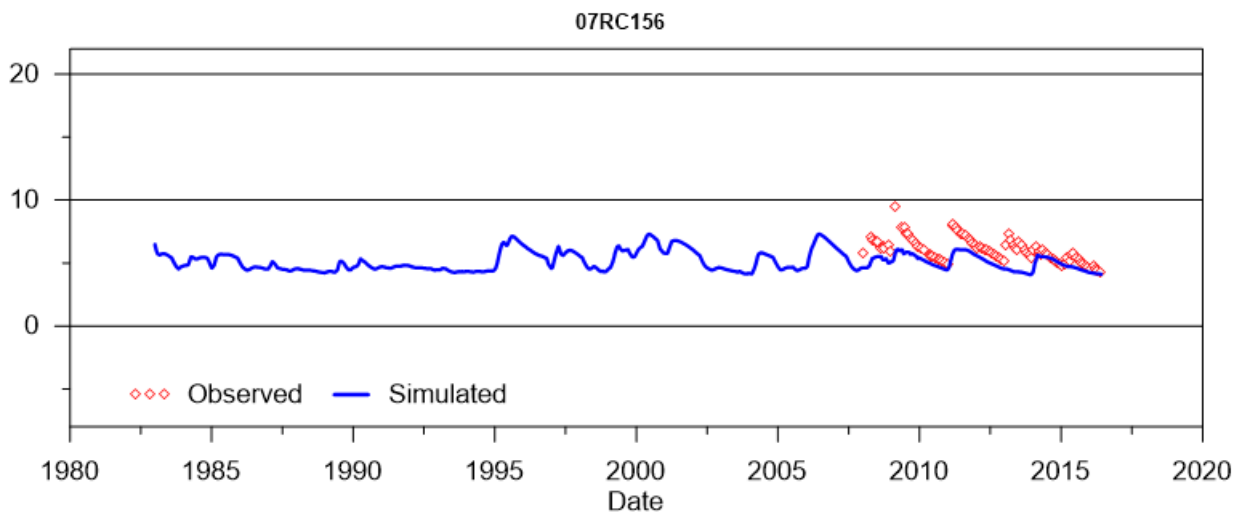
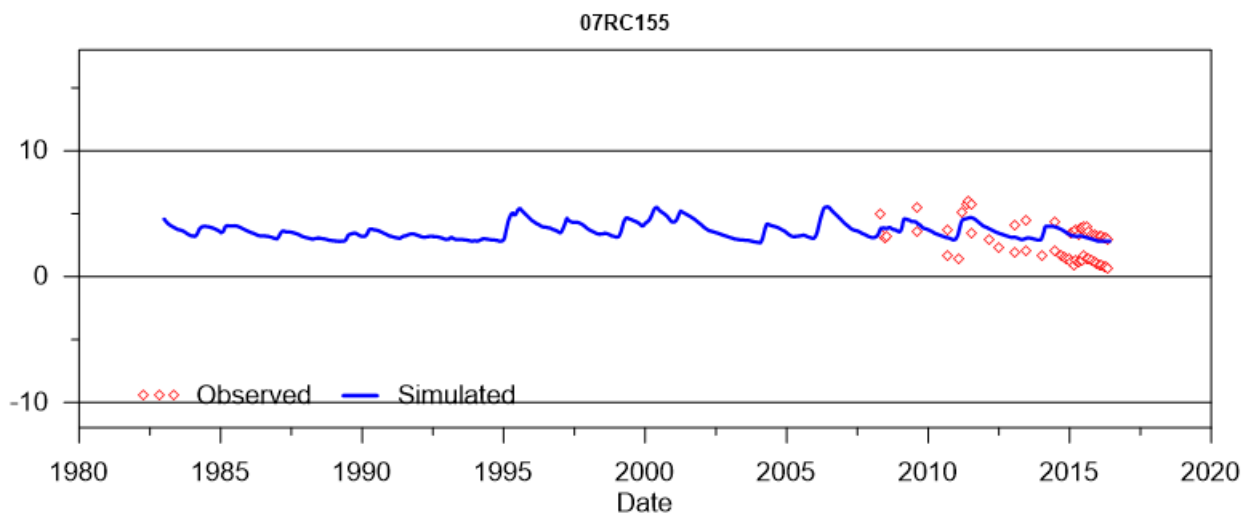
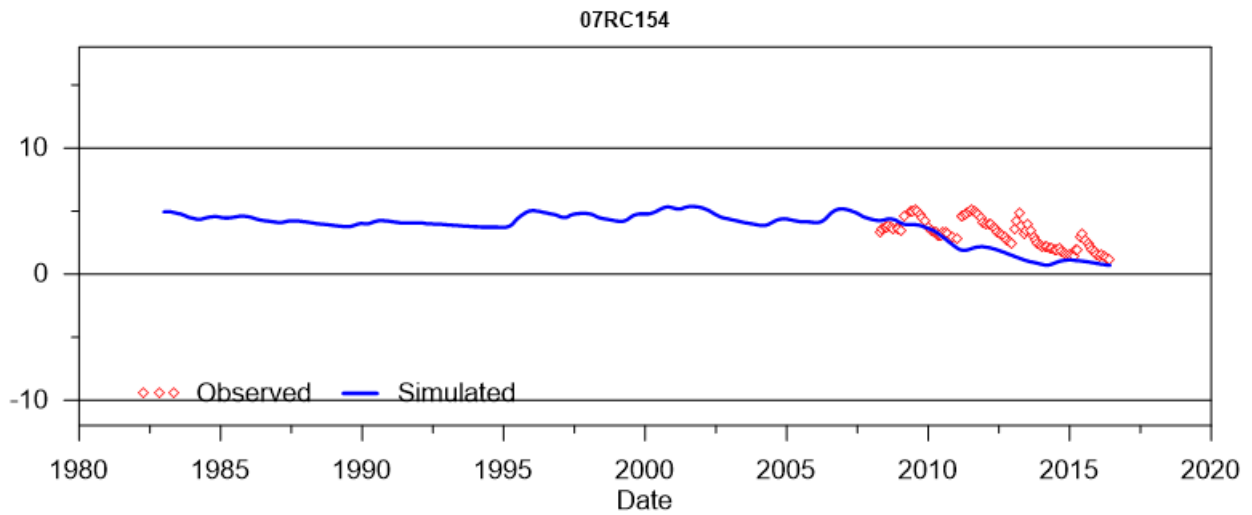
07RC149



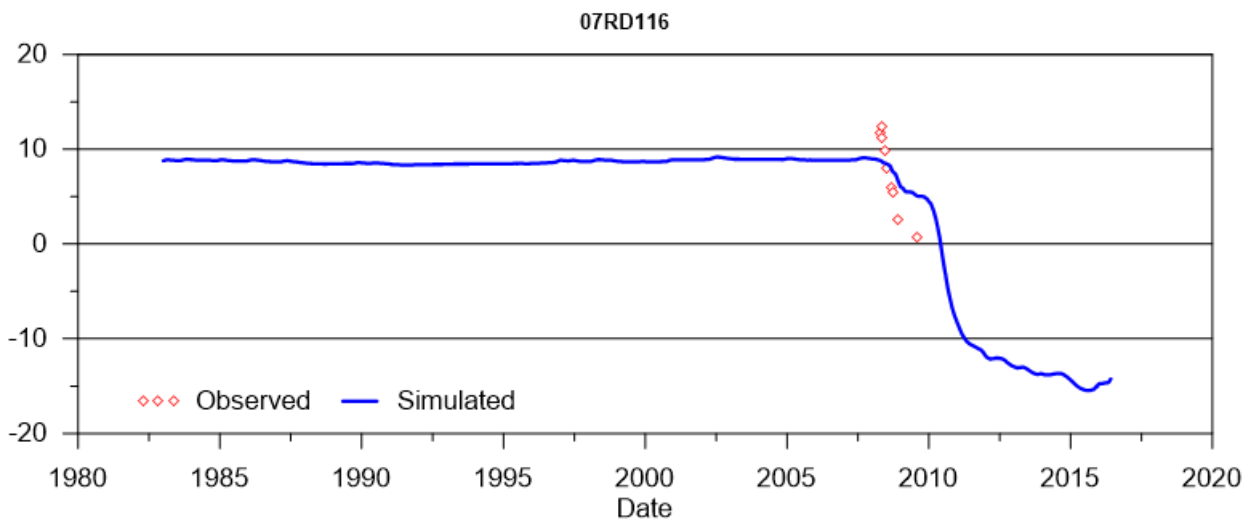
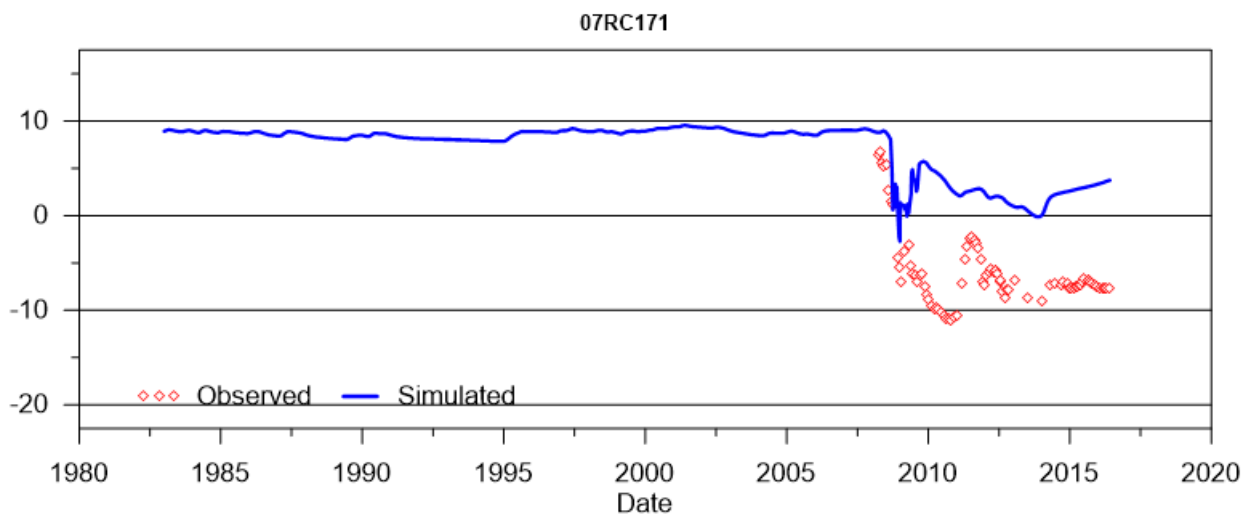
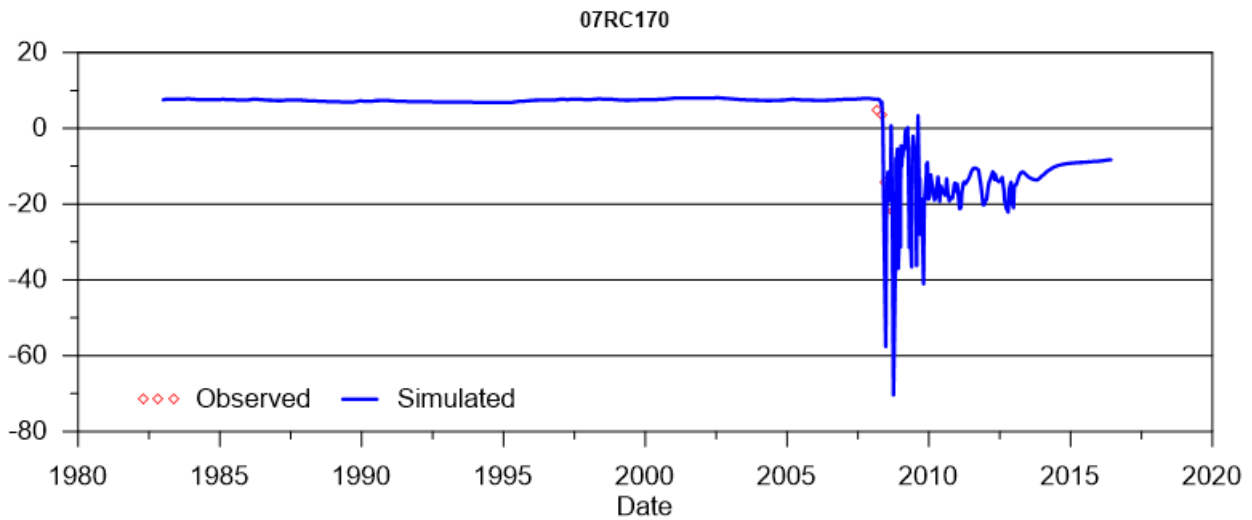
SINO EXPANSION LIFE OF MINE GROUNDWATER MODEL
APPENDIX E –Calibrated standpipe groundwater levels



SINO EXPANSION LIFE OF MINE GROUNDWATER MODEL
APPENDIX E –Calibrated standpipe groundwater levels

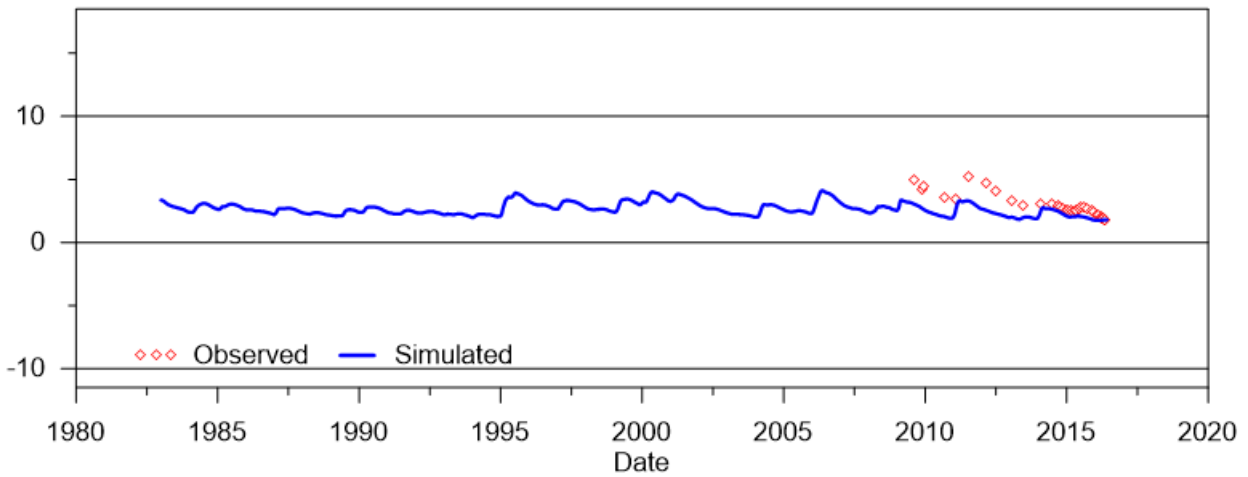


SINO EXPANSION LIFE OF MINE GROUNDWATER MODEL
APPENDIX E –Calibrated standpipe groundwater levels

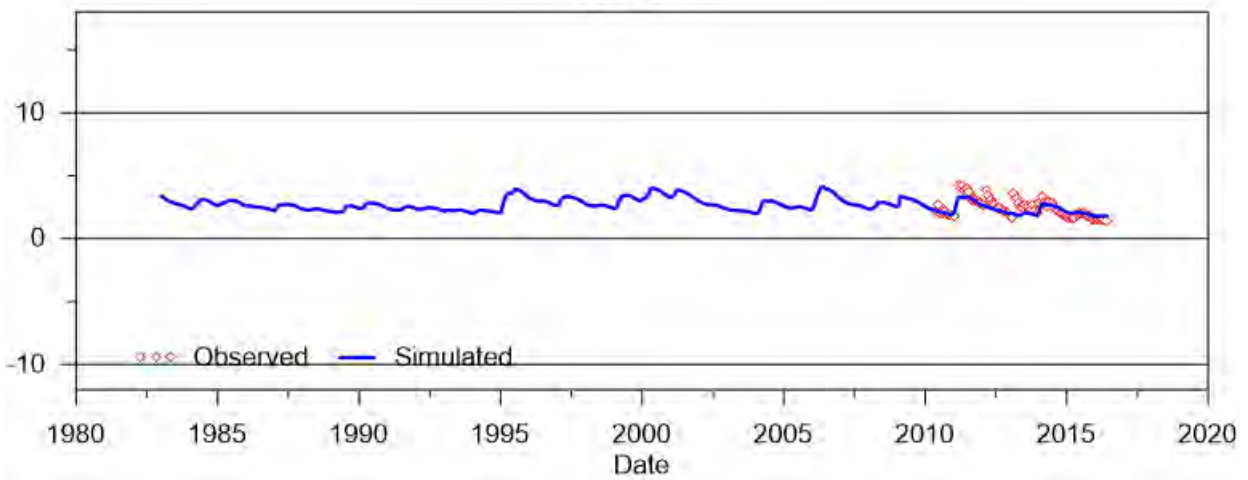


SINO EXPANSION LIFE OF MINE GROUNDWATER MODEL
APPENDIX E –Calibrated standpipe groundwater levels

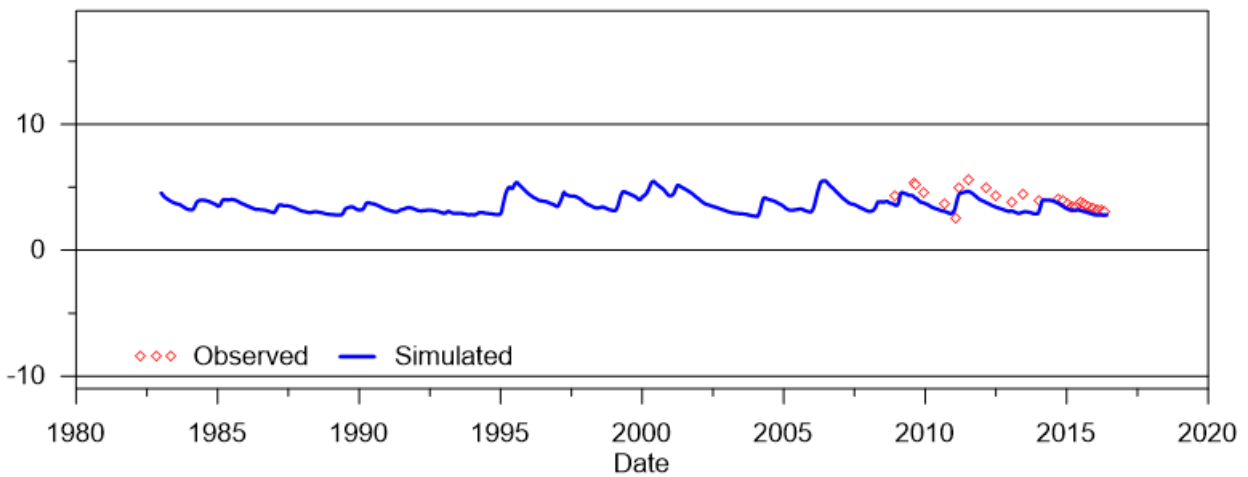
08AC283



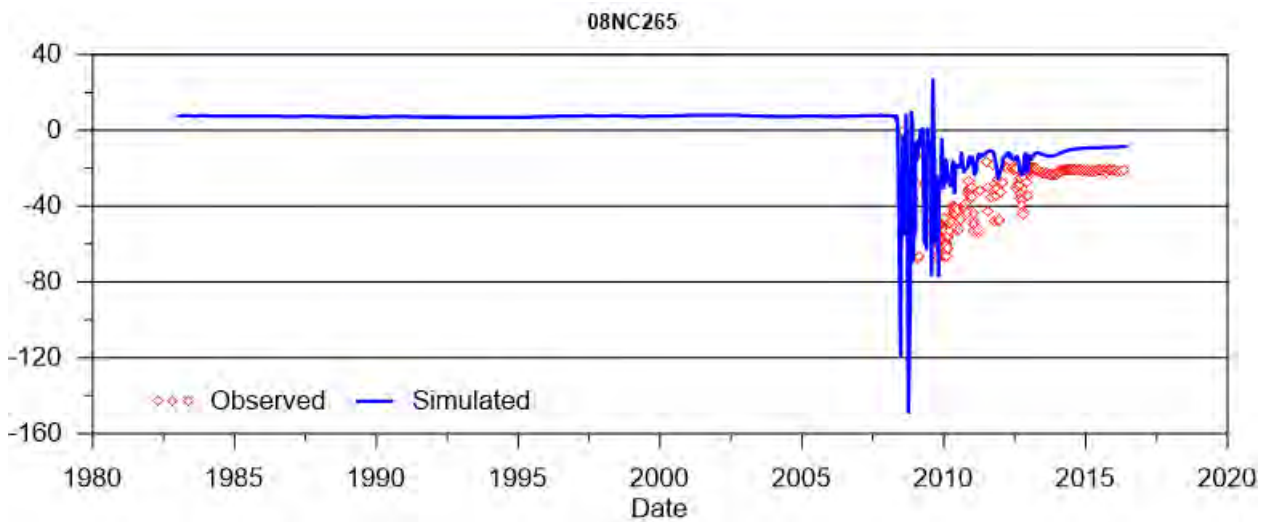
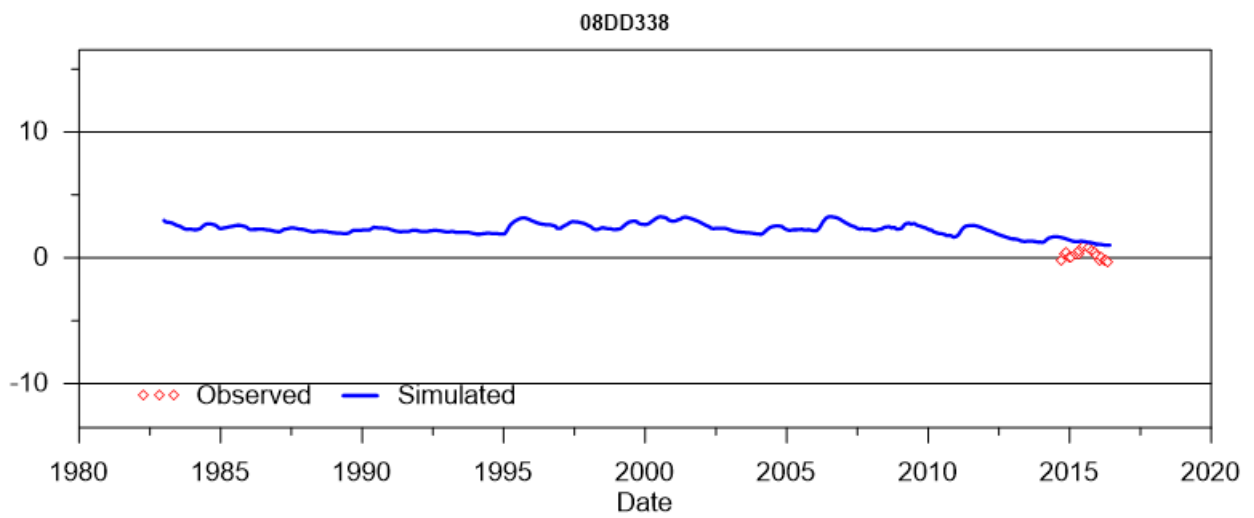
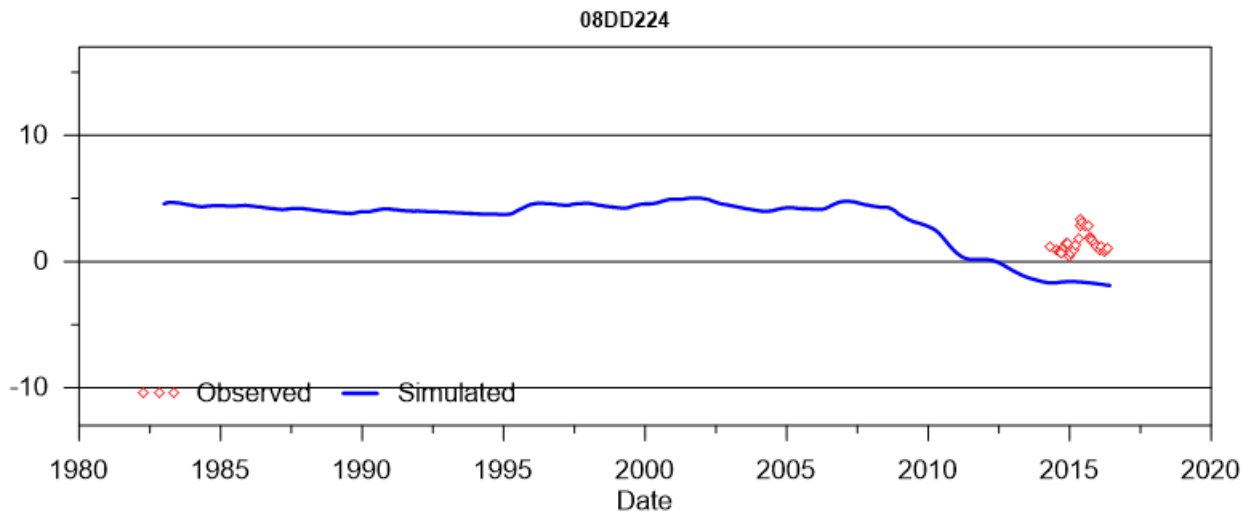
08AC284



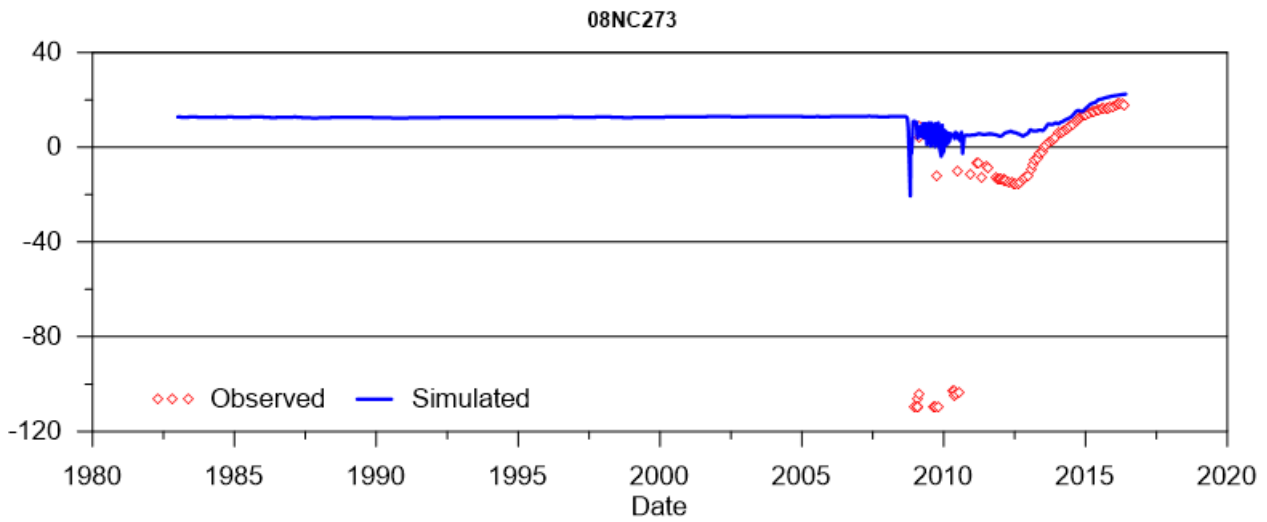
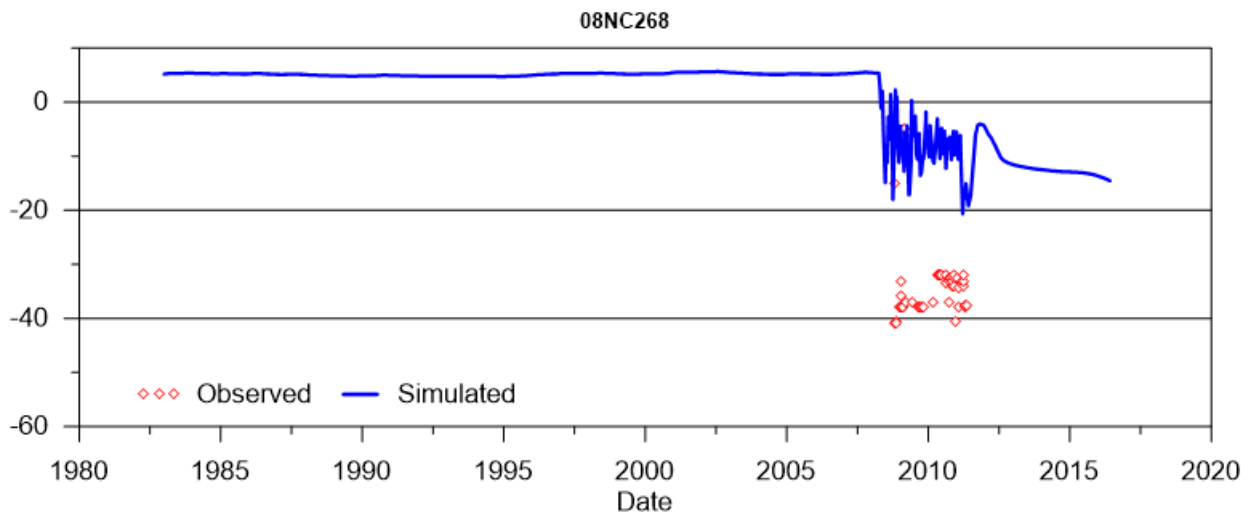
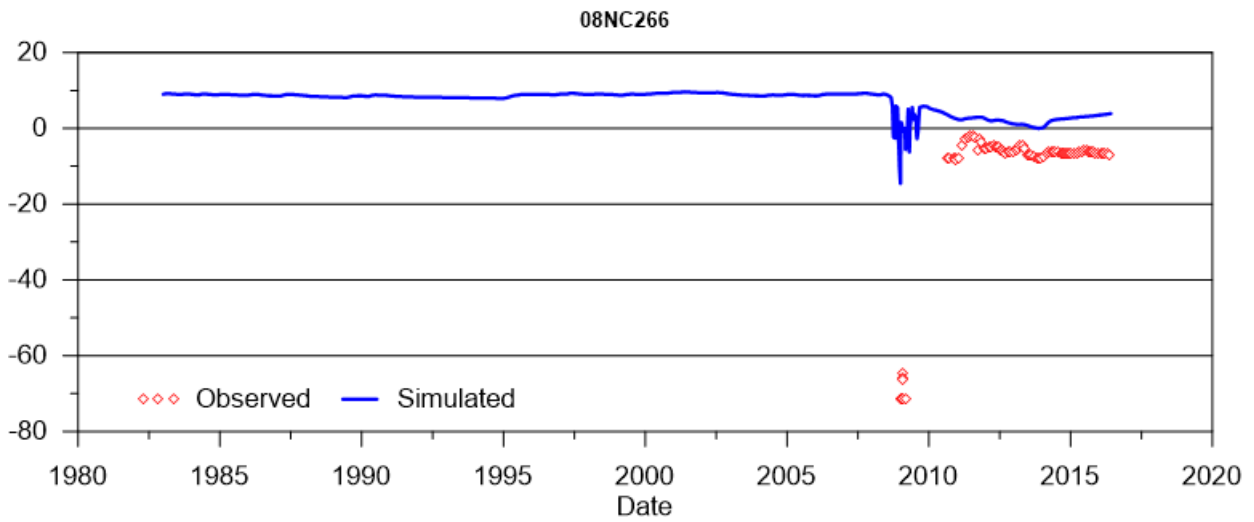
08AC285



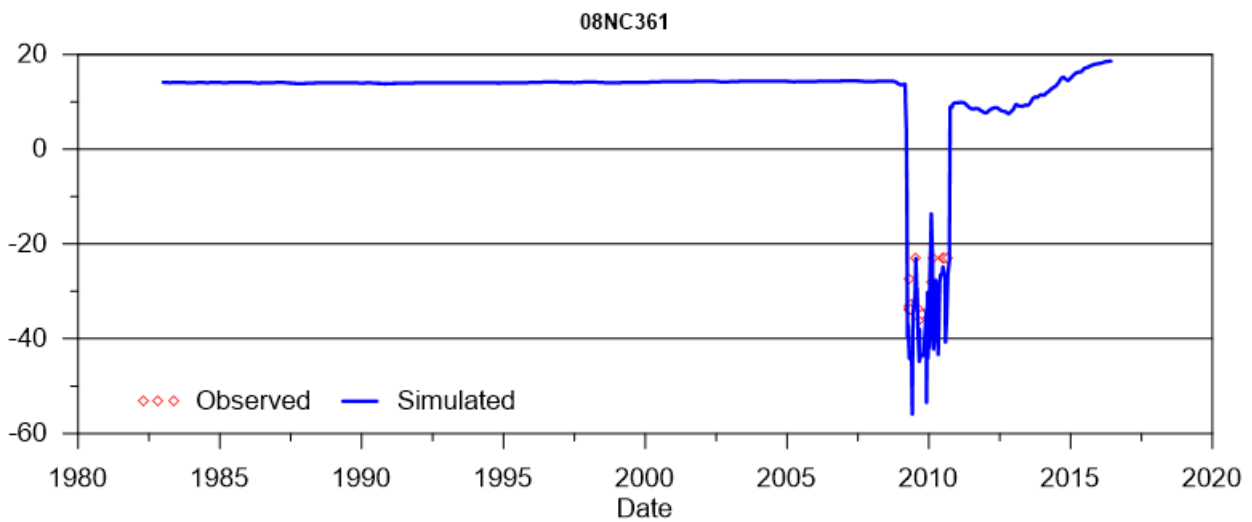
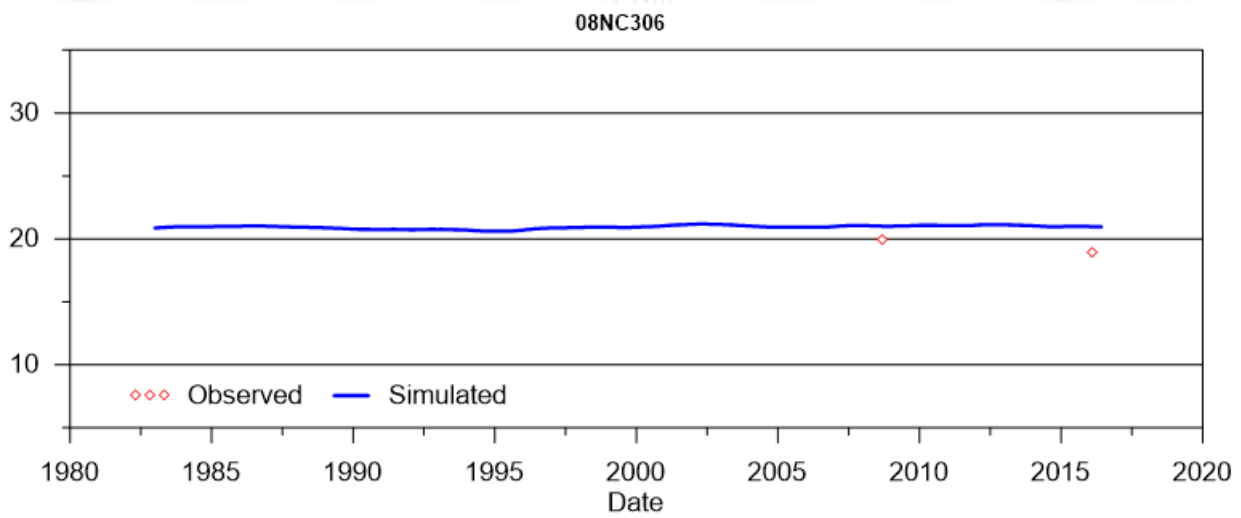
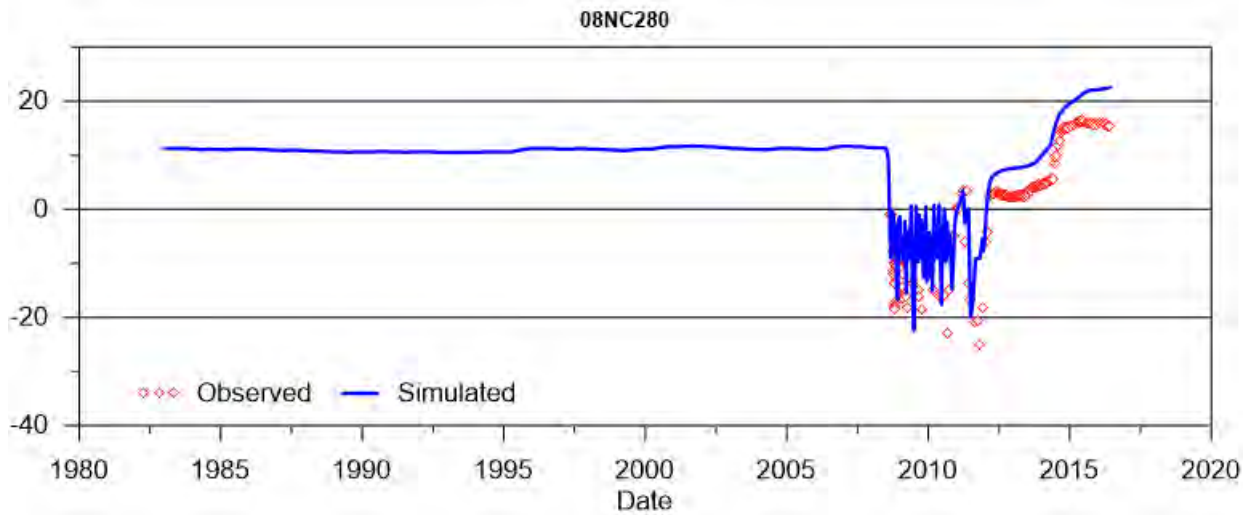
SINO EXPANSION LIFE OF MINE GROUNDWATER MODEL
APPENDIX E –Calibrated standpipe groundwater levels



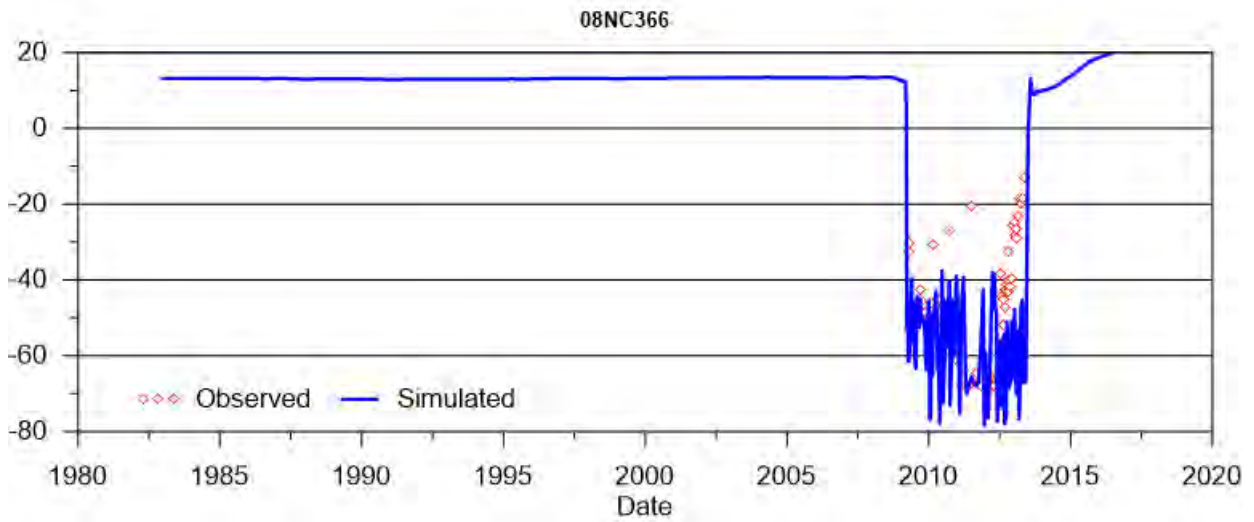
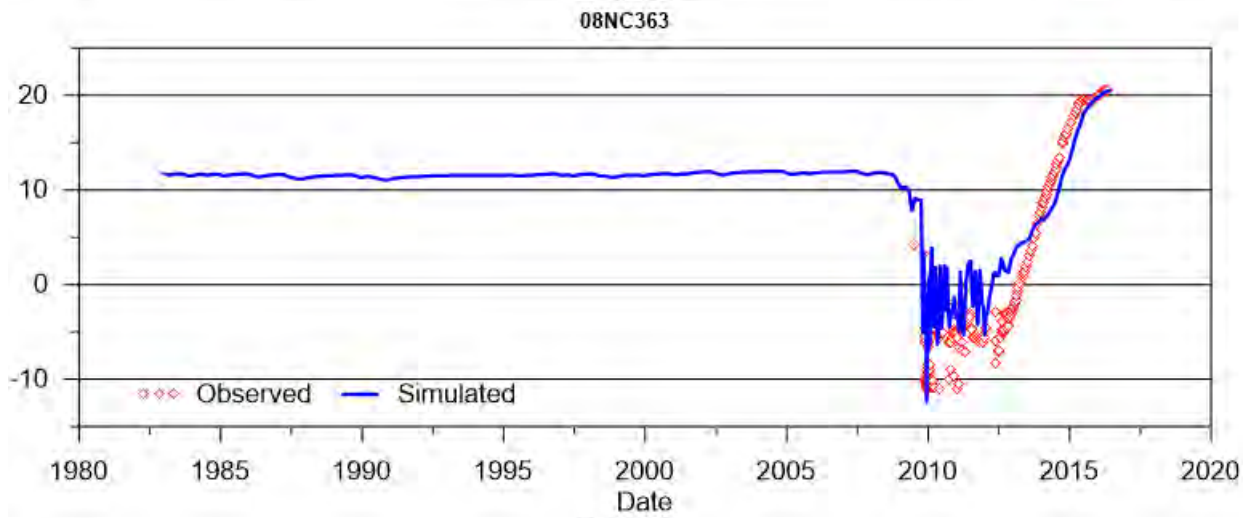
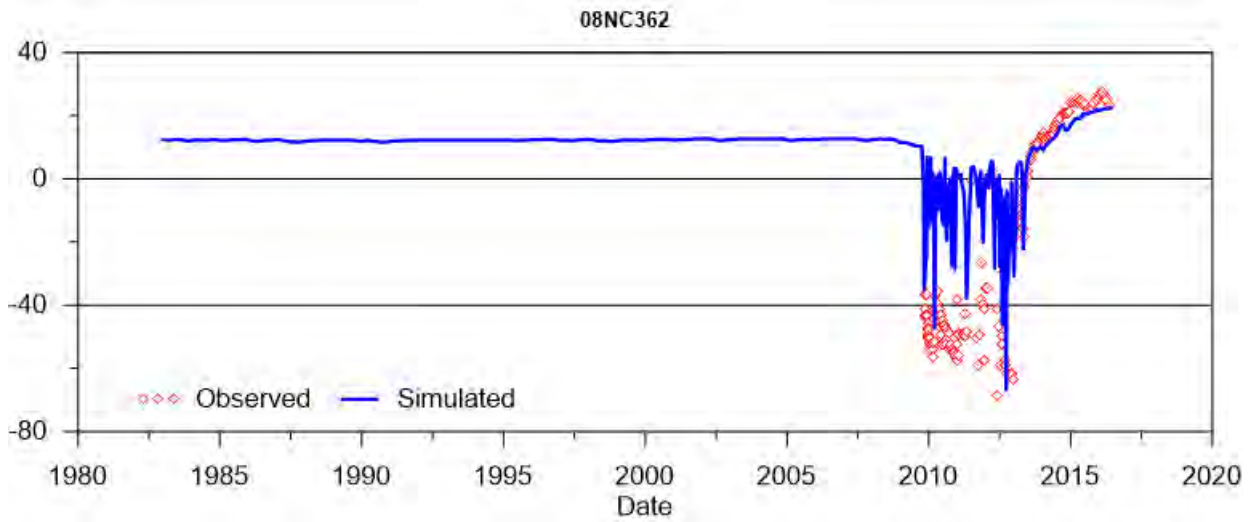
SINO EXPANSION LIFE OF MINE GROUNDWATER MODEL
APPENDIX E –Calibrated standpipe groundwater levels



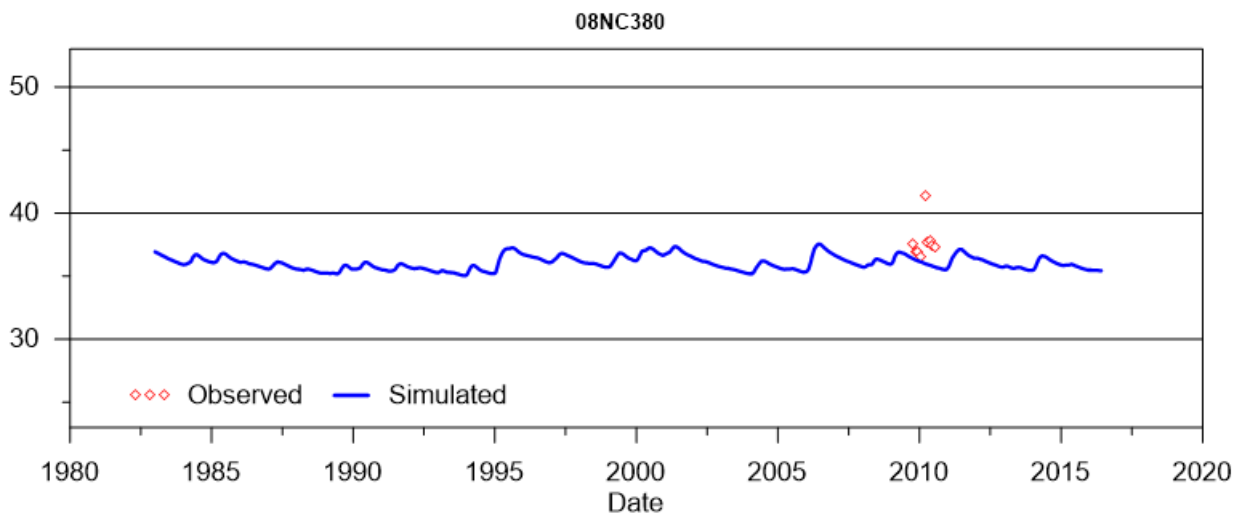
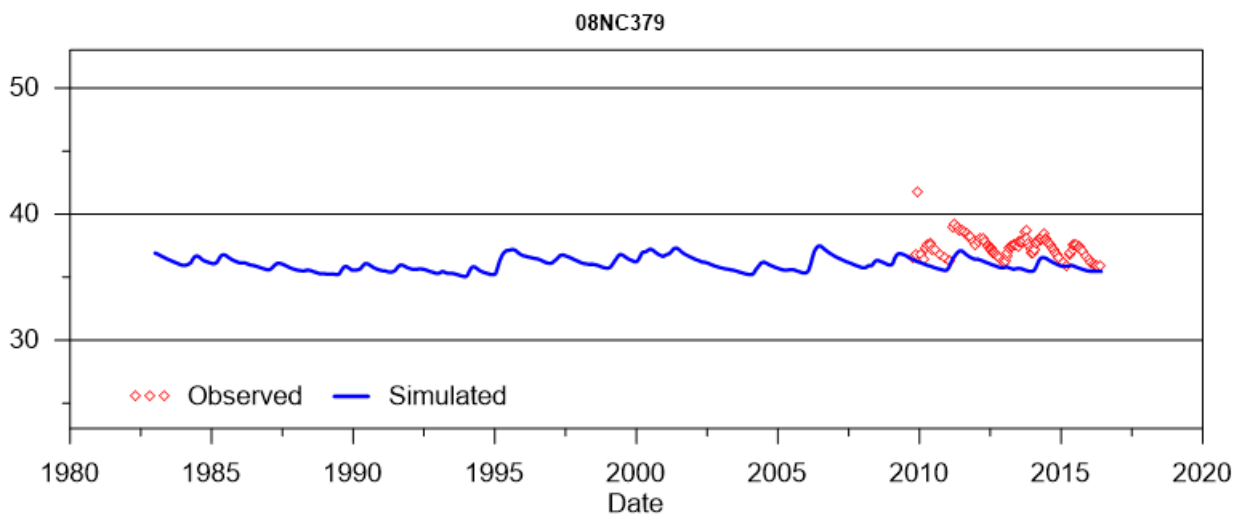
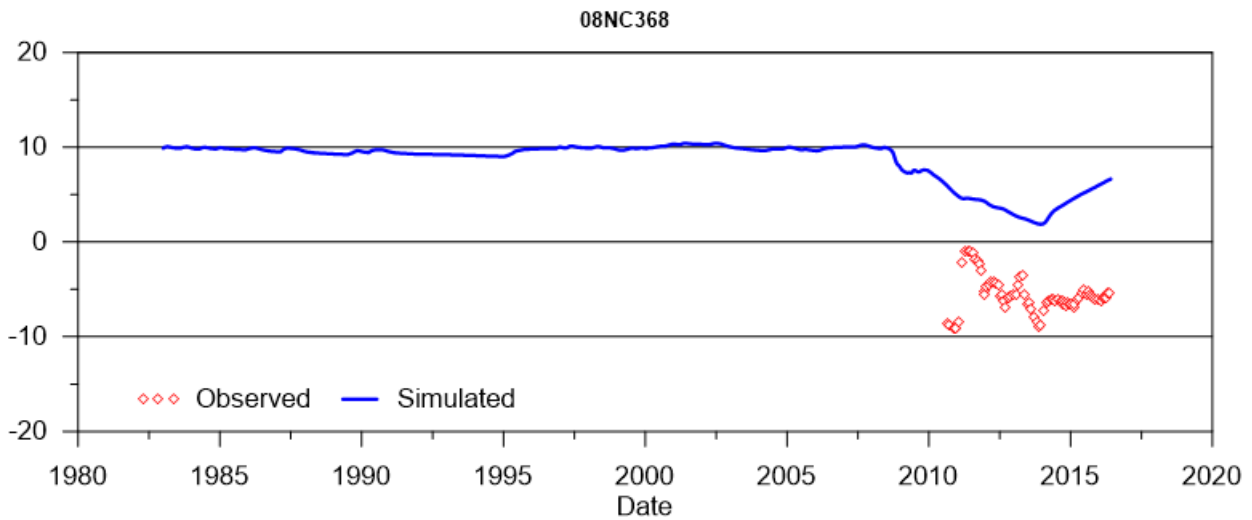
SINO EXPANSION LIFE OF MINE GROUNDWATER MODEL
APPENDIX E –Calibrated standpipe groundwater levels



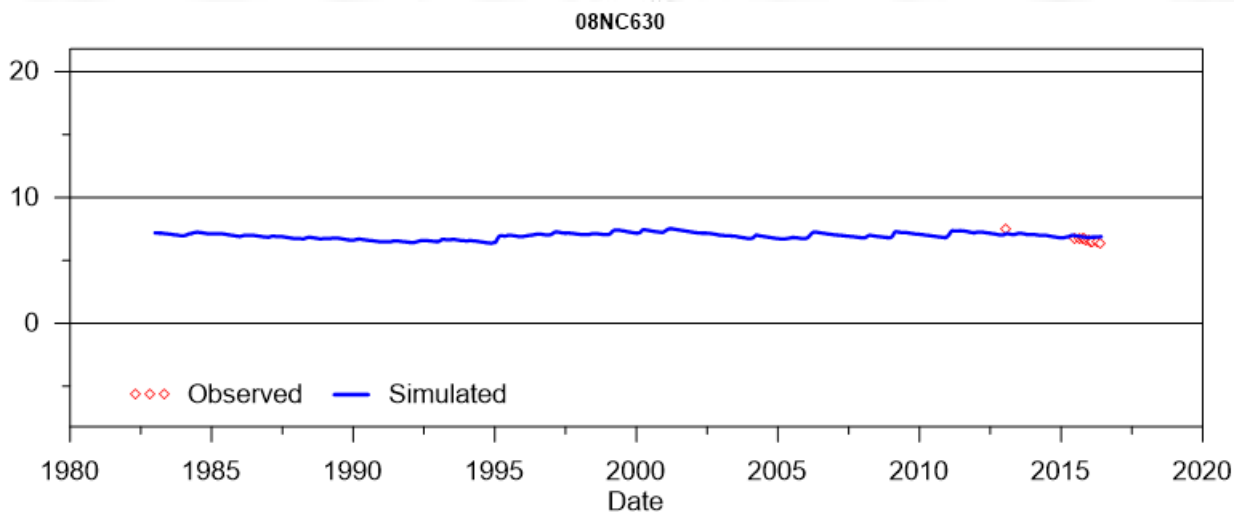
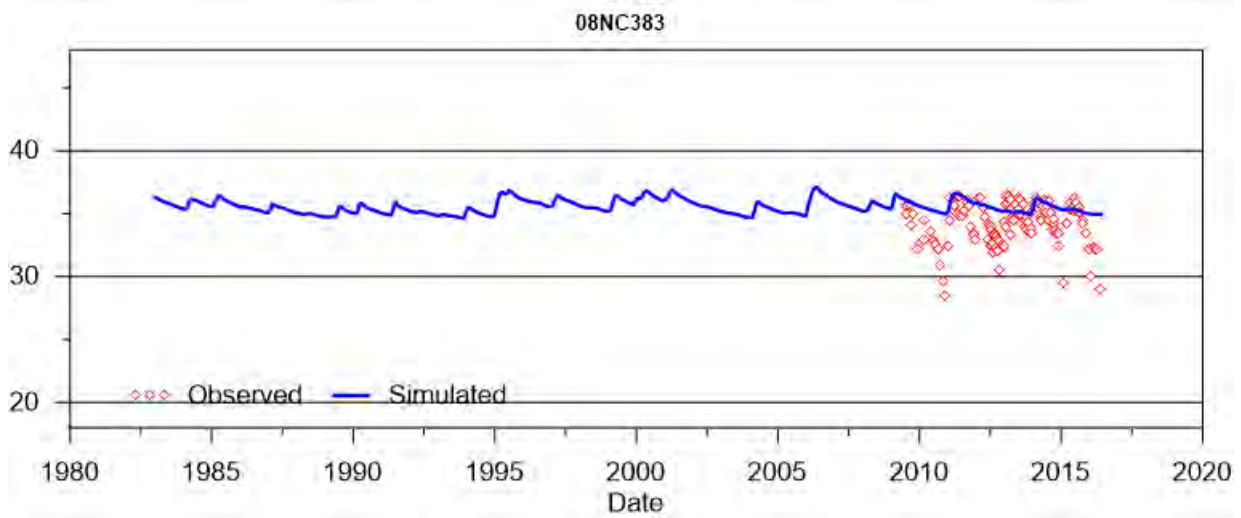
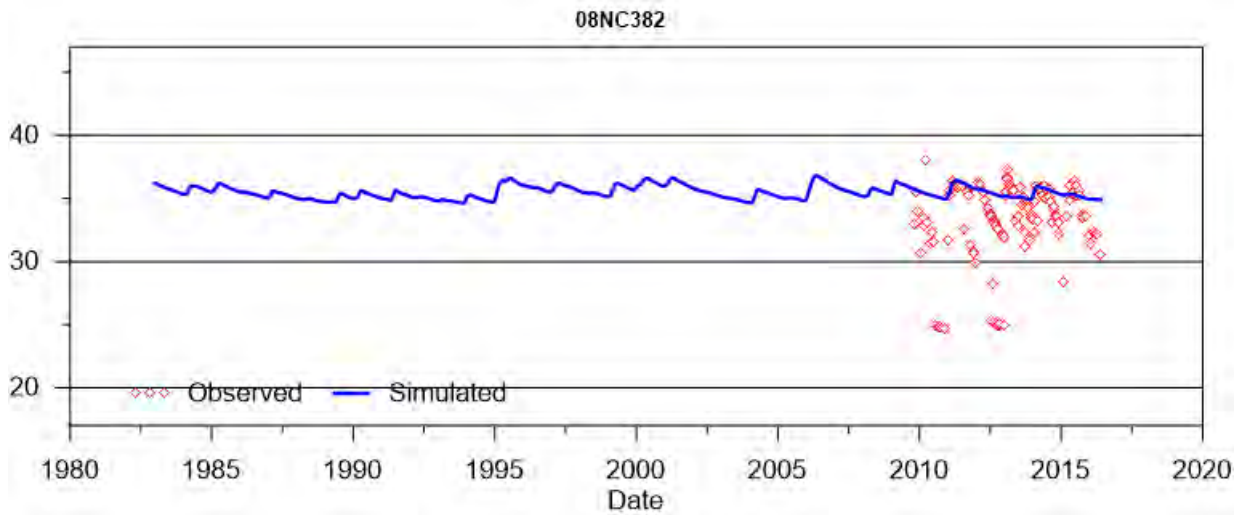
SINO EXPANSION LIFE OF MINE GROUNDWATER MODEL
APPENDIX E –Calibrated standpipe groundwater levels



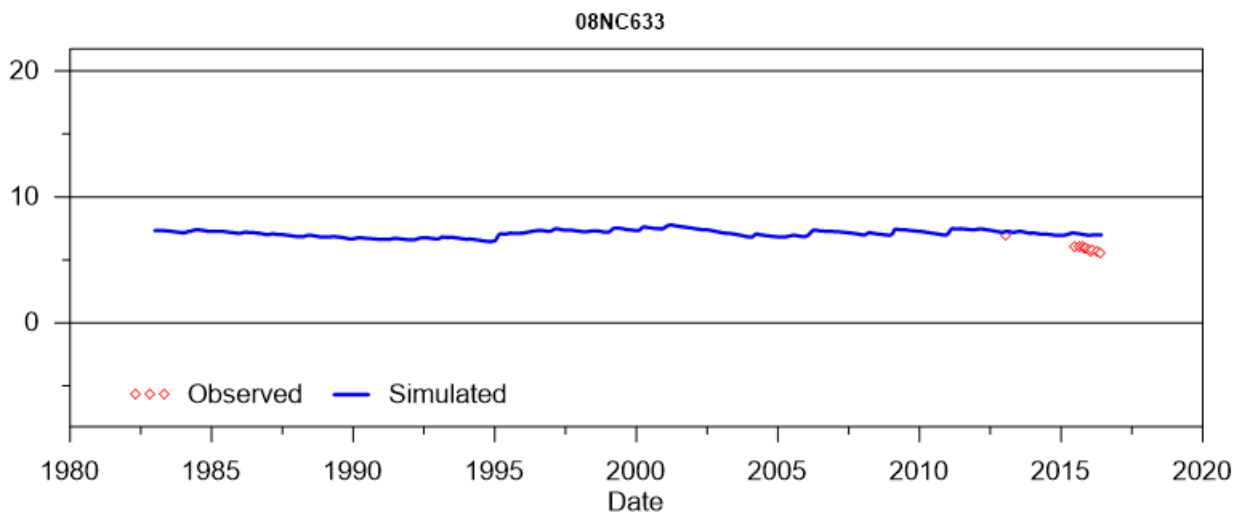
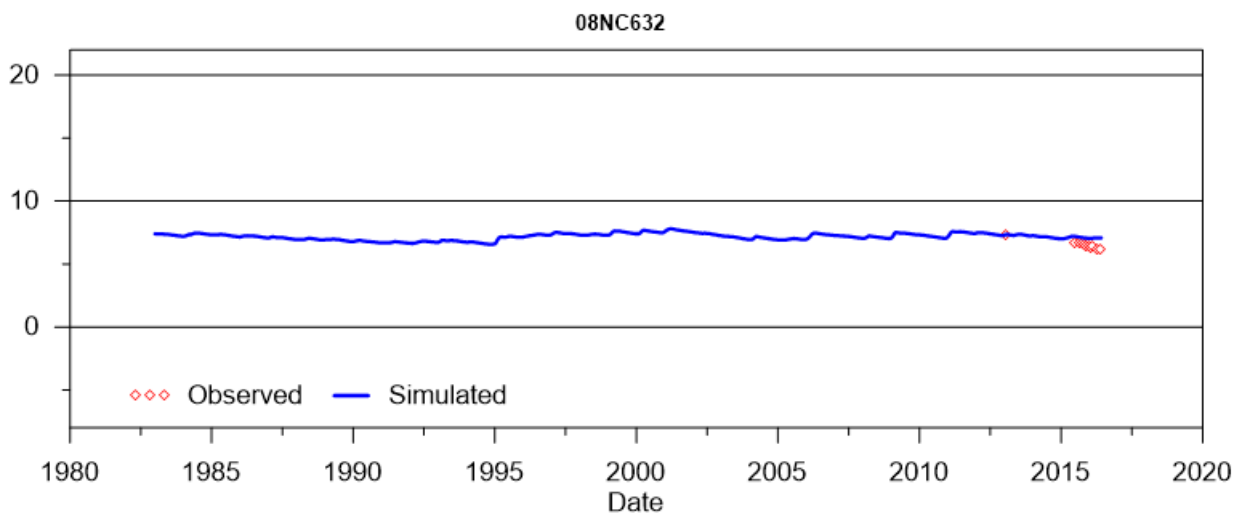
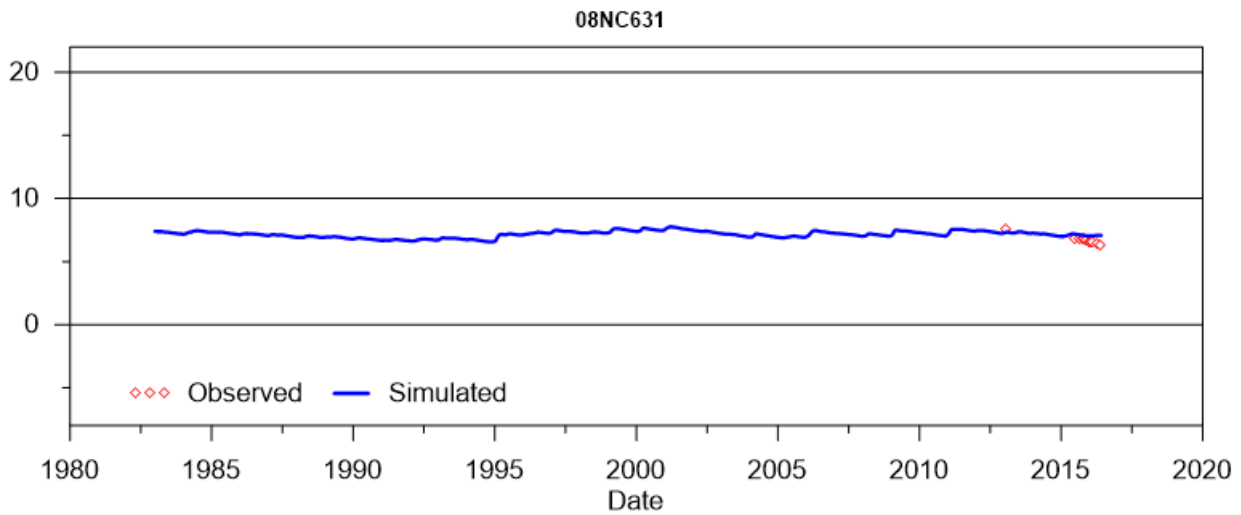
SINO EXPANSION LIFE OF MINE GROUNDWATER MODEL
APPENDIX E –Calibrated standpipe groundwater levels



SINO EXPANSION LIFE OF MINE GROUNDWATER MODEL
APPENDIX E –Calibrated standpipe groundwater levels

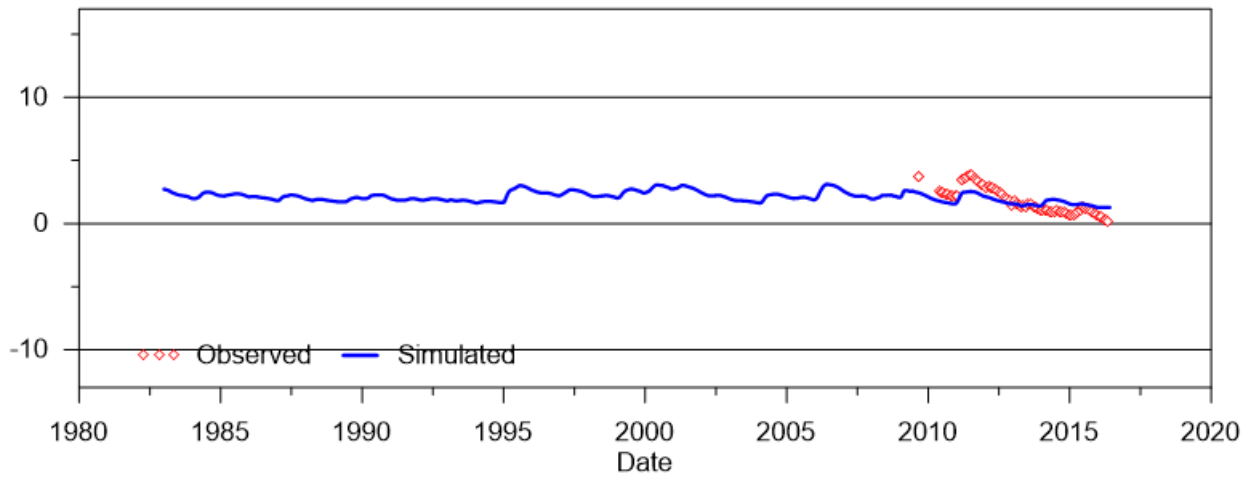


SINO EXPANSION LIFE OF MINE GROUNDWATER MODEL
APPENDIX E –Calibrated standpipe groundwater levels

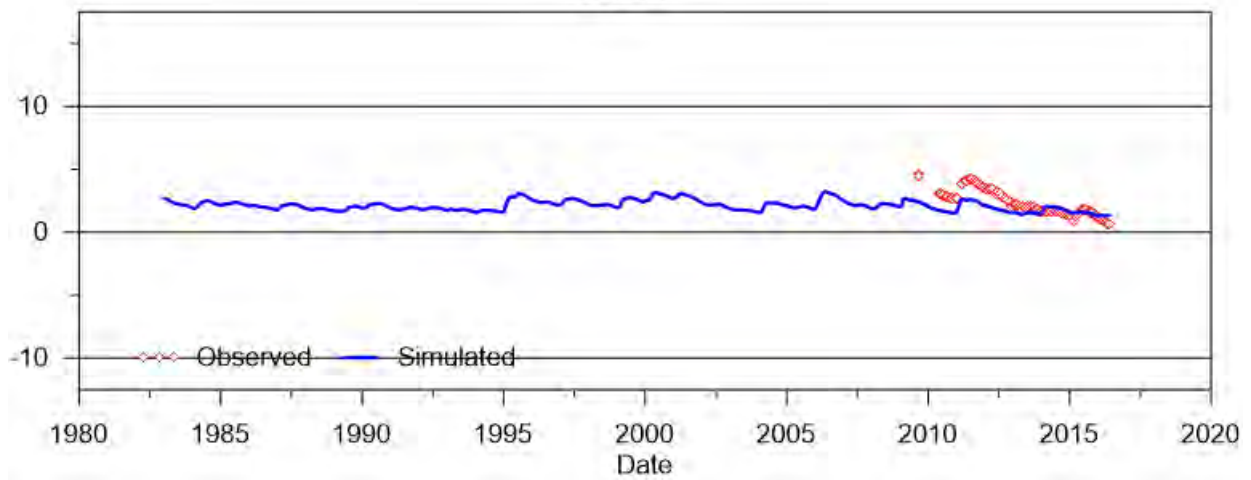


SINO EXPANSION LIFE OF MINE GROUNDWATER MODEL
APPENDIX E –Calibrated standpipe groundwater levels

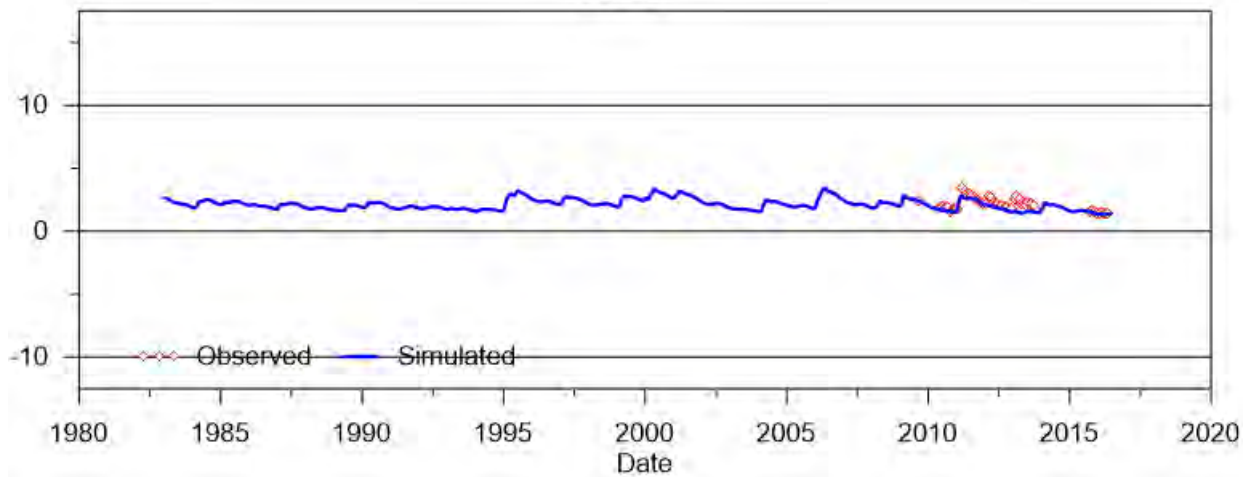
09AC487



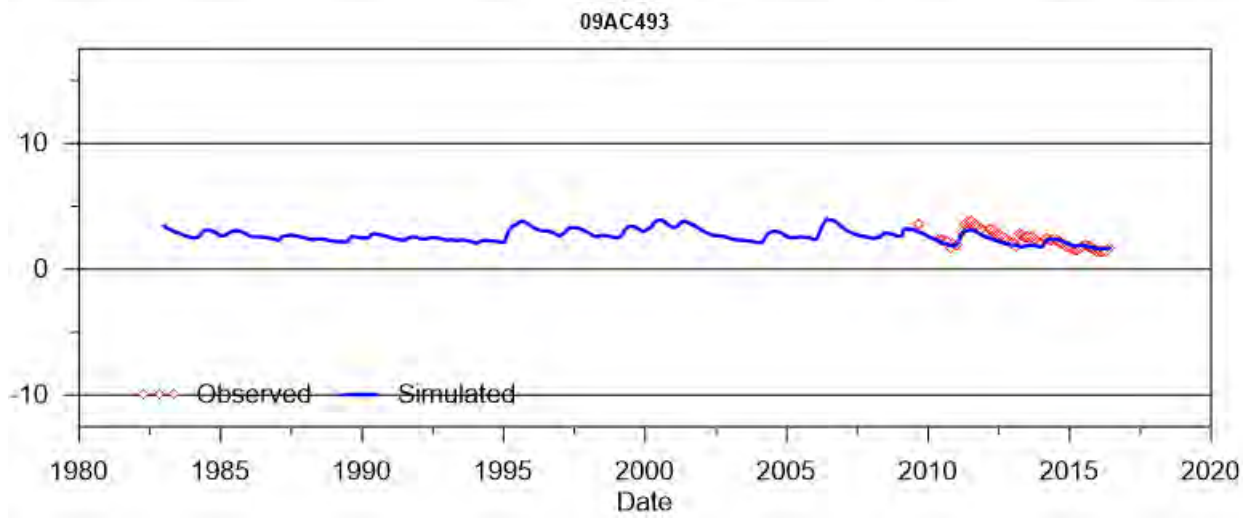
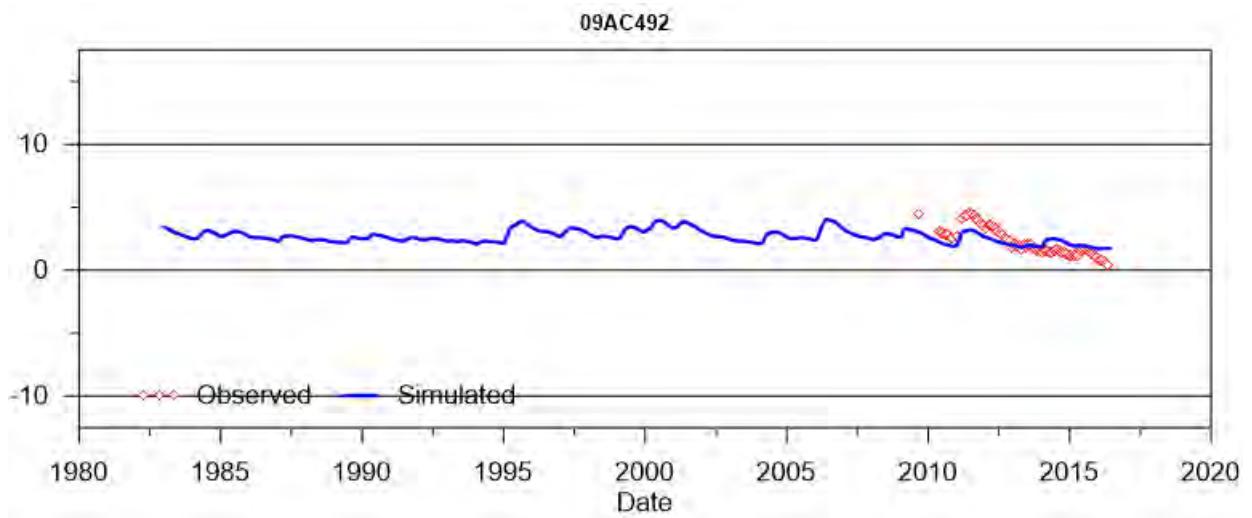
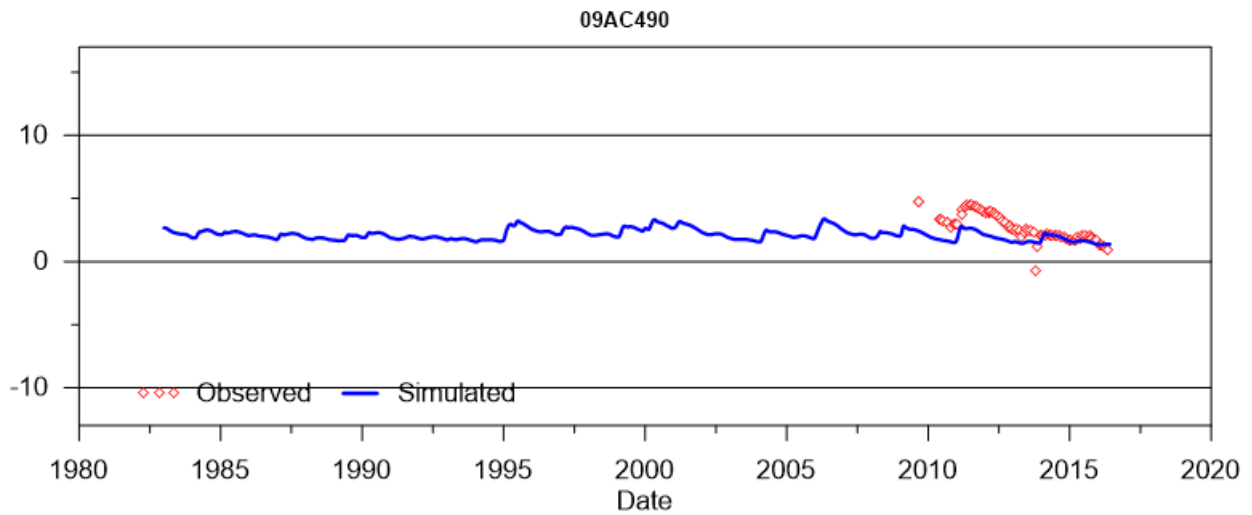
09AC488



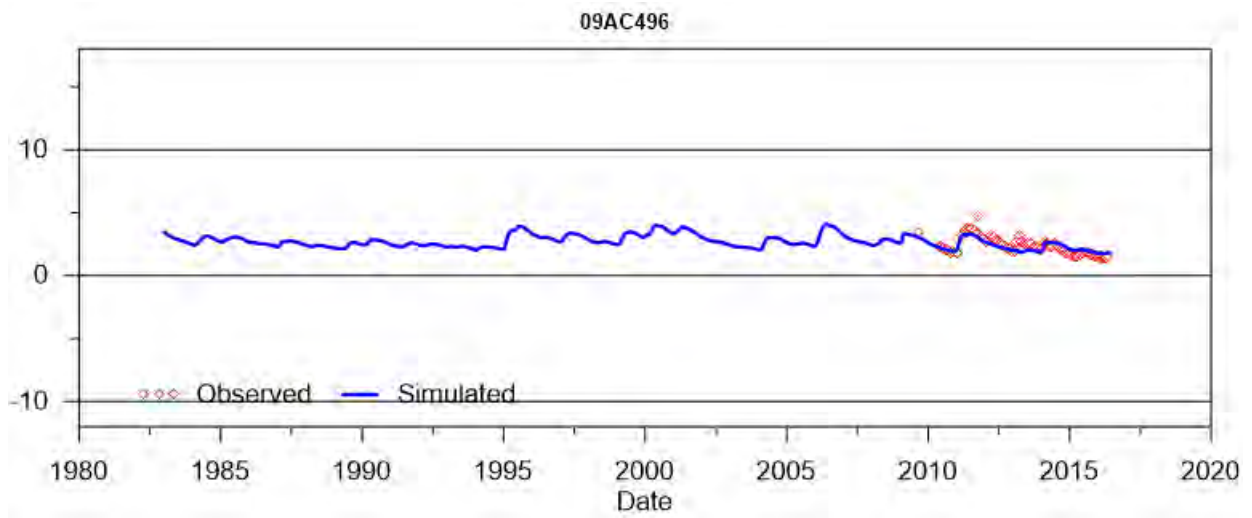
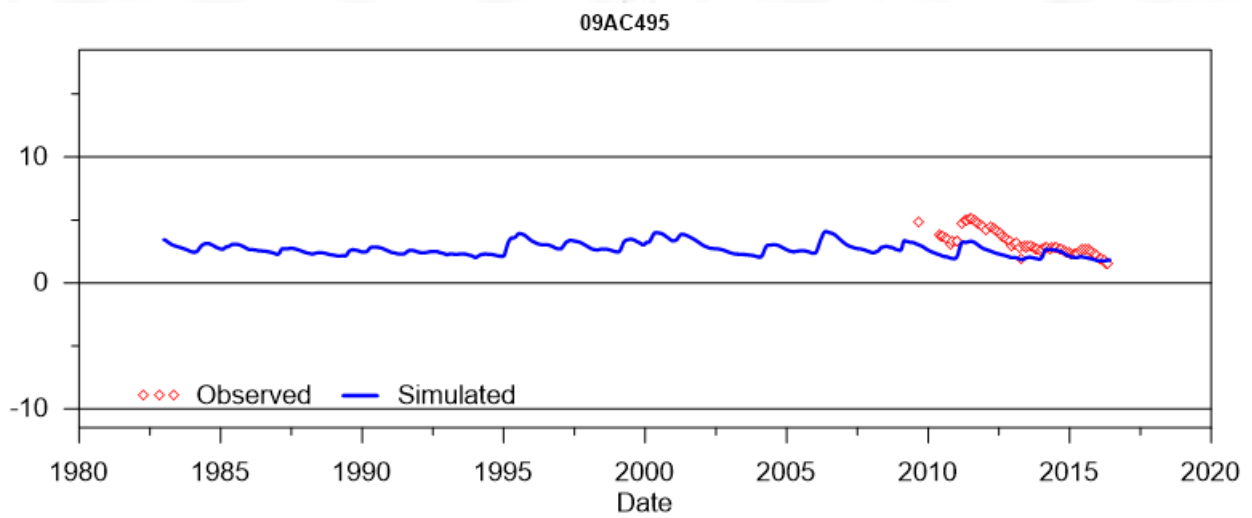
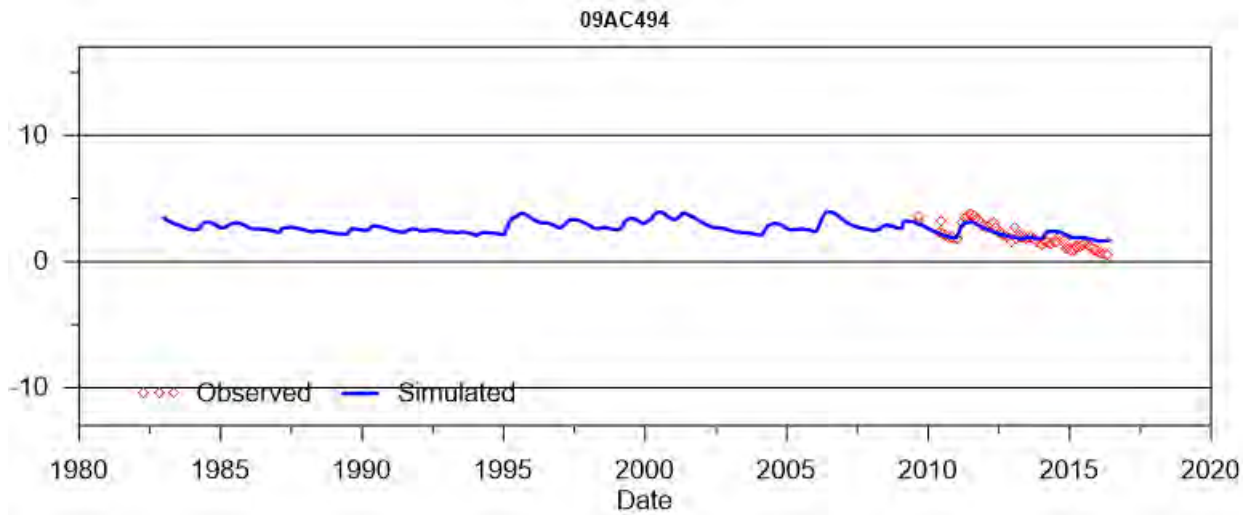
09AC489



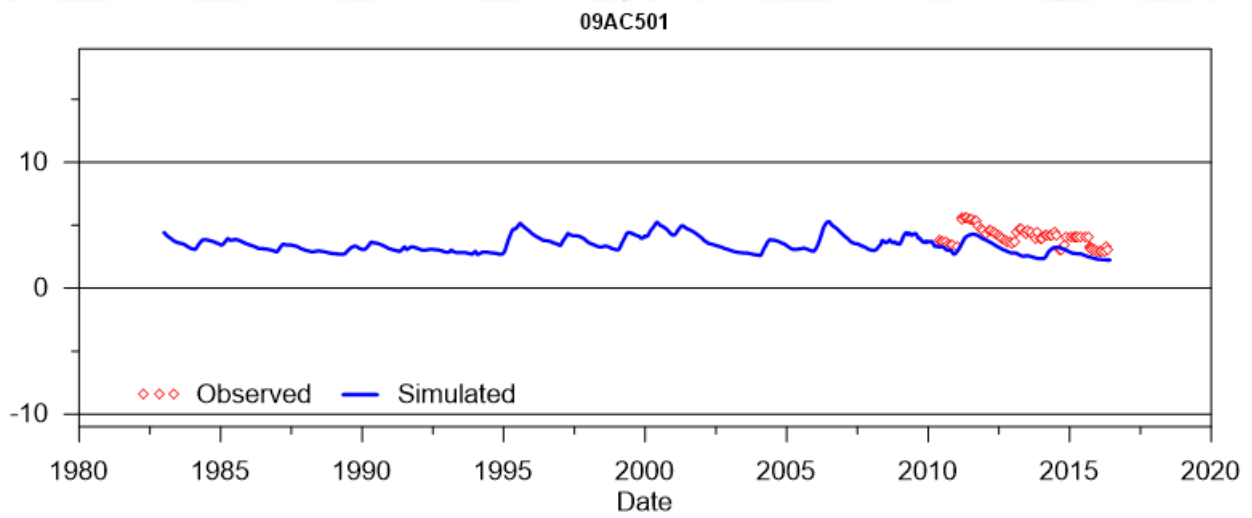
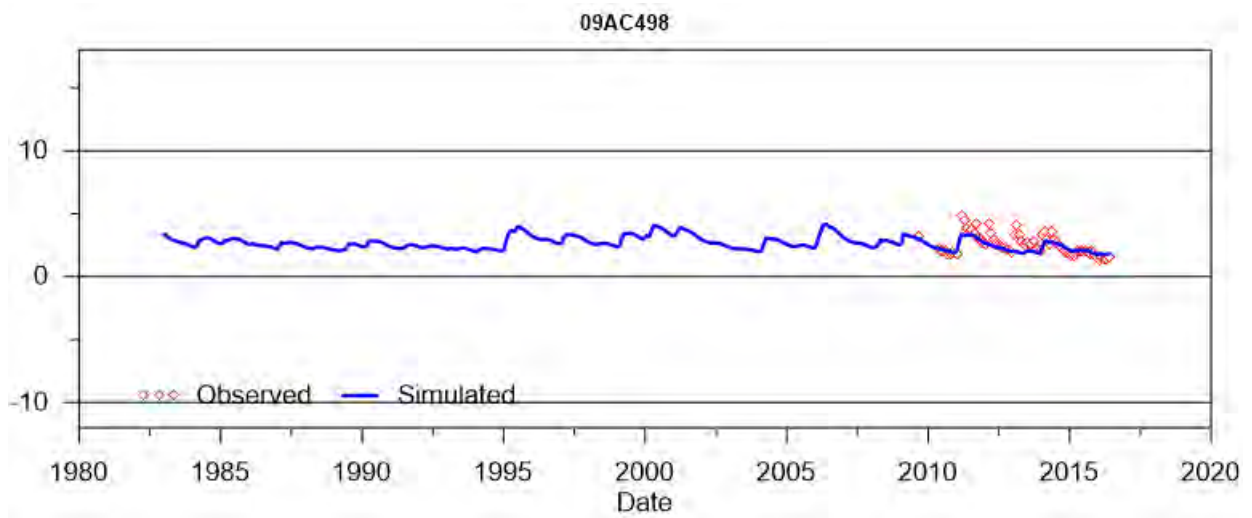
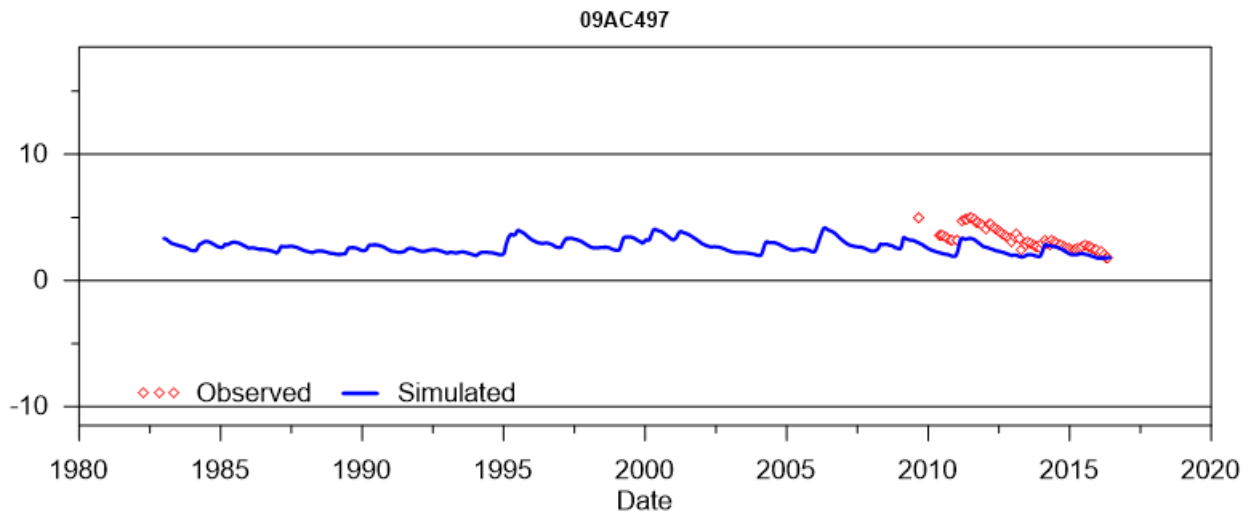
SINO EXPANSION LIFE OF MINE GROUNDWATER MODEL
APPENDIX E –Calibrated standpipe groundwater levels



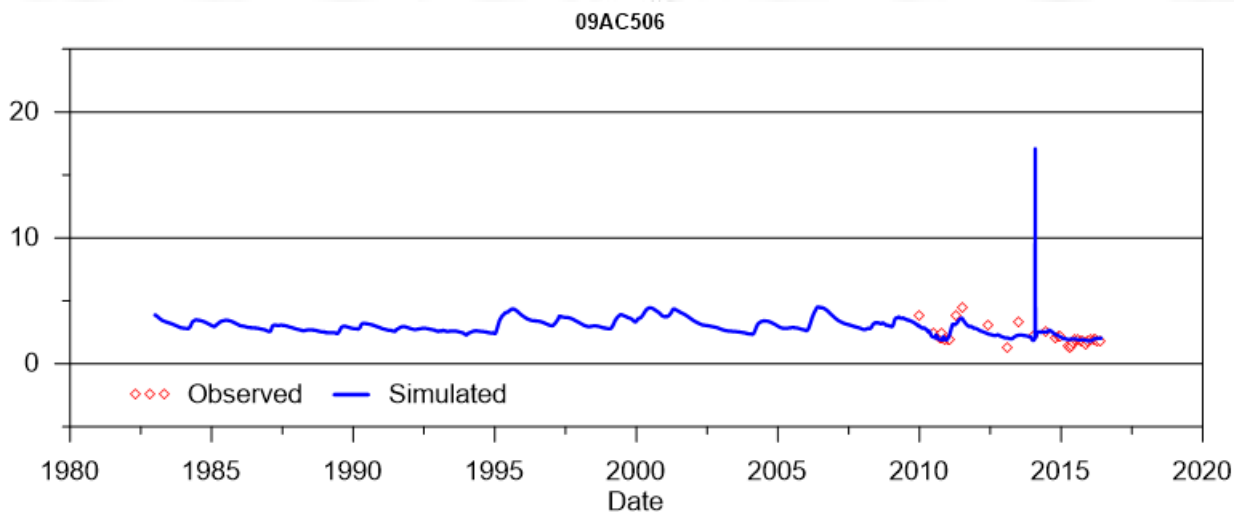
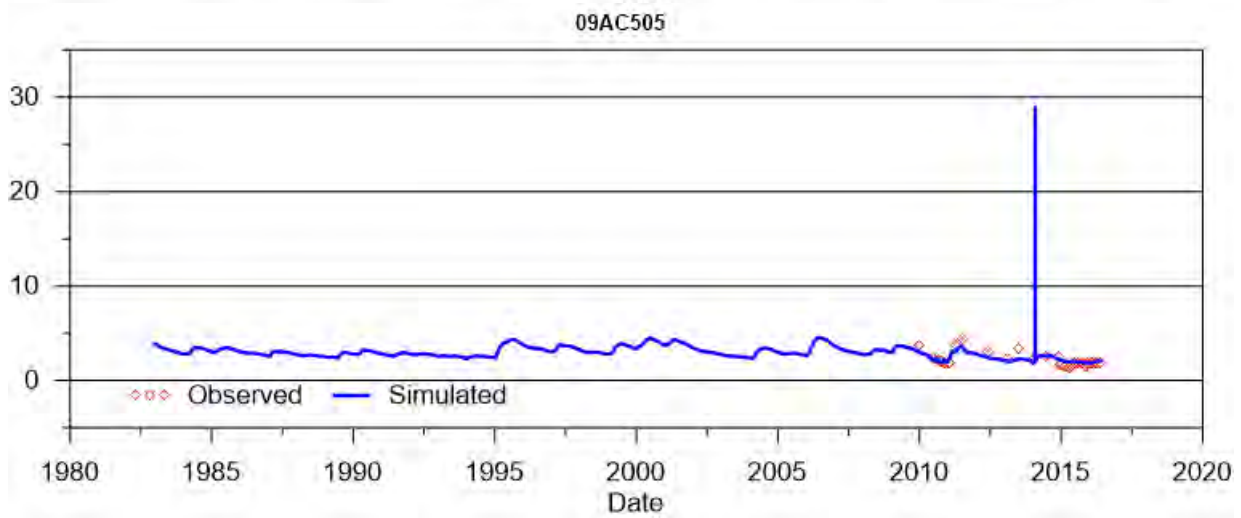
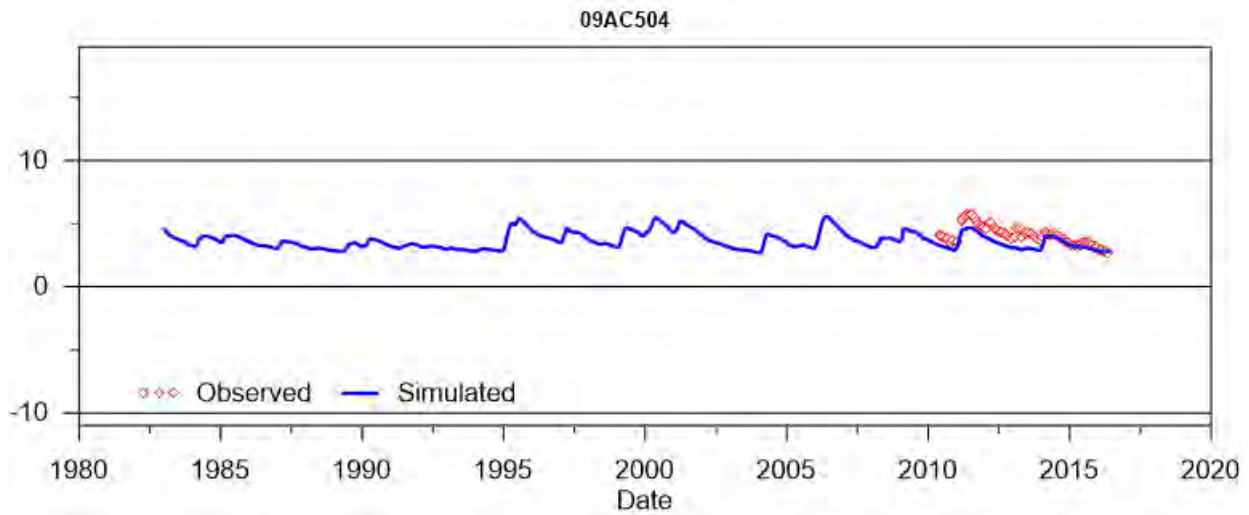
SINO EXPANSION LIFE OF MINE GROUNDWATER MODEL
APPENDIX E –Calibrated standpipe groundwater levels



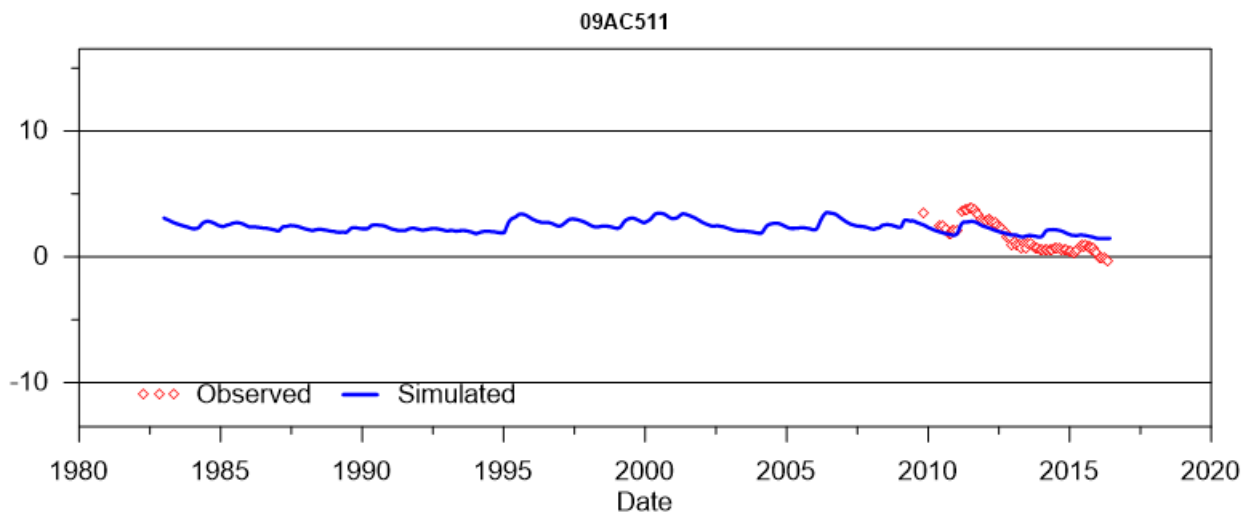
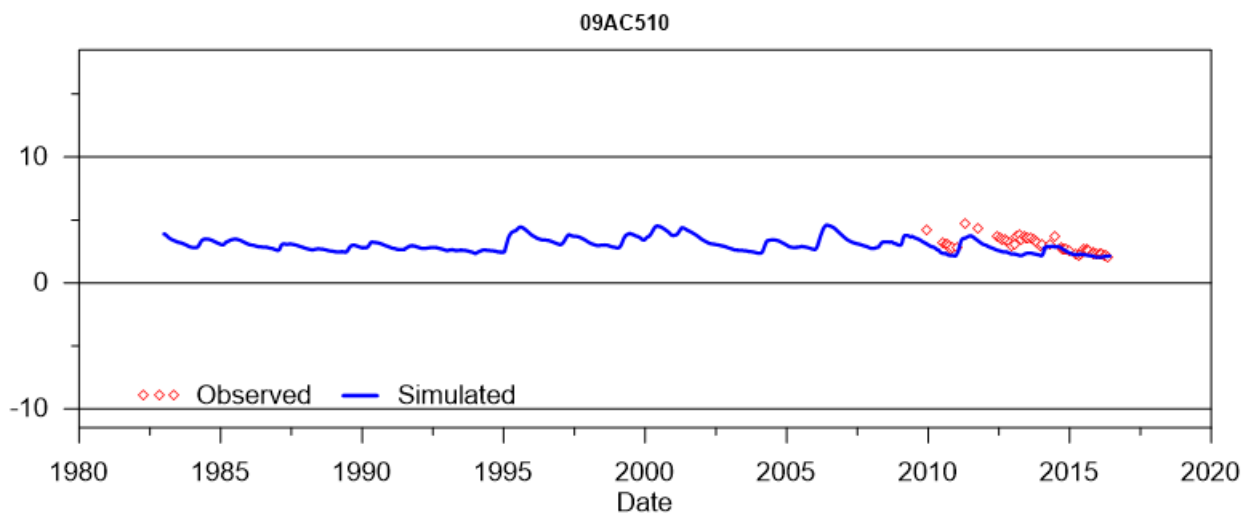
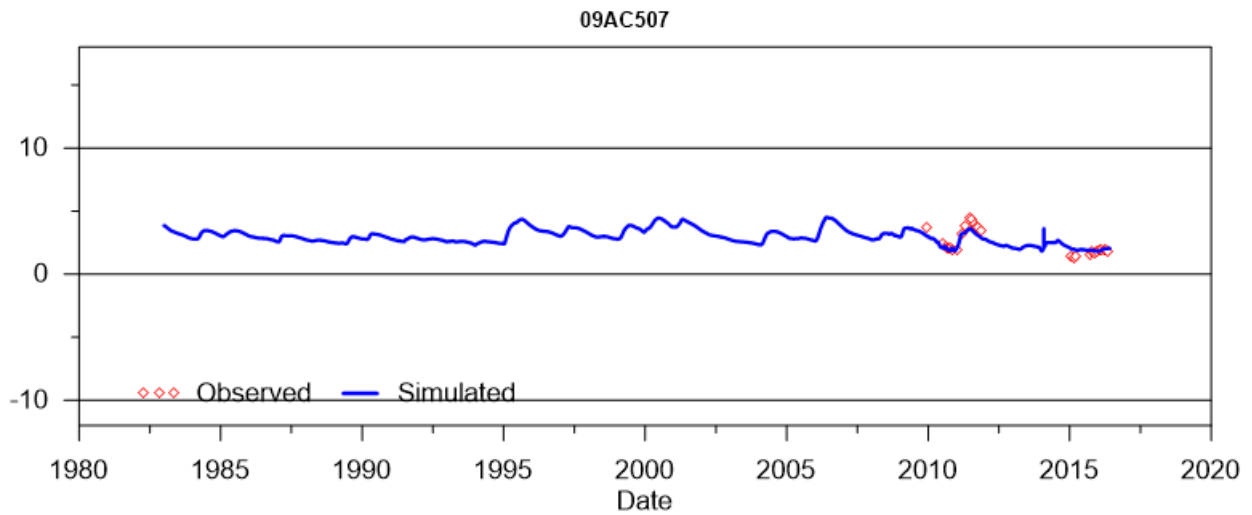
SINO EXPANSION LIFE OF MINE GROUNDWATER MODEL
APPENDIX E –Calibrated standpipe groundwater levels



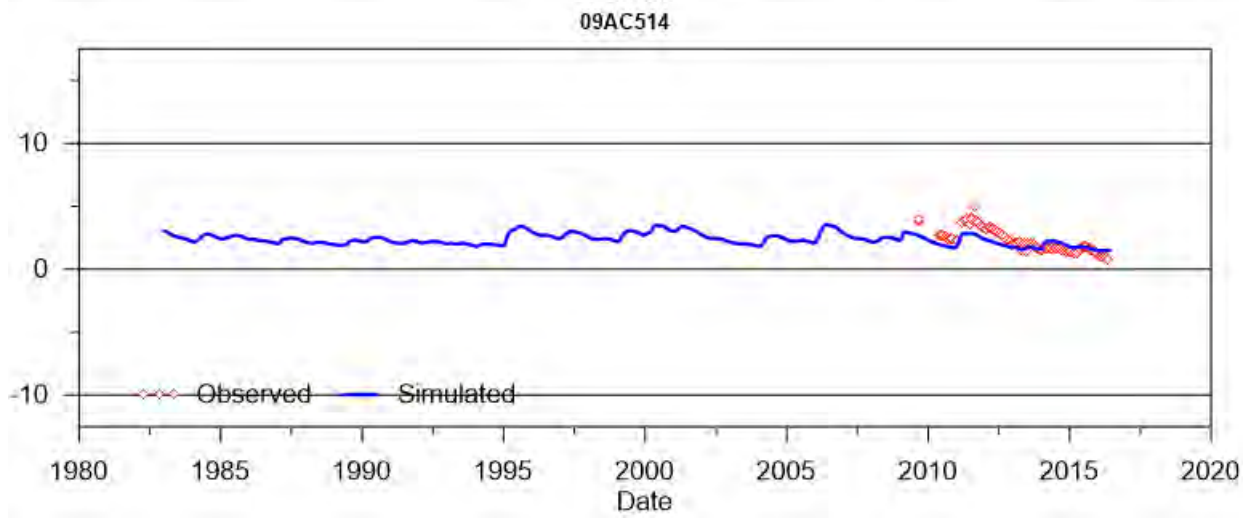
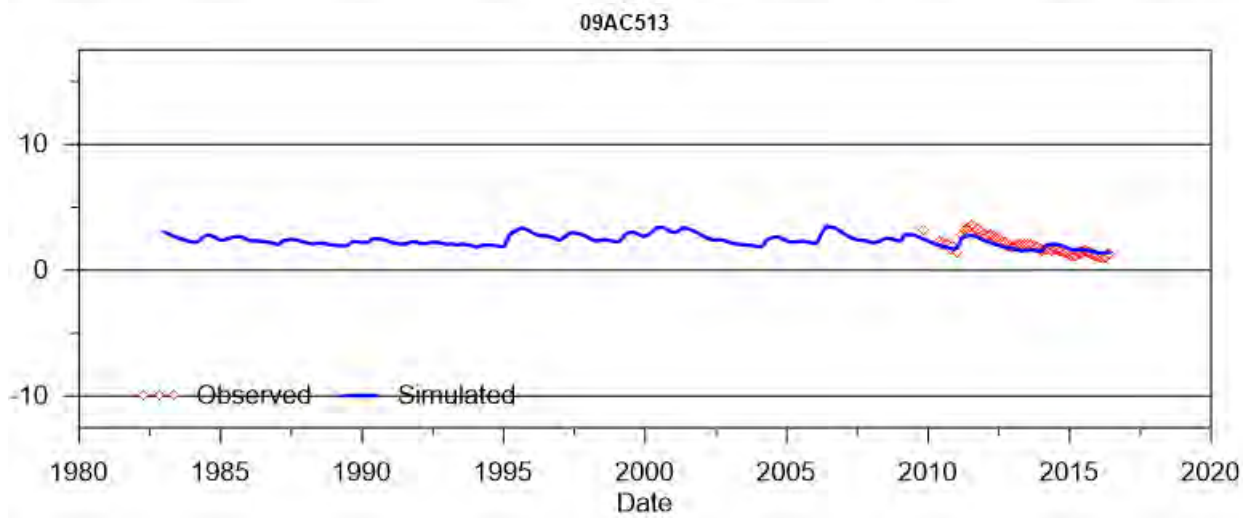
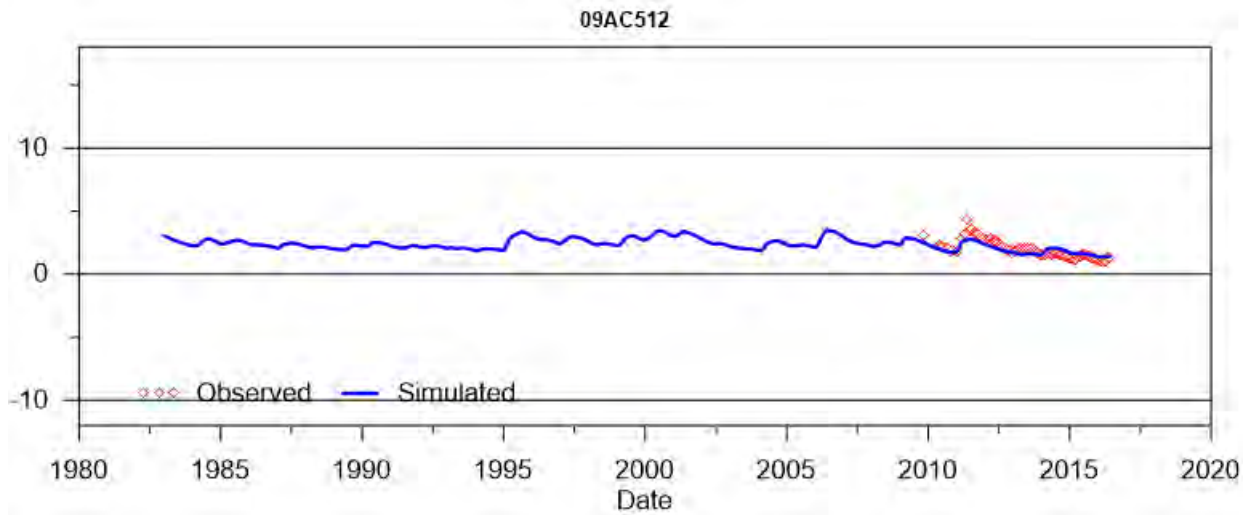
SINO EXPANSION LIFE OF MINE GROUNDWATER MODEL
APPENDIX E –Calibrated standpipe groundwater levels



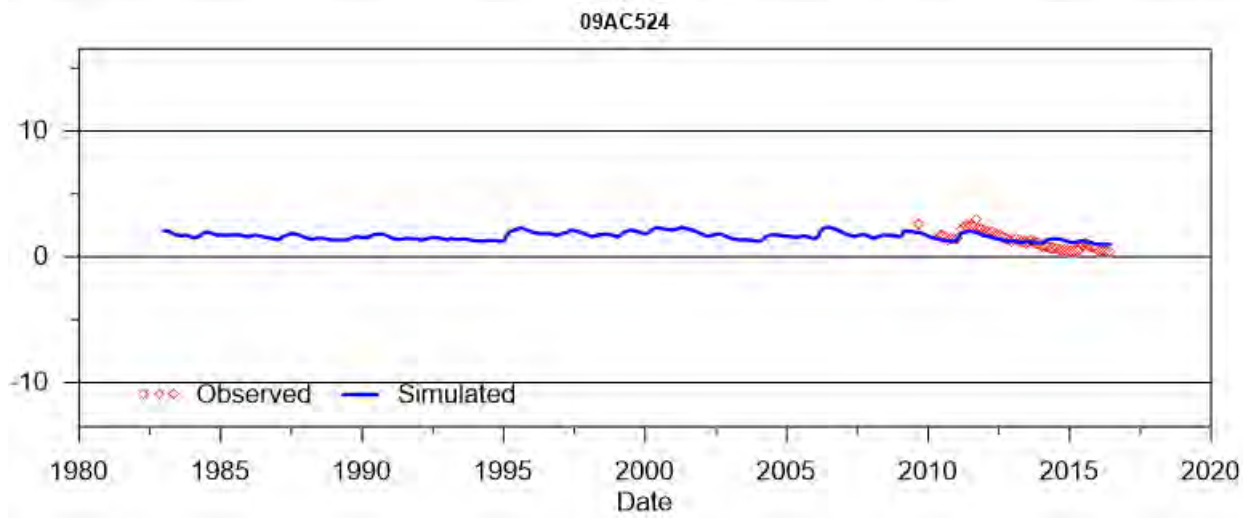
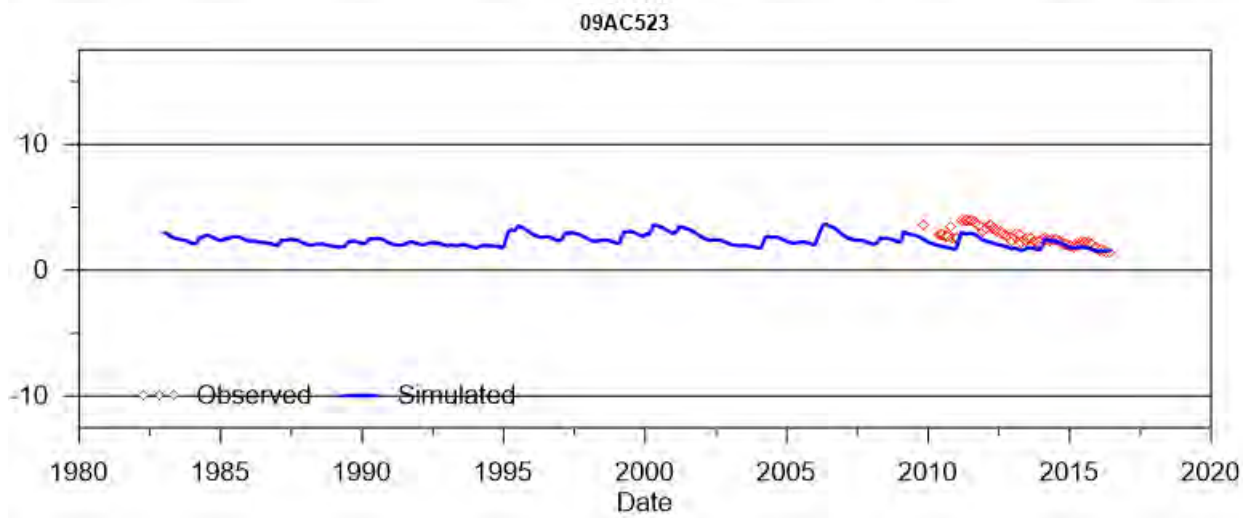
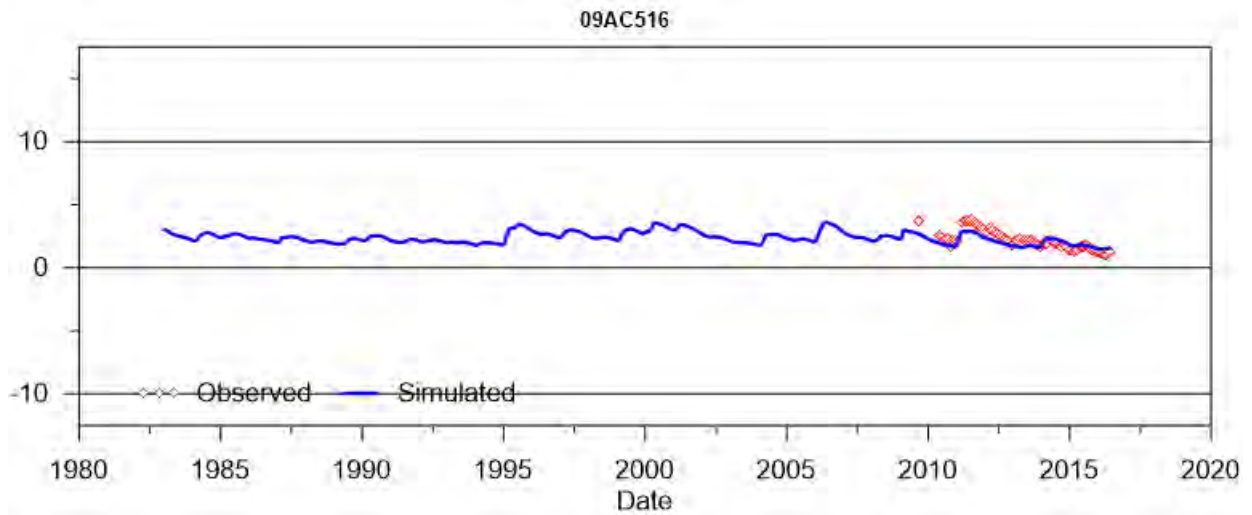
SINO EXPANSION LIFE OF MINE GROUNDWATER MODEL
APPENDIX E –Calibrated standpipe groundwater levels



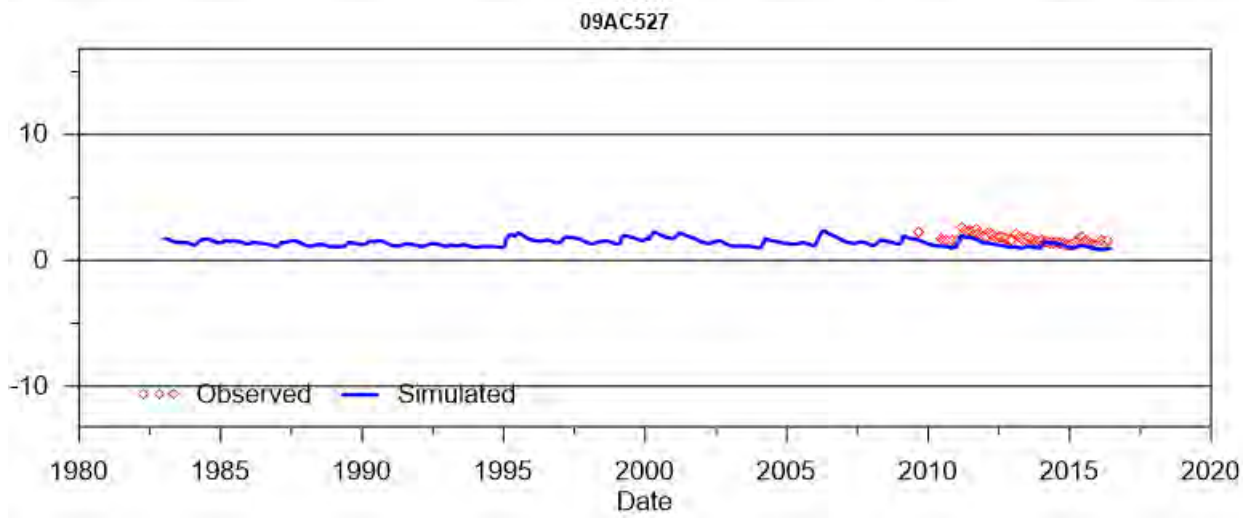
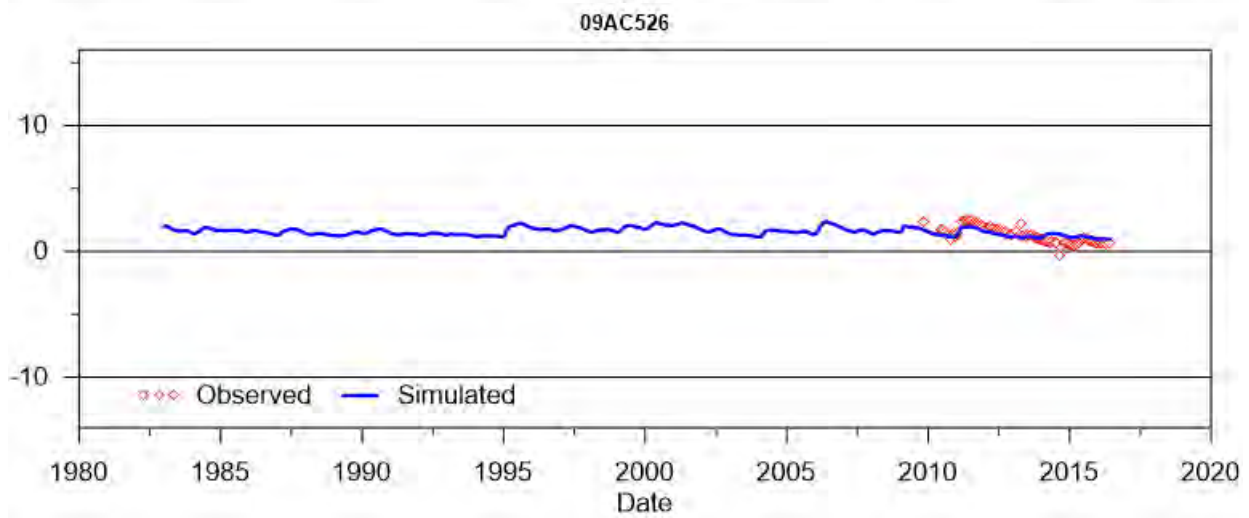
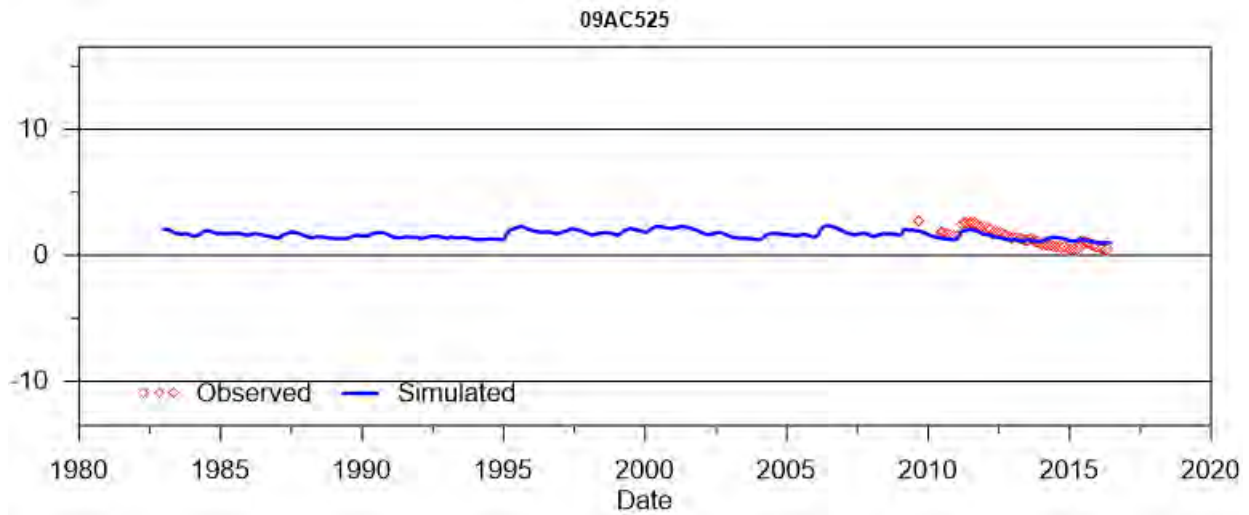
SINO EXPANSION LIFE OF MINE GROUNDWATER MODEL
APPENDIX E –Calibrated standpipe groundwater levels



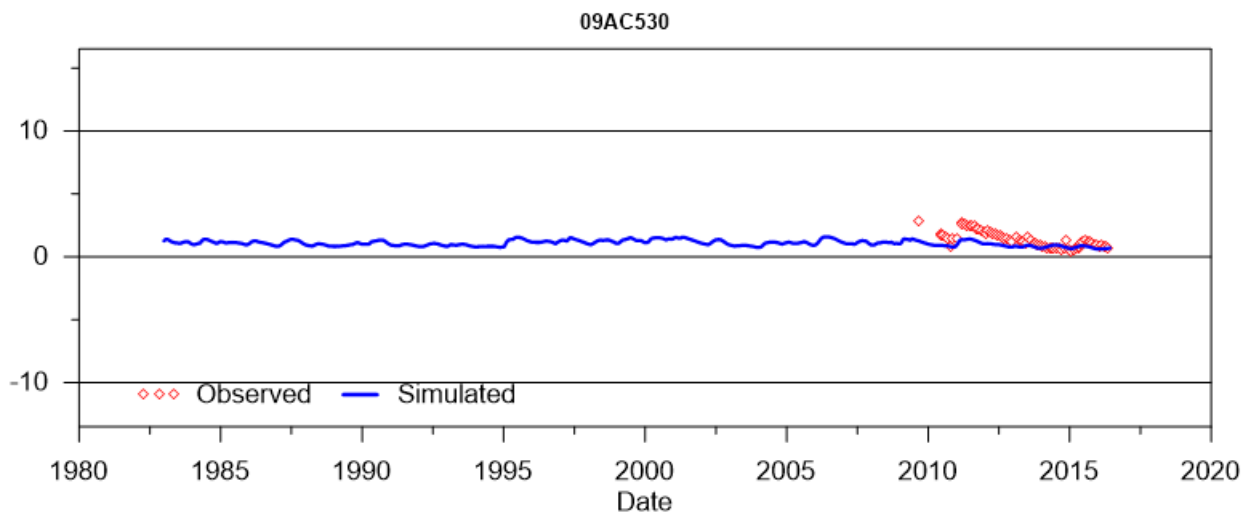
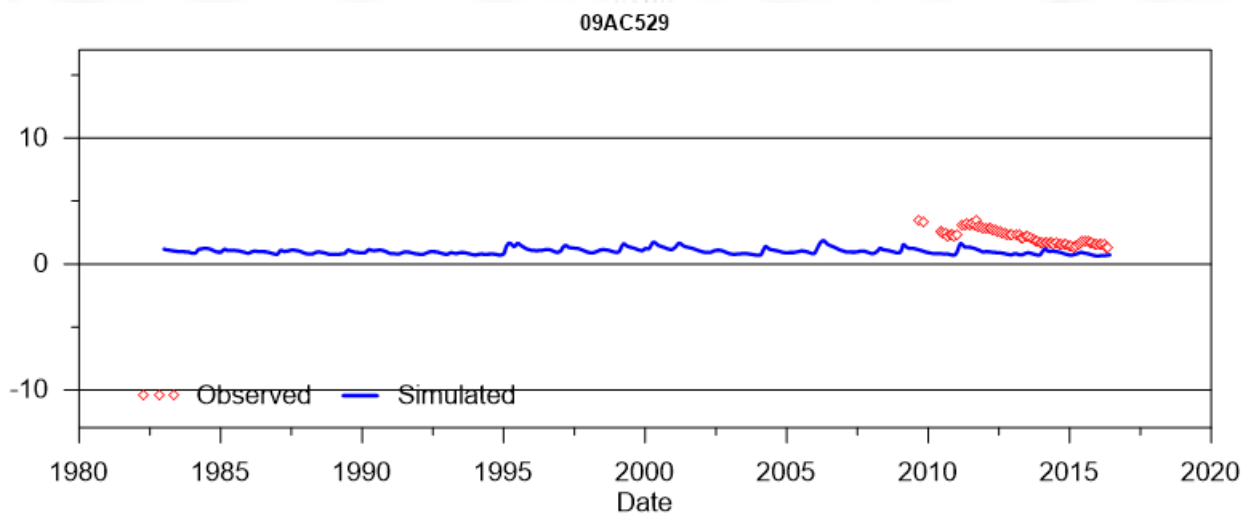
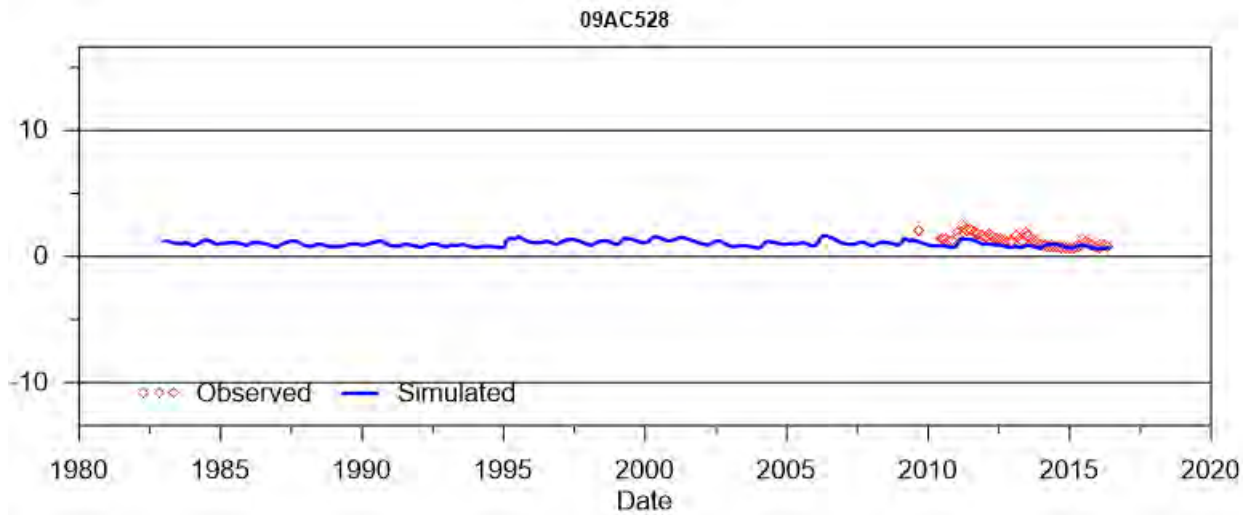
SINO EXPANSION LIFE OF MINE GROUNDWATER MODEL
APPENDIX E –Calibrated standpipe groundwater levels



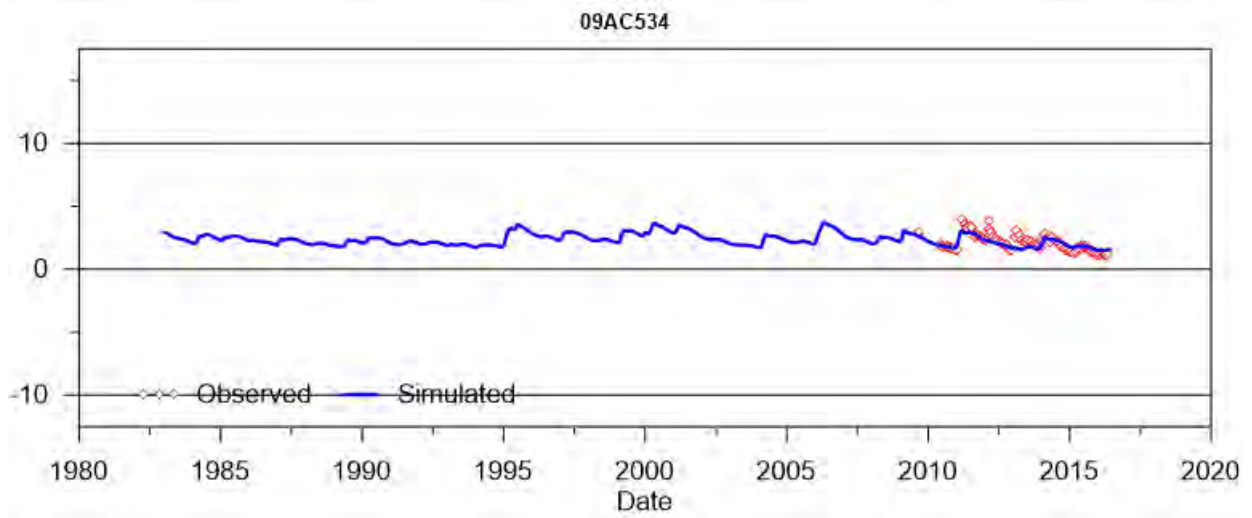
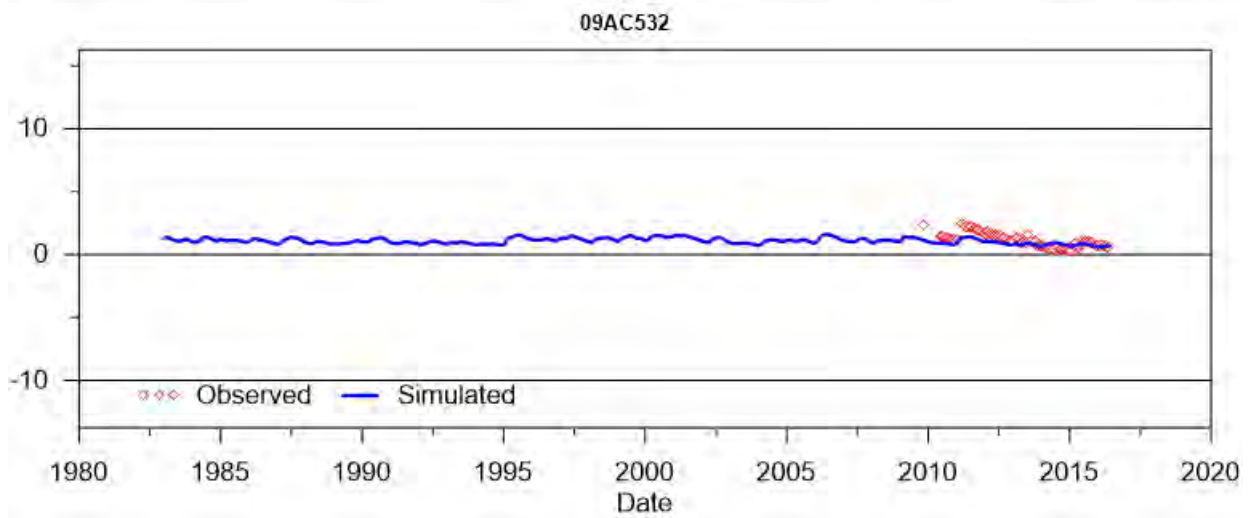
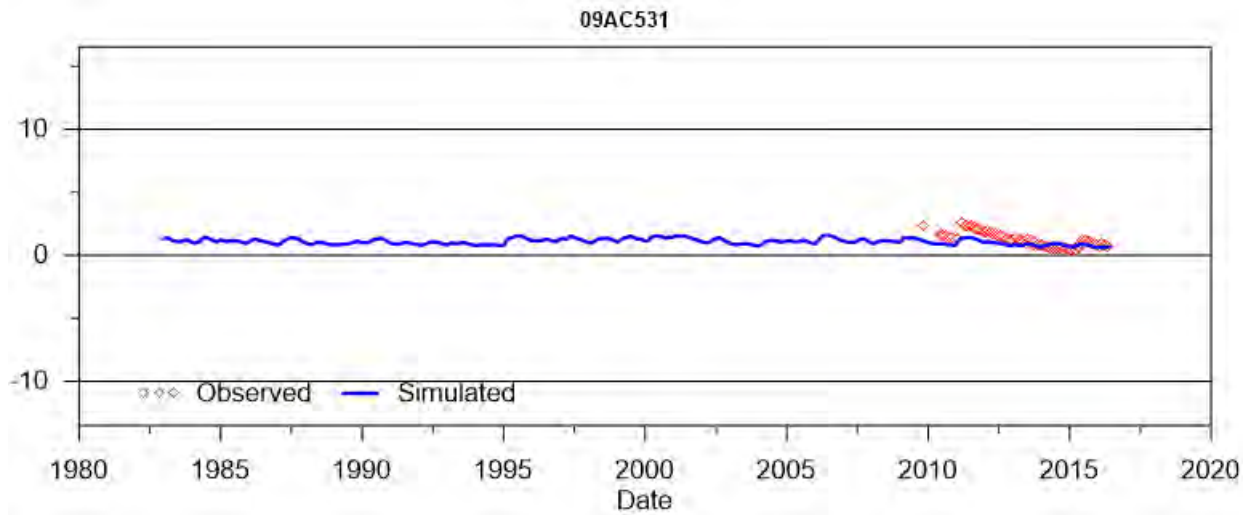
SINO EXPANSION LIFE OF MINE GROUNDWATER MODEL
APPENDIX E –Calibrated standpipe groundwater levels



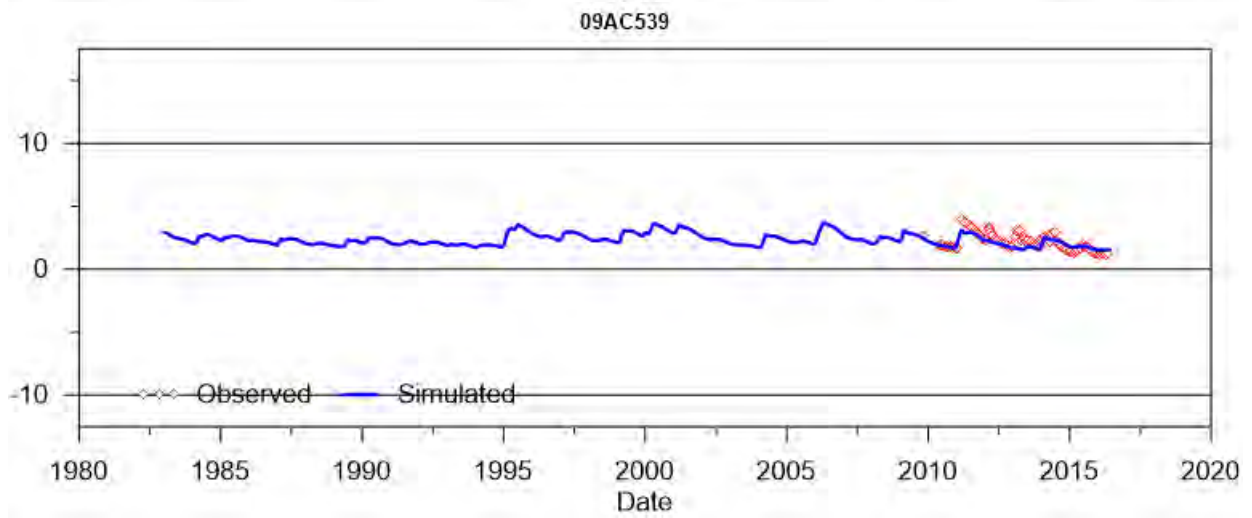
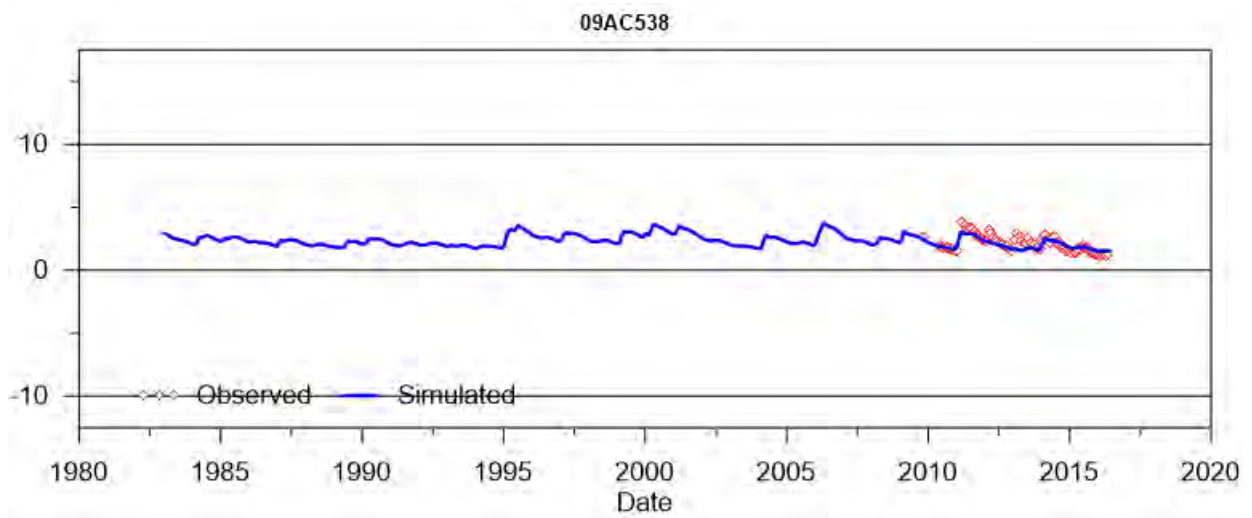
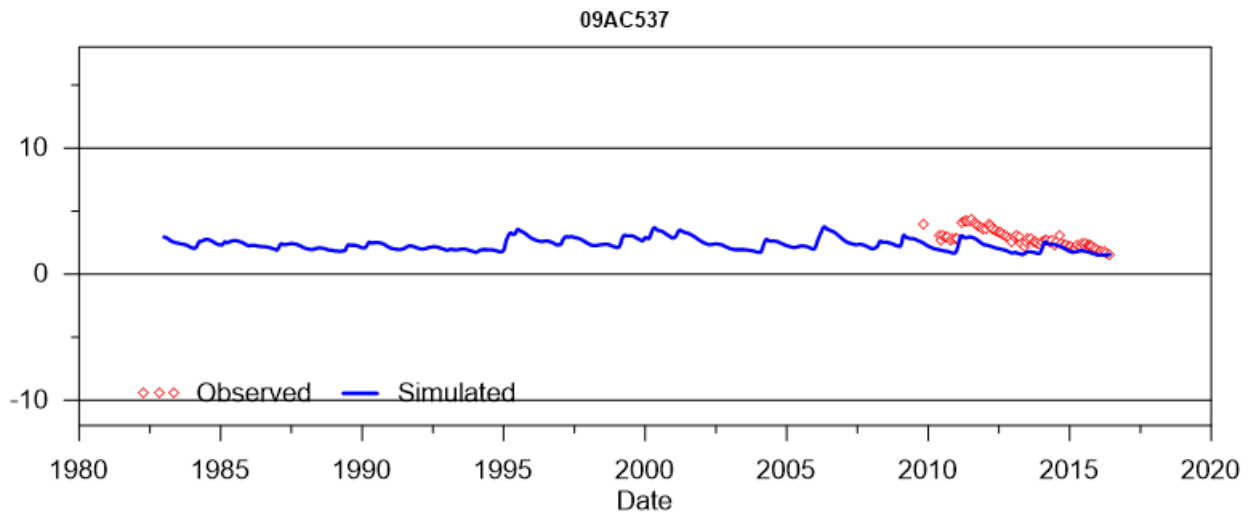
SINO EXPANSION LIFE OF MINE GROUNDWATER MODEL
APPENDIX E –Calibrated standpipe groundwater levels



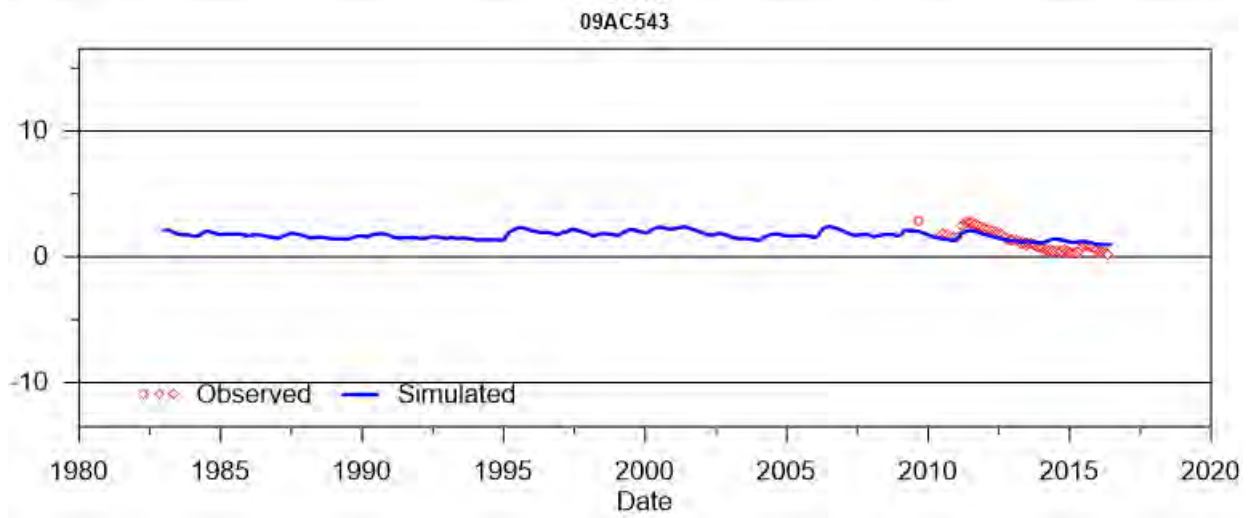
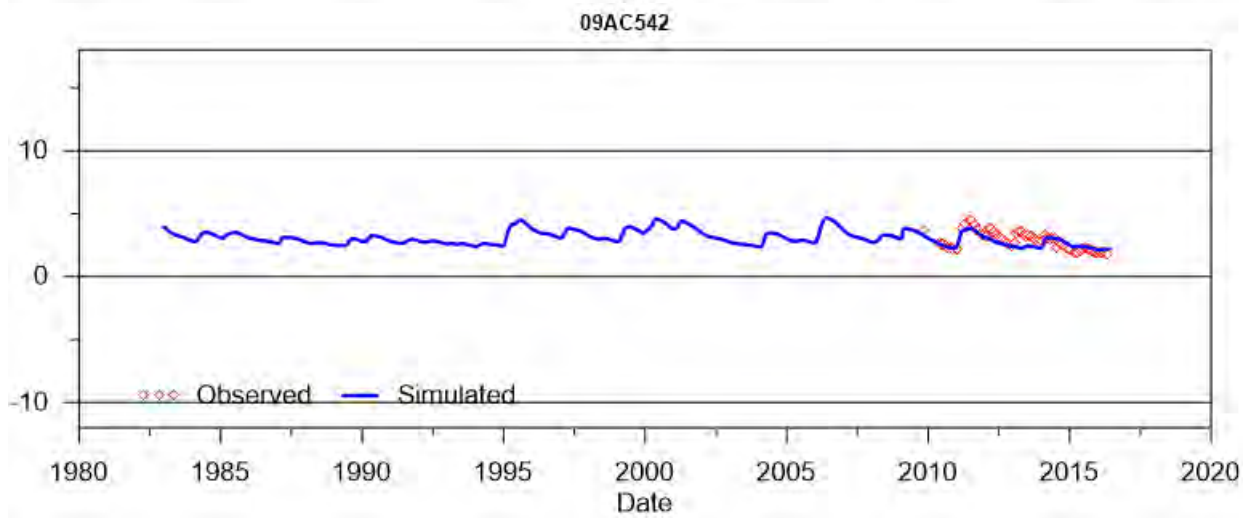
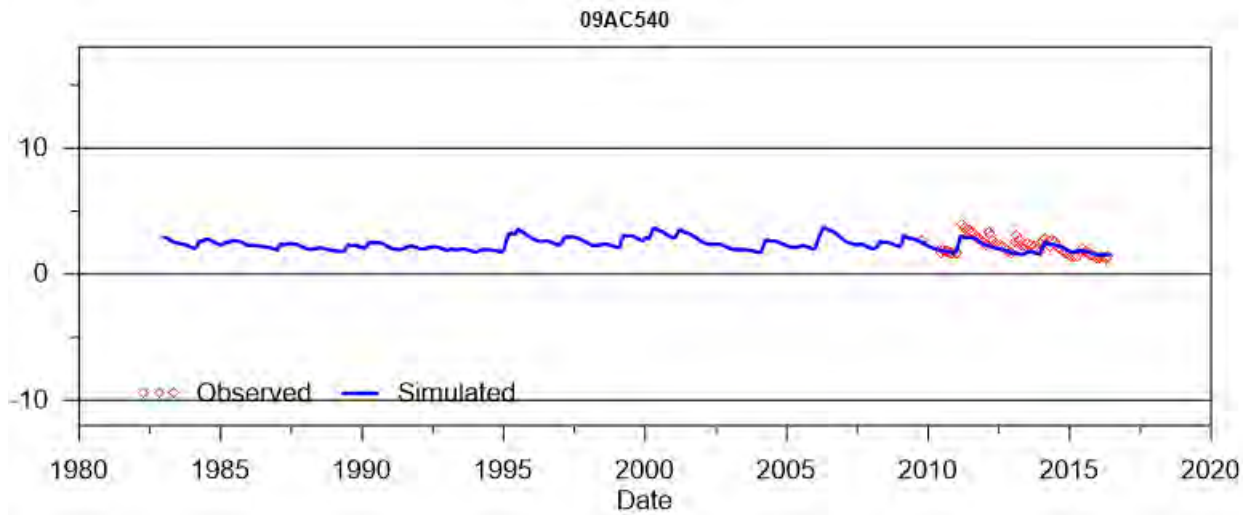
SINO EXPANSION LIFE OF MINE GROUNDWATER MODEL
APPENDIX E –Calibrated standpipe groundwater levels



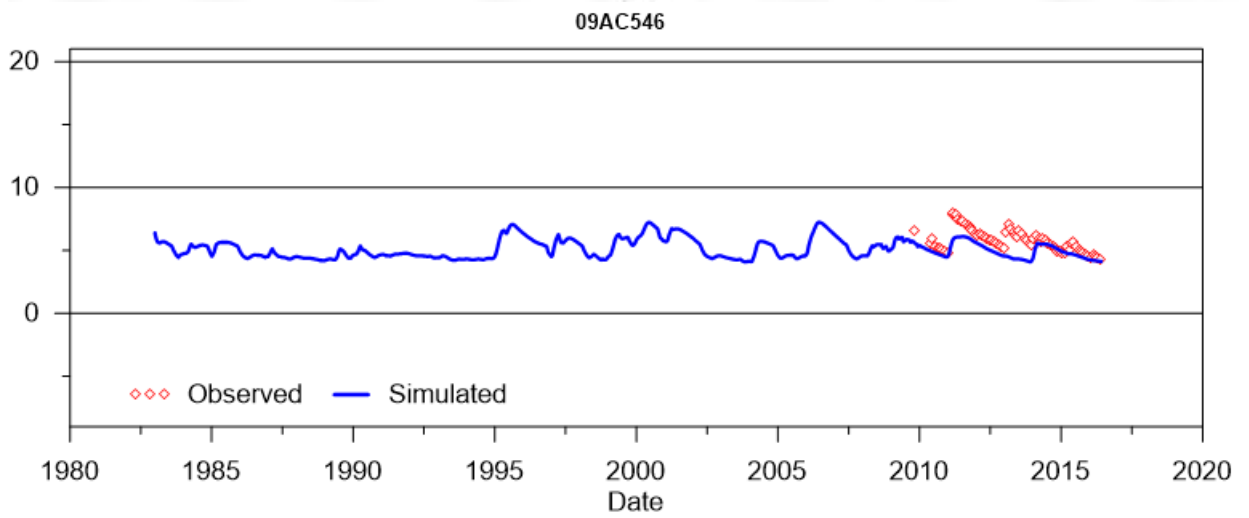
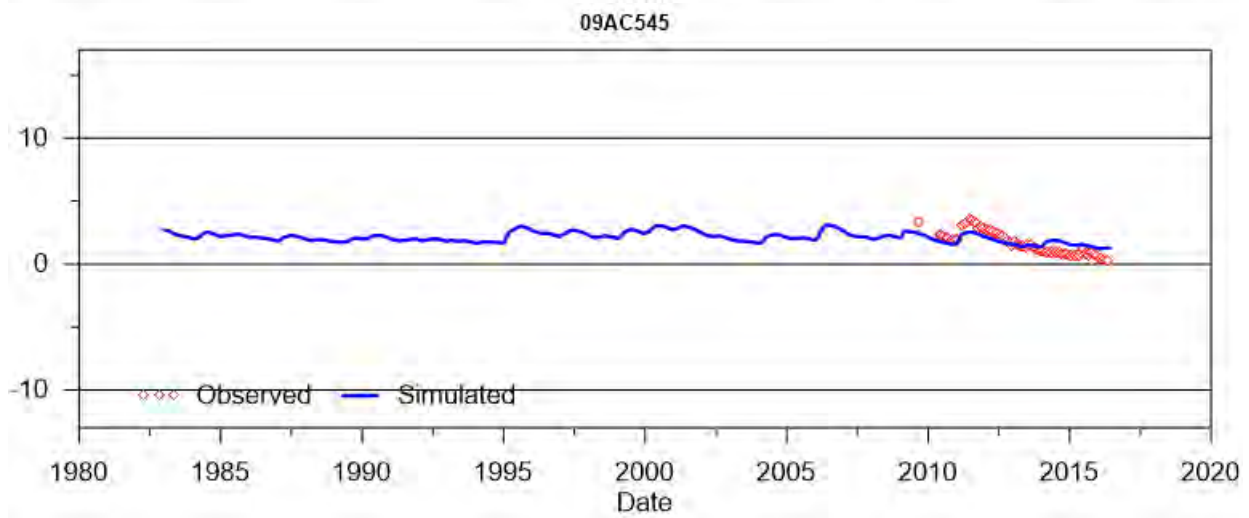
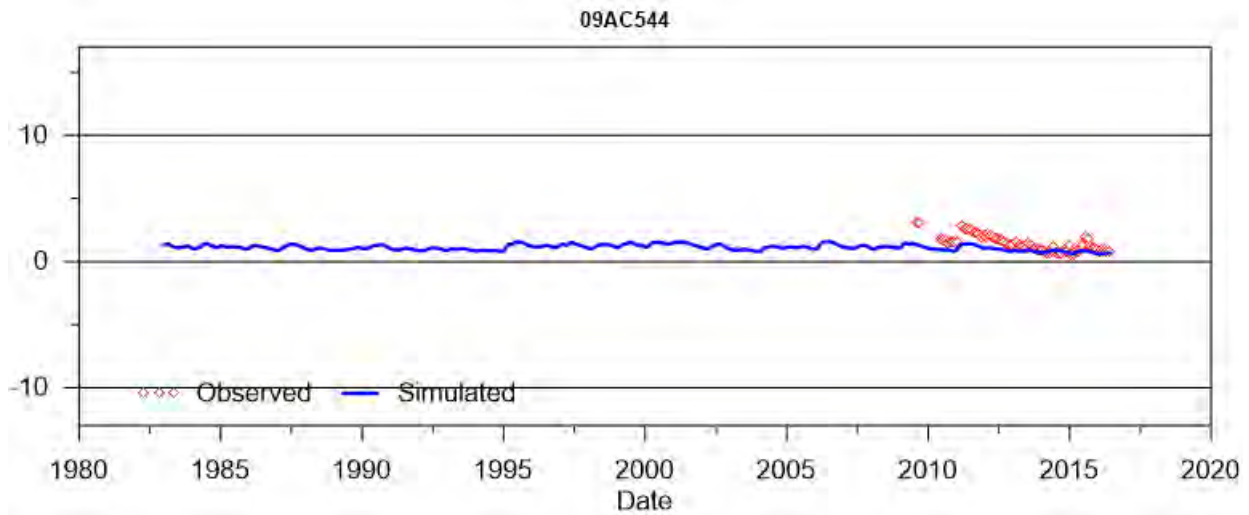
SINO EXPANSION LIFE OF MINE GROUNDWATER MODEL
APPENDIX E –Calibrated standpipe groundwater levels



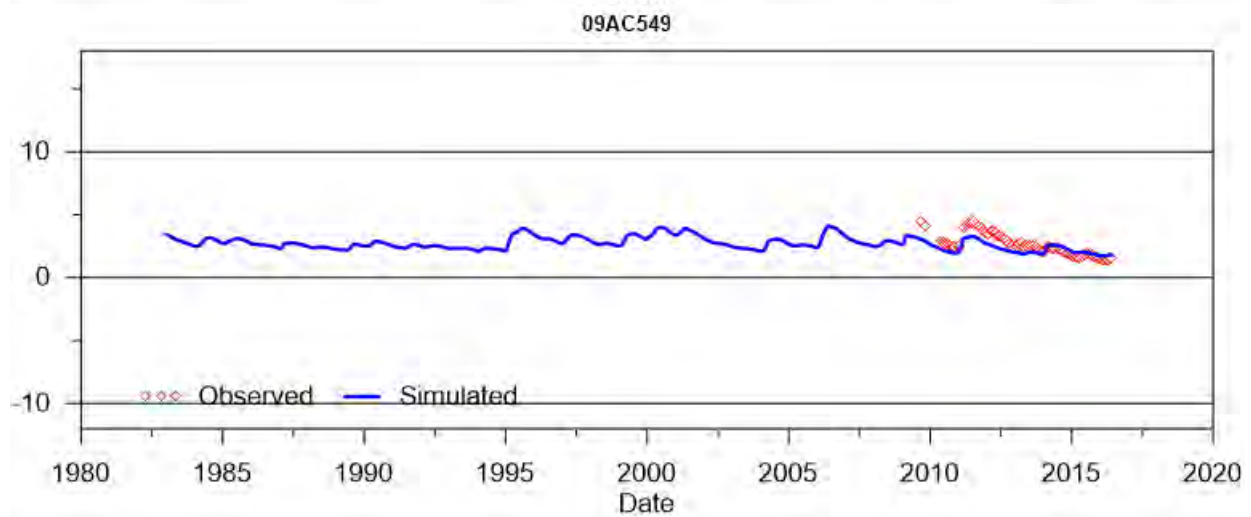
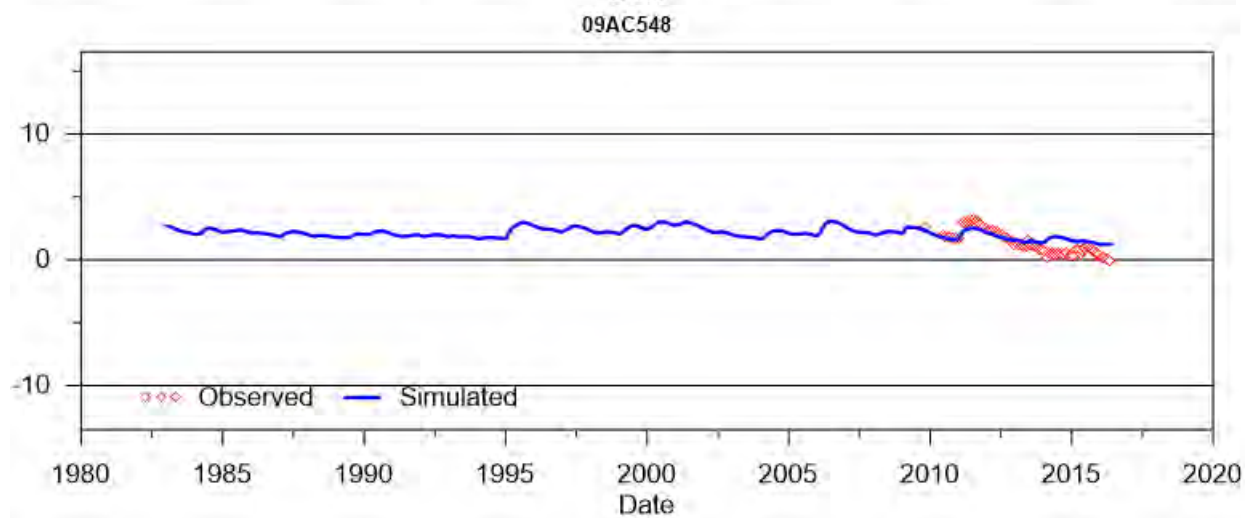
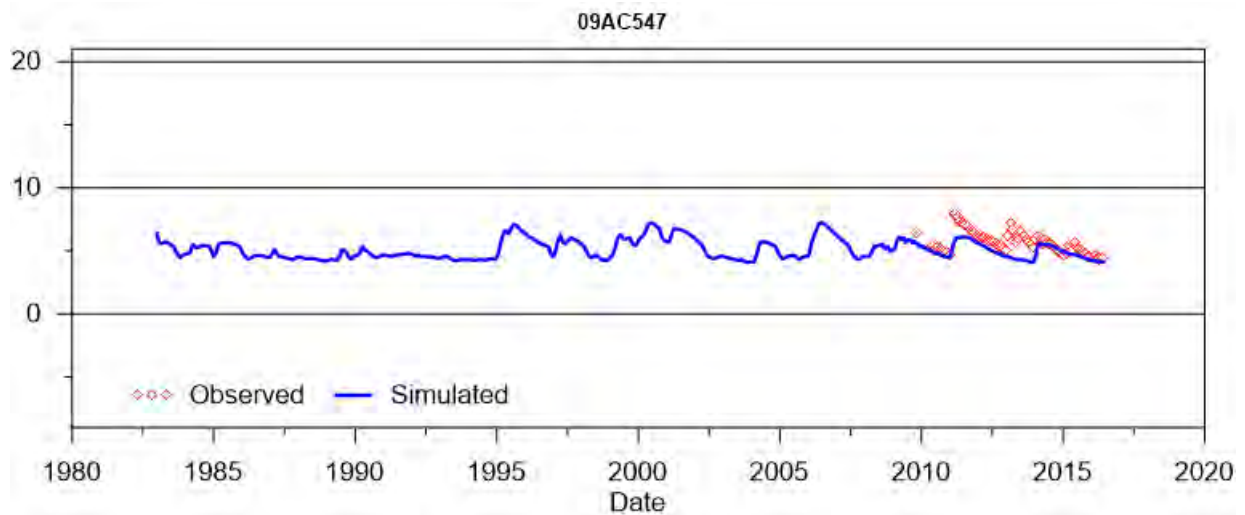
SINO EXPANSION LIFE OF MINE GROUNDWATER MODEL
APPENDIX E –Calibrated standpipe groundwater levels



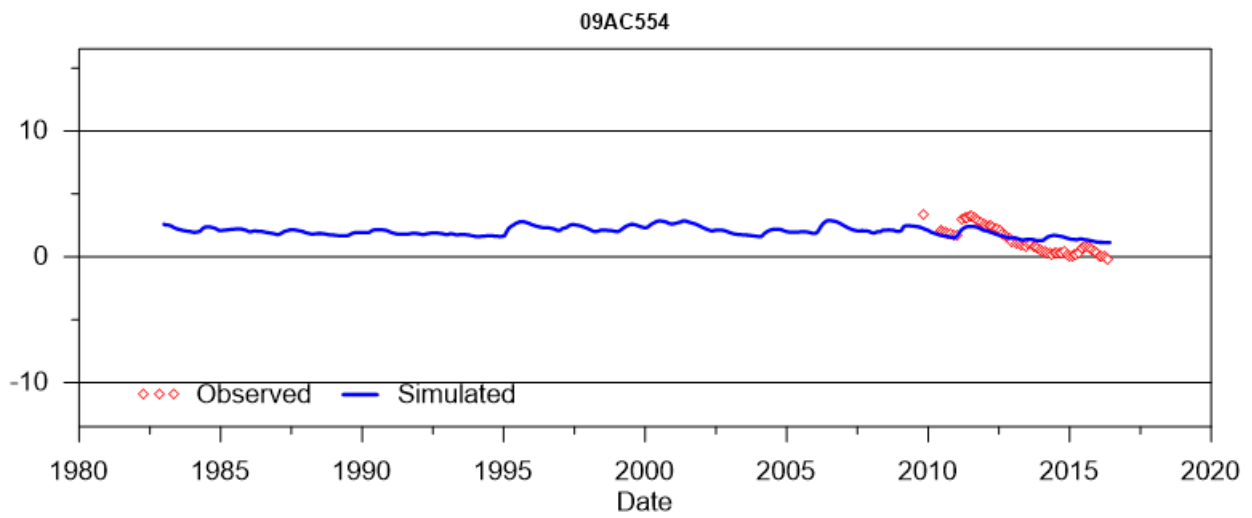
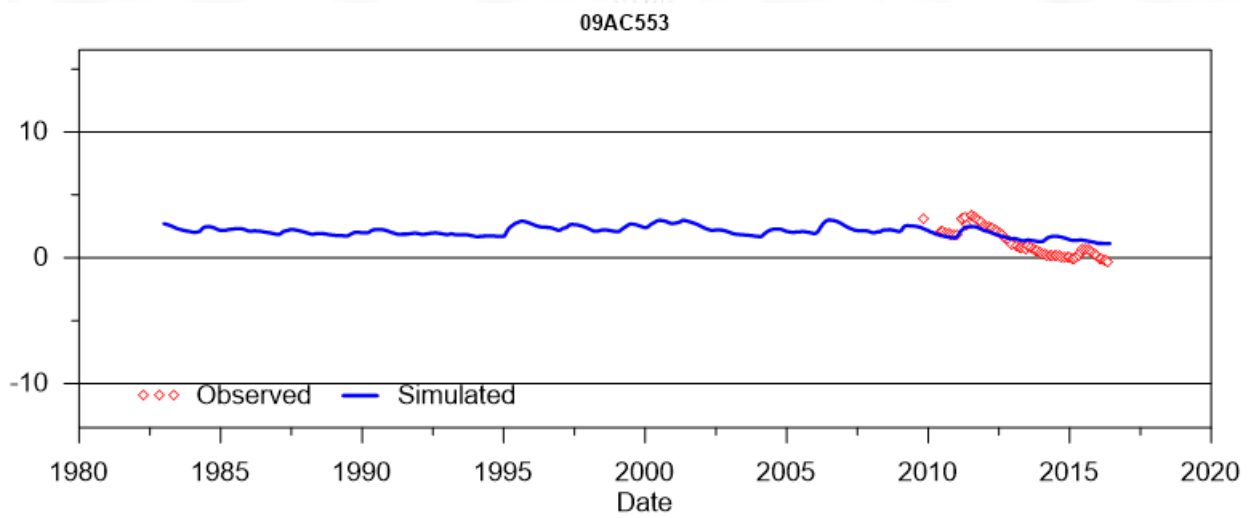
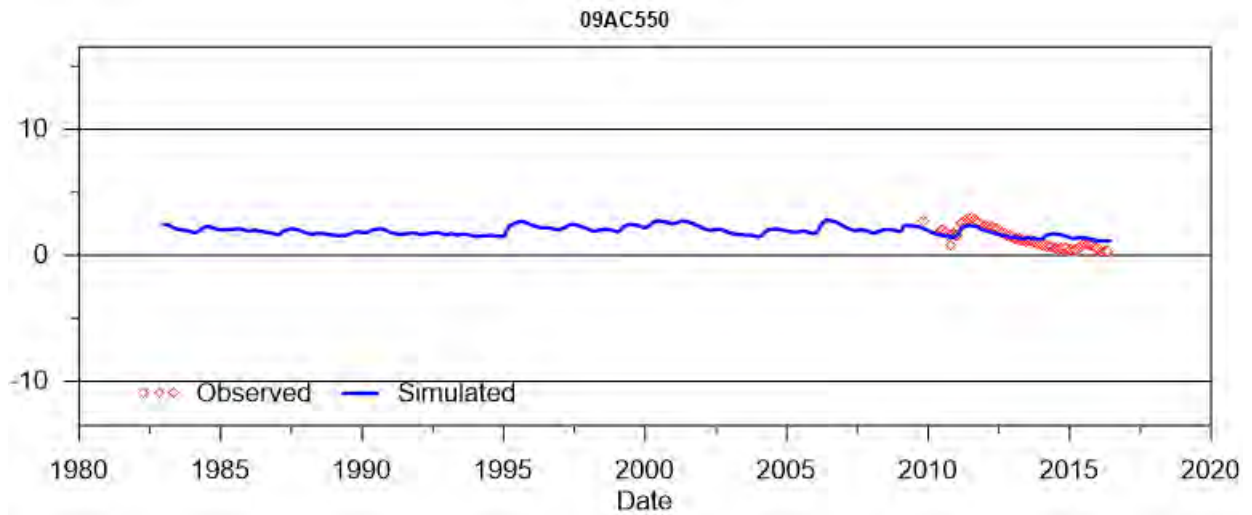
SINO EXPANSION LIFE OF MINE GROUNDWATER MODEL
APPENDIX E –Calibrated standpipe groundwater levels



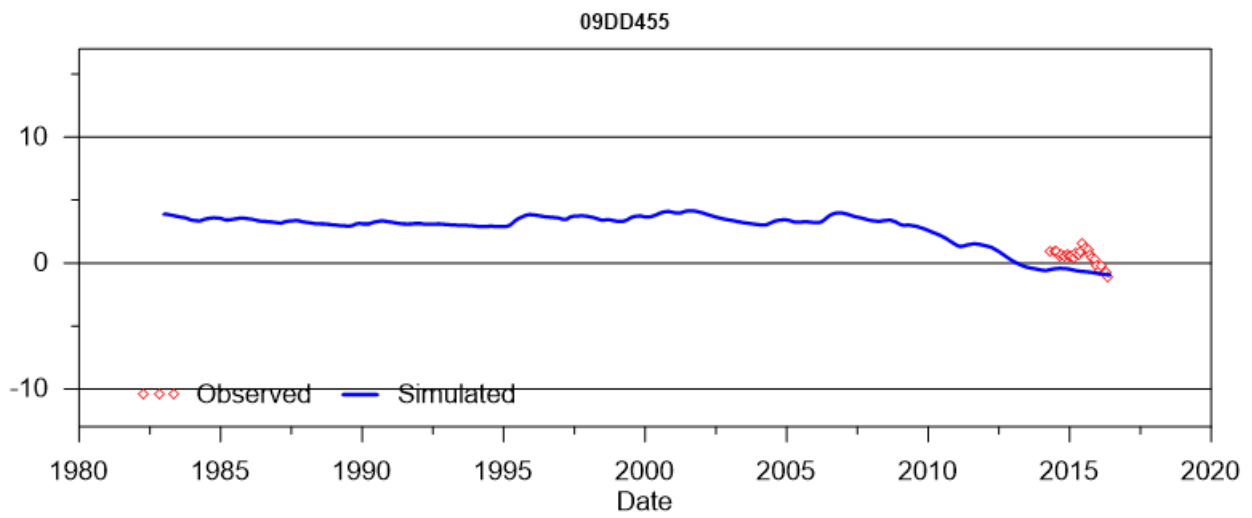
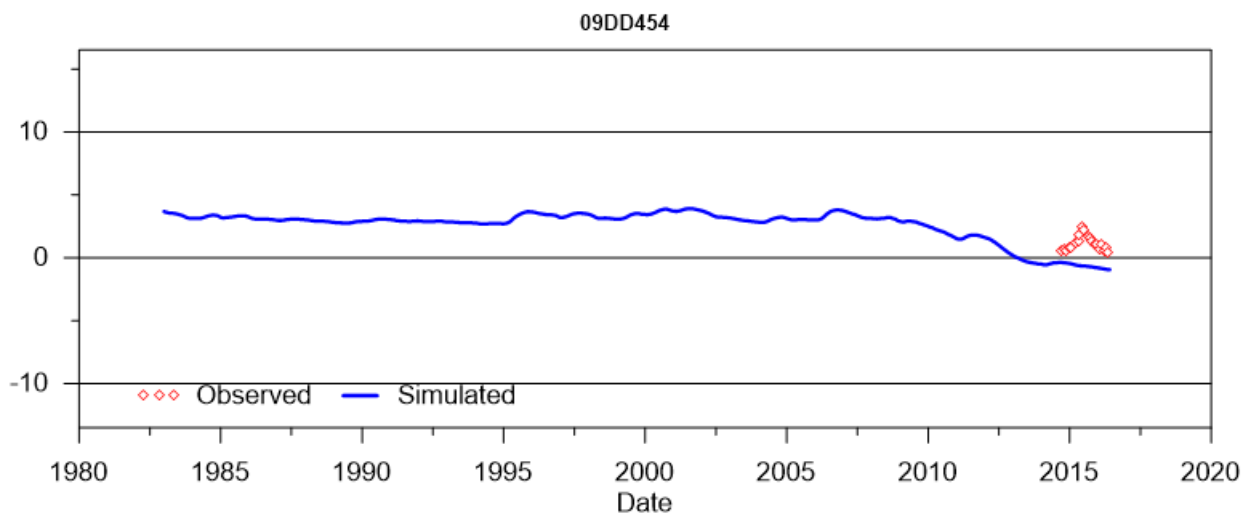
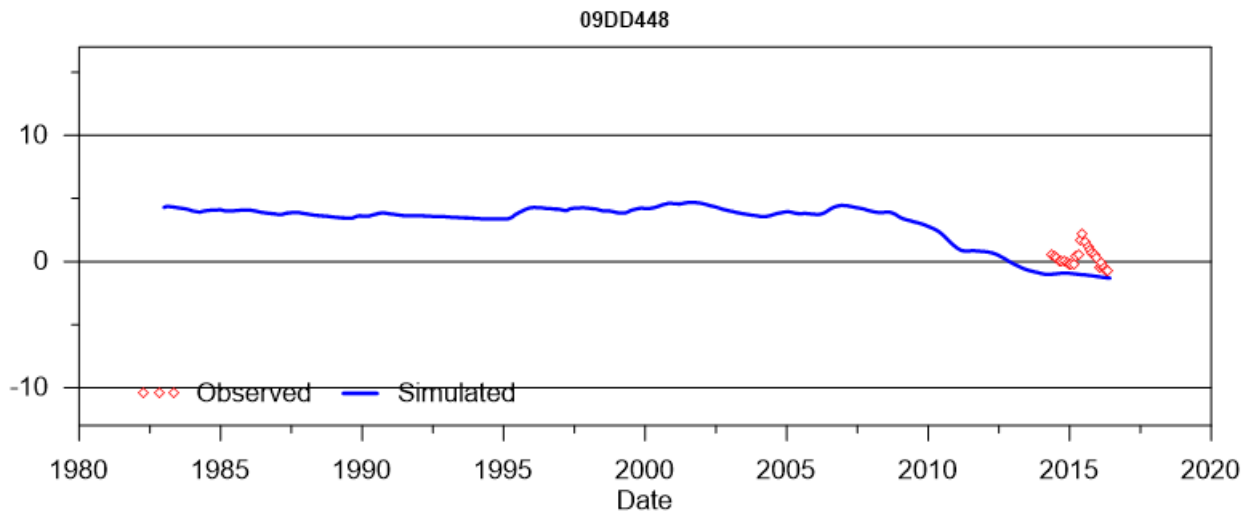
SINO EXPANSION LIFE OF MINE GROUNDWATER MODEL
APPENDIX E –Calibrated standpipe groundwater levels



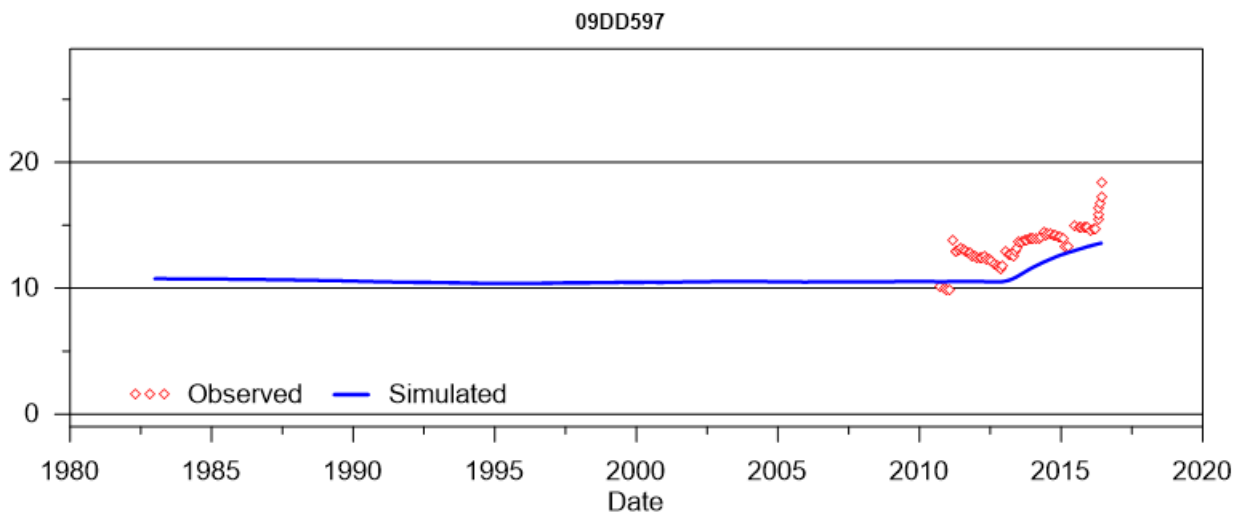
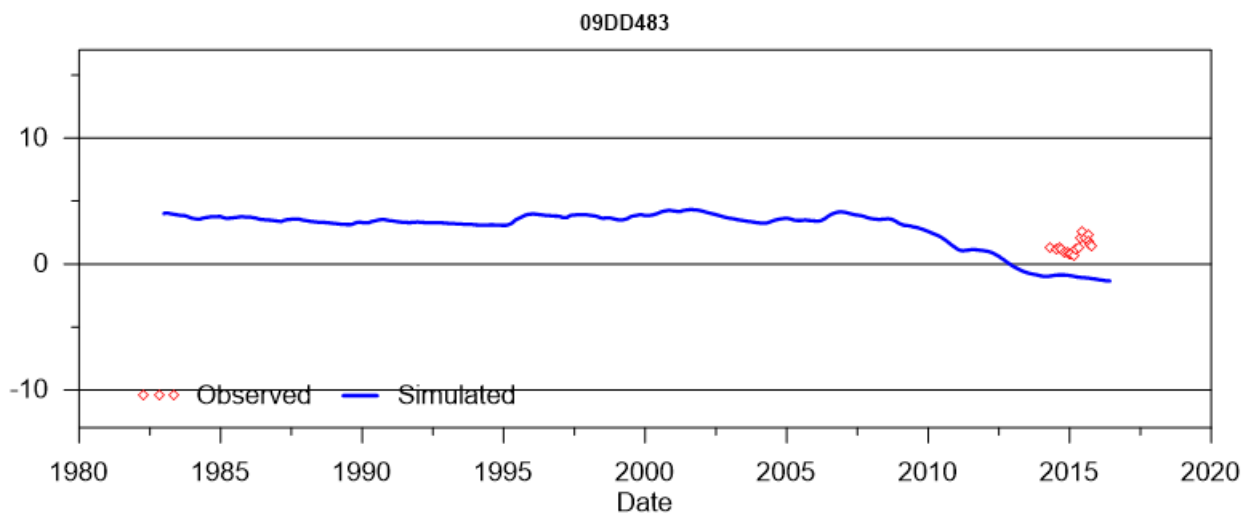
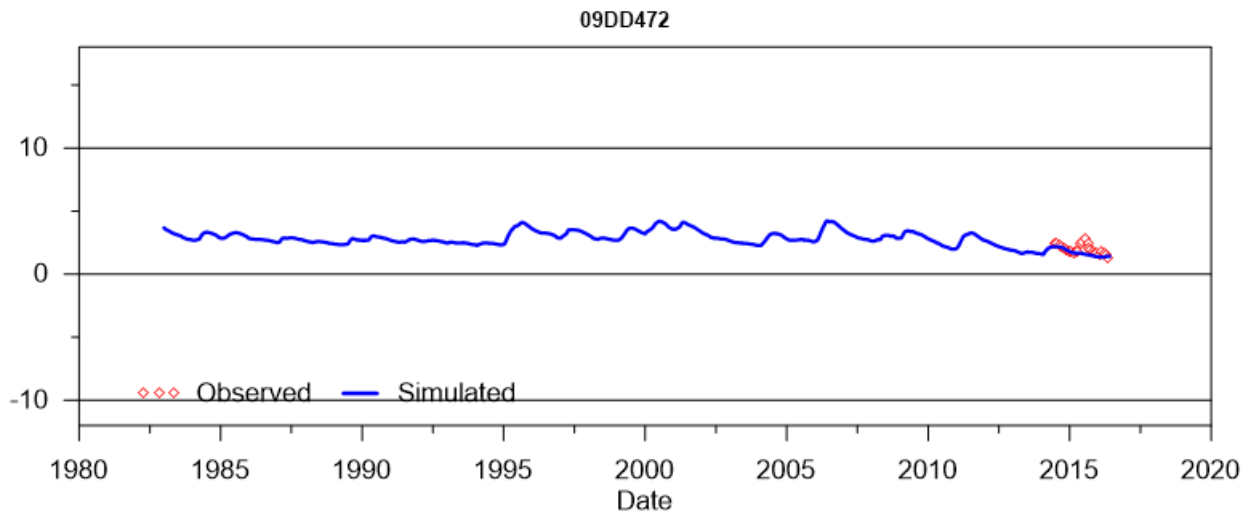
SINO EXPANSION LIFE OF MINE GROUNDWATER MODEL
APPENDIX E –Calibrated standpipe groundwater levels



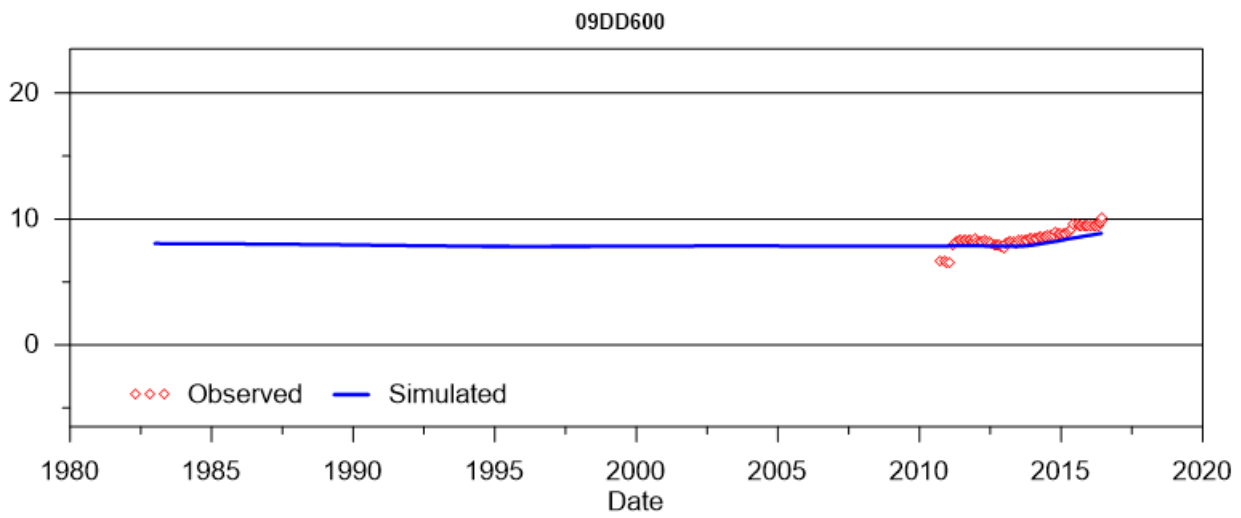
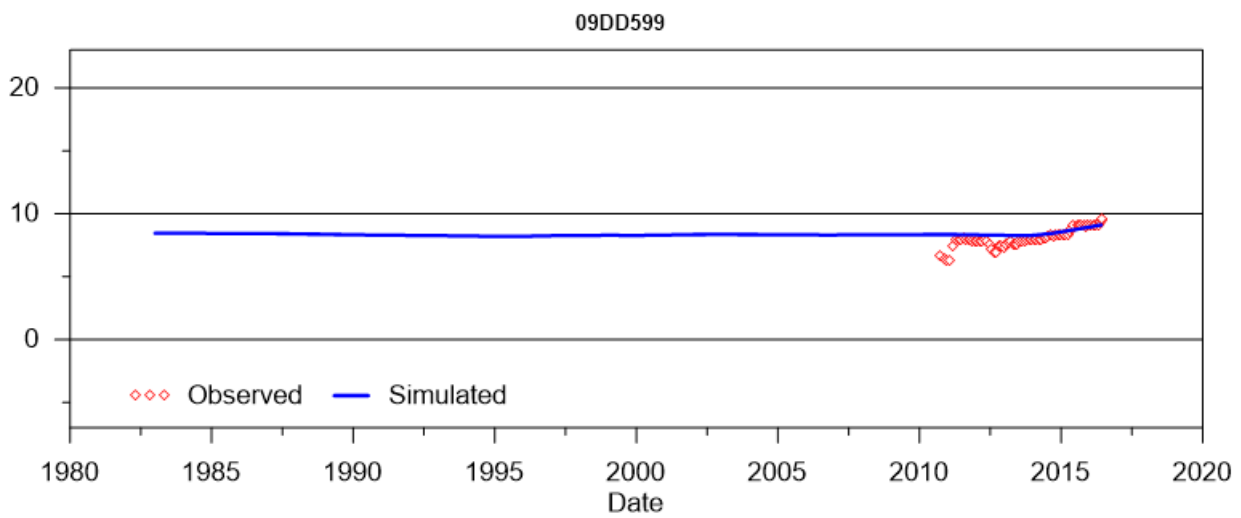
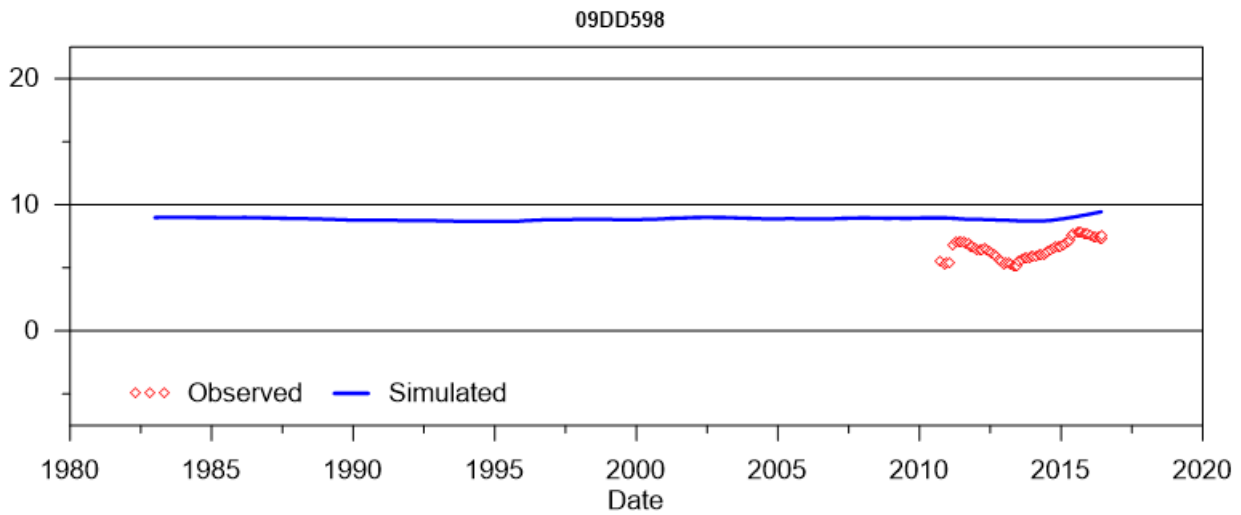
SINO EXPANSION LIFE OF MINE GROUNDWATER MODEL
APPENDIX E –Calibrated standpipe groundwater levels



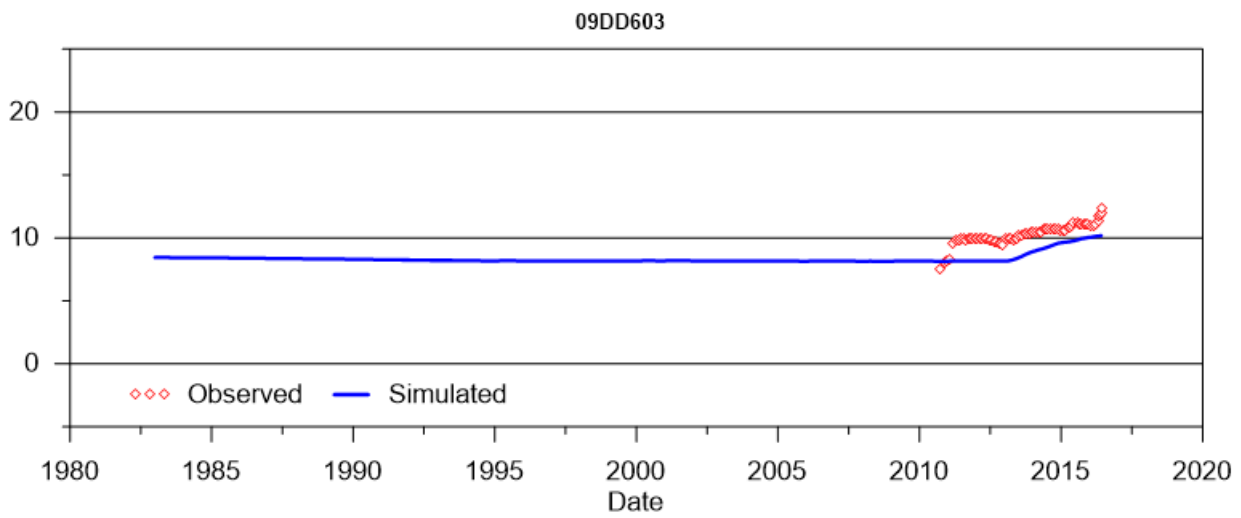
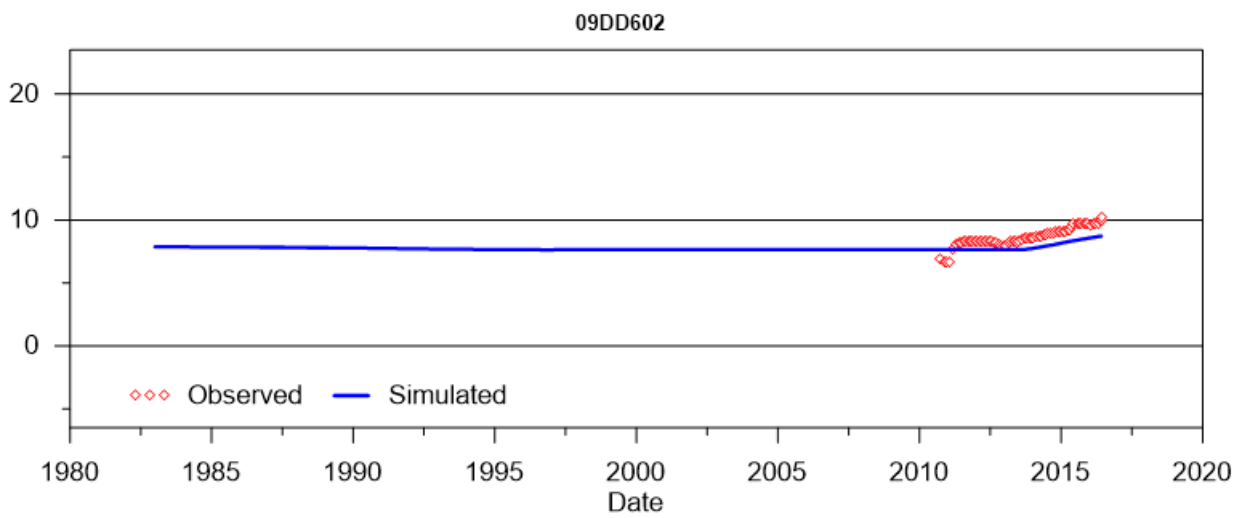
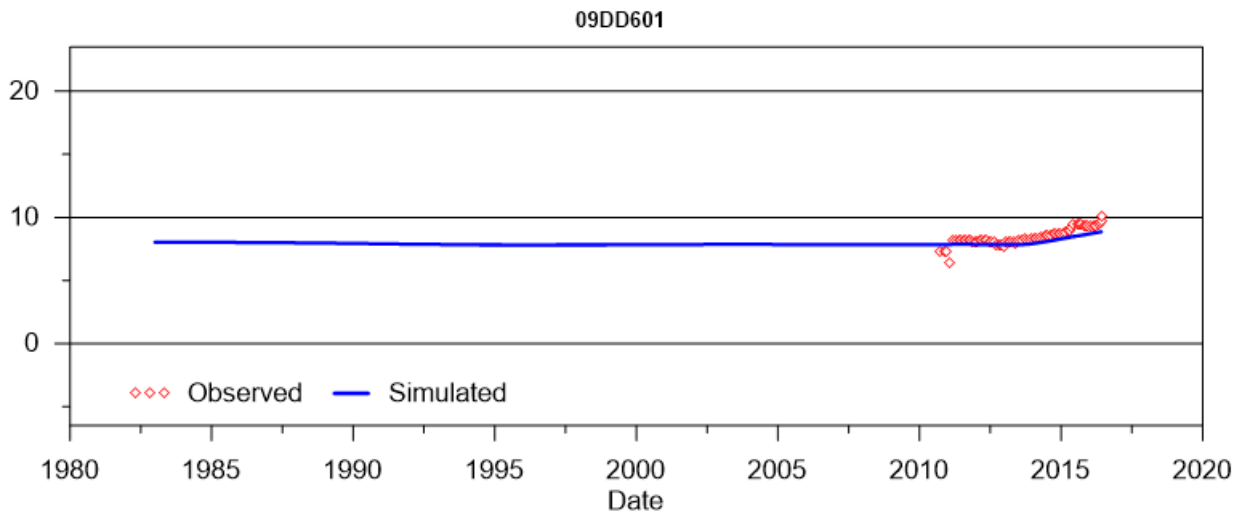
SINO EXPANSION LIFE OF MINE GROUNDWATER MODEL
APPENDIX E –Calibrated standpipe groundwater levels



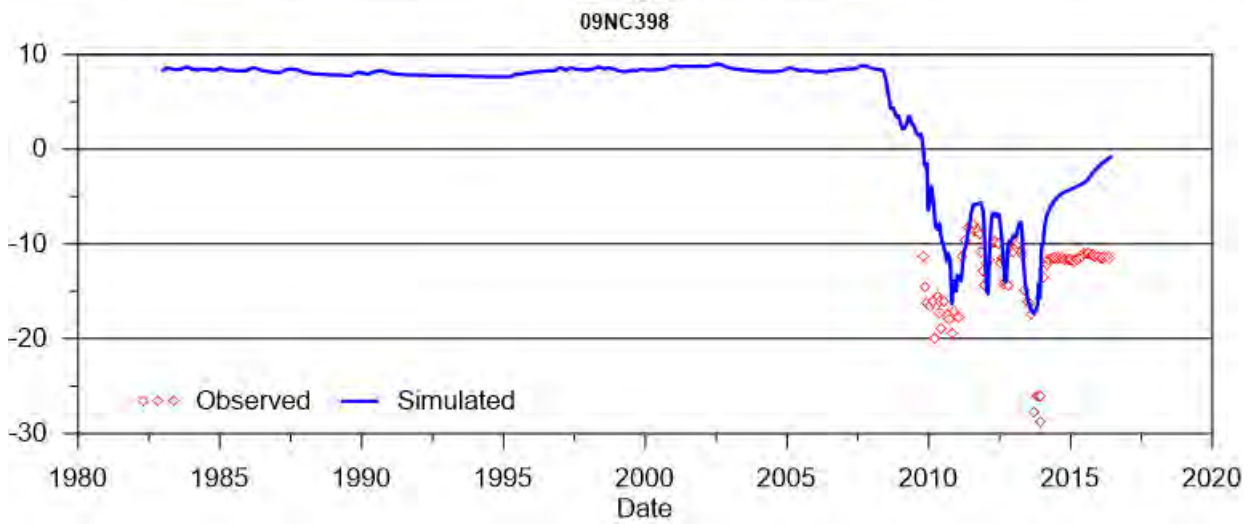
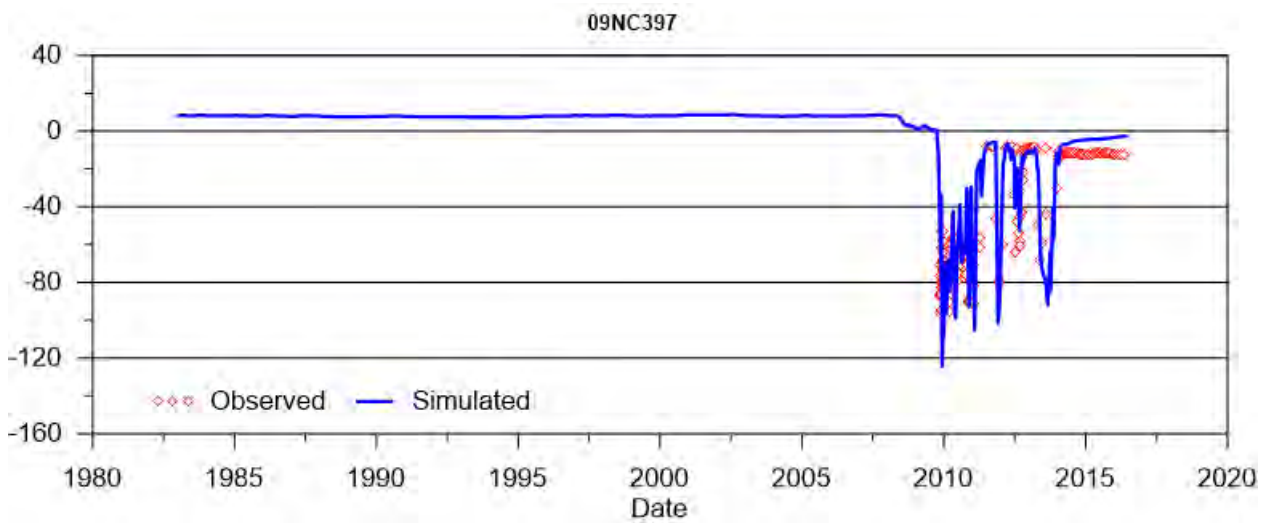
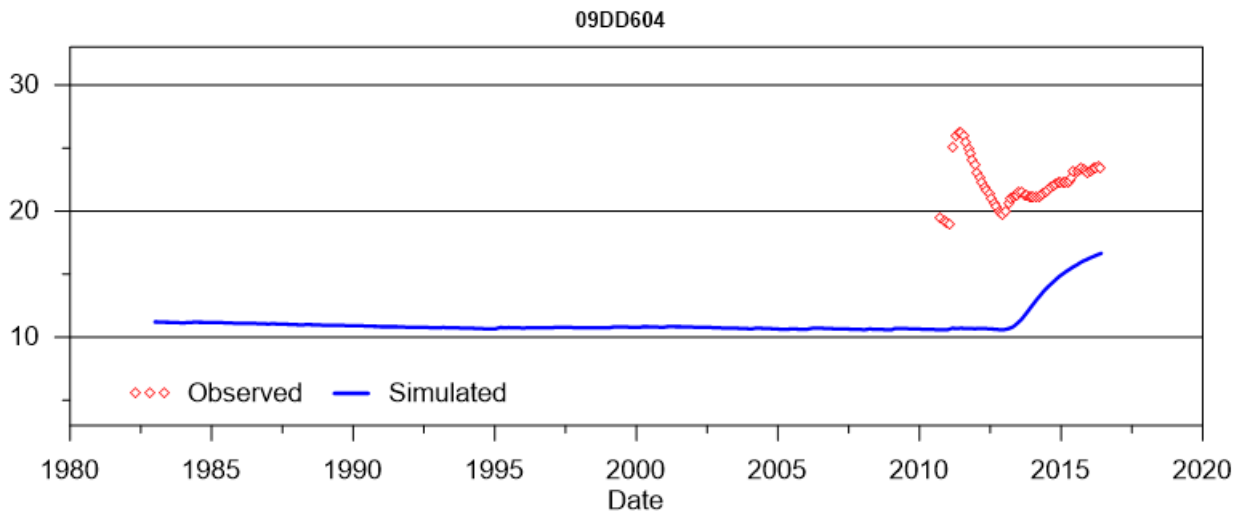
SINO EXPANSION LIFE OF MINE GROUNDWATER MODEL
APPENDIX E –Calibrated standpipe groundwater levels



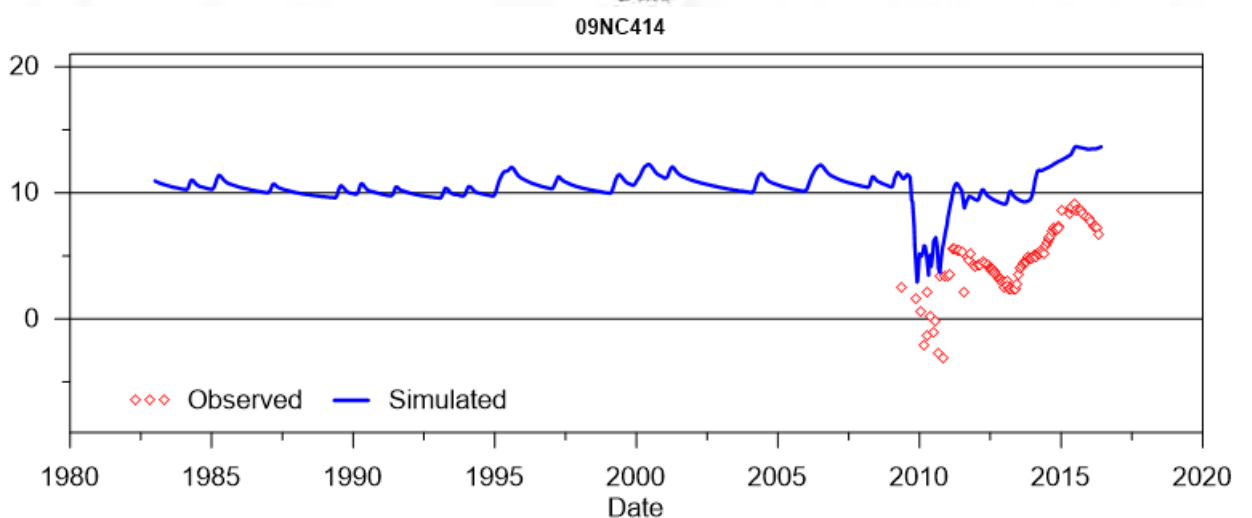
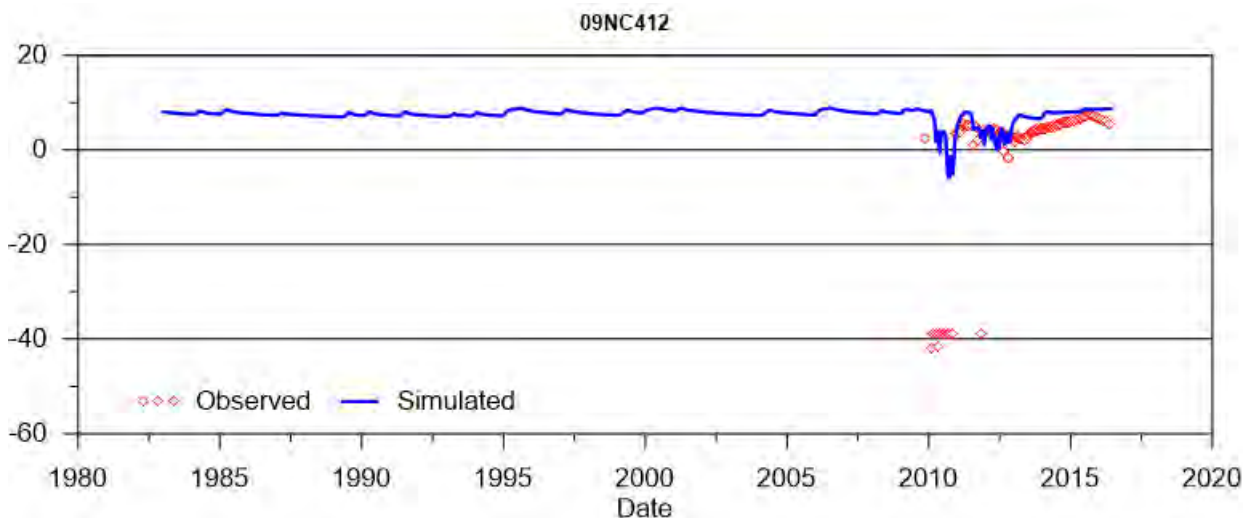
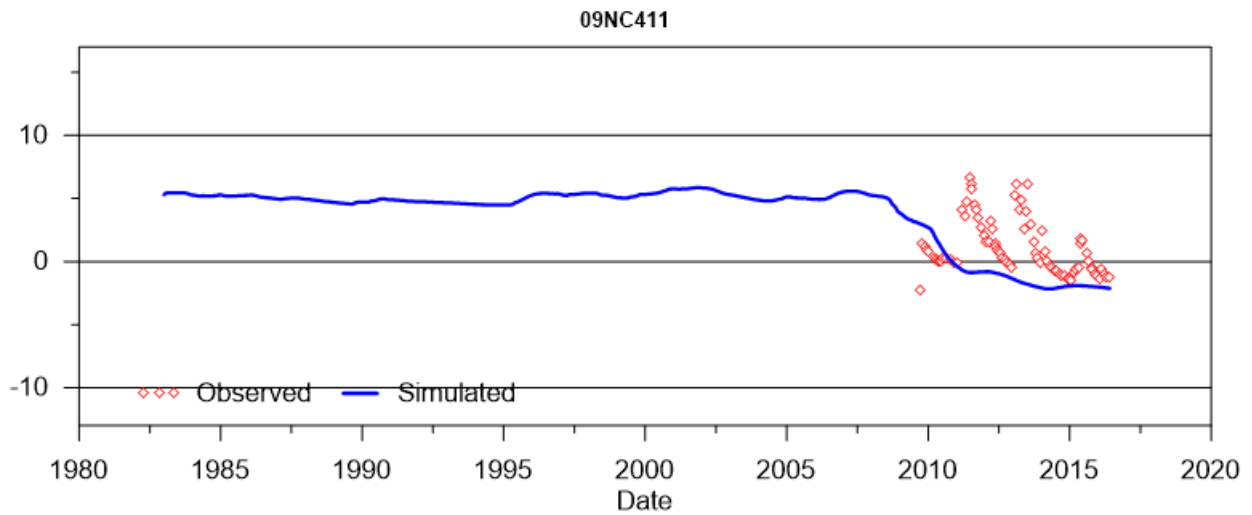
SINO EXPANSION LIFE OF MINE GROUNDWATER MODEL
APPENDIX E –Calibrated standpipe groundwater levels



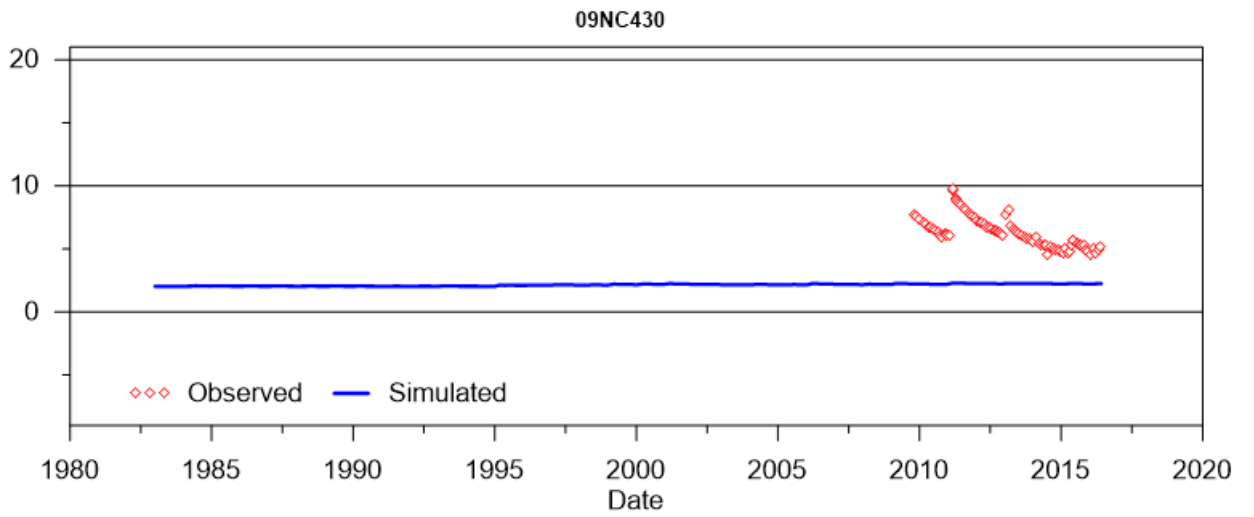
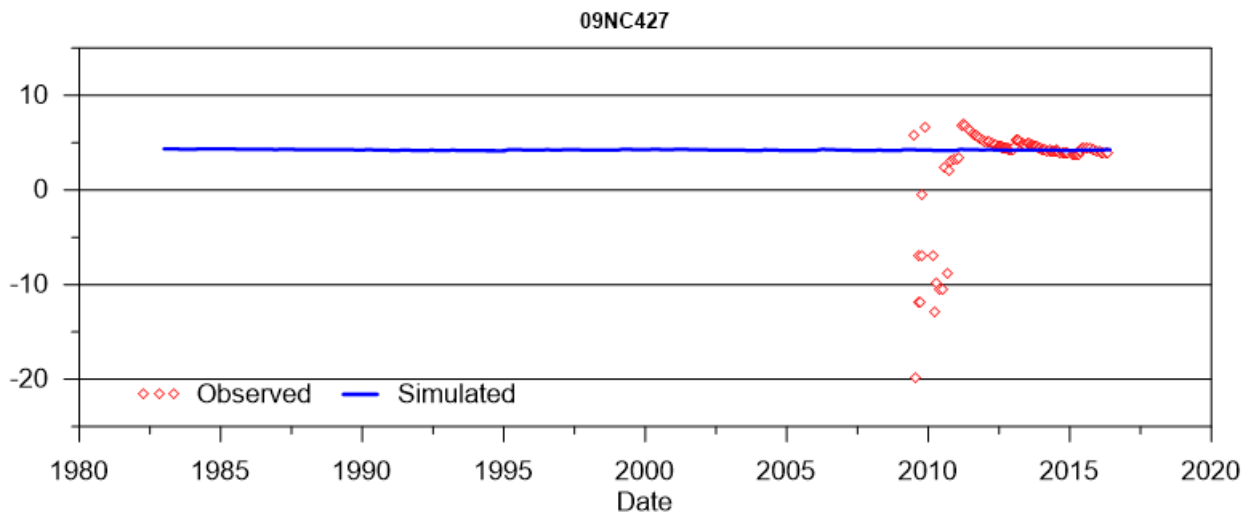
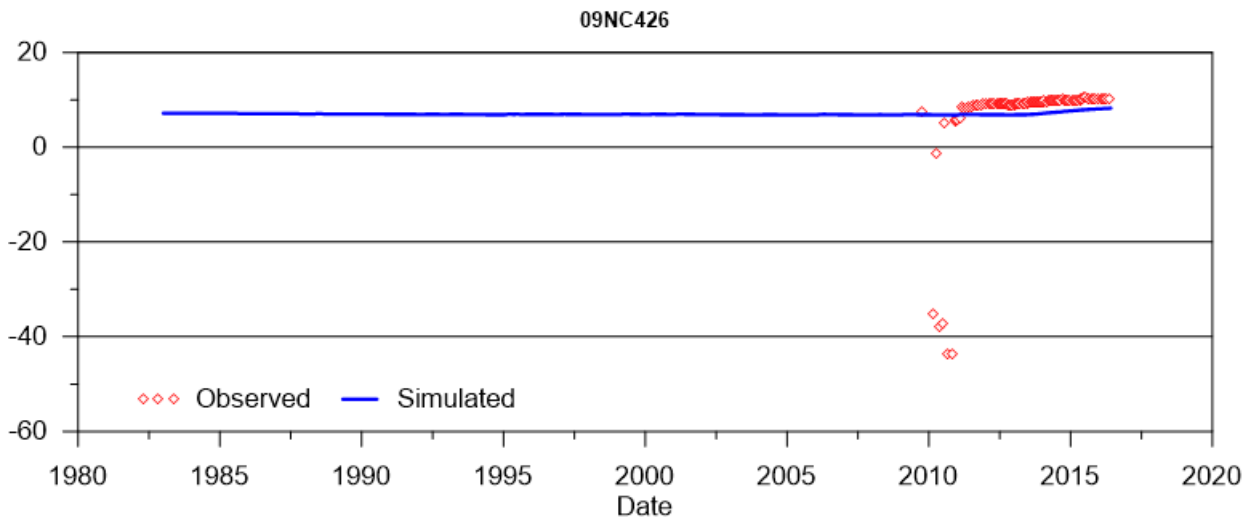
SINO EXPANSION LIFE OF MINE GROUNDWATER MODEL
APPENDIX E –Calibrated standpipe groundwater levels



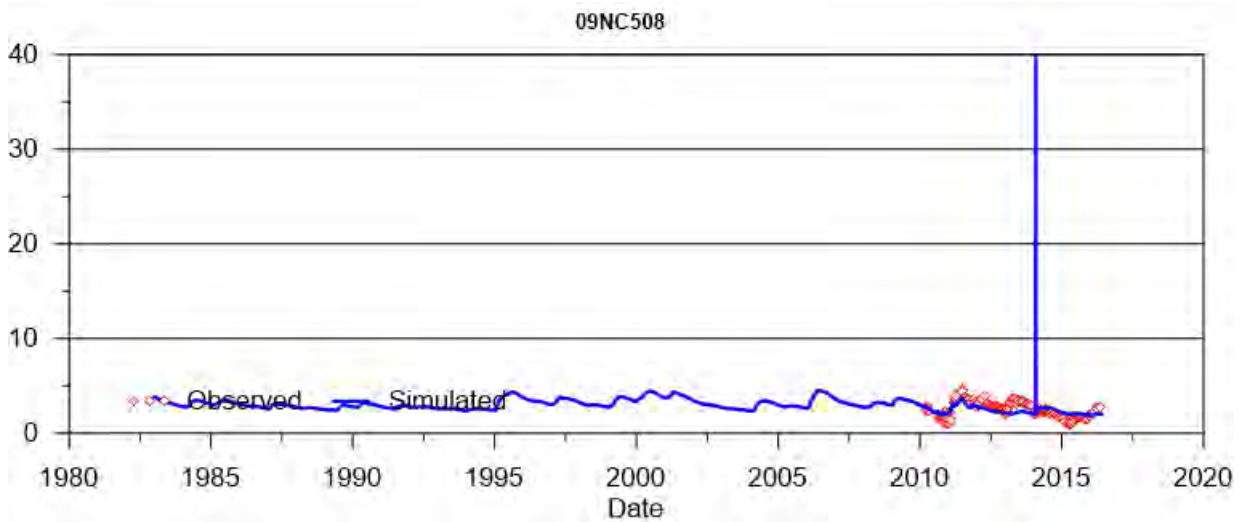
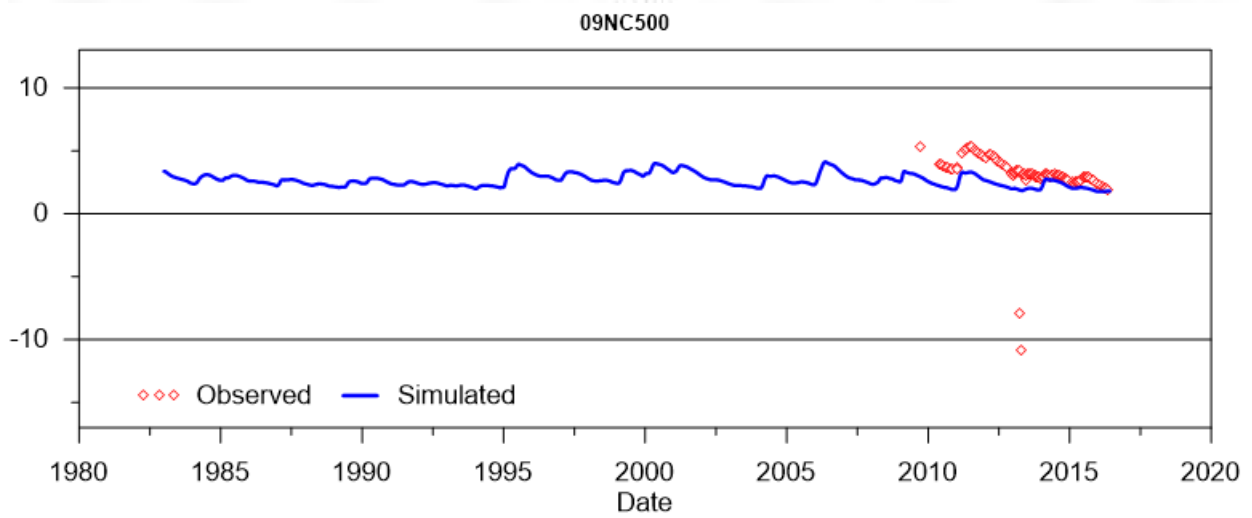
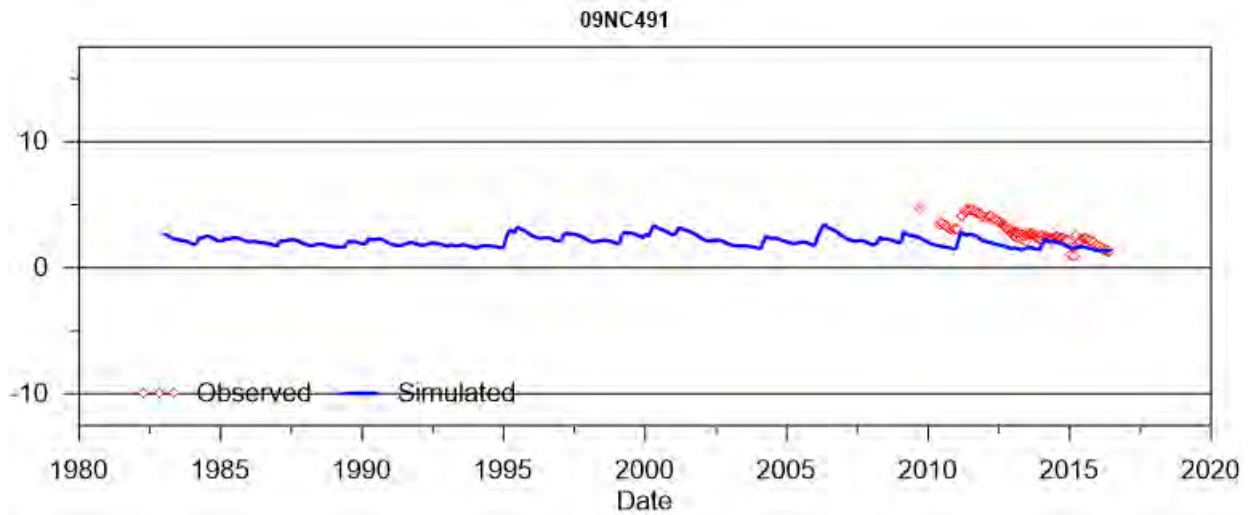
SINO EXPANSION LIFE OF MINE GROUNDWATER MODEL
APPENDIX E –Calibrated standpipe groundwater levels



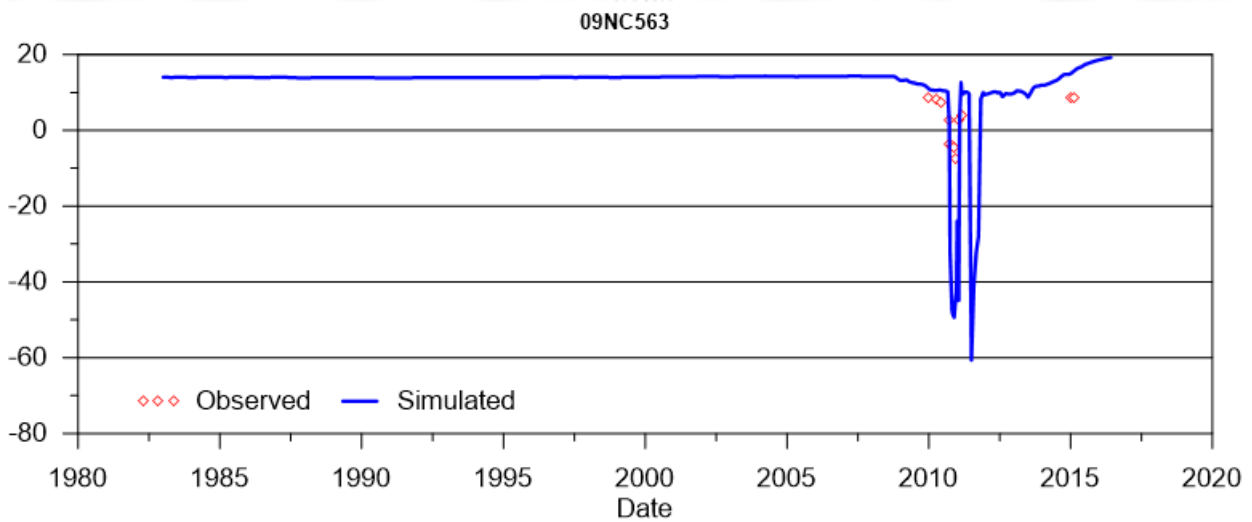
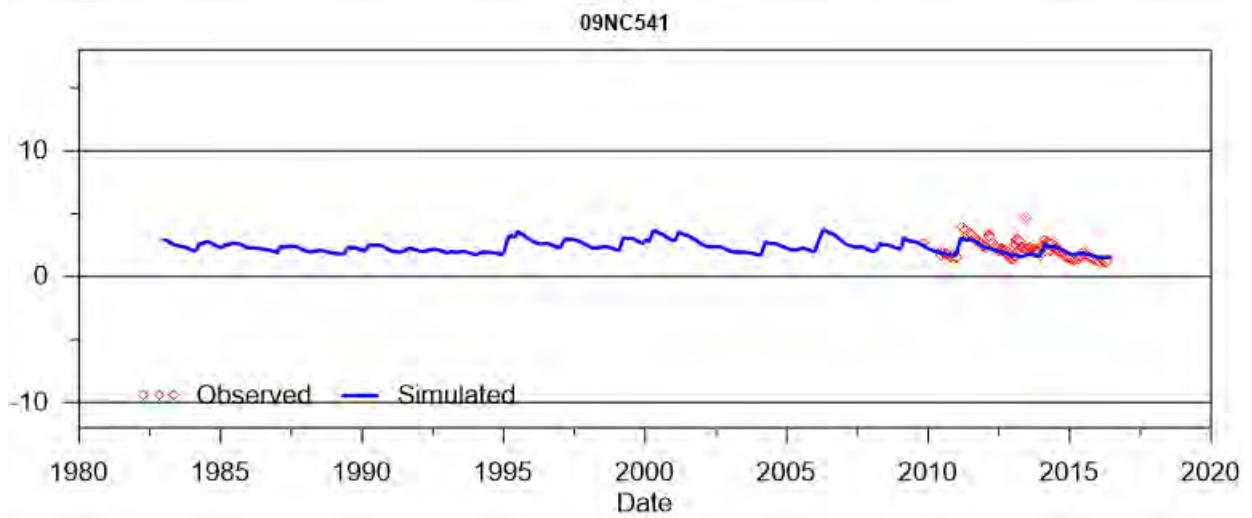
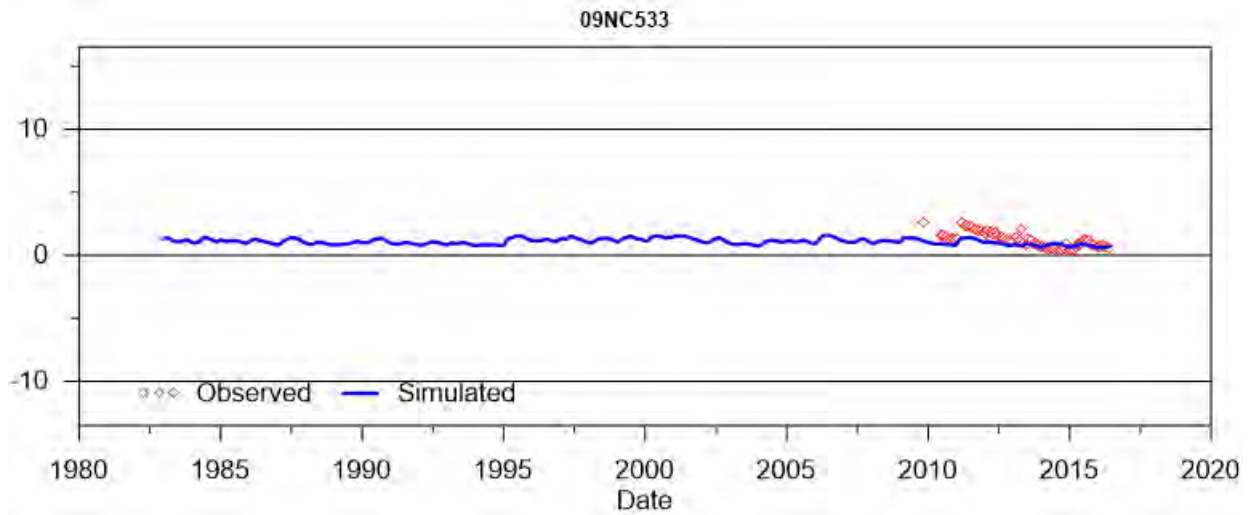
SINO EXPANSION LIFE OF MINE GROUNDWATER MODEL
APPENDIX E –Calibrated standpipe groundwater levels



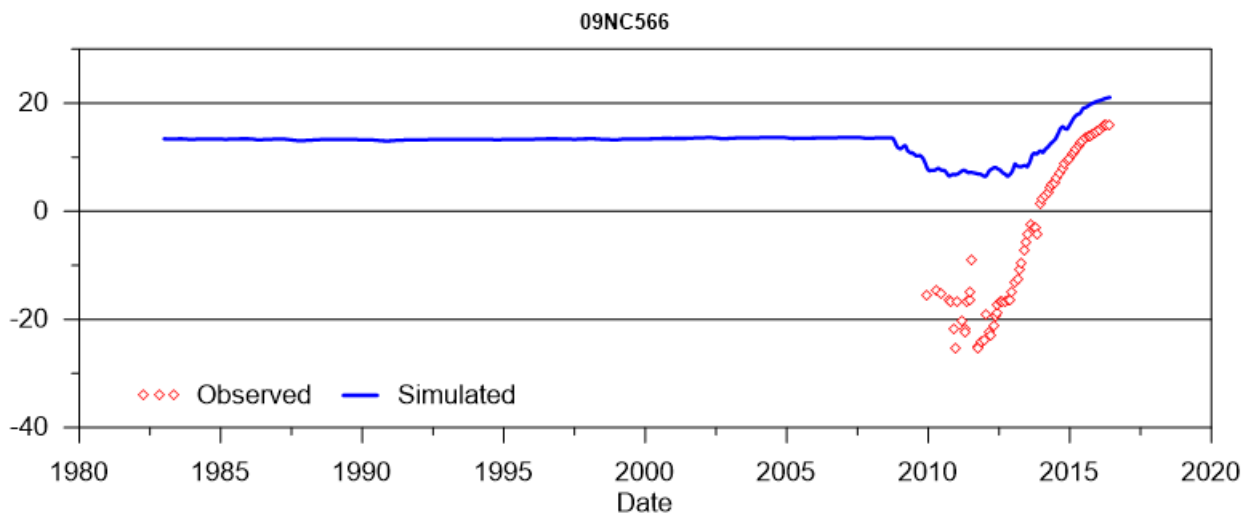
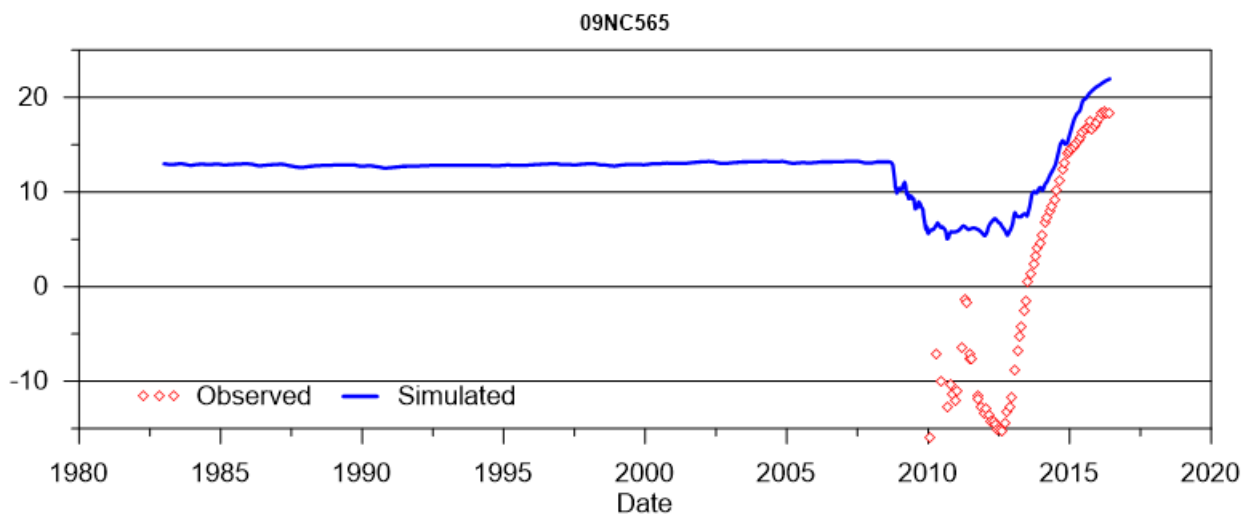
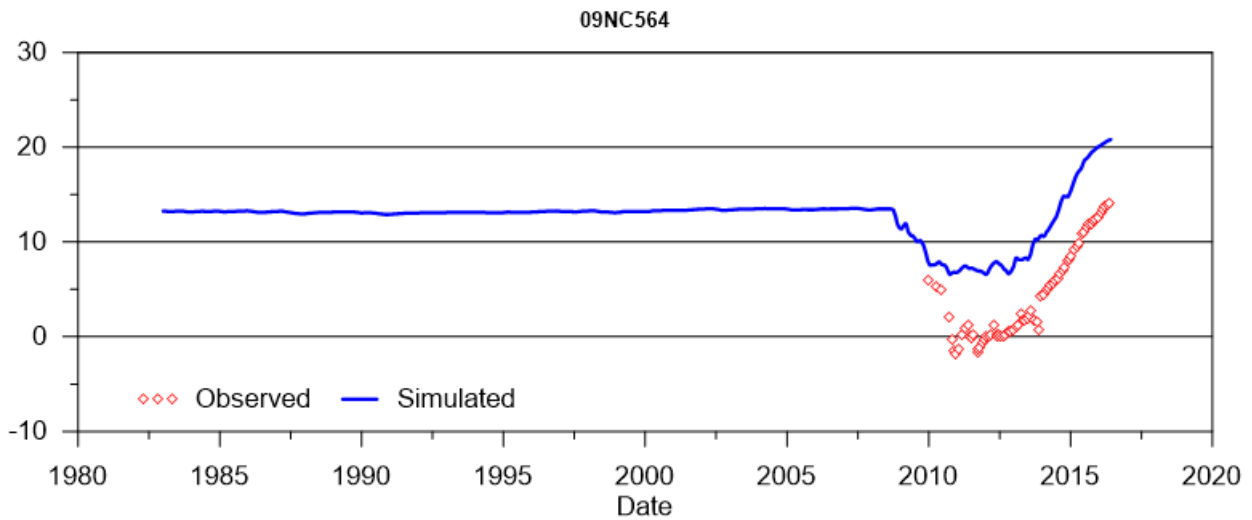
SINO EXPANSION LIFE OF MINE GROUNDWATER MODEL
APPENDIX E –Calibrated standpipe groundwater levels



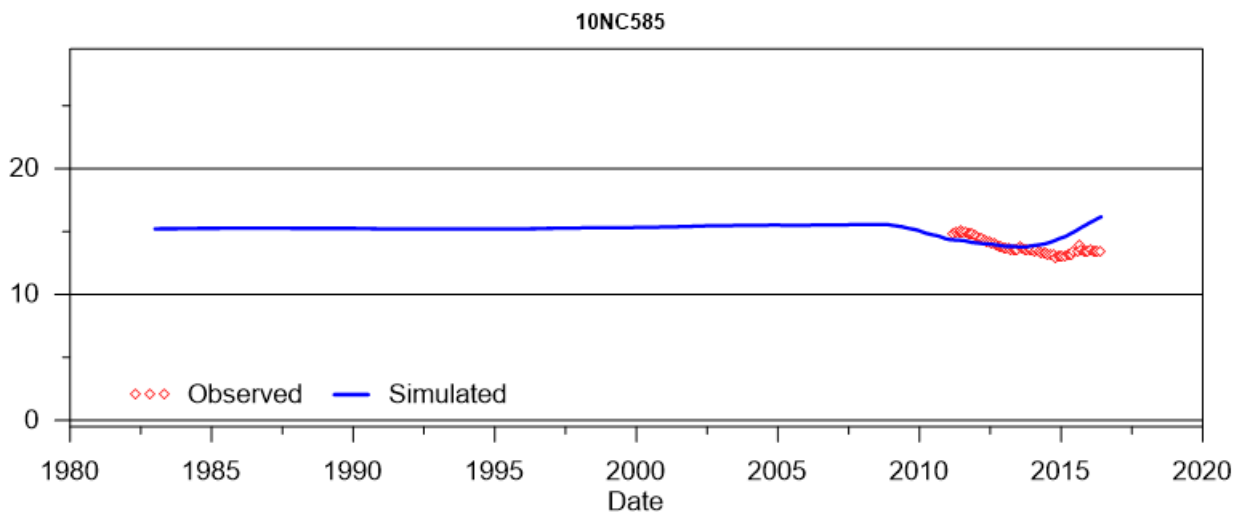
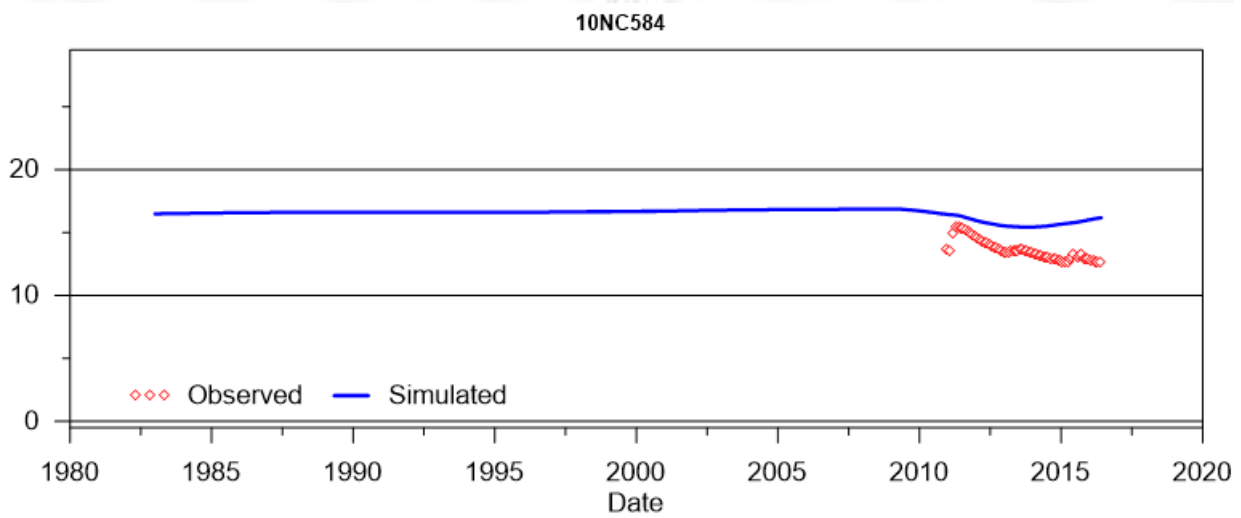
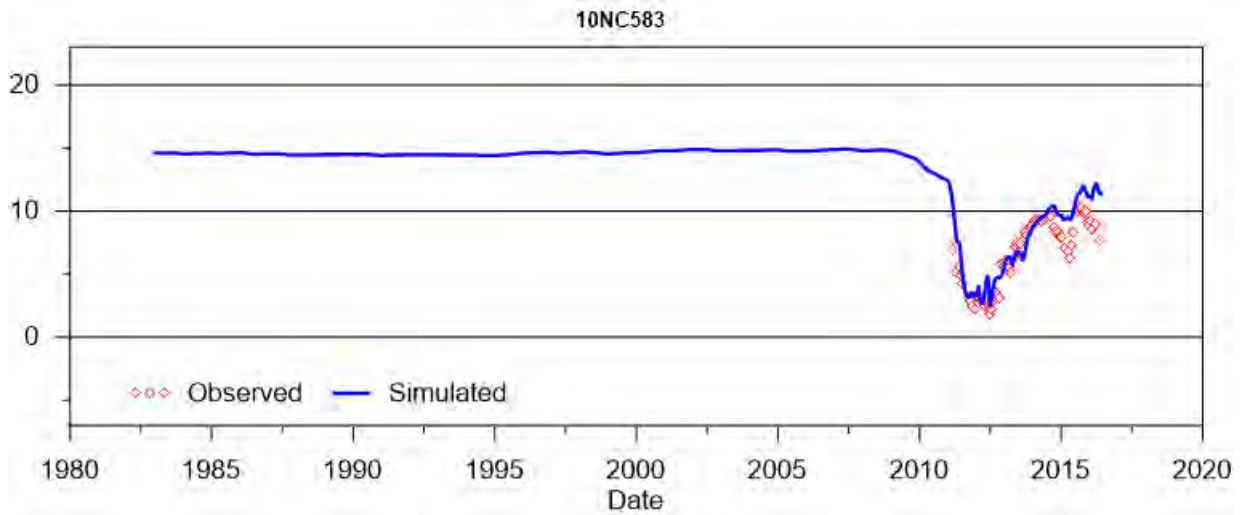
SINO EXPANSION LIFE OF MINE GROUNDWATER MODEL
APPENDIX E –Calibrated standpipe groundwater levels



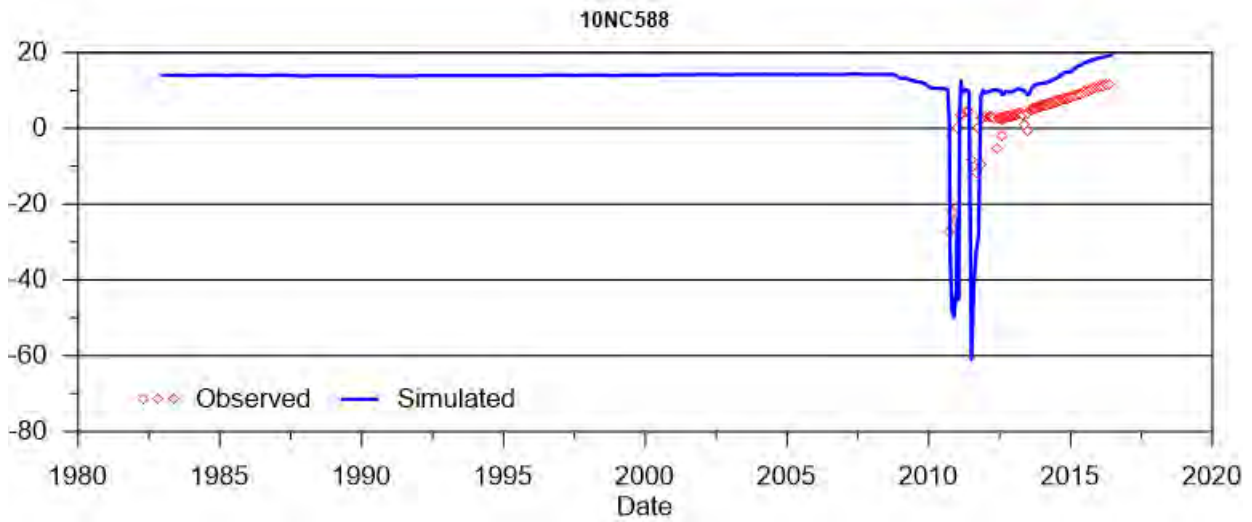
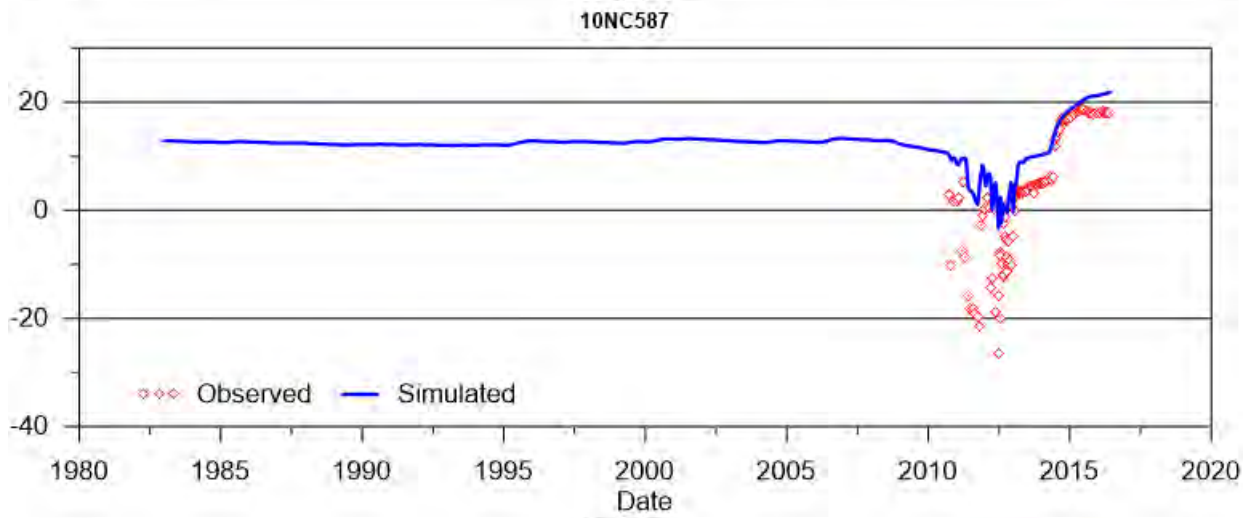
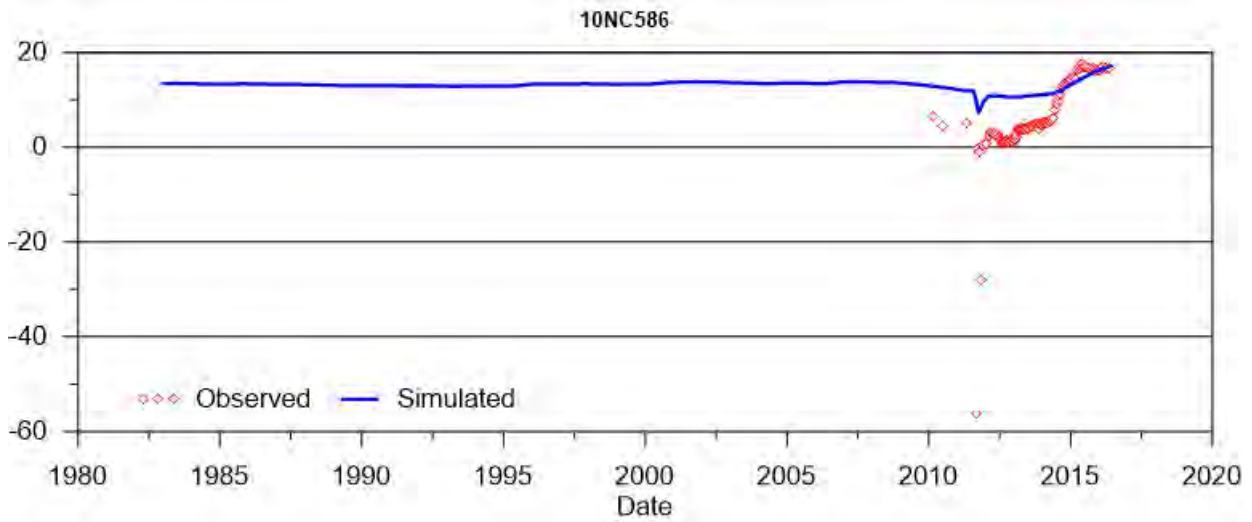
SINO EXPANSION LIFE OF MINE GROUNDWATER MODEL
APPENDIX E –Calibrated standpipe groundwater levels



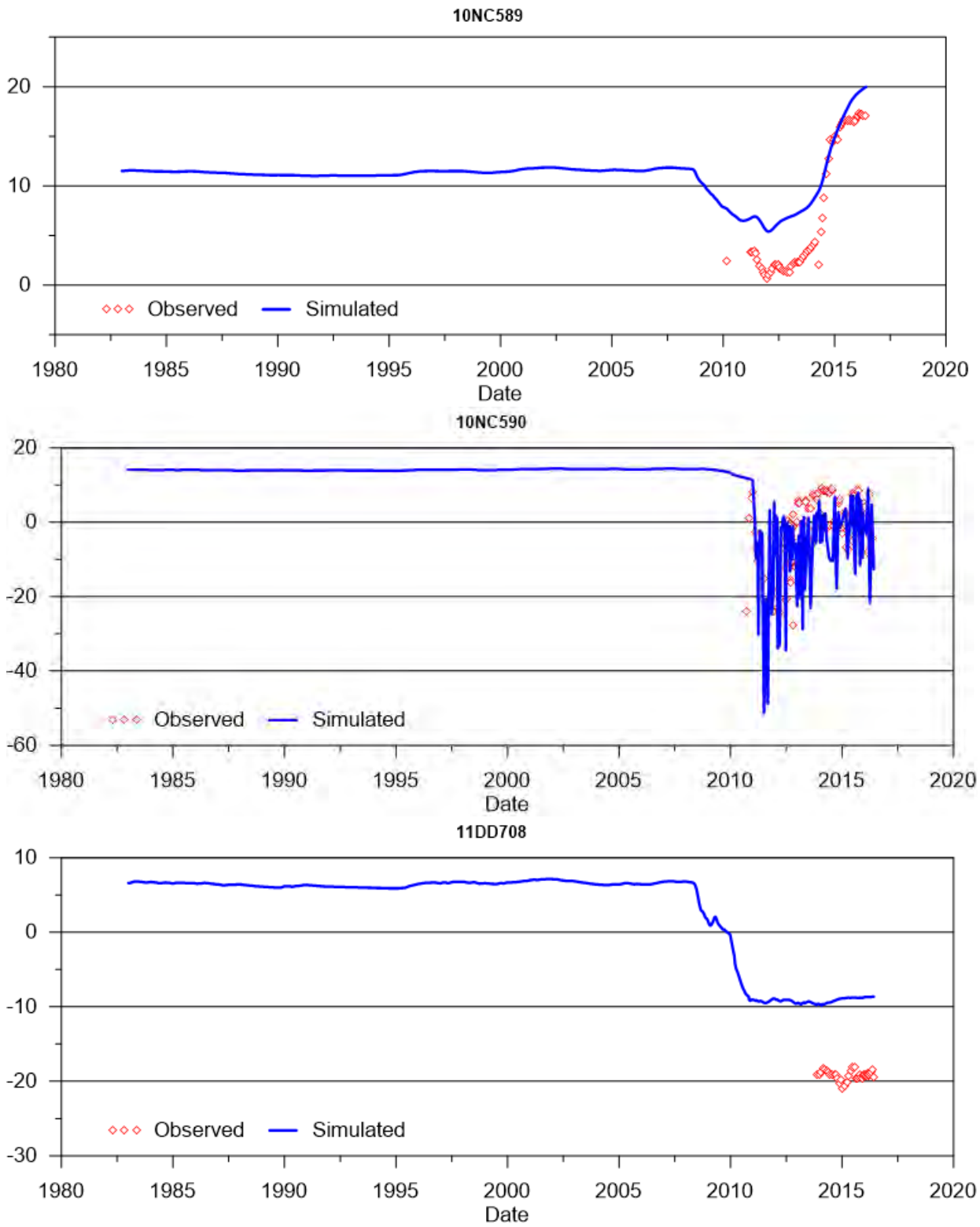
SINO EXPANSION LIFE OF MINE GROUNDWATER MODEL
APPENDIX E –Calibrated standpipe groundwater levels



SINO EXPANSION LIFE OF MINE GROUNDWATER MODEL
APPENDIX E –Calibrated standpipe groundwater levels

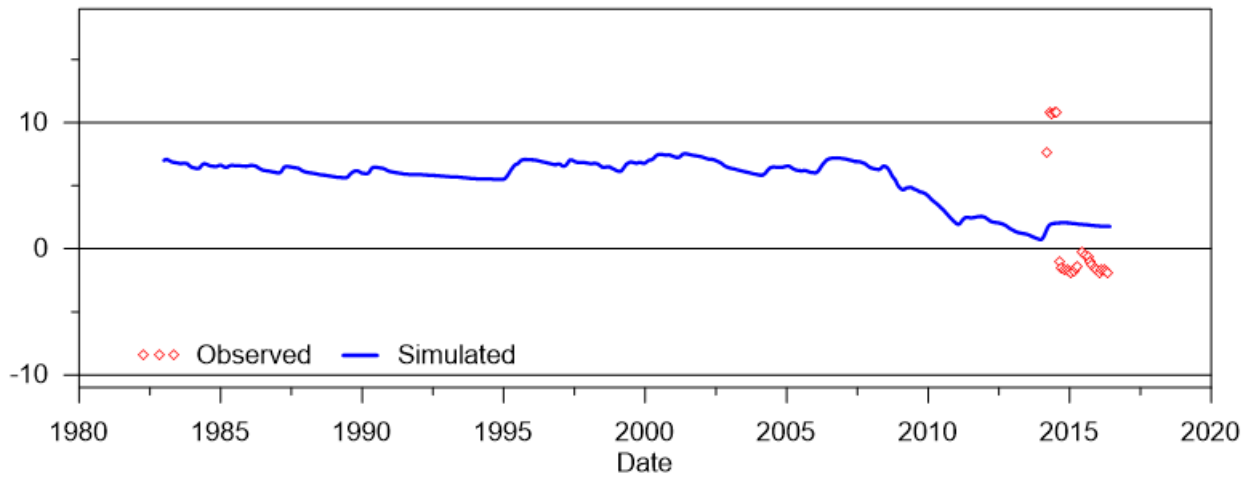


SINO EXPANSION LIFE OF MINE GROUNDWATER MODEL
APPENDIX E –Calibrated standpipe groundwater levels

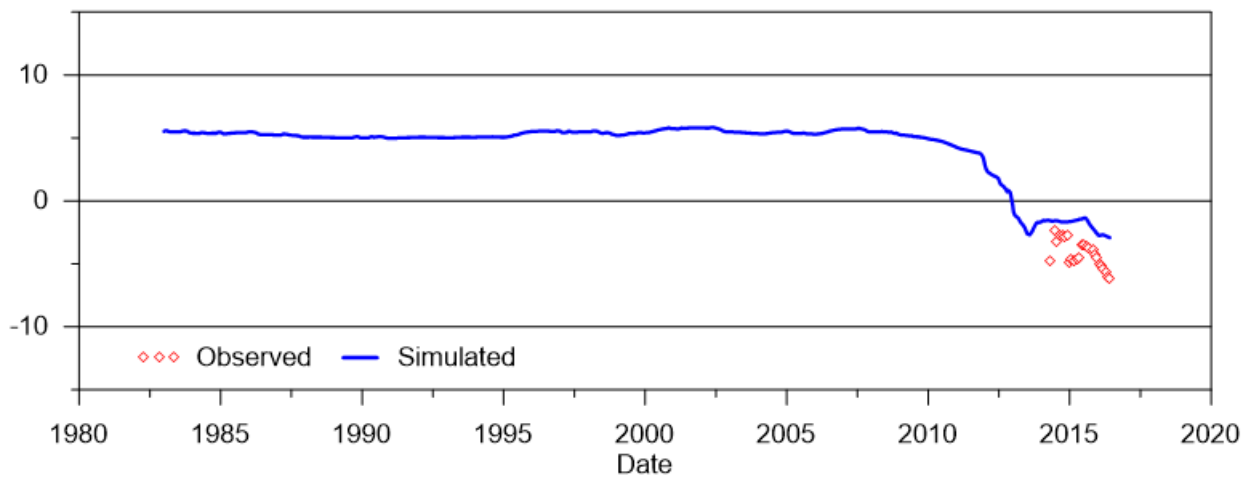


SINO EXPANSION LIFE OF MINE GROUNDWATER MODEL
APPENDIX E –Calibrated standpipe groundwater levels

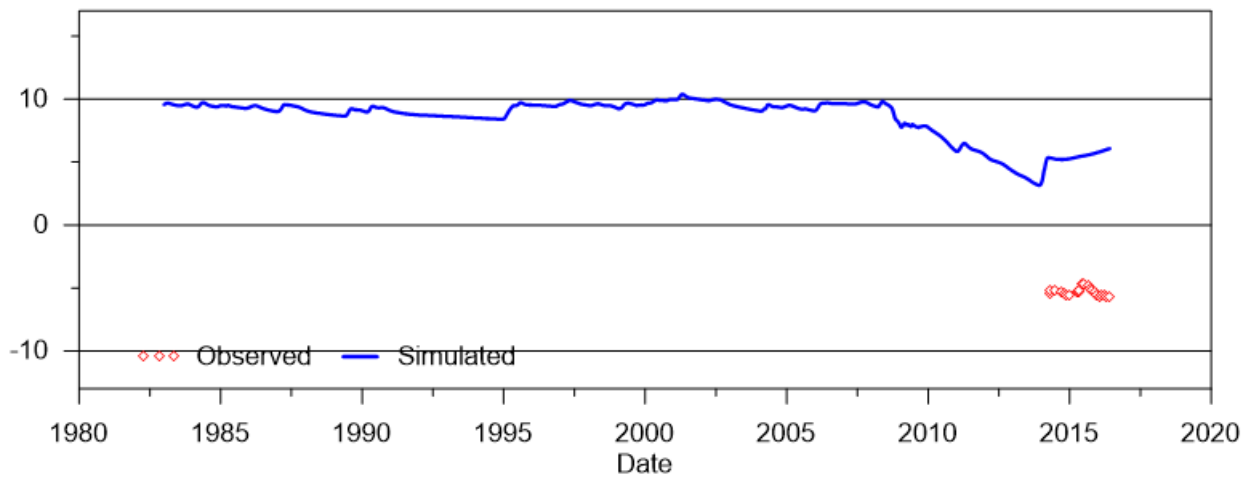
11DD712



12DD721

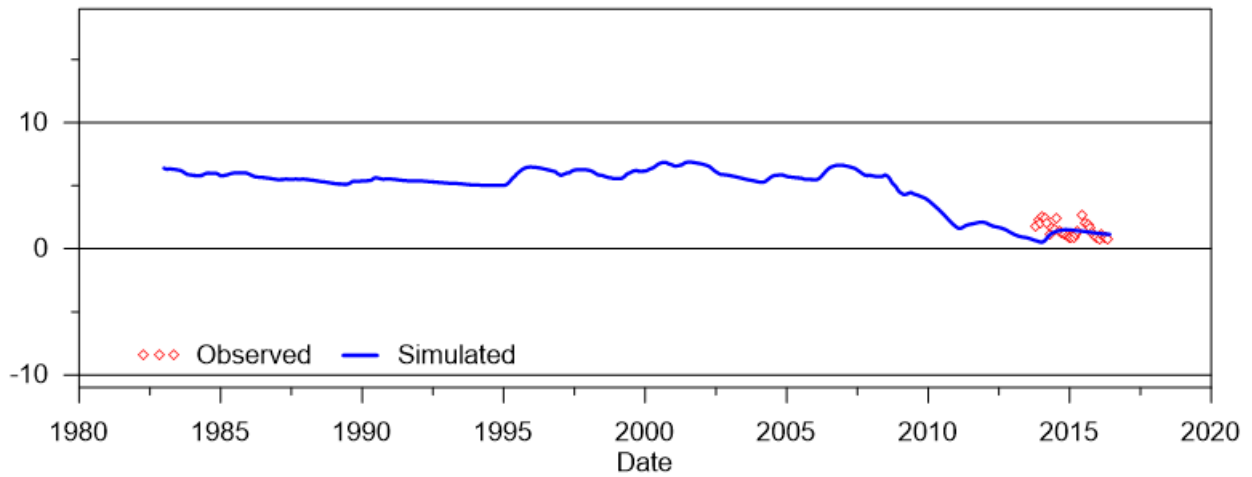


12DD727

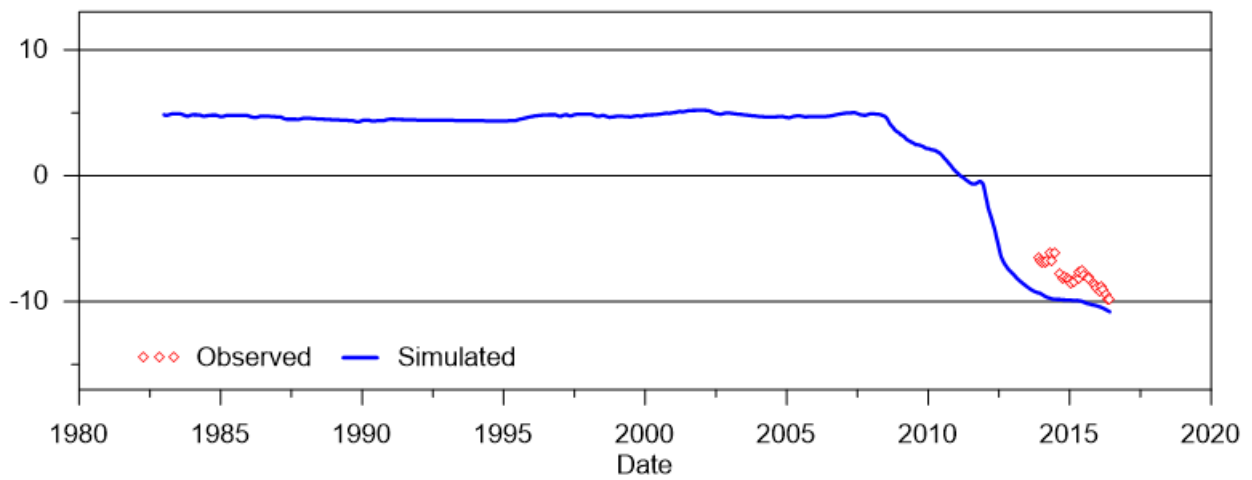


SINO EXPANSION LIFE OF MINE GROUNDWATER MODEL
APPENDIX E –Calibrated standpipe groundwater levels

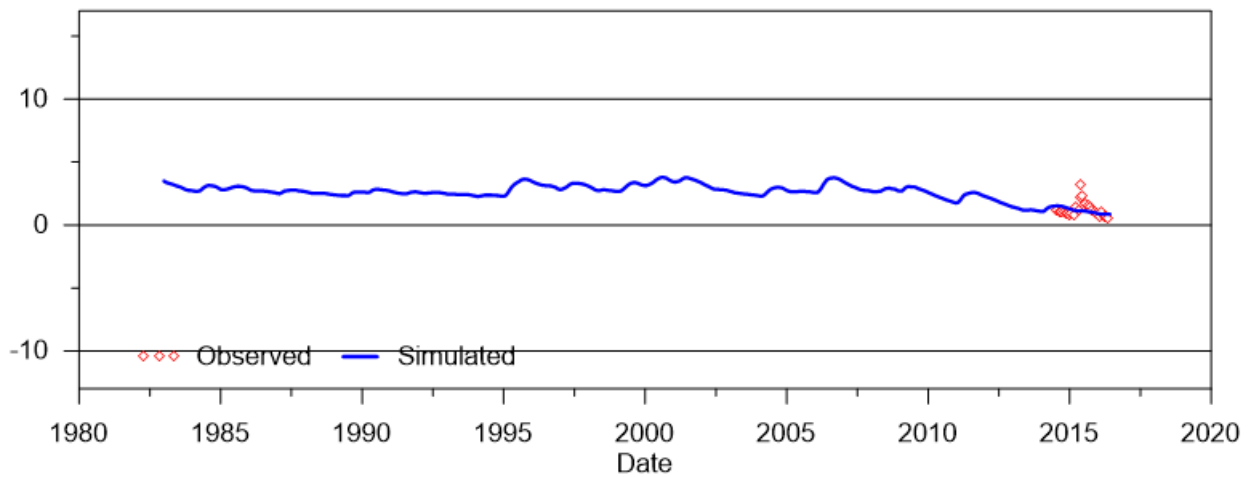
12DD728



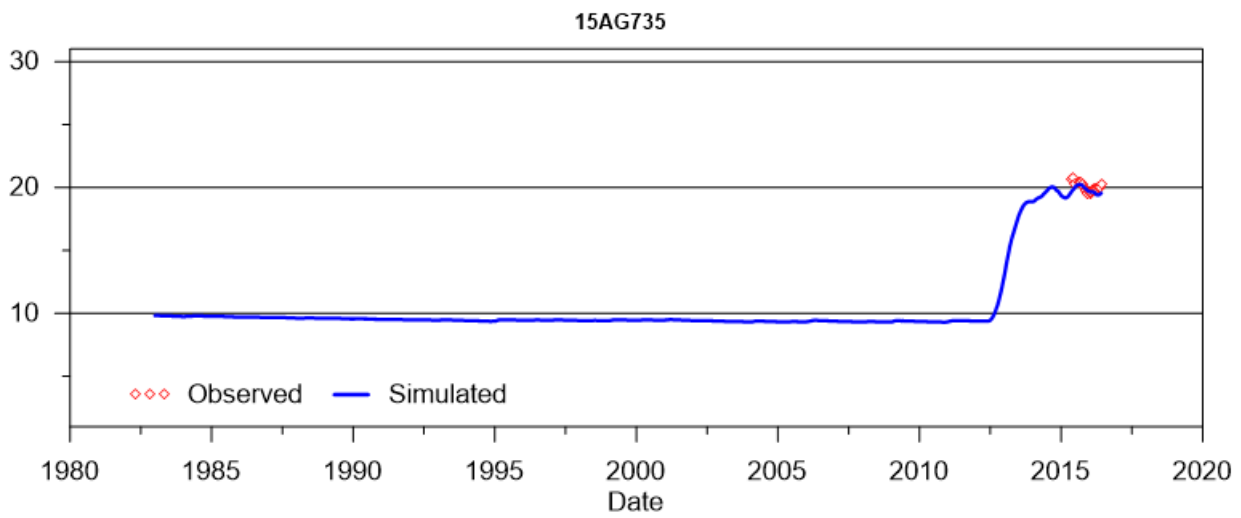
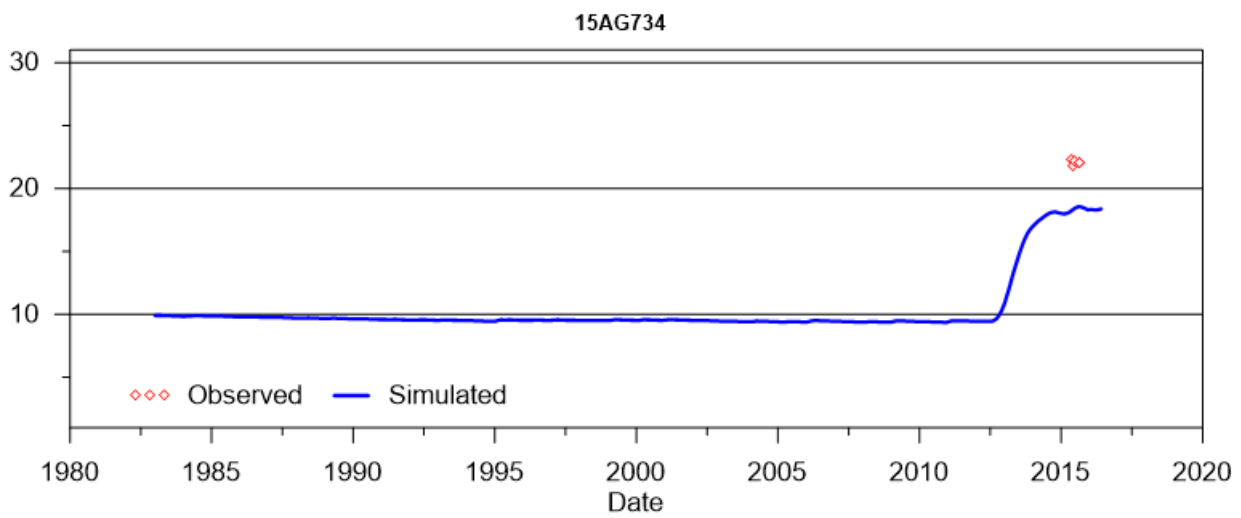
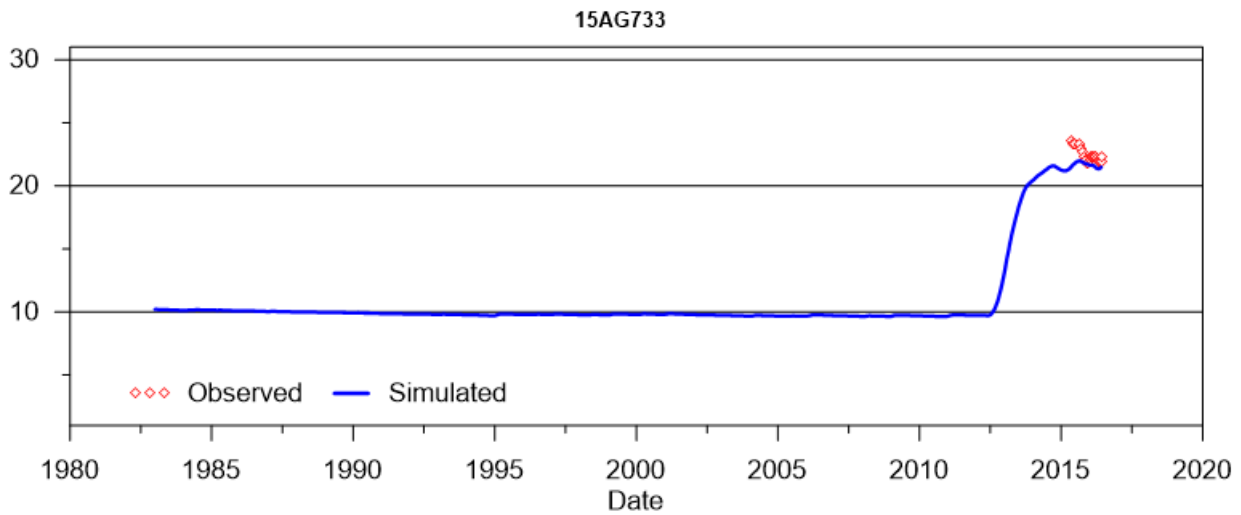
12DD730



13DD732

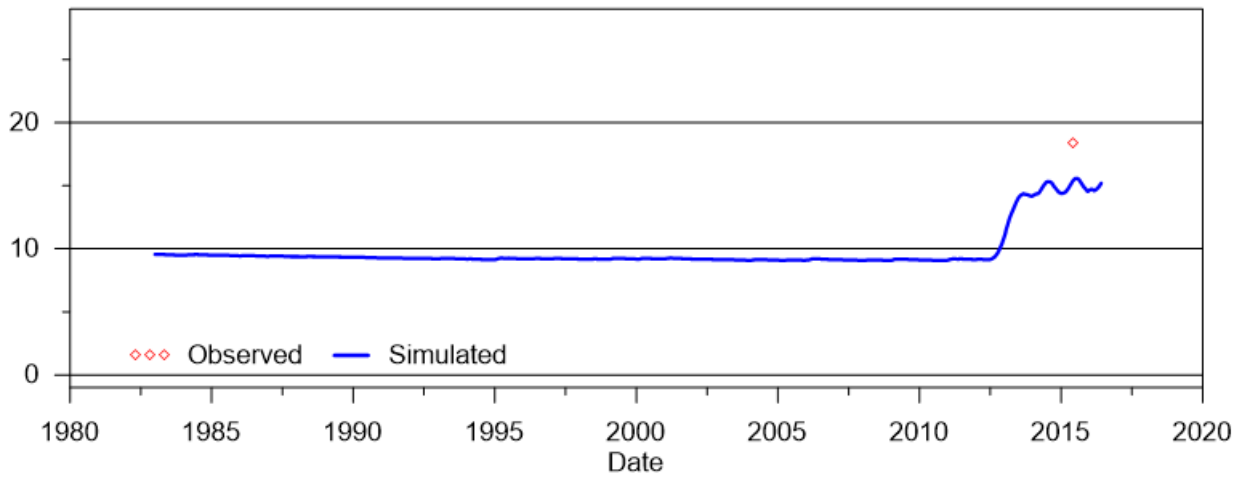


SINO EXPANSION LIFE OF MINE GROUNDWATER MODEL
APPENDIX E –Calibrated standpipe groundwater levels

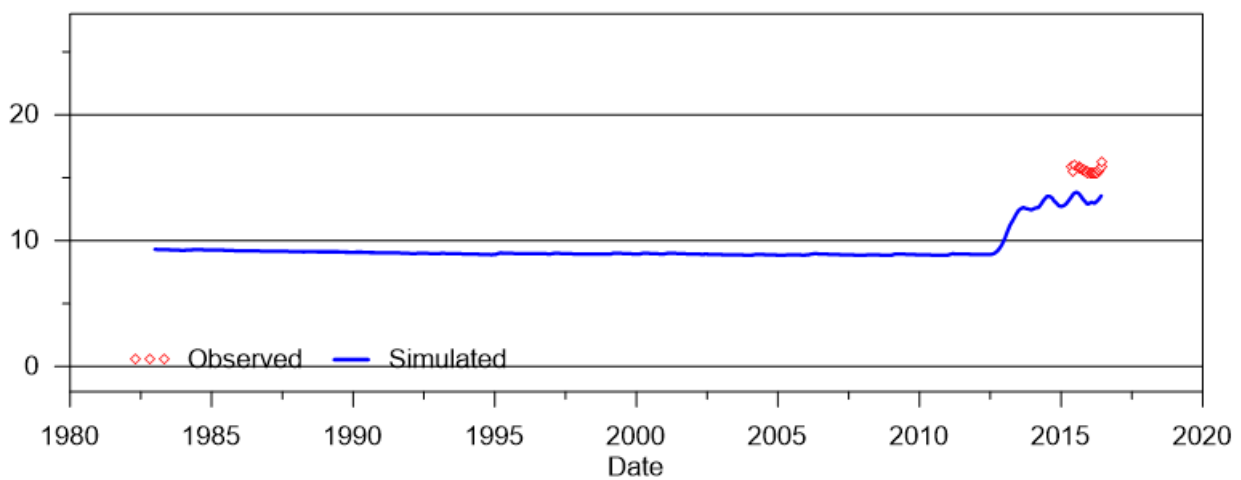


SINO EXPANSION LIFE OF MINE GROUNDWATER MODEL
APPENDIX E –Calibrated standpipe groundwater levels

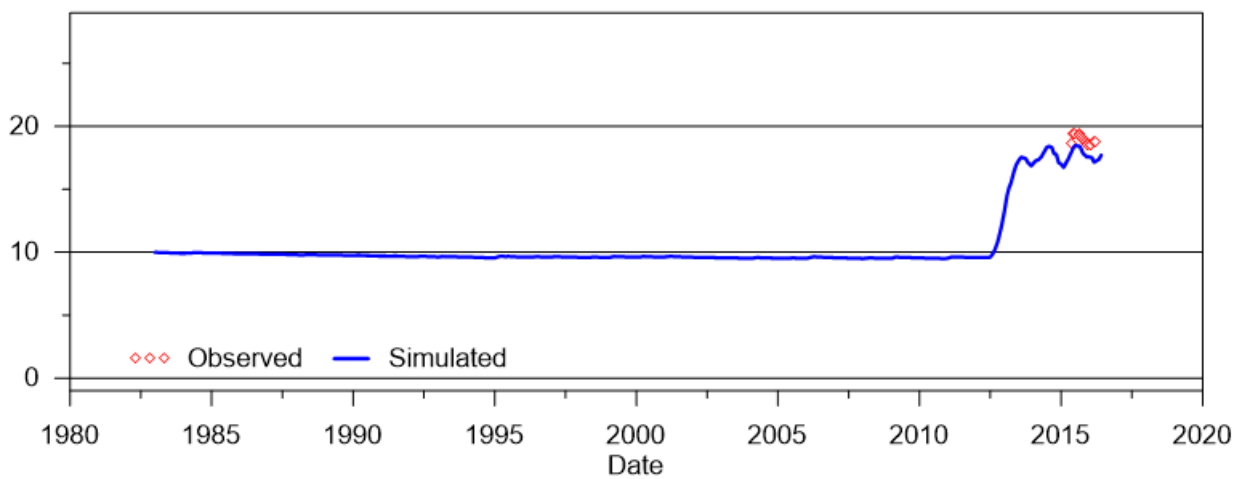
15AG737



15AG738

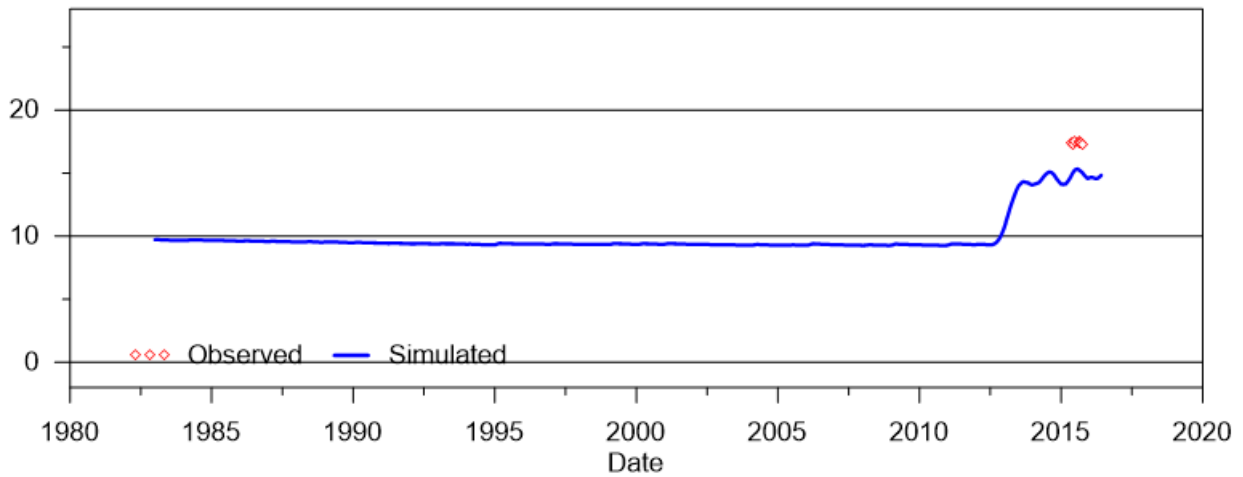


15AG739

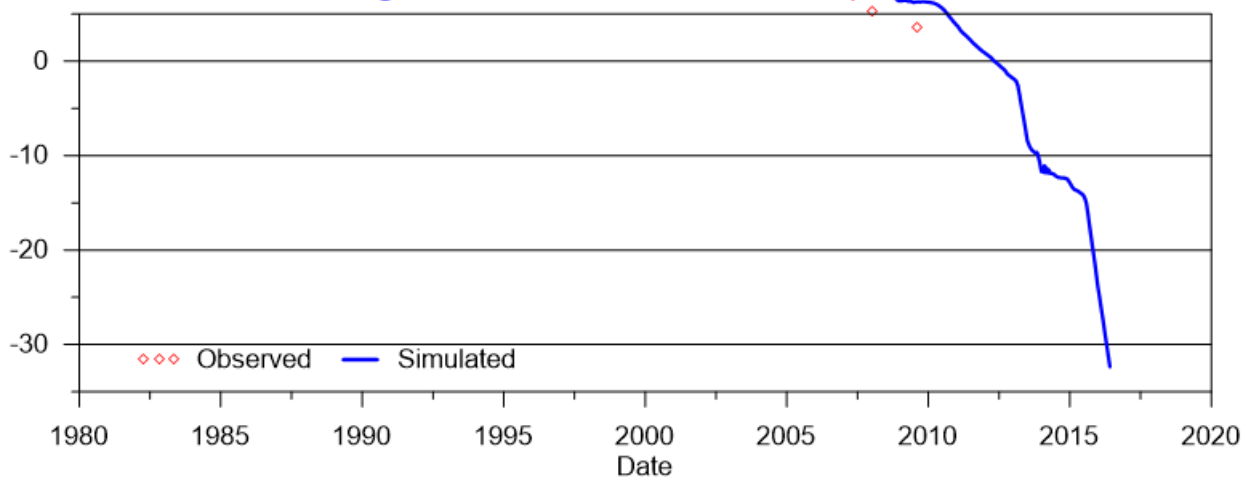


SINO EXPANSION LIFE OF MINE GROUNDWATER MODEL
APPENDIX E –Calibrated standpipe groundwater levels

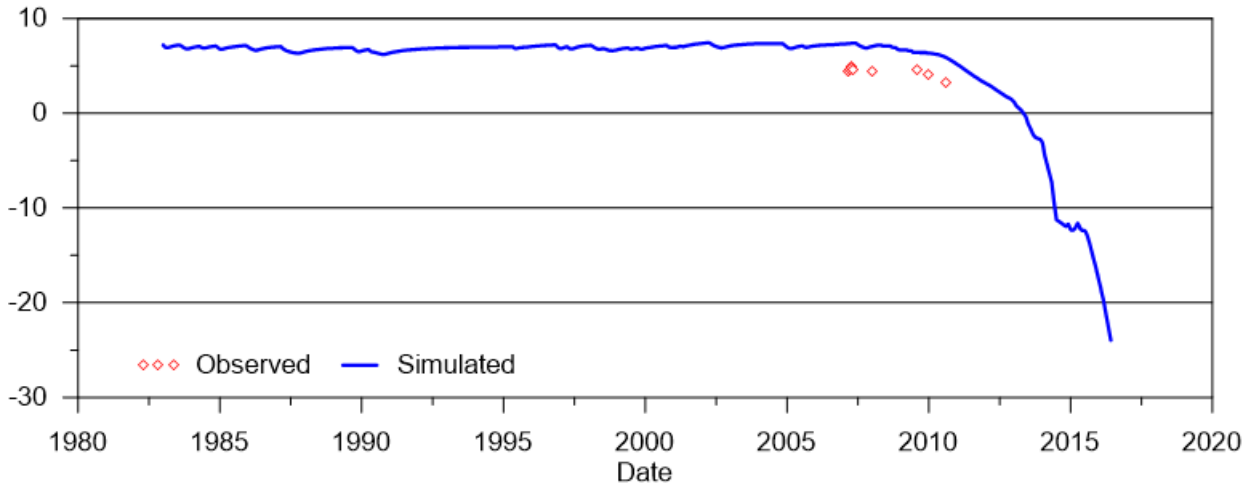
15AG740



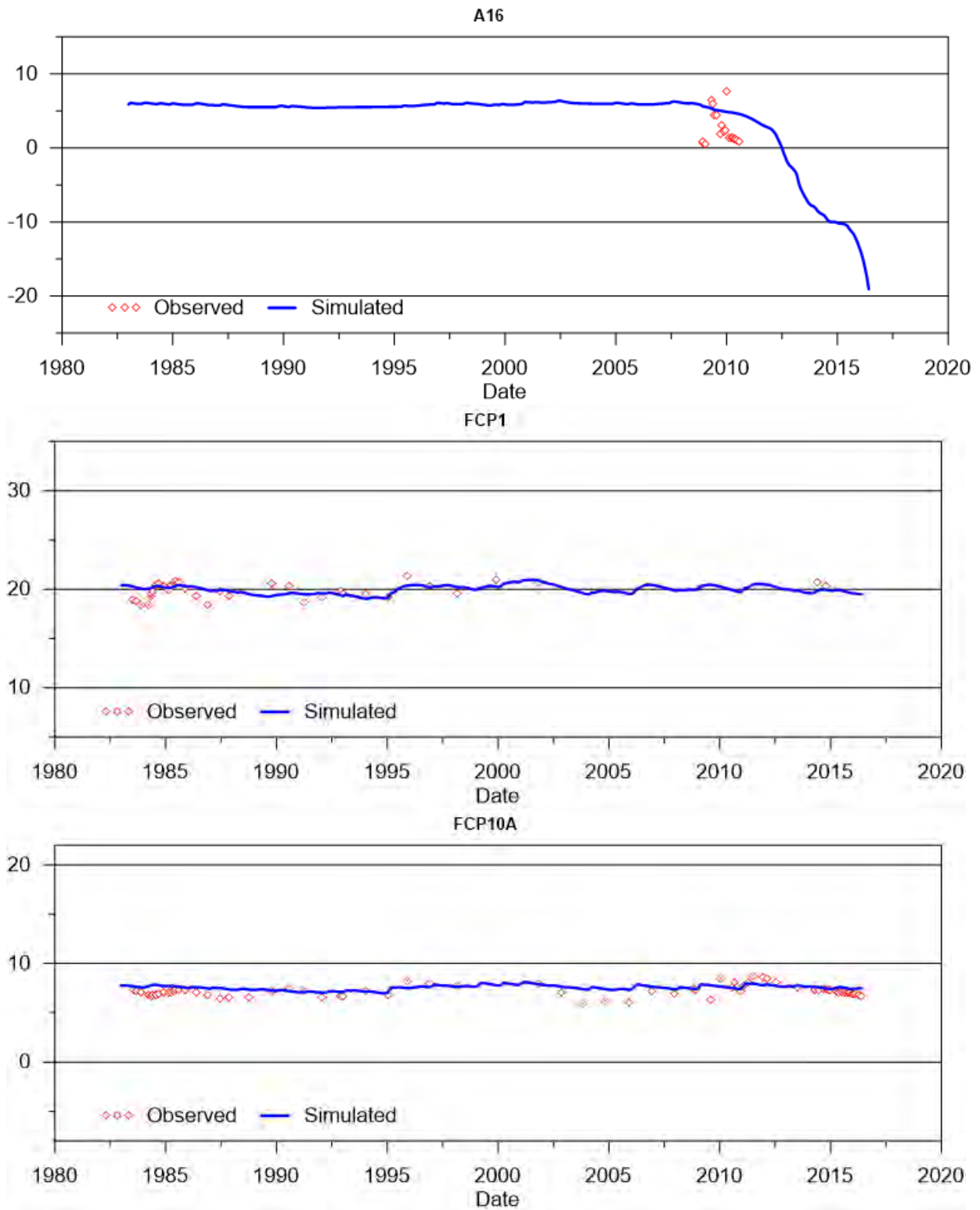
A06



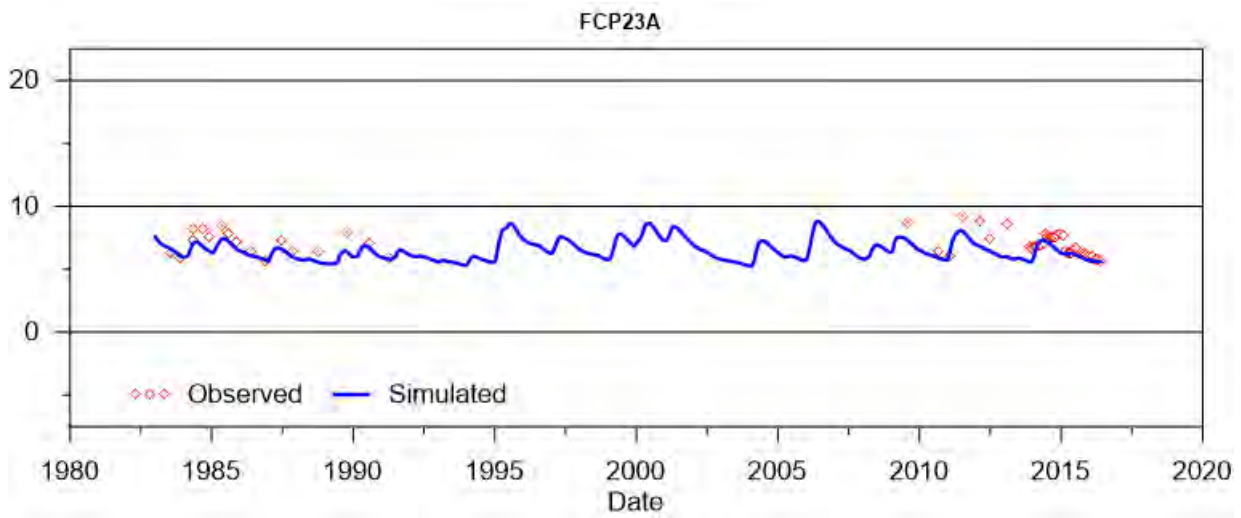
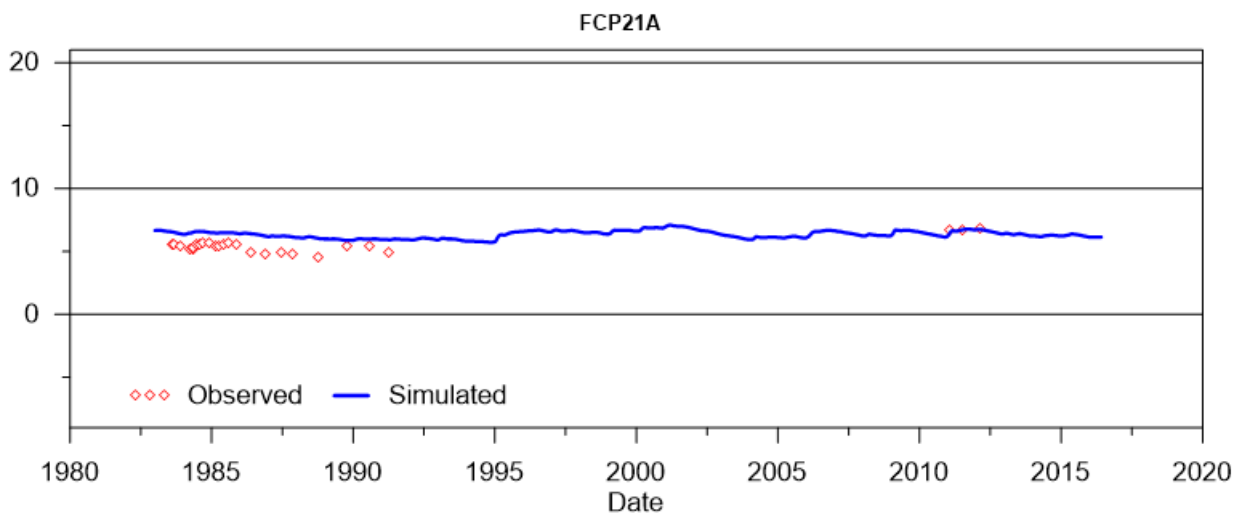
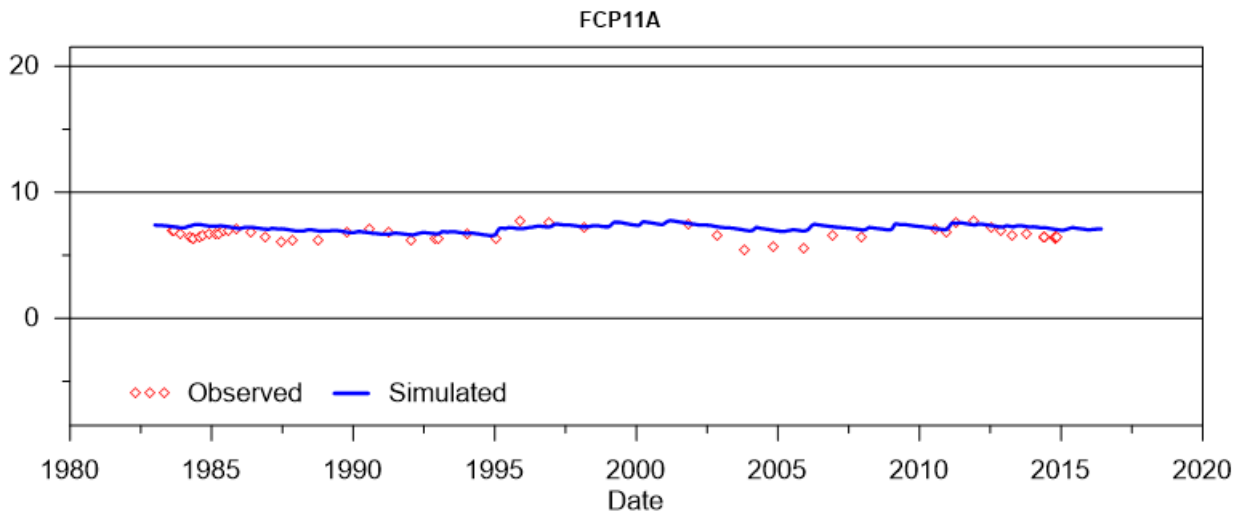
A13



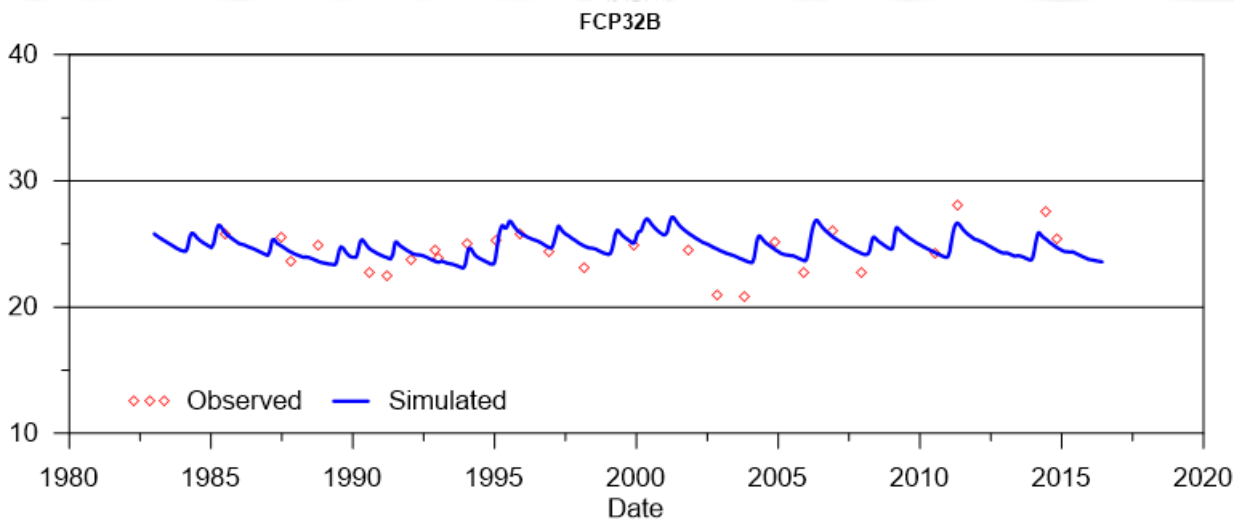
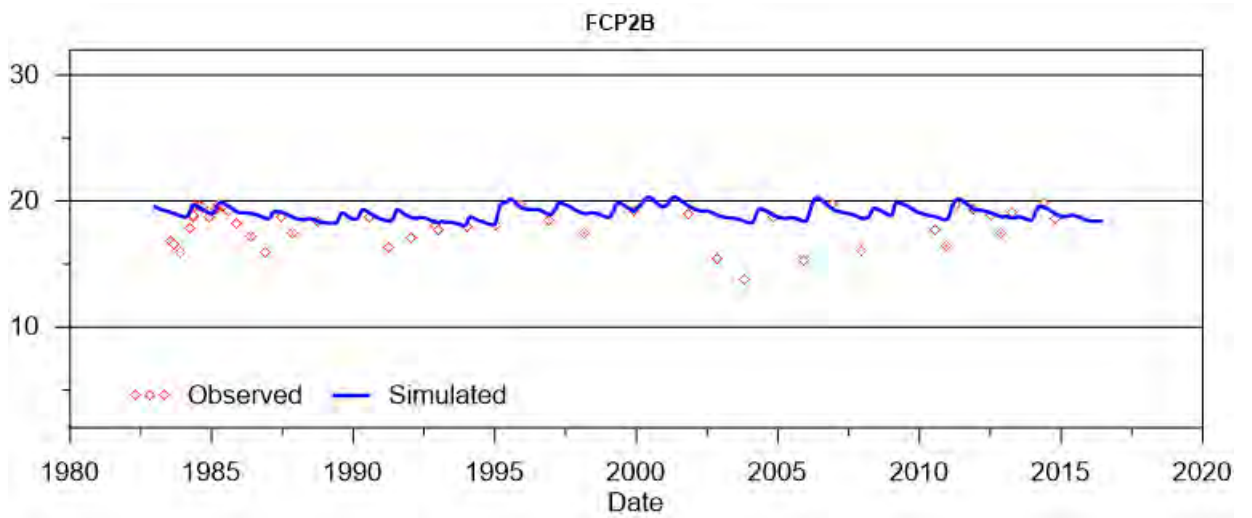
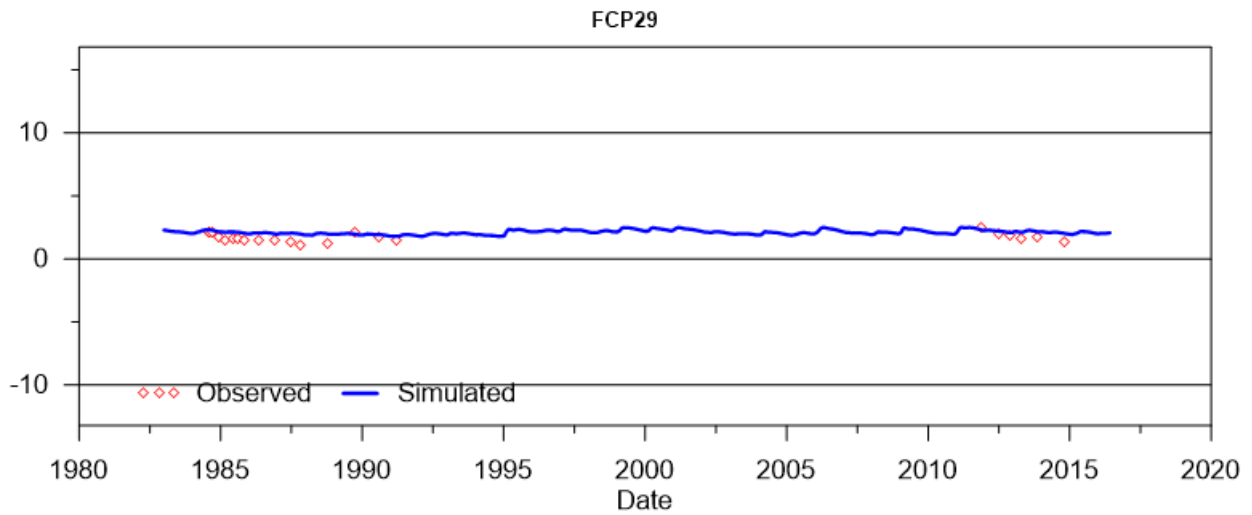
SINO EXPANSION LIFE OF MINE GROUNDWATER MODEL
APPENDIX E –Calibrated standpipe groundwater levels



SINO EXPANSION LIFE OF MINE GROUNDWATER MODEL
APPENDIX E –Calibrated standpipe groundwater levels



SINO EXPANSION LIFE OF MINE GROUNDWATER MODEL
APPENDIX E –Calibrated standpipe groundwater levels



SINO EXPANSION LIFE OF MINE GROUNDWATER MODEL
APPENDIX E –Calibrated standpipe groundwater levels

